Climatological Isentropic Analysis: Identifying Patterns Associated with Tornado Occurrences Across the United States

by

Matthew Brandon Pace

A Dissertation Presented in Partial Fulfillment
of the Requirements for the Degree
Doctor of Philosophy

Approved April 2012 by the
Graduate Supervisory Committee:

Randall Cerveny, Chair
Nancy Selover
Anthony Brazel

ARIZONA STATE UNIVERSITY

May 2012

ABSTRACT

Isentropic analysis is a type of analysis that is based on using the concept of potential temperatures, the adiabatically established temperature at 1000 hPa. In the 1930s and 1940s this type of analysis proved to be valuable in indicating areas of increased moisture content and locations experiencing flow up or down adiabatic surfaces. However, in the early 1950s, this type of analysis faded out of use and not until the twenty-first century have some researchers started once again to examine the usefulness of isentropic analysis. One aspect in which isentropic analysis could be practical, based on prior research, is in severe weather situations, due to its ability to easily show adiabatic motion and moisture. As a result, I analyzed monthly climatological isentropic surfaces to identify distinct patterns associated with tornado occurrences for specific regions and months across the contiguous United States. I collected tornado reports from 1974 through 2009 to create tornado regions for each month across the contiguous United States and corresponding upper air data for the same time period. I then separated these upper air data into tornado and non-tornado days for specific regions and conducted synoptic and statistical analyses to establish differences between the two. Finally, I compared those results with analyses of individual case studies for each defined region using independent data from 2009 through 2010. On tornado days distinct patterns can be identified on the isentropic surface: (1) the average isentropic surface lowered on tornado days indicating a trough across the region, (2) a corresponding increase in moisture content occurred across the tornado region, and (3) wind shifted in such a manner to produce flow

up the isentropic trough indicating uplift. When comparing the climatological results with the case studies, the isentropic pattern for the case studies in general was more pronounced compared to the climatological pattern; however, this would be expected as when creating the average the pattern/conditions will be smoothed. These findings begin to bridge the large gap in literature, show the usefulness of isentropic analysis in monthly and daily use and serve as catalysts to create a finer resolution database in isentropic coordinates.

ACKNOWLEDGMENTS

I would like to first thank Dr. Randall Cerveny, committee chair, for his time, valued comments and support during this process as well as throughout my entire undergraduate and graduate career. Thanks as well to my other committee members, Dr. Nancy Selover and Dr. Anthony Brazel for their time and feedback on this dissertation. I would also like to thank Dr. Kimberly DeBiasse and Dr. Bohumil Svoma for their support and suggestions. Lastly, I would like to thank my parents Barbara and Richard Pace, for their support and encouragement throughout my entire educational career. Without any of the above mentioned individuals the completion of this dissertation would not have been as successful.

TABLE OF CONTENTS

CHAPTER Page

CHAPTER Page

Page

LIST OF TABLES

LIST OF FIGURES

Fig Page

Fig Page

Fig Page

Chapter 1

CLIMATOLOGICAL ISENTROPIC ANALYSIS IN TORNADO OCCURRENCE

a. Introduction

Isentropic analysis is a type of analysis that is based on using the concept of potential temperatures. Potential temperature is defined as the temperature of an air parcel that is brought down to 1000hPa of pressure through an adiabatic process (Holton 1992). Analysis of potential temperatures (or isentropes, often termed as such because potential temperature inherently conserves entropy) was found to be useful as mapping the elevations of a given isentropic surface indicates areas of flow up and down those adiabatic surfaces and also in displaying areas of moisture, since troughs (areas of lower heights/higher pressures) on isentropic surfaces are closely linked to higher moisture content (Namias 1938; Namias 1939). For a visual example, Fig 1.1 displays the 300K isentropic pattern for 12Z on March 19, 2012, with the solid lines indicating the pressure, in hPa, that the 300K potential temperature occurs and the shading displays the moisture content on the 300K surface, with the darker grey representing higher mixing ratio values.

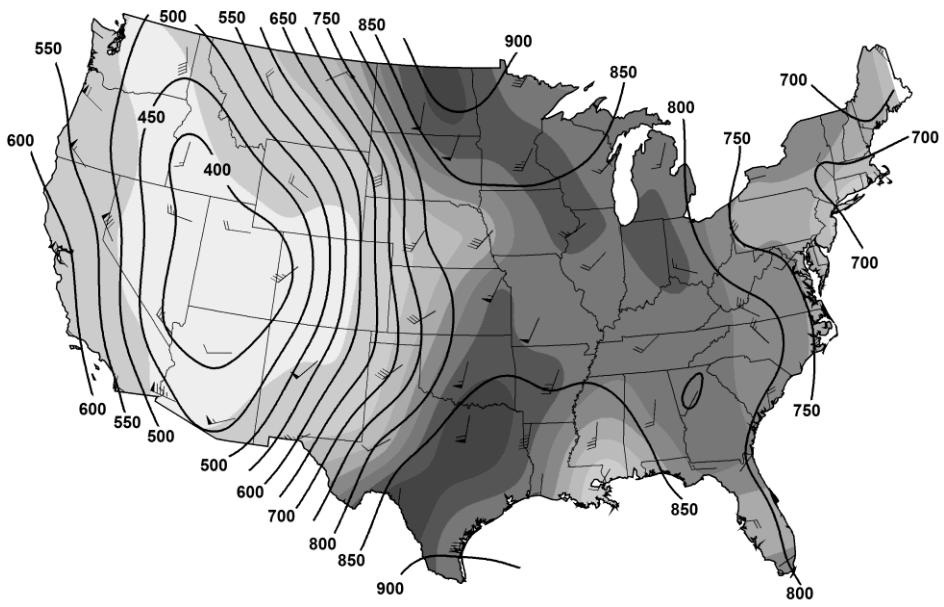

Fig. 1.1. 300K Isentropic map with solid lines representing the pressure at which the 300K potential temperatures occurs in hectopascals, shaded region displays mixing ratio (for that surface) with dark grey indicating higher mixing ratio value and wind speed and direction represented with traditional wind plots (for that surface).

In Fig. 1, a pronounced isentropic ridge exists over the western United States. Over the southern United States, especially over Texas and Louisiana, is an isentropic trough recognized by the high pressure values on the surface. The strongest flow oriented up the isentropic surface (indicating adiabatic uplift) is noted over Texas and Louisiana. Flow oriented down the isentropic slope (indicating adiabatic heating) is seen across the Texas panhandle and New Mexico. Lower mixing ratio values correspond to the isentropic ridge over the western United States and higher values within the isentropic trough over the southern United States. These parameters (e.g., adiabatic uplift) and variables (e.g., moisture advection), quickly identifiable with isentropic analysis as seen in Fig. 1.1, can supply forecasters with valuable information (de Coning 2000).

Consequently, isentropic analysis was once the primary forecasting tool around the time it was developed in the 1930s and 1940s. It first appeared in research by Sir Napier Shaw (1926) and was more fully developed in the 1930s by Byers, Namias and Wexler (e.g., Byers 1938; Pierce 1938; Namias 1938; Namias 1939; Wexler and Namias 1939; Namias 1940). However, while this type of analysis appeared to be promising in the mid to late 1940s, it began to fade out of use due to four main reasons: (1) the aviation community desired constant pressure charts, (2) fast computers to quickly conduct the analysis were not available, (3) a flaw in the Montgomery Stream function made isentropic analysis appear as though the flow on the surfaces were incorrect, and (4) isentropic data were not transmitted with the upper air observations (de Coning 2000; Saucier 1955).

As a result of these four main issues, isobaric (constant pressure surface) analysis became the primary analysis in daily forecasting. This also resulted in little, if any, research published with regard to isentropic analysis from the late 1940s through the twenty-first century resulting in a large gap in literature. Not until the twenty-first century did isentropic analysis start to gain more interest when de Coning (2000) examined precipitation in South Africa, Cerveny et al. (2011) re-examined Wexler and Namias' work from the 1930s, as well as examined the climatological isentropic patterns associated with drought conditions, and Balling et al. (2011) investigated trends in precipitation and the corresponding isentropic surface.

With this renewed interest in potential temperatures' climatic characteristics, isentropic analysis has begun to reprove itself as a useful forecasting technique to analyze vertical motion in the atmosphere and areas of moisture, both of which were discussed in the example above (Fig 1.1). With modern advances in meteorology and climatology over the past seventy years, including a denser network of upper air stations, faster computers, and the above mentioned atmospheric conditions easily identified on isentropic surfaces, more closely examining isentropic analysis with respect to severe weather could yield beneficial results for forecasters and possibly lead to isentropic analysis being brought back into daily use. Another broad-scale goal of this research in isentropic analysis is to serve as a catalyst to create a gridded database in isentropic coordinates such as is currently available for the isobaric coordinate system, in order to more closely analyze the small scale features on the given isentropic surfaces.

b. Problem Statement and Hypothesis

With prior research conducted in the 1930s and 1940s showing isentropic analysis being able to accurately indicate areas of moisture and vertical motion in the atmosphere (e.g, Shaw 1929; Byers 1938; Pierce 1938; Namias 1938; Namias 1939; Wexler and Namias 1939; Namias 1940), as well as noting the large gap in literature dealing with isentropic analysis, I set out to answer the following question: *to what degree does climatological (monthly) isentropic analysis, based on modern weather observations, show identifiable distinct patterns associated with the occurrence of tornadoes within the contiguous United States?*

With the above question in mind and examining the literature base, which will be reviewed in Chapter 2, my hypothesis is that the following features will be found on the isentropic surface during tornado events:

(1) A well-defined isentropic trough will be located across the given region experiencing tornadoes;

(2) With isentropic troughs linked to an increase in moisture, I also hypothesize that moisture will significantly increase in a region experiencing tornadoes;

(3) The wind direction on the given isentropic surface for a given region experiencing tornadoes will shift in a direction resulting in up sloping flow on the isentropic surface, meaning the flow would be from an area of high pressures (low heights) to low pressures (high heights) which would result in added lift in the atmosphere; and

(4) Wind speed will increase across a given region experiencing tornadoes which would result in added uplift as such an increase would be coupled with the switch in wind direction flowing up the isentropic trough.

c. Organization

In Chapter 2, I will examine prior literature dealing with isentropic analysis starting with Sir Napier Shaw's work in 1926 and ending at present time. This will result in a detailed timeline of the development and growth of isentropic analysis starting in the 1930s and 1940s, which quickly then turned into the demise of isentropic analysis in the 1950s up until around the turn of the twenty-

first century when additional work began emerging (de Coning 2000; Balling et al. 2011; Cerveny et al. 2011).

The study area, data used, and the methods I employed to conduct this research will be discussed in Chapter 3. This will include a detailed look at the quality controls used on the tornado data, rawinsonde data and include the statistical tests and mapping tools used.

Chapter 4 will examine the climatological patterns of the isentropic surface on tornado and non-tornado days. This will be completed using statistical tests and maps comparing non-tornado days and tornado days for each month for selected regions across the United States. Following these results, Chapter 5 will examine select tornado outbreaks for each of the fifteen regions discussed in Chapter 4. These case studies were created using an independent data set of tornadoes between 2010 and 2011. For each of the case studies, I first examined the overall isentropic pattern for the given day and then analyzed how that case study pattern was similar or different compared to the climatological isentropic pattern on tornado days for the given region.

This research will conclude with Chapter 6, in which I will summarize the results presented in Chapter 4 and 5, discuss future work that should be conducted based off the findings of this research and, finally, reiterate the significance of this research. However, to begin study of the significance of isentropic analysis in tornado occurrence, it is necessary to review the pertinent literature associated with isentropic analysis.

Chapter 2

LITERATURE REVIEW

a. Introduction

With the goal of enhancing the ability to forecast tornadic weather events, understanding the uplift within the atmosphere and moisture content are crucial. While constant pressure charts can depict where moisture is at certain levels within the atmosphere, the ability to view and forecast vertical velocities, as well as moisture transport, is almost non-existent. One forecasting analysis that shows both of these severe weather inducing features is isentropic analysis. Isentropic analysis is based on the concept of potential temperature, the temperature that a parcel of air would have if it were adiabatically positioned to 1000 hPa. As a result, I set out in this dissertation to answer the question: *to what degree does climatological (monthly) isentropic analysis, based on modern weather observations, show identifiable distinct patterns associated with the occurrence of tornadoes within the contiguous United States?*

My hypothesis for this question, based on prior research that will be discussed within this chapter, is the isentropic pattern will yield the following on tornado days:

(1) a well-defined isentropic trough will be located across the area experiencing tornadic events

(2) moisture will significantly increase in the selected region due to the isentropic trough

(3) the wind direction on the given isentropic surface will shift in a direction resulting in up sloping flow on the isentropic surface, meaning the flow would be from an area of high pressures (low heights) to low pressures (high heights) which would result in added lift in the atmosphere (4) wind speed will increase across the region which would result in added uplift as it would be coupled with the switch in wind direction flowing up the isentropic trough.

This chapter will be first structured in a chronological fashion when examining the history (development, decline, and slow rebirth) and research of isentropic analysis. Within the main section, specific comparisons about isentropic surfaces and constant pressure surfaces will be made to gain a better understanding about which analysis is useful for certain conditions. This section will conclude with some final remarks of the direction research in this area should turn based on the findings in the presented material.

Isentropic analysis, first drafted by Sir Napier Shaw (1926) and, later, more fully developed by Jerome Namias in the 1930s, was one of the first methods created once upper air data became available to the meteorological community within the United States. Several other methods were put into practice across the world as well, which included constant pressure charts, used by German meteorologists and a number of other European countries, and constant height charts which were being used by meteorologists within the United States (Bleck, 1973). With different agencies using varying methods, a desire to become more uniform across the meteorological community, as well as a push from the

aviation community to use constant pressure maps, the isobaric coordinate systems were put into daily practice and are still used today (Bleck 1973). While the overall community began to solely use this type of analysis, Namias, Rossby and a handful of other research meteorologists such as Byers, Pierce and Shaw, continued an attempt to set in motion the method of isentropic analysis by carrying out a number of research projects proving its ability to be a valuable forecast tool allowing the interpretation of the atmosphere in three dimensions (Byers 1938; Pierce 1938; Namias 1938; Namias 1939; Wexler and Namias 1939; Namias 1940).

The main advantage over any other analysis technique is that isentropic analysis allows the forecaster to view and understand the atmosphere in three dimensions, which is not possible using isobaric (constant pressure) charts. This allows for the visual clues of both down slope and up slope flow areas within the atmosphere, which can induce or hinder the development of precipitation/severe weather (Green 1966). The other major advantage, which will be discussed in detail below, is the ability to determine where moisture is being transported within an isentropic surface, possibly allowing for the ability to better forecast positioning of dry lines within the atmosphere. In fact, Benjamin (2004) as well as Johnson et al. (1993) found that when examining moisture and potential vorticity on an isentropic surface, it allowed for a more accurate depiction of where precipitation was occurring or would likely occur. They contributed this to the idea that a parcel is likely to stay on a given isentropic surface, meaning there is little cross-mixing between isentropic surfaces, whereas a given parcel will likely

pass through (leave) a surface of constant pressure. These two advantages serve as an initial basis for why isentropic analysis would be a helpful tool to be placed back into mainstream service.

b. Isentropic Analysis

Isentropic analysis is conducted by determining the potential temperature, which is the temperature a parcel of air would have if brought to 1000 hPa adiabatically, for a network of upper air stations. Potential temperature (θ) as derived from one of the three Poisson's relationships (Holton 1992), and can be expressed as:

$$\theta = T\left(\frac{p_s}{p}\right)^{\frac{R}{c_p}} \tag{2.1}$$

where T is ambient temperature (K), p_s is a standard reference pressure (100 kPa or 1000 hPa), p is pressure, R is the gas constant for dry air (287 J K^{-1} kg^{-1}), and c_p is the specific heat of dry air at constant pressure (1004 J K^{-1} kg^{-1}).

From the above calculation, a given potential temperature is chosen and the pressure levels associated with that potential temperature are plotted on a map with contour lines drawn in. Locations that have low pressure levels (higher heights) for a given potential temperature surface are termed "isentropic ridges", whereas locations with high pressure levels (lower heights) are called "isentropic troughs". In many cases, which will be discussed in the following sections, isentropic ridges are associated with colder temperatures and a drier atmosphere, whereas isentropic troughs are associated with areas of moisture and warmer temperatures (de Coning 2000). Plotting wind direction for the given isentropic surface allows the forecaster

to see if air flow is moving up or down the ridges/troughs, allowing for the determination of how much vertical motion is taking place, something that is not easily/directly interpreted off of a constant pressure chart.

Other elements to plot on isentropic maps that can be beneficial are mixing ratios, saturation vapor pressure, Montgomery stream flow, and isentropic potential vorticity for the given potential temperature surface. Each of these elements will be briefly outlined here and discussed further in forthcoming sections. Mixing ratio, which is the mass of water vapor to the mass of dry air (Saucier 1955), as well as the saturation vapor pressure, the pressure level at which saturation occurs (Saucier, 1955), allows for an effective way to observe areas of saturation as well as moist and dry air advection. Areas of saturation are easily determined when the saturation vapor pressure is added to the isentropic surface. Where saturation vapor pressure and the pressure of the given isentropic surface are equal, saturation is evident (Saucier, 1955). The Montgomery stream flow function is mathematically defined as: (Bleck 1973):

$$M = gz + c_p T \tag{2.2}$$

where g is the acceleration of gravity (9.8 ms^{-2}), z is the height (m) of the given isentropic surface. It is essentially the geostrophic wind on the isentropic surface and allows for the indication of flow on the given surface. Geostrophic flow above the surface is generally parallel to the isentropic pressure lines (Saucier, 1955). Plotting the isentropic potential vorticity (curl) is beneficial to identifying areas of

potential strengthening of upper and surface based low pressure areas (Hoskins 1985).

c. Creation and Interpretation of Isentropic Maps

The previous section discussed techniques regarding what isentropic analysis is mathematically (Equation 2.1 and 2.2) and elements to include on an isentropic surface. This section will discuss how an isentropic surface is created and how to interpret this type of analysis. This will be completed in three phases: (1) an examination into thermodynamic soundings, (2) linking the sounding to an isentropic surface, and, most importantly, (3) how to analyze the isentropic map.

i. Thermodynamic Sounding

The foundation of isentropic analysis is the thermodynamic sounding. With the information gathered from the sounding (temperature, dew point, wind speed and wind direction) throughout the atmosphere, the potential temperature can be derived for each hectopascal of the given sounding. It should be mentioned that for the analysis of isentropic surfaces to be conducted with the best results, the network of stations should be as dense as possible as Namias (1940) noted. Not only is a dense network of upper air stations beneficial but the thermodynamic soundings themselves should be of fine resolution (more than just the mandatory levels) so when the potential temperature is interpolated for each hectopascal the pressure gap between actual observed measurement is as small as possible. Additional information regarding interpolation of data between observed pressure levels is discussed in detail within Chapter 4.

Since the potential temperature, as defined by Equation 2.1, is simply the temperature an air parcel would have if brought down adiabatically to 1000 hPa it is rather straight forward to find a given potential temperature and pressure level at which that given temperature occurs. Fig 2.1 shows the location of the 315K potential temperature and the pressure level at which it occurs on the thermodynamic sounding. This was found by first, at 1000 hPa, finding the 315 K (~41.9°C) temperature and then rising adiabatically (dashed red line on Fig 2.1) until the environment temperature is reached. The pressure level at which that occurs, in this case approximately 810 hPa, is the location of the 315 K isentropic level for that given sounding. At that pressure level the wind direction, wind speed and mixing ratio would also be calculated for the given station to be used on the isentropic map.

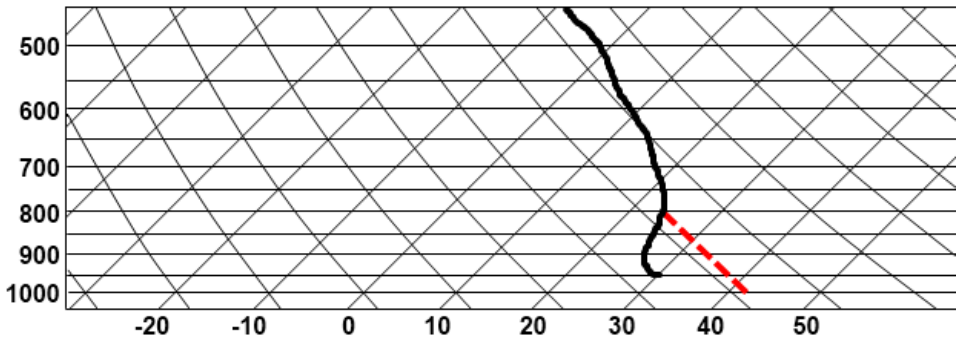

Fig. 2.1. Thermodynamic sounding showing environment temperature (black line) and the 315K potential temperature line (red). Note that the 315K level for this sounding is ~810 hPa.

The above discussed the basics of visually finding a specific isentropic pressure level using a thermodynamic sounding. For the study completed in the subsequent chapters, this procedure was done using Equation 2.1 to obtain an exact pressure

level for the given potential temperature. This process is carried out for every upper air station available (using a FORTRAN program discussed in Chapter 4) within the network and the isentropic map is created which will be outlined in the following section.

ii. The isentropic surface

Before anything else, the first aspect that needs to be determined prior to creating a given isentropic surface is what potential temperature is best suited for the analysis. When determining a proper isentropic surface it is necessary to choose a surface that is as close to the ground as possible without going below ground level across the study region. However, the surface should also be high enough off the ground that it is out of the surface boundary layer. Namias (1940) devised a table showing the best isentropic surface to be used in each season (Table 2.1). All these recommendations follow the underlying principle that with warmer temperatures a higher potential temperature surface is needed and with cooler temperatures a lower potential temperature needs to be used.

Table 2.1. Recommended isentropic level for each season (Namias 1940)

Season	Isentropic Level
Winter	290 – 295 K
Spring	295 – 300 K
Summer	310 – 315 K
Fall	300 – 305 K

After the proper isentropic level is selected, the isentropic map can be created. With the pressure levels for the given potential temperatures calculated from each thermodynamic sounding in the network, as briefly outlined in Section 2.c.i, and in more detail in Chapter 4, all that needs to be completed is the creation of the map. Along with the pressure level of the given potential temperature, wind direction, wind speed and mixing ratio are also plotted on the isentropic map.

iii. Interpreting the isentropic surface

Once the map has been created as discussed in the section above a detailed analysis of the surface can be completed. The first thing to note when examining an isentropic surface is the individual completing the analysis needs to reverse their frame of reference as compared to examining an isobaric map. The two most prominent features on an isentropic map are troughs and ridges. A trough is an area of high pressure values (low heights); whereas a ridge is an area of low pressure values (higher heights). Fig 2.2 shows an isentropic ridge axis from North Dakota down into Arizona and an isentropic trough axis from Louisiana up through Illinois. These are key features as isentropic troughs have been linked to moisture and isentropic ridges have been link to dry conditions (Byers 1938; Namias 1938; Wexler and Namias 1939; Cerveny et al. 2011). This is the case in Fig 2.2 as the highest mixing ratios are seen within the trough and the lowest values within the ridge. Examining the placement of the trough/ridge pattern as well as wind speed/direction can yield important information as well.

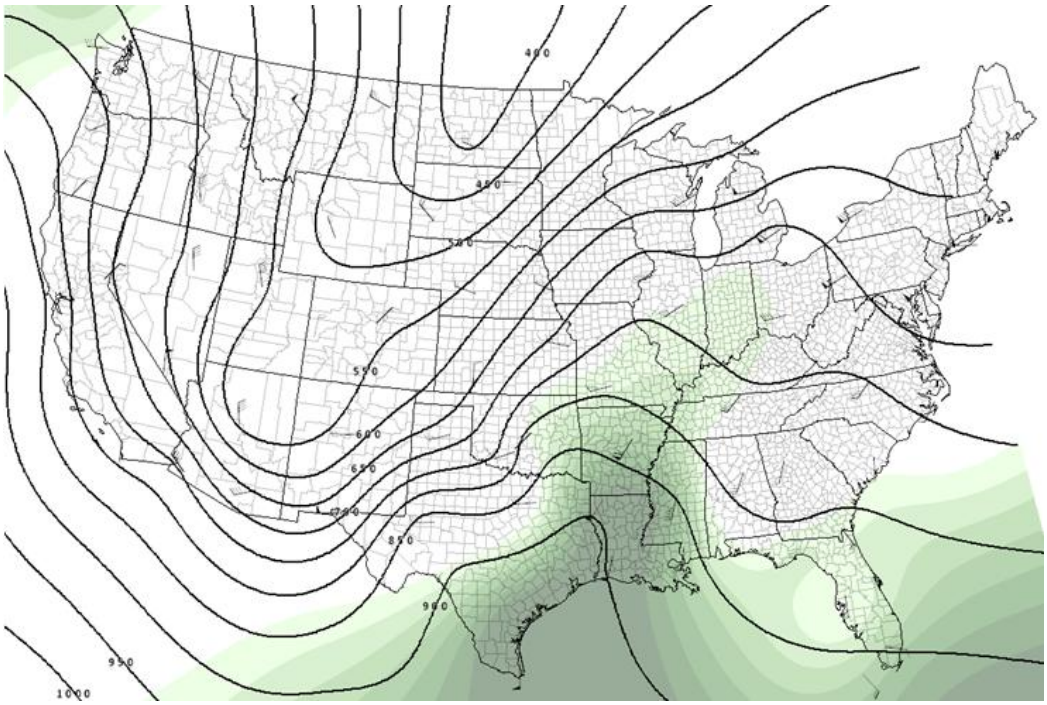

Fig. 2.2. 315K Isentropic map with solid lines representing the pressure at which the 315K potential temperatures occurs, shaded region displays mixing ratio with dark greens indicating higher mixing ratio value and wind speed and direction represented with traditional wind plots.

Wind direction and speed on an isentropic surface can indicate areas of upslope and down slope flow. Keeping in mind that a three dimensional picture of the atmosphere is obtained when examining an isentropic surface since the vertical flow can easily be seen. If winds are moving from an isentropic ridge (lower pressure/higher heights) into an isentropic trough (higher pressure/lower heights) this would indicate down sloping flow and potentially adiabatic warming as the parcels move down within the atmosphere. The reverse is true when wind is moving from an isentropic trough onto an isentropic ridge. In this case, air would be forced up into the atmosphere. In Fig 2.2 down sloping flow can be seen across Montana, Utah and Wyoming and upslope flow is noted across nearly the entire southeastern United States.

Not only can moisture flow and uplift be easily identified on an isentropic map but also nearness to saturation or areas of saturation can also be seen. If the saturation vapor pressure is plotted on the given isentropic map, where the saturation vapor pressure and pressure level of the isentropic surface are near or the same would indicate areas of saturation.

The aspects of analysis outlined in this section are the basic features to examine when conducting an isentropic analysis. These, as well as additional aspects, will be discussed in more detail within the subsequent sections of this Chapter and in Chapters 5 and 6.

d. The Beginning

The first mention and use of isentropic analysis was by Sir Napier Shaw (1926); however, with an extremely limited number of upper air stations, in-depth research did not begin until the late 1930s. The main ideas of isentropic analysis were developed through research by Namias, Rossby and Wexler, with Rossby focusing his study on two themes: (1) to study how large scale air currents moved across large regions; and (2) to investigate the flow of moisture across large regions (de Coning, 2000). With these goals in mind, Namias, Rossby and Wexler embarked to research isentropic analysis to create both long-term and short-term forecasts. Namias, in the mid to late 1930s, conducted numerous research projects using isentropic analysis; however, in the 1930s collection of upper air data was just beginning to commence. Consequently, the analyses he could apply were limited due to the lack of a network of stations spaced fairly evenly apart from one another. Indeed, both Namias and Rossby discovered that a denser network of upper air

stations was needed and the frequency of observations markedly increased to obtain more accurate representation of the atmosphere (Namias 1939). While Namias was surprisingly successful in his findings using isentropic analysis with only having thirty stations, there appears to be a potential improvement to his work through reexamination of his analyses using sixty plus upper air stations recording twice a day that are currently available (Cerveny et al. 2011). Such an improved network in turn, as Namias mentioned, gives an even better representation of the atmosphere, possibly allowing the type of analysis to gain more credibility as a useful forecasting tool.

With a continued motivation to promote isentropic analysis as a forecast tool, from 1938 through 1940, Namias, Byers, and Wexler produced numerous articles regarding how isentropic analysis could successfully be used in analyzing/forecasting different weather phenomena. In 1938, Namias researched isentropic analysis and short-term forecasting and discovered some interesting comparisons between isentropic analysis and constant pressure charts. He found that isentropic surfaces gave a more detailed and accurate representation of the actual state of the atmosphere compared to surface charts and tephigrams (a type of vertical thermodynamic diagram), which are used to view raw sounding data (Namias 1938). This was a promising finding for these early days of forecasting inspiring Namias to conduct a case study in which he forecasted precipitation first by using only surface maps and tephigrams and then forecasted for the same time period where rainfall should occur based on isentropic analysis. The major finding from his case study was identifying that upper level mechanisms initiated rainfall,

depicted by the isentropic maps and not surface maps. It should be noted that Namias was comparing the surface maps to isentropic maps, which meant the isentropic maps were the only maps examining the upper atmosphere. To enhance this case study, and to further validate the usefulness of using isentropic analysis, it would have been worthwhile to also analyze the constant pressure charts during the time period to show the strengths and weakness of both analysis tools.

With the successful introduction of isentropic analysis displayed by Namias, in 1938 Byers discussed the thermodynamics behind isentropic charts, which continued to show how isentropic analysis can be employed as a successful forecast tool (Byers 1938). He was able to show several key points that set isentropic maps apart from constant pressure charts, which included: (1) moisture content and flow is depicted more accurately compared to constant pressure charts, (2) isentropic charts allow the forecaster to easily tell the nearness to condensation, and (3) areas of condensation can be displayed directly off the map if condensation pressure is presented (Byers 1938).

One of the other major findings that Byers' (1938) research identified was the ability to determine where areas of instability and stability were located by taking the pressure level where the 295K potential temperature occurred minus the pressure at which the 299K potential temperature occurred. Areas that had a greater pressure difference were areas of greater instability (Byers, 1938). Byers was convinced of this possibility and stated, "There appears to be no reason why the type of charts advocated here is not preferable for practically all uses, and if only one chart is drawn in daily synoptic practice, the one recommended here is

distinctly preferable" (p. 68). As Byers' study showed, isentropic analysis remains worthwhile to research in the present day with regard to forecasting severe weather. With positive results from short-term forecasting using isentropic analysis, in 1939 Wexler and Namias began dealing with the idea of long-term analysis of precipitation using monthly mean isentropic surfaces. To do this they calculated the mean isentropic values for the month of August for the years 1934, 1935, 1936 and 1937 and compared those maps with departure from average rainfall maps across the United States. They noted that areas of high isentropic heights matched closely with areas of drought; while in contrast, areas of low isentropic heights were closely matched with areas of above normal precipitation (Wexler and Namias 1939). Since this is simply comparing the analysis technique to an observed condition, rainfall, it is possible that this study could be updated so that isentropic analysis can be used in long range forecasting for pattern recognition. Associated with this study, Namias established that isentropic eddies can form and dramatically change the moisture content throughout an area (Namias 1938).

These two correlated studies (Wexler and Namias 1938; Namias 1938) reveal, once again, that even when the network of upper air stations is rather sparse, and the length of record is small, a reasonable pattern could be discerned within the isentropic maps that can be correlated to the relative abundance of rainfall across a region. Similar to the prior study referenced, no comparison was made to the constant pressure charts that were being used at the time. However, moisture flow on constant pressure charts does not show up as prominently, as moisture is not likely to remain on a constant pressure surface. As a result, the correlation of a

constant pressure surface, e.g., 500 hPa pattern, and rainfall is not likely to be as noticeable as with isentropic analysis.

With the findings in the studies mentioned above, and use of isentropic charts on a regular basis across the United States, by the early 1940s, this type of analysis was promising as a long-term and short-term forecasting tool (Namias 1940). However, with the start of World War II there was a push from the aviation community to adopt the more widely used forecast tool of constant pressure charts. With this desire from the aviation community the 1940s time period was the beginning of the end for isentropic analysis, at least until the 1960s (de Coning, 2000). In fact, isentropic data were no longer transmitted after 1945, which, when combined with the lack of computing power, made the calculations even more time consuming. (Saucier 1955).

e. The Decline of Early Isentropic Analysis

With isentropic analysis leading the way into the 1940s with research and use in daily forecasts, isentropic analysis's future was bright; however, in the mid-1940s several conflicting factors came into play. Four main factors halting the progress of isentropic analysis were (1) the lack of fast computers, (2) the occurrence of World War II leading to an increase in the needs of aviation weather, (3) a flaw in the calculations originally done regarding the Montgomery stream function (de Coning, 2000), and (4) isentropic data were no longer transmitted within upper air weather observations (Saucier, 1955).

The calculations that needed to be computed for potential temperature as well as any moisture or vorticity variable that needed to be displayed on the isentropic

maps was laborious in nature and, with limited computers, creating maps was often time consuming, resulting in slow forecasting. This was one of the main disadvantages that limited the usefulness of isentropic analysis as a short-term forecast tool in the 1940s. The aviation community during World War II, one of the largest users of weather-related products, heavily pushed for the switch from isentropic maps to constant pressure charts, as pilots dealt with altimeters, which are solely based on pressure. Also, the incorrect calculation of the Montgomery stream function was being used. Instead of interpolating the values g and z (equation 2.2) at the same time they were interpolated separately, which was found to cause an error in the Poisson's relationships (Bleck, 1973). Due to this error resulting in isentropic geostrophic flow being represented incorrectly, some researchers simply believe the basic flow principles would not work on an isentropic surface. This in turn pushed them further away from the analysis technique altogether (Bleck, 1973).

With the three factors mentioned above, slow computers, the aviation community, and an incorrectly derived equation, isentropic analysis was phased out as a real-time technique employed in forecast analysis and was replaced with what is currently used today, isobaric (constant pressure) charts. Following this operational judgment, little, if any, research was done regarding the analysis until the 1960s when computers became faster, the Montgomery stream function was corrected, and there were more stakeholders outside of the aviation community that required short-term and long-term forecasts.

f. The slow rebirth in the 1960s to present

After a twenty-year gap in research from the demise of early isentropic analysis in the early 1940s, researchers began to reexamine isentropic analysis as a reliable forecast tool. The main reason for the rebirth of research in this area was due to three developments: (1) the correction in the Montgomery stream flow function (Danielsen, 1959), (2) faster computers were becoming available, and (3) the need for more accurate forecasts were being required for many additional organizations other than aviation. Also, researchers saw the changing ideology and need to forecast the actual weather (pressure patterns in the atmosphere) as compared to what had been done up to this point which was simply forecasting the pressure for a given location (Reed and Danielsen, 1960). Such a shift would require forecasters to examine the atmosphere in three dimensions, as is possible with isentropic analysis.

With the suggestions by Danielsen (1961), calling for isentropic analysis to be brought back into practice to forecast the actual weather, one of the first studies to emerge from the lull in the interest of isentropic analysis was by Green (1966), dealing with the flow on an isentropic surface. This paper was primarily based around the idea of trajectory set forth by Danielson (1961) in which he found that computing isentropic vs isobaric trajectory yielded strikingly different results. Because of these large deviations, it was found that isentropic analysis was a far better means of showing the true movement of water vapor as well as other gases, with Reiter (1963) even examining the flow of radioactive material using isentropic surfaces. Just as discussed in the early research by Namias and Wexler, Green (1966) and Danielson (1961) also concluded that isentropic analysis shows the

overall flow of the atmosphere in a more accurate way compared to that of constant pressure charts. Green also noted that, with isentropic analysis, a given parcel could be traced from day to day, adding to the accuracy of distinguishing how areas within the atmosphere have been, or will be, influenced through time.

Shortly after Green's (1966) research, Tubbs (1972) published on isentropic analysis and focused on summer thunderstorms over southern California. When examining the amount of moisture in the area that could produce thunderstorms, Tubbs turned to the early work by Namias and Wexler regarding moisture transport. As a result, Tubbs created isentropic maps for the time frame of interest and found that an isentropic tongue of moisture would shift in and out of California (Tubbs 1972) resulting in increased or decreased precipitation events. This, yet again, shows that isentropic analysis is a useful tool in showing moisture. An interesting note is when Tubbs discussed anything dealing with moisture, the analysis of constant pressure charts was not used, but instead he turned to isentropic charts for the answer.

Other researchers utilized the concept of potential temperature being an adiabatic process, Mitchell (1967) dealt with dividing the western United States into climate regions based on areas with similar potential temperatures. His findings suggest that the classification by potential temperature is far more accurate in representing air mass boundaries compared to the traditional Köeppen and Thornthwaite method (Mitchell 1967). While not dealing with isentropic analysis completely, this shows that potential temperature, which is used in this analysis, is a conservative property, and elevation does not affect it.

Another groundbreaking study into the practicality of isentropic analysis involved atmospheric blocking conditions (Crum and Stevens 1987). An atmospheric blocking pattern, which is the presence of a large stationary ridge, can lead to devastating droughts in one region and an abundance of rain in another, so predicting these occurrences with accuracy allows for further preparedness. In their examination, Crum and Stevens (1987) were focusing on isentropic potential vorticity, which they speculated is a large factor in the block setting up.

It should be noted that Crum and Stevens (1987) mentioned isentropic analysis as an effective tool to use for potential vorticity compared to constant pressure charts. With isentropic surfaces there is no need to calculate vertical velocity when calculating the vorticity equation; however, with constant pressure charts calculating vertical velocity becomes a daunting task as constant pressure charts do not easily display vertical flow. After examining the potential vorticity, they found that the block developed and continued to remain in an area of low potential vorticity (Crum and Stevens, 1987). This was a useful finding, as it demonstrates that isentropic analysis can be used for moisture, upslope/downslope flow, and potential vorticity in order to determine where large ridges of high pressure may develop.

An earlier study also dealing with isentropic potential vorticity by Hoskins et al. (1985) showed additional functionality of isentropic analysis. In this study the authors found that examining vorticity on the isentropic surface can add to the understanding of how low pressure systems, both at the surface and aloft, will develop/deepen within areas of high potential vorticity. They concluded it was

advantageous to use isentropic potential vorticity versus potential vorticity on an isobaric surface as the vertical motion of the potential vorticity could be effortlessly seen by examining the flow.

Most recently published research dealing with isentropic analysis is being carried out in South Africa. In 2000, de Coning studied how isentropic analysis can be used as an operational forecast tool in South Africa. In conducting a number of case studies, de Coning discovered that the transportation of moisture is more clearly evident on an isentropic chart than on isobaric charts. She also determined that parcels of air will normally stay on the same potential temperature surface so forecasters are able to plot a time series showing a parcels movement resulting in a better ability to make short term forecasts (de Coning, 2000). After completing the case studies under consideration, de Coning found that isentropic analysis was indeed a beneficial way to forecast precipitation due to the ability to easily track moisture, verifying work done by Namias and Wexler in the 1930s.

Cerveny et al. (2011) have also carried out work dealing with isentropic analysis. Their work primarily reevaluated research conducted by Wexler and Namias in the 1940's, by utilizing a denser network of upper air stations presently available. The three major findings with this work included: (1) reinforced the idea that moisture flowed up isentropic troughs and dry air existed in areas of isentropic ridges, (2) demonstrated the prominence of the isentropic trough (moisture tongue) associated with the North American Monsoon, allowing the visual clue as to where the moisture source is located, and, most importantly, (3) an isentropic wave was noted over the Great Plains, correlating to the area of highest tornado density.

So far this discussion of isentropic analysis has identified mostly positive attributes that this analysis possesses; however, it is also important to look at some of the disadvantages that come with using isentropic analysis. De Coning (2000) identified some of the most noted disadvantages which include: (1) the proper potential temperature surface must be chosen, and (2) the forecaster needs to think outside of the pressure coordinate system, which has been, and is still, the preferred coordinate system since the early 1940s.

De Coning 's first point is that a good isentropic surface should not intersect the ground but be close enough to the ground to obtain near surface conditions (de Coning, 2000). The issue with this, theoretically, is that the isentropic surface that can be used in one season cannot necessarily be used in others due to temperature changes. In warmer seasons, higher potential temperature surfaces need to be employed, while in cooler seasons a lower potential temperature surface can be used. Table 2.1 suggests the following isentropic levels for each season based on Namias (1940). With the need to adjust the potential temperature level used, based on surface temperature, from a forecaster's standpoint, it might be found that selecting a proper level may be too time consuming to produce a short term forecast. Conversely, it might be beneficial to use a selection of potential temperature levels in order to gain a full picture of the entire atmosphere. At present, I have not discovered any research that dealt specifically with the best way to determine the potential temperature to use, and whether or not using potential temperatures that occur further from the surface are actually better. This is an idea that will require additional study to completely fulfill the purpose of this research.

De Coning ’s second potential disadvantage of having the forecaster think outside the pressure coordinate system could be addressed through practice. Once forecasters became accustomed to switching between the pressure coordinate system and the potential temperature coordinate system, it may be found that forecasters have a better understanding of the overall structure/workings of the atmosphere. For this to be verified, the first step is to attempt to have isentropic analysis rejoin the group of regularly used tools.

g. Conclusions

A specific subject matter not fully considered in the research discussed above is the use of isentropic analysis in severe weather forecasting, particularly tornadic episodes. With a denser network of stations now present across the United States, it may also be highly advantageous to reexamine work done in the 1930s by Namias and Wexler to determine if additional information can be deduced from their studies to aid in forecasting severe weather. For example, to see if a more in-depth examination of eddies, which Namias originally found in 1938, within the isentropic flow may yield using a higher resolution dataset. This may result in the finding of even smaller eddies which could enhance or decrease the amount of rain or severe weather a location might experience.

With the articles presented above, it is plausible that severe weather events could be more accurately forecasted using isentropic analysis versus the current constant pressure charts and would be a beneficial endeavor to undertake. As mentioned, with numerous studies being conducted in the 1930s and, then again, in the 1960s regarding moisture transport on isentropic surfaces, it seems necessary to delve

back into isentropic research during the current time period now that a denser network of upper air stations is in place. With isentropic analysis, being a widely used tool in the 1930s, it is well worth the research to discover how this type of analysis can further enhance both long-term and short-term forecasting of severe weather events. The goal of this research is to take all the varying aspects of isentropic analysis discussed in this chapter and discover the distinct patterns associated with the isentropic surfaces on tornado days across the contiguous United States. In doing so, all companies, organizations, and the public that rely on accurate severe weather forecasts will be better aided.

To assess the hypothesis outlined in this chapter long-term and short-term databases will need to be utilized in order to examine both the climatological and meteorological aspects of forecasting tornadoes using isentropic analysis The following chapter will outline these data sources used to create the isentropic maps as well as the severe weather database which was employed to determine specific dates and time frames to be used in the analysis.

Chapter 3

STUDY AREA, DATA AND METHODS

a. Introduction

The previous chapter examined literature associated with isentropic analysis and its ability to be used as a forecast tool. One of the key findings is that precipitation and moisture flow using isentropic analysis has yielded beneficial results (Byers 1928; Pierce 1938; Namias 1938; Namias 1939; Wexler and Namias 1939; Namias 1940). This is mainly due to the fact that isentropic analysis represents a three-dimensional view of the atmosphere compared to that of constant pressure charts. By plotting winds on the given isentropic surface, up-sloping and down sloping flow can easily be recognized. However, even with these results, no examination of patterns on isentropic surfaces associated with severe weather events has been conducted. With this sizeable gap in literature and isentropic analysis already found to be a useful tool with some aspect of forecasting, this dissertation is designed to determine what patterns exist on the isentropic surface that are associated with tornado occurrences across the contiguous United States

This chapter will outline how the research question presented in chapter one was conducted, which was: *to what degree does climatological (monthly) isentropic analysis, based on modern weather observations, show identifiable distinct patterns associated with the occurrence of tornadoes within the contiguous United States?* This chapter will be broken into the following sections: (1) defining the study area in general as well as how the study area was broken

into smaller regions in order to more closely examine the usefulness of isentropic analysis within certain parts of the country, (2) discussion of tornado data used, (3) analysis of the upper air (radiosonde) data employed to create the isentropic maps and carry out statistics on given stations, (4) analysis techniques in both the visual and statistical sense, and (5) case study selections.

To determine the usefulness of isentropic analysis with regard to tornadoes, this dissertational research was accomplished in two separate steps. The first involved determining climatological patterns with respect to isentropic level, mixing ratio, wind direction, and wind speed. Once I had determined the significant variables and patterns through visual examination of isentropic maps as well as statistical tests, those parameters were examined in a number of case studies using an independent dataset to verify the results.

b. Study Area and Defining Smaller Regions

To examine the usefulness of isentropic analysis in forecasting tornado events within the United States the study area examined incorporates the conterminous United States. At times, the study area was reduced to specific regions to obtain a more detailed image of the synoptic pattern associated with severe events; however, the conterminous United States was still required for analysis to determine what may potentially advect into a given region. This size study area was also needed in order to determine if isentropic analysis could be used throughout varying regions of the United States. Within the study region, sixty-two upper air stations were available (Fig 3.1). A more in-depth examination of upper air data will be made in the following section; however, it

should be noted here that not all stations mapped in Fig 3.1 were used in each case as the station had to have at least 70 percent of data for the given time period to be used.

Fig. 3.1. Map of the study region with black dots indicating the locations of the sixty-two available upper air stations.

While tornadoes occur in different regions throughout the year within the United States, analyzing different tornado regions for each month is crucial in determining if isentropic analysis is beneficial in forecasting severe weather events. For this dissertational research, every month throughout the year had at least one smaller region defined across the United States in order to more specifically focus on the most dense tornado region for the given month. To define these smaller tornado regions, all tornado reports between the years of 1974 and 2009 were mapped and a density plot for tornadoes per 100 square miles was created for each month. From these density maps/data the density had to be four standard deviations from the mean or greater to be considered a region. Using four standard deviations from the mean allowed two things: (1) the ability

to straightforwardly detect where the highest density of tornadoes occurred in each month since 99.9 percent of the densities should be within four standard deviations of the mean thereby permitting the extreme density cases to clearly stand out, and (2) the creation of regions that were small enough to geographically analyze, as selecting too large of regions could result in the masking of potentially important variables and patterns that might counteract one another on opposite sides of a large region .Most months had only one well-defined region of high density of tornado events, while three months had two well-defined areas of tornadoes. It should also be noted that I required at least one upper air station in each region in order to have upper air data representative of the conditions within the defined region. Fig 3.2 shows the location of each region for every month as well as the shading indicating the areas where density was four standard deviations from the mean. There was slight cartographic license in drawing the borders of each region to ensure, first and foremost, that the maximum numbers of stations were within a given region while also maintaining the densest area of tornadoes. Table 3.1 displays the regions for each month, the number of tornado reports for the given region, the number of days between January 1974 through December 2009 that tornadoes occurred within that region, and the upper air stations located within each area.

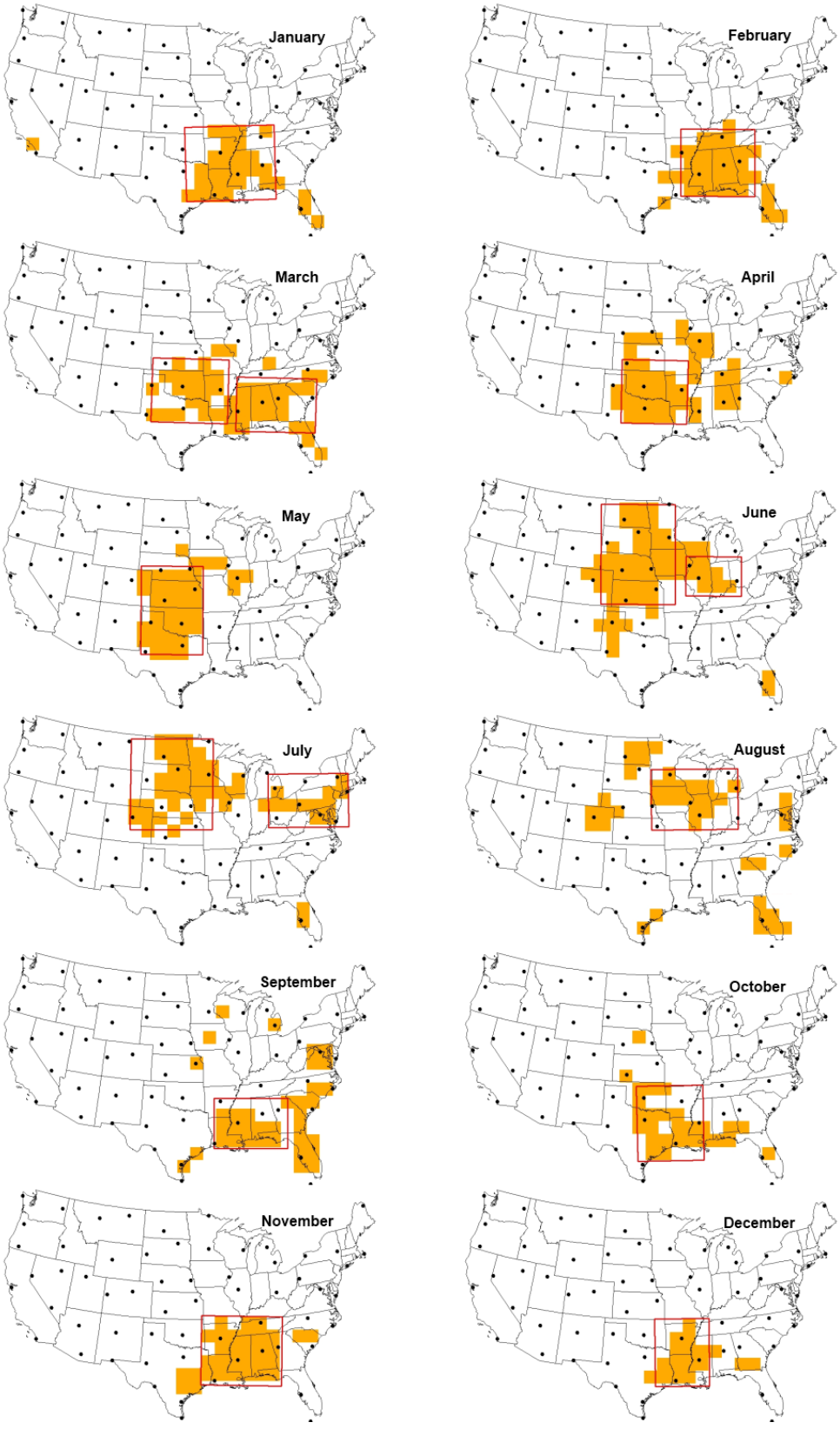
January
February
March
April
May
June
July
August
September
October
November
December

Fig. 3.2. Red boxes indicate the region(s) for each month with yellow shading indicating areas where tornado density was four standard deviations from the mean, with black dots indicating the upper air station.

Table 3.1. Region characteristics for each month including the month, region number, number of tornado reports, number of tornado days, and station locations/WMO numbers within the region.

Month	Area	# of Reports	# of days	Upper Air Stations
January	1	583	100	Lake Charles, LA: 72240 Little Rock, AR: 72340 Jackson, MS: 72235 Shelby, AL: 72230 Nashville, TN: 72327
February	1	471	95	Little Rock, AR: 72340 Jackson, MS: 72235 Shelby, AL: 72230 Nashville, TN: 15672327 Peachtree City, GA: 72215
March	1	714	156	Little Rock, AR: 72340 Ft Worth, TX: 72249 Amarillo, TX: 72363 Norman, OK: 72357 Dodge City, KS: 72451
March	2	417	162	Jackson, MS: 72235 Peachtree City, GA: 72215 Shelby, AL: 72230 Charleston, SC: 72208
April	1	1438	249	Little Rock, AR: 72340 Ft Worth, TX: 72249 Norman, OK: 72357 Dodge City, KS: 72451
May	1	3355	490	Ft Worth, TX: 72249 Amarillo, TX: 72363 Norman, OK: 72357 Dodge City, KS: 72451 Topeka, KS: 72456 Omaha, NE: 72558 North Platte, NE: 72562 Midland, TX: 72265

Table 3.1 (continued)

June	1	2981	552	Dodge City, KS: 72451 Topeka, KS: 72456 Omaha, NE: 72558 North Platte, NE: 72562 Rapid City, SD: 72662 Aberdeen, SD: 72659 Bismark, ND: 72764 Chanhassen, MN: 72649
June	2	653	178	Davenport, IA: 74455 Lincoln, IL: 7456 Wilmington, OH: 72426
July	1	2665	515	Dodge City, KS: 72451 Topeka, KS: 72456 Omaha, NE: 72558 North Platte, NE: 72562 Rapid City, SD: 72662 Aberdeen, SD: 72659 Bismark, ND: 72764 Chanhassen, MN: 72649 Denver, CO: 72469
July	2	602	218	Wilmington, OH: 72426 White Lake, MI: 72632 Pittsburgh, PA: 72520 Buffalo, NY: 72528 Albany, NY: 72518 Upton, NY: 72501 Sterling, VA: 72403
August	1	567	217	Topeka, KS: 72456 Omaha, NE: 72558 Chanhassen, MN: 72649 Davenport, IA: 74455 Lincoln, IL: 74560 Wilmington, OH: 72426 White Lake, MI: 72632 Green Bay, WI: 72645 Gaylord, MI: 72534

Table 3.1 (continued)

September	1	402	84	Lake Charles, LA: 72240 Little Rock, AR: 72340 Jackson, MS: 72235 Shelby, AL: 72230 Peachtree City, GA: 72215
October	1	511	114	Lake Charles, LA: 72240 Little Rock, AR: 72340 Jackson, MS: 72235 Ft Worth, TX: 72249 Norman, OK: 72357
November	1	845	138	Little Rock, AR: 72340 Jackson, MS: 72235 Shelby, AL: 72230 Nashville, TN: 72327 Peachtree City, GA: 72215 Lake Charles, LA: 72240
December	1	379	81	Little Rock, AR: 72340 Jackson, MS: 72235 Lake Charles, LA: 72240

c. Tornado Data

To examine the density of tornadoes across the United States and to find dates with significant tornado events to be examined for case studies, I collected tornado reports from the Storm Prediction Center Warning Coordinator Meteorologist site (Storm Prediction Center, 2011). The tornado reports were in comma delimited format and included a number of attributes including year, month, day, time, f-scale, start latitude, start longitude, end longitude, fatalities, damage, states impacted, counties impacted, path length and number of segments but for this study only the year, month, day, time, f-scale, start latitude, and start longitude were used. A sample of the raw output for each report can be seen in Fig 3.2. While length of path and tornado width would be of interest to study, the

goal of this research is to introduce isentropic analysis into forecasting severe weather and serve as a catalyst to further examine these types of variables. Also, these types of variables were only available for large tornadoes and for only the most recent years. These particular reports use the Fujita scale and not the more recently created enhanced Fujita scale (Doswell and Brooks 2009). As a result, throughout the rest of this study, the Fujita scale will be used.

In	Year	month	day	Date	Time	TZ	State	State_Fips	State_Count	F_Scale	Injuries	Fatalities	P_Loss	C_Loss	Lat_Start	Lon_Start	End_Lat	End_Lon	Length_Miles	Width_Yards
171567	2009	5	13	5/13/2009	16:52:00	3	KS	20	0	0	0	0	0	0	38.2921	-95.6327	38.292	-95.633	0.1	25
171574	2009	5	13	5/13/2009	17:00:00	3	KS	20	0	0	0	0	0	0	38.2696	-95.5289	38.27	-95.529	0.01	25
158827	2009	5	13	5/13/2009	17:55:00	3	KS	20	0	0	0	0	0	0	37.2976	-96.6361	37.297	-96.621	0.81	75
175772	2009	5	13	5/13/2009	18:20:00	3	KS	20	0	1	0	0	0.1	0	37.9437	-95.0702	37.849	-94.872	12.62	300
158830	2009	5	13	5/13/2009	20:49:00	3	KS	20	0	0	0	0	0	0	37.0086	-95.0774	37.009	-95.073	0.26	50
159705	2009	5	15	5/15/2009	15:57:00	3	KS	20	0	0	0	0	0	0	37.75	-97.8	37.743	-97.79	0.76	50
159706	2009	5	15	5/15/2009	16:31:00	3	KS	20	0	0	0	0	0	0	37.66	-97.61	37.661	-97.604	0.36	50
159709	2009	5	15	5/15/2009	16:58:00	3	KS	20	0	0	0	0	0	0	37.42	-97.9	37.42	-97.872	1.52	75
159711	2009	5	15	5/15/2009	17:25:00	3	KS	20	0	0	0	0	0	0	37.36	-97.61	37.361	-97.605	0.3	50
164044	2009	5	25	5/25/2009	13:45:00	3	KS	20	0	0	0	0	0	0	38.6117	-101.92	38.612	-101.92	0.25	20
551	2008	5	1	5/1/2008	17:50:00	3	KS	20	0	0	0	0	0	0	37.36	-96.18	37.37	-96.17	0.7	50

Fig. 3.3. Sample of the attributes associated with the tornado reports collected from the Storm Prediction Center Warning Coordinator Meteorologist site (http://www.spc.noaa.gov/gis/svrgis/).

I collected reports from 1940 through 2009; however, only the time period of 1974 through 2009 were utilized as prior to 1970 a number of tornado reports were incomplete. To quality control these reports, I constructed a FORTRAN program that ensured the F-scale was not missing and that there were no duplicate reports which could alter the density maps that were used to create the region as was discussed in the above section. For use in the independent case studies, the same data source was used; however, tornadoesfrom 2010 to 2011 were utilized.

d. Radiosonde Data

In order to create isentropic patterns and datasets to be analyzed for this dissertation, I acquired raw radiosonde data from the CD-ROM "Radiosonde Data of North America 1946-1996" produced by Forecast System Laboratory, supplemented with data between the years of 1997 through 2010 using data

supplied online via National Climatic Data Center (Forecast Systems Laboratory 1997). For this dissertational research, sixty-two upper air stations were utilized (Fig 3.1). Not all sixty-two upper air stations were used in each analysis. If, for a given time frame, the station was missing more than 20percent of its data, it was not used. For this dissertation, I only employed 12Z soundings for analysis as my goal was determine the pattern associated with tornadoes with regard to forecasting and the morning12Z soundings would be what forecasters would utilize to produce their initial daily forecasts. While the spatial extent of this network of upper air stations is indeed more dense compared to that of other work done in the past (Namias, 1938; Namias, 1939; Wexler and Namias, 1939; Namias 1940), it would be beneficial to have an even denser network of stations to fine-tune minor disturbances within the pattern even further, such as data sources like NCEP/NCAR or other model output sources currently available for mandatory pressure levels. Unfortunately, these types of gridded data sources simply do not currently exist for isentropic analysis.

The NCEP/NCAR Reanalysis Dataset only has the mandatory pressure levels which are spaced too far apart vertically for any interpolation between layers (Kalnay et al., 1996). The European Center for Medium range Weather Forecasting (ECMWF) does have an isentropic analysis output; however, it is only for 300K and 315K levels and for this research the 300K, 305K, 310K and 315K all need to be analyzed in order to gain a full picture of the atmosphere (ECMWF, 2011). Using ECMWF for the research would mean for part of the study time frame the 300K surface would be under the ground and the 315K

would be of too high an altitude to gain a proper depiction of near surface conditions. With this lack of gridded data, as noted above, research was conducted using raw (non-gridded) radiosonde data. One of the goals of this research, aside from discovering another forecasting tool for tornadoes, is to eventually create a gridded isentropic surface database such as is presently available for constant pressure charts.

Since raw radiosonde data were used, I had to undertake a number of steps to actually create a given isentropic surface. I first had to collect the RAOB data for each station across the United States in FSL Original Format. These data include pressure level, height, temperature, dew point, wind direction, and wind speed. To take these data and turn them into an output file suitable for mapping and calculating additional variables for the isentropic analysis, I then constructed a FORTRAN program. This program had multiple purposes as described below:

(1) A quality check was run on each sounding used. This ensured that the sounding reached at least 300 hPa and that the missing data did not compose more than ten percent of the sounding.

(2) Using trigonometric functions as seen in equation 3.1 and 3.2, where *d* is the wind direction in radians and *s* is the wind speed, I broke the wind direction into U and V components in order to obtain an accurate lapse rate which will be discussed in Step 5.

$$U = \cos(d) * s \tag{3.1}$$

$$V = \sin(d) * s \tag{3.2}$$

(3) The temperatures were converted to Kelvin.

(4) I converted the dew point into mixing ratio in units of grams/kilogram in two steps. The first step was to calculate the vapor pressure as defined by equation 3.3, where *e* is the vapor pressure and *D* is the dew point in Celsius. After that was completed, the mixing ratio could be determine using equation 3.4 where *w* is mixing ratio, *e* is the vapor pressure and *p* is the pressure in hectopascals (National Weather Service, 2010)

$$e = 6.11 * 10^{\frac{7.5 \cdot D}{237.7+D}} \tag{3.3}$$

$$w = 621.97 * \frac{e}{p - e} \tag{3.4}$$

(5) Algorithms created within the program calculated for each hectopascal, from the surface to the top of the given sounding, temperature (in Kelvin), mixing ratio, wind speed, and wind direction. To do this, the program used two pressure levels within the sounding, computed the pressure difference and calculated a lapse rate for each of the variables found above. Using the lapse rate, the algorithms determined the meteorological conditions, at each hectopascal between the known pressure levels, including the potential temperature (equations 3.5) where *R* is the gas constant for dry air (287 J K^{-1} kg^{-1}), *T* is the ambient temperature in Kelvin, c_p is the specific heat of dry air at constant pressure (1004J K^{-1} kg^{-1}), p_s is the standard reference pressure (1000 hPa) and *p* is the pressure of the given potential temperature Θ (Holton 2004):

$$\theta = T\left(\frac{p_s}{p}\right)^{\frac{R}{c_p}} \tag{3.5}$$

Another quality check was built into the program with this step. If the pressure difference between two known pressure levels was greater than 100 hPa, the entire sounding was removed from the dataset. This ensured that the lapse rate technique of deducing data was not used for large pressure gaps where the large interpolation could lead to errors within these data.

(6) After conditions were obtained for each hectopascal throughout a sounding, the pressure levels of following potential temperature values, the conditions described in Step 5 were stored and placed into respective files: 300K, 305K, 310K, and 315K. Nothing below a potential temperature of 300K was used as within the study region it would have run into the ground.

Using the program as described above, every station within the study area had four files created, one for each isentropic level (300K, 305K, 310K, and 315K) containing the pressure level at which the isentropic surface was located, its mixing ratio, its wind direction, and its wind speed.

Another FORTRAN program was created to construct files for tornado and non-tornado days. For each month, tornado reports that were contained within a given region, as described in Section 3.b, were categorized and the specific Julian day for each tornado report was determined. Using the days of the tornado reports and the station isentropic files, the program created a nominative categorization scheme by identifying the days with tornadoeswith a “1” and days without tornadoes within the region with a “0.”

The resulting data matrix for each station had twenty-seven columns, which included each isentropic surface and associated mixing ratio, wind direction, and wind speed for each isentropic level, pressure difference between isentropic levels, and the tornado/non-tornado day indicator. In this format the files were imported into MiniTab and ArcMap for statistical and visual analysis.

e. Analysis Techniques

To determine the usefulness of isentropic analysis in forecasting severe weather events, I conducted two different analyses. The first was examining the station data within each region through statistical analysis. This entailed using Kruskal-Wallis test to examine difference in means between tornado and non-tornado days for each given isentropic level is determine if there was significant difference in the isentropic level of tornado days versus non-tornado days. This test determines if the median of two datasets are statistically different and is calculated using equation 3.1 which calculates the H statistic (Hollander and Wolfe 1999):

$$H = \frac{12}{N(N+1)}\left(\sum \frac{\tau_i^2}{n}\right) - 3(N+1) \tag{3.1}$$

where H is the H statistic, N is the total sample size, n is the sample size of the individual group and τ is the sum of the variables in the given group. For this research, I elected to use an alpha value of 0.050 (95 percent confidence level) resulting in the critical H value being 3.84146 obtained for the chi-square probability table. This means, when conducting the Kruskal-Wallis test, any variable that has an H statistic greater than 3.84146 can be assumed to have a statistically significant difference in the median value. For my results, the

corresponding *p*-value will be given which demonstrates the significance of the difference.

The second method used was synoptically identifying critical patterns for each month/region. The type of anomalies and patterns I will address include: the position of isentropic troughs and ridges, the depth of the given troughs, moisture content on the given surface and the wind flow on the surface which can result in up sloping or down sloping flow.

These two steps allowed for, not only determining which variables were significantly different on tornado versus non-tornado days, but also allowed for examination of the visual pattern of the isentropic surface that cannot be statistically tested.

After statistically analyzing the data and determining which variables were most significant with respect to difference in median between tornado and non-tornado days using a Kruskal-Wallis test, synoptic pattern analysis is also needed. This was an important step as while the statistical tests allowed for examination of which variables had the most significant change for tornado and non-tornado days, it did not allow for evaluation of the specific synoptic features associated with tornado events. For this examination, I created a FORTRAN program that averaged the isentropic surface and the conditions associated with each isentropic surface as described in Section 3.4 for each day that tornadoes occurred in the given region between January 1974 and December 2009. These files were then mapped in ArcGIS, using Universal Kriging to map the isentropic level, mixing ratio, twenty-four hour difference, and difference between the isentropic surfaces.

Universal Kriging is an interpolation algorithm that uses weighted averages and a probability model to create a given spatial output. Equation 3.8 shows the general Universal Kriging model where Z(s) is the point value, μ(s) is the spatial trend and ε(s) is the spatially-autocorrelated error (Cressie 1991, Isaaks, and Srivastava 1989).

$$Z(s) = \mu(s) + \varepsilon(s) \tag{3.8}$$

I then plotted wind direction and wind speed using traditional station model wind flags/barbs and located tornado events using their start latitude and longitude. A sample 305K isentropic map for 12Z May 22, 2011 is shown in Fig 3.4.

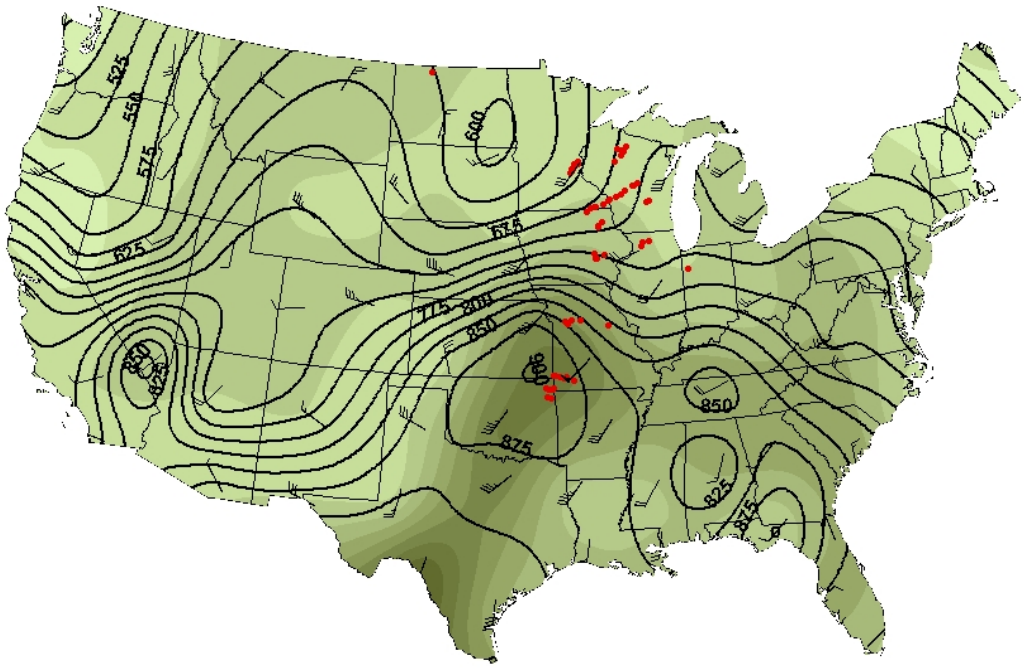

Fig. 3.4. Sample output map showing the 12Z May 22, 2011 305K isentropic surface. The solid lines are the pressure in hectopascals at which the 305K potential temperature is found, the shaded regions indicate mixing ratio with darker shading indicating higher mixing ratio values, and red dots are tornado reports.

f. Case Study Selection

In Section 3.e, I described how the climatological isentropic pattern was analyzed using both statistics and visual analysis. This process allows for the examination of which variable on the isentropic surface and which isentropic surface itself are the most significant to analyze and the synoptic pattern associated with tornado events. Using this information, I analyze a case study for each region using the information obtained from the climatological analysis. This determines if the isentropic tornado results can be used in an operational sense.

To select case studies, I evaluated tornado reports as discussed in Section 3.c, but used the years from 2010 through 2011 in order to select case studies from an independent dataset. The largest tornado outbreak within each region, which was defined in section 3.b, was determined and the case studied was created. Each of the case studies will be outlined in Chapter 5, with the dates and number of tornadoes for each outbreak listed in Table 3.2.

Table 3.2. Case studies dates that were examined, including the region they were in and the number of tornado reports.

Month	Region	Date	Number of Tornadoes
January	Lower Mississippi River Valley	January 20, 2010	21
February	Southeastern Mississippi River	February 24, 2011	27
March	Central Southern Plains	March 10, 2010	7
March	Southeastern United States region, excluding Florida	March 9, 2011	25

Table 3.2 (continued)

April	Southern Plains	April 25, 2011	59
May	Central Great Plains	May 10, 2010	42

June	Upper Great Plains	June 17, 2010	115
June	Great Lakes	June 5, 2010	67
July	Upper Plains	July 10, 2011	15
July	Mid-Atlantic	July 24, 2010	7
August	Great Lakes/Midwest	August 23, 2011	5
September	Gulf States	September 4, 2011	19
October	Southern Great Plains	October 24, 2010	20
November	Gulf States	November 29, 2010	25
December	Lower Mississippi River	December 31, 2010	66

g. Summary

Past research has suggested that isentropic analysis can be a useful forecasting tool with regard to moisture transport and up-sloping and down-sloping flow. Due to this success, I set out to determine if isentropic analysis could be used in forecasting severe weather, in particular tornadoes. To complete this, I first compiled and quality-controlled tornado reports from the Storm Prediction Center Warning Coordinator Meteorologist site from the time period of 1974 through 2009 to create tornado density maps. From these maps, the areas that demonstrated a density that was four standard deviations from the mean were considered for being tornado regions. I selected at least one region for each month with each region displayed in Fig 3.2. The days for which tornadoes occurred were identified and based on those days in each region, the average isentropic surface including each surface's mixing ratio, wind speed, and wind speed and direction was created for visual analysis. I obtained the isentropic conditions by collecting the raw radiosonde data from the Forecast System Laboratory and National Climatic Data Center and running them through a FORTRAN program

to create the given isentropic surface. Station files were also created for stations that were within a given region with the isentropic conditions, as defined above, for tornado and non-tornado days. Using these files, I then conducted a Kruskal-Wallis test on each variable to examine if there was a significant difference in means on tornado versus non-tornado days. With this visual and statistical analysis for each month for varying regions, I was able to determine the locations where isentropic analysis was best representative of tornado events.

Using the information gathered from both the visual and statistical climatological analysis, I created a number of case studies for each month for varying regions of the country. This allowed for the ability to determine if the variables found significant within the climatological portion of this dissertation held true in daily case examples.

This chapter examined the study area, the two data sources used to obtain tornado and raw radiosonde files, the visual and statistical analysis of data, and the case studies which were examined. Chapter 4 will examine the results, which will include a detailed look at the descriptive statistics for each variable for each station in the defined tornado regions, a suite of maps and discussion of isentropic maps for each tornado regions, and will conclude with an examination of fourteen case studies.

Chapter 4

RESULTS AND DISCUSSION

a. Introduction

In this chapter I will show and discuss the results of the statistical tests and mapped results that were created to answer the question posed in this dissertation, specifically: *to what degree does climatological (monthly) isentropic analysis, based on modern weather observations, show identifiable distinct patterns associated with the occurrence of tornadoes within the contiguous United States?* While addressing this question was the main goal of this dissertation, my underlying theme was to place isentropic analysis back into mainstream weather forecasting and to show the need for more high resolution datasets in isentropic coordinates such as currently available for constant pressure surfaces.

To address my research question, I employed two datasets which included tornado reports obtained from the Storm Prediction Center Warning Coordinator Meteorologist site (Storm Prediction Center, 2011) and rawinsonde data for upper air stations across the contiguous United States obtained from the CD-ROM "Radiosonde Data of North America 1946-1996" produced by Forecast System Laboratory, supplemented with data between the years of 1997 through 2009 using data supplied online via National Climatic Data Center (Forecast Systems Laboratory 1997). Both of these datasets were run through quality controls before use which were discussed in Chapter 3.

Using these two datasets, the first step was to determine the region to analyze in each month throughout the year across the contiguous United States.

To determine these regions I calculated the total density of tornado reports across the contiguous United States from 1974 through 2009 and mapped the areas that had a tornado density at or exceeding four standard deviations from the mean. Using four standard deviations from the mean allowed two things: (1) the ability to straightforwardly detect where the highest density of tornadoes occurred in each month since 99.9 percent of the densities should be within four standard deviations of the mean thereby permitting the extreme density cases to clearly stand out, and (2) the creation of regions that were small enough to geographically analyze, as selecting too large of regions could result in the masking of potentially important variables and patterns that might counteract one another on opposite sides of a large region. In Chapter 3, I discussed the creation of the regions with Fig 3.2 showing the location of each region for each month.

After the regions were selected, the specific calendar days on which tornadoes occurred in each given region were determined. This information was later used in FORTRAN programs to calculate the average isentropic pattern for each region on tornado and non-tornado days.

After the regions were selected and the days on which tornadoes occurred in each of the regions were identified, I used rawinsonde data to calculate not only the average isentropic pattern for non-tornado and tornado days for mapping but for each upper-air station within each region. I then created a list of the conditions including the pressure level of the given isentropic surface, mixing ratio, wind direction and wind speed on each of the isentropic levels for each day and nominally categorized that day with a “0” for a non-tornado day and a “1” for

tornado days. This type of array for each station allowed me to conduct statistical tests to analyze differences on tornado and non-tornado days.

Using each station's daily isentropic data file as described above, the main statistical test I used to analyze the upper air data in each region was a non-parametric one-way analysis of variance, the Kruskal-Wallis test. This test determines if the median of two datasets are statistically different and is calculated using equation 4.1 which calculates the H statistic (Hollander and Wolfe 1999):

$$H = \frac{12}{N(N+1)}\left(\sum \frac{\tau_i^2}{n}\right) - 3(N+1) \tag{4.1}$$

where H is the H statistic, N is the total sample size, n is the sample size of the individual group and τ is the sum of the variables in the given group. For this research, I elected to use an alpha value of 0.050 (95 percent confidence level) resulting in the critical H value being 3.84146 obtained for the chi-square probability table. This means, when conducting the Kruskal-Wallis test, any variable that has an H statistic greater than 3.84146 can be assumed there is a statistically significant difference in the median value. For my results, the corresponding p-value will be given which demonstrates the significance of the difference.

This chapter is divided into the fifteen different regions that were defined in Chapter 3. Each region is discussed in the same manner starting with a brief overview of the given region, as a more in-depth description of each region can be found in Chapter 3. I then examine how the pressure level on each given

isentropic surface is changed on tornado versus non-tornado days, which will be followed by the alterations to wind speed/direction and mixing ratio. Each section has a brief conclusion outlining the important aspects that were found within each region and I will also state the best isentropic level forecasters should use in the given region/month. This chapter concludes with an overarching conclusion of how isentropic analysis can be used as a useful forecasting tool when examining tornado events within the United States.

b. January – Region 1 (Lower Mississippi)

For January, I selected a region that was located in the southern United States and contained 583 (48 percent) of the 1,216 tornadoes reported from 1974 to 2009 (Fig 4.1). Five upper air stations were utilized in this region which included: Lake Charles, LA (72240), Little Rock, AR (72340), Jackson, MS (72235), Shelby, AL (72230) and Nashville, TN (72327).

Fig. 4.1**.** Red box is the boundary for the study region for January. Black dots indicate tornado reports within the region from January 1974 through December 2009. This region contained 583 (48 percent) of the 1,216 tornado reports during this timeframe.

The first aspect that I analyzed was the pressure level a given isentropic surface was at for tornado and non-tornado days. I evaluated if there was a statistically significant difference in median using a Kruskal-Wallis test. Of the four isentropic surfaces (315K, 310K, 305K and 300K) for the five stations within the study region, all four were found to have a statistically significant difference in the median at the 95 percent confidence level. In each of the cases the pressure level of the given isentropic surface was at a higher pressure (lower height) during tornado events compared to that of non-tornado event days (Table 4.1). The level that had the greatest change was that of the 300K surface, with the average pressure rise in the isentropic trough to be on the order of 56hPa. This indicates that during tornado days, a deeper isentropic trough exists across the region which may not only enhance uplift, but it may also aid in advecting higher moisture content from the Gulf of Mexico.

Table 4.1**.** Kruskal-Wallis test results for the 300K isentropic level for the following variables. Pressure level (hPa), wind direction (º from N), wind speed (kts) and mixing ratio (g/kg) for the five stations within study region 1 for January. Bolded values indicate those that were not significant at the 95 percentile confidence interval ($p < 0.05$). The entire table for the 315K, 310K, 305K and 300K can be found in the Appendix A.

		300K Pressure Level (hPa)	300K Wind Direction (°)	300K Wind Speed (knots)	300K Mixing Ratio (g/kg)
Lake Charles, LA	Non-Event	755	261	22	2.1
	Event	811	224	32	6.29
	Difference	56	-37	10	4.19
	p-value	0	0	0	0
Little Rock, AR	Non-Event	675	270	34	1.2
	Event	717	240	37	3.1

Table 4.1 (continued)

	Difference	42	-30	3	1.9
	p-value	0	0	0.003	0
Jackson, MS	Non-Event	725	266	28	1.62
	Event	776	233	24	5.05
	Difference	51	-33	-4	3.43
	p-value	0	0	0.001	0
Shelby, AL	Non-Event	714	269	**33**	1.45
	Event	765	227	**32**	4.84
	Difference	51	-42	**-1**	3.39
	p-value	0	0	**0.696**	0
Nashville, TN	Non-Event	636	268	**41**	0.99
	Event	715	241	**40**	2.93
	Difference	79	-27	**-1**	1.94
	p-value	0	0	**0.294**	0

Although statistical analysis indicated that during tornado days, the isentropic trough across the study region deepens, it is also important to visually assess the pattern spatially to see where the highest pressure rises and falls on the isentropic surface occur. To examine this pattern an anomaly map was created by taking the average 300K isentropic surface for tornado days and subtracting it from the average 300K isentropic surface on non-tornado days. As a result, a positive value indicates areas of a lowering isentropic surface (troughing) and negative values indicates areas where the isentropic surface was rising (ridging).

Fig 4.2 displays the 300K pressure anomaly map (all four isentropic surfaces had similar patterns) which showed the largest differences. Pronounced troughing is observed over the study region and across the entire eastern United States. This is matched by a large area of ridging over the western United States. Of additional specific interest are the axis of greatest pressure rise and the

location of the zero-change from positive to negative pressure differences. The axis of greatest pressure rise (troughing) is noted from Louisiana through West Virginia and into Michigan, with the largest difference occurring in eastern Michigan. Also, of note is the location of the zero-change line and the gradient displayed on the western edge of the study region. This pattern indicates a strengthening isentropic trough located directly next to a strengthening isentropic ridge, which promotes uplift as it moves through the given region. With this feature located on the western edge of the study region at 12Z (morning) of the tornado day, it would likely move through the area throughout the day. That would promote thunderstorm development due to the ascent up the isentropic surface.

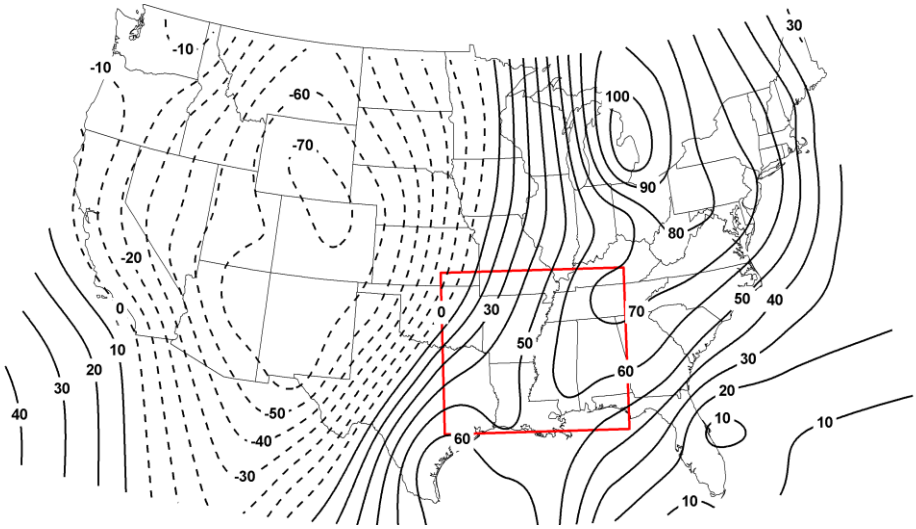

Fig. 4.2**.** 300K January Isentropic surface pressure difference calculated by taking the average pressure level of the 300K isentropic surface on tornado days minus the pressure level on non-tornado days.

While the basic isentropic pattern as discussed above is an important indicator for tornado forecasting, wind speed and direction on an isentropic surface determines whether air is either descending or ascending on the

given isentropic surface. Descending air inhibits thunderstorm growth and ascending air up an isentropic surface aids in thunderstorm development, as a result for the most uplift to occur, the wind direction needs to be perpendicular to the isentropic pressure contours and flowing from high pressure areas (lower heights) to areas of lower pressure (higher heights).

When conducting a Kruskal-Wallis test on wind direction for the four isentropic surfaces, (similar to the analyses for pressure level of a given isentropic surface above), each station within the study region demonstrated a statistically significant change in wind direction on tornado days compared to non-tornado days at the 95 percent confidence level (Table 4.1). At each station on non-tornado days, the winds were primarily westerly and on non-tornado days backing (more southwesterly) winds were noted, (Fig 4.2).

Once again, the 300K isentropic surface had the highest change in wind direction with an average backing wind of 34º for the five stations. Though this change is statistically significant, it was important to see how the change in wind direction impacted upslope or downslope flow on the isentropic surfaces. Since the 300K isentropic surface for this region shows the greatest change, for brevity I will discuss only that isentropic level. Fig 4.3 shows the average 300K isentropic surface with wind speed and direction for non-tornado days (top) and tornado days (bottom) from 1974 through 2009. During non-tornado days a zonal isentropic pattern is noted with winds flowing nearly parallel to the isentropic surface indicating little, if any, isentropic lift or decent across the region. Conversely, during tornado days an amplified trough across the region has winds

flowing up the isentropic trough from southwest to northeast resulting in uplift along the isentropic surface. Consequently, the change in isentropic surface and the wind direction identifies enhanced areas of uplift that may lead to the production of tornado events.

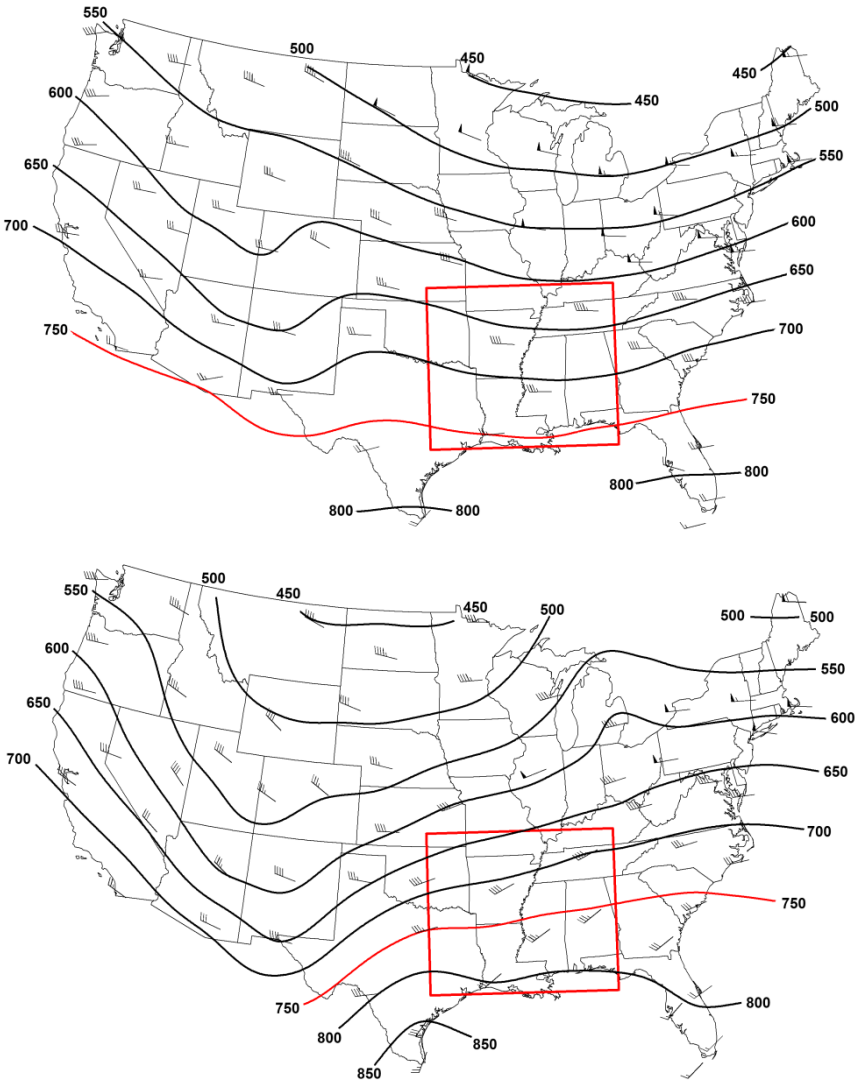

Fig. 4.3**.** (a) average 300K January isentropic surface and wind direction/speed for non-tornado days from 1974 through 2009 (b) same as the above but for tornado days. The 750 hPa isobar is highlighted in red to be able to easily note how the pattern changed from non-tornado to tornado days.

With regard to wind speed changes on the given isentropic surfaces for tornado versus non-tornado days, no uniform significant change is evident. Lake

Charles, LA and Nashville, TN did display a significant change but Nashville displayed an increase while Nashville displayed a decrease of wind speed on tornado days, so it does not appear for the month of January in this study region wind speed is a factor that should be looked at on any isentropic level (Table 4.1).

Mixing ratio is another key aspect to examine when conducting an isentropic analysis of tornado versus non-tornado occurrence. It has already been found that isentropic troughs are rather closely linked to an increase in moisture (Byers, 1938; Namias, 1938; Wexler and Namias, 1939; Cerveny et al., 2011). When performing a Kruskal-Wallis test on mixing ratio for the five stations in the study region, just like for wind direction and isentropic pressure level, I determined that all stations had a statistically significant change in mixing ratio values from tornado versus non-tornado days. The 300K isentropic surface displayed the highest change with an average increase in mixing ratio of 2.31g/kg. The axis of highest mixing ratio for the 300K isentropic surface follows closely with the axis of greatest pressure rise (Fig 4.4). A fairly tight dry to moist gradient is also located along the western edge of the study region which coincides with the boundary between pressure falls and rises as seen in Fig 4.2.

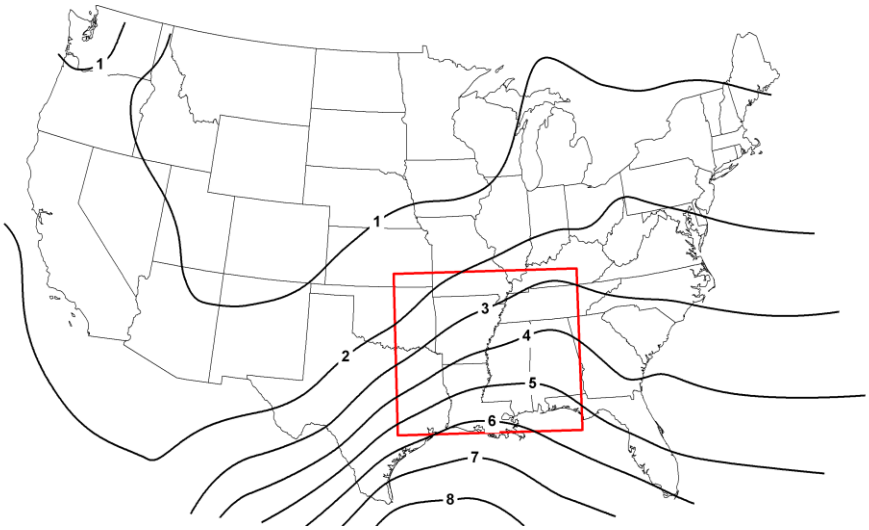

Fig. 4.4**.** Average mixing ratio on the 300K January isentropic surface for tornado days from 1974 through 2009.

Overall, for this study area in January, the key aspects on any of the four isentropic surfaces (300K, 305K, 310K and 315K) for tornado versus non-tornado days are the synoptic-scale isentropic pattern, the changes in wind direction and changes in mixing ratio. These variables showed a statistically significant change in median value for non-tornado days compared to tornado days. Over the study region for January, I found:

(1) The isentropic trough deepens with the axis of greatest deepening running from Louisiana up through Michigan.

(2) The boundary between troughing and ridging was located along the western boundary of the study region at 12Z and, as it shifts east throughout the day, could result in greater uplift.

(3) During tornado days wind direction flowed up the isentropic trough from southwest to northeast which would result in greater uplift.

And (4), during tornado days the mixing ratio was found to increase on average 2.31g/kg across the region on the 300K isentropic surface, which could substantially aid in thunderstorm development/strengthening.

Finally, while these same variables have similar differences on each of the isentropic surfaces, they displayed the greatest change on the 300K surface and as a result that would be the recommended surface to use in this region in January.

c. February – Region 1 (southeastern Mississippi River)

The month of February consisted of a single region which was located in the southeastern United States and contained Mississippi, Alabama, Tennessee, western/central Georgia and eastern Arkansas and eastern Louisiana. This region experienced 471 (32 percent) of all the tornadoes reported within the contiguous United States for the month of February from 1974 through 2009 (Fig 4.5). The upper air stations I used in this region included: Peachtree City, GA (72215), Shelby, Al (72230), Jackson, MS (72235), Nashville, TN (72327) and Little Rock, AR (72340).

Fig. 4.5**.** Red box is the boundary for the study region for February. Black dots indicate tornado reports within the region for February from 1974 through 2009. This region contained 471 (32 percent) of the 1,216 tornado reports during this timeframe.

To begin the examination of isentropic analysis in tornado forecasting for January, I first examined the difference in the pressure at the 315K, 310K, 305K and 300K isentropic surfaces which occurred from non-tornado days and tornado days using a Kruskal-Wallis test. I found that each station within the study region had a statistically significant difference in median pressure level for all four isentropic surfaces on tornado days compared to non-tornado days (Table 4.2). Each of the stations displayed an increase in pressure (decrease in height) on the given isentropic surface for tornado days. Similar to January results (section 4b), the 300K isentropic surface showed the greatest change between tornado versus non-tornado days with Peachtree City, GA increasing pressure by 41hPa, Shelby, AL, increasing 54hPa, Jackson, MS, increasing 57hPa Nashville, TN increasing 89hPa and Little Rock, AR, increasing by 47hPa.

Table 4.2**.** Kruskal-Wallis test results for the 300K isentropic level for the following variables: pressure level (hPa), wind direction (º from N), wind speed (kts) and mixing ratio (g/kg) for the five stations within study region 1 for February. Bolded values indicate those that were not significant at the 95 percentile confidence interval ($p < 0.05$). The entire table for the 315K, 310K, 305K and 300K can be found in the Appendix A.

		300K Pressure Level (hPa)	300K Wind Direction (°)	300K Wind Speed (knots)	300K Mixing Ratio (g/kg)
Peachtree City, GA	Non-Event	719	267	**32**	1.36
	Event	760	235	**33**	4.5
	Difference	41	-32	1	3.14
	p-value	0	0	**0.892**	0

Table 4.2 (continued)

Shelby, AL	Non-Event	721	267	**31**	1.22
	Event	775	230	**33**	4.86
	Difference	54	-37	**2**	3.64
	p-value	0	0	**0.674**	0
Jackson, MS	Non-Event	727	266	27	1.53
	Event	784	234	35	5.37
	Difference	57	-32	8	3.84
	p-value	0	0	**0**	0
Nashville, TN	Non-Event	634	268	**39**	0.98
	Event	723	237	**35**	4.24
	Difference	89	-31	**-4**	3.26
	p-value	0	0	**0.39**	0
Little Rock, AR	Non-Event	678	270	31	1.18
	Event	725	240	36	3.8
	Difference	47	-30	5	2.62
	p-value	0	0	0.002	0

In order to analyze the overall change in isentropic pattern for tornado days compared to non-tornado days, I calculated the average isentropic pressure level for non-tornado and tornado days within the region and from that result, I created an isentropic anomaly map showing the areas of greatest pressure rises and falls. This type of analysis/map was created for each of the four isentropic levels analyzed but for brevity only the 300K map will be shown as it displayed the greatest change (Fig 4.6).

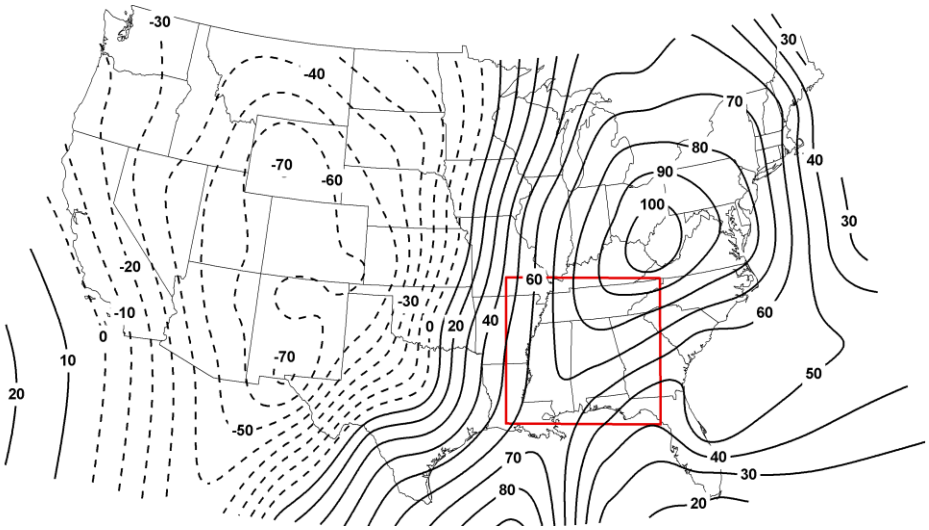

Fig. 4.6**.** 300K February Isentropic surface pressure difference calculated by taking the average pressure level of the 300K isentropic surface on tornado days minus the pressure level on non-tornado days. Solid lines indicate areas of increasing pressure (lowering heights) and dotted lines indicate areas of rising pressures (rising heights).

Similar to the January analysis (section 4b), the largest rise in pressure of the isentropic surface is over the eastern United States, indicating a deepening trough, whereas a strengthening isentropic ridge is building over the entire western United States. The other two keys points are (1) the location of the axis of greatest pressure rise which runs nearly through the center of the study region from eastern Louisiana up to the northeast into West Virginia, and (2) the position of the tightest gradients from troughing to ridging which was located across Oklahoma. The axis of greatest pressure rise on the isentropic surface indicates that there is a deepening isentropic trough across the region, which not only increases uplift but also moisture content since moisture has been linked to isentropic troughs as noted in Chapter 2 (Moore and Smith 1989). The isentropic trough to ridge location could indicate a frontal system which likely moves through the region throughout the day resulting in additional uplift to aid in

thunderstorm development. These two aspects will be discussed in greater detail below when analyzing the actual 300K pattern.

An additional aspect is uplift on the isentropic surface, which can be easily shown by examining the actual isentropic pattern and wind direction (Fig 4.7). As was the case with the pressure level of the given isentropic surface, each station within the study region noted a statistically significant change in wind direction on tornado days compared to non-tornado days, with the greatest change in median wind direction noted once again on the 300K surface, so that will be the level on which I focus. The average change in wind direction for the five stations within the region on the 300K isentropic surface was 32.4 degrees, or switching wind direction from 268 degrees (west) on non-tornado days to 235 degrees (southwest) on tornado days (Fig 4.7). This marked shift in wind direction allows for flow up the isentropic trough leading to added uplift. On non-tornado days, the winds are nearly parallel to the contours indicating no up-sloping or down-sloping flow within the atmosphere. While these findings suggest wind direction is an important factor to synoptic isentropic analysis of tornado events, wind speed was found to be a non-significant statistical component in isentropic analysis of tornado versus non-tornado days. Only on two levels (300K and 305K) and two stations (Nashville, TN and Peach Tree, GA) was wind speed found to be statistically significant and, even with that, the direction of change (increasing or decreasing wind speed) varied from level to level and station to station, leading to the assumption that for this region, variations in isentropic levels wind speeds between tornado and non-tornado days is not statistically distinguishable.

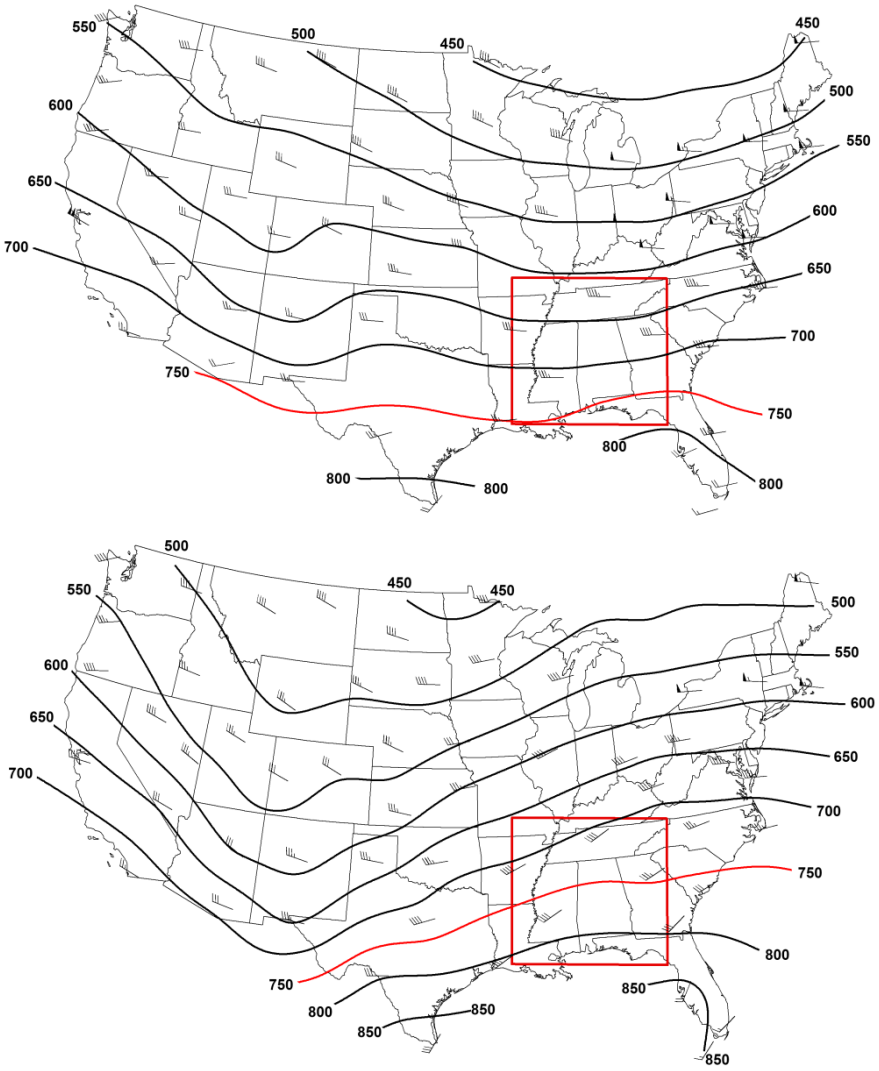

Fig. 4.7**.** (a) average 300K February isentropic surface and wind direction/speed for non-tornado days from 1974 through 2009 (b) same as the above but for tornado days. The 750 hPa isobar is highlighted in red to easily identify the shift in pattern on non-tornado versus tornado days.

So far, it has been found that additional uplift occurs across the study region as the result of a more amplified isentropic trough and up-sloping flow within the region. With uplift in place, moisture is another ingredient needed in order to develop thunderstorms within the region. I conducted a Kruskal-Wallis test on mixing ratios between tornado versus non-tornado days. I found for each isentropic level, and for each station within the region, the median mixing ratio

was significantly higher on tornado days compared to that on non-tornado days. As was the case for isentropic pressure level and wind direction, the greatest change in mixing ratio was found on the 300K isentropic surface, where median values increased on average 3.29g/kg across the region for tornado days. The axis of moisture increase is noted stretching from eastern Louisiana up into Kentucky (Fig 4.8) which follows a very similar pattern to that of the pressure difference map (Fig 4.6). This is not surprising considering that presence of isentropic troughs normally indicate an increase in low-level moisture.

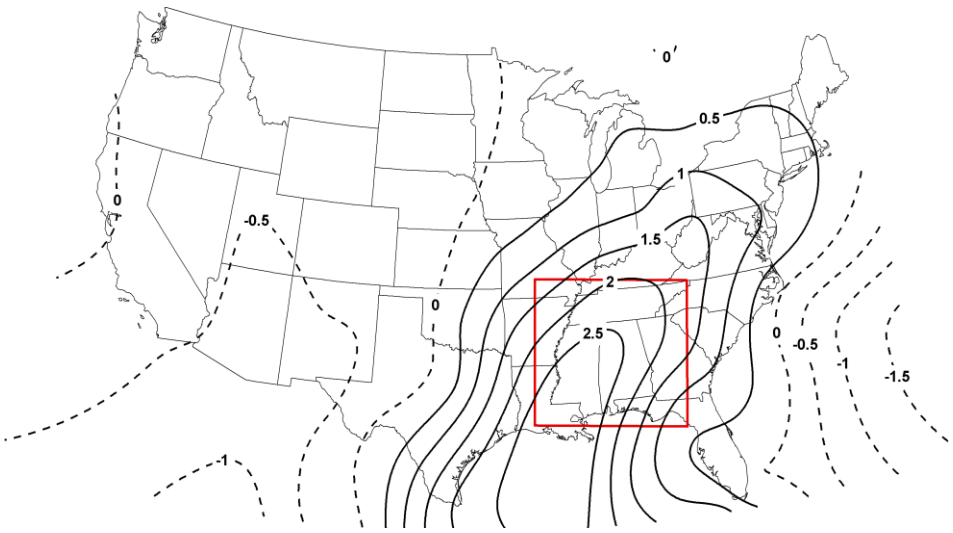

Fig. 4.8**.** 300K February Isentropic surface mixing ratio difference in g/kg calculated by taking the average mixing ratio of the 300K isentropic surface on tornado days minus the average mixing ratio on non-tornado days. Solid lines indicate areas of increased mixing ratio and dotted lines indicate areas of decreased mixing ratio.

In summary, for February, in this gulf state region, I found that isentropic pressure level, wind direction and mixing ratio were all key aspects to examine. Each of the four isentropic levels displayed these variables to be statistically significant; however, the 300K level showed each of the variables had the greatest change in median for tornado versus non-tornado days. At each station, the

isentropic pressure level increased for tornado days indicating isentropic troughing over the region. This deeper trough across the study region led to an increase in moisture with the mixing ratio increasing on average 3.29g/kg on the 300K isentropic surface. The wind direction within the region was backing to more meridional flow on tornado days which lead to additional uplift within the isentropic trough, compared to the more zonal flow on non-tornado days. All these variables were found to have the greatest change on the 300K isentropic surface and as a result recommend it as the isentropic surface to use in this region during February.

d. March – Region 1 (central Southern Plains)

For the month of March, two prominent region of tornado occurrence were identified through standard deviation density of tornadoes and, as a result, I defined two discrete regions for March isentropic analysis. The first region I selected had 714 (20 percent) of the 3,650 tornado reports within its boundaries for the time period of 1974 through 2009. This region is located in the southern Plains and contained the states of Oklahoma, northeastern/north central Texas, northern Louisiana, Arkansas, southwest Missouri and southern Kansas (Fig 4.9). This region contains five upper air stations that were used for analysis and include: Little Rock, AR (72340), Fort Worth, TX (72249), Amarillo, TX (72363), Norman, OK (72357) and Dodge City, KS (72451).

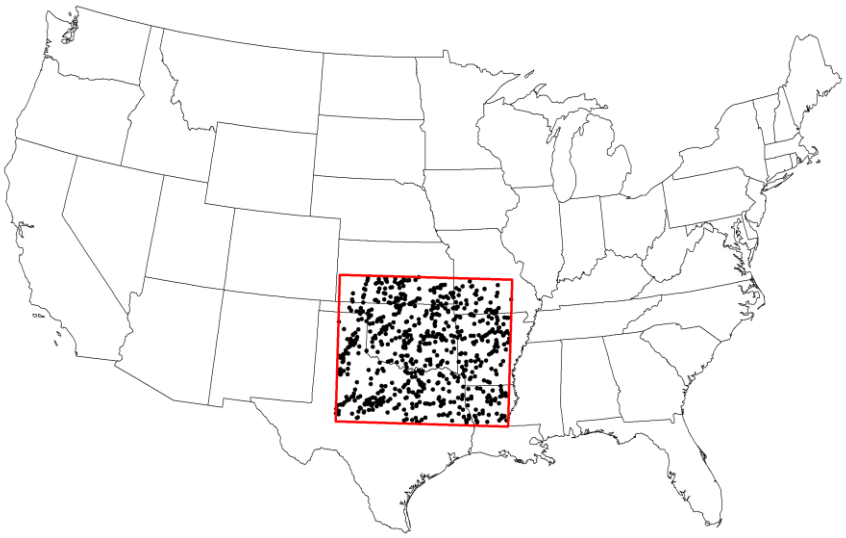

Fig. 4.9**.** Red box is the boundary for the study region 1 for March. Black dots indicate tornado reports within the region for March from 1974 through 2009. This region contained 714 (20 percent) of the 3,650 tornado reports during this timeframe.

When analyzing the pressure level at which the four isentropic surfaces (315K, 310K, 305K and 300K) occur using a Kruskal-Wallis test each station for each level (with the exception of Amarillo, TX), displayed a statistically significant difference in pressure level of the isentropic surface for tornado days compared to non-tornado days (Table 4.3). Each station displayed an increase in pressure (lowering in height) of the isentropic surface on tornado days. Even the Amarillo, TX upper air station which did not have a statistically significant change still display an overall increase in pressure level of the isentropic surface on tornado days. Again, the 300K isentropic level had the largest change in pressure level on tornado days with an average pressure increase of the five upper air stations within this region being 56hPa between tornado and non-tornado days. The largest difference was at Norman, OK with an 80hPa rise in pressure of the 300 K isentropic surface on tornado days compared to non-tornado days.

Table 4.3**.** Kruskal-Wallis test results for the 300K isentropic level for the following variables: pressure level (hPa), wind direction (º from N), wind speed (kts) and mixing ratio (g/kg) for the five stations within study region 1 for March. Bolded values indicate those that were not significant at the 95 percentile confidence interval ($p < 0.05$). The entire table for the 315K, 310K, 305K and 300K can be found in the Appendix A.

		300K Pressure Level (hPa)	300K Wind Direction (°)	300K Wind Speed (knots)	300K Mixing Ratio (g/kg)
Little Rock, AR	Non-Event	712	271	28	1.69
	Event	786	229	27	4.96
	Difference	74	-42	-1	3.27
	p-value	0	0	0	0
Fort Worth, TX	Non-Event	761	252	24	2.95
	Event	827	209	36	7.21
	Difference	66	-43	12	4.26
	p-value	0	0	0	0
Amarillo, TX	Non-Event	726	256	24	2.15
	Event	749	232	31	2.83
	Difference	23	-24	7	0.68
	p-value	0.01	0	0	0
Norman, OK	Non-Event	726	260	26	2.08
	Event	806	220	32	5.75
	Difference	80	-40	6	3.67
	p-value	0	0	0.004	0
Dodge City, KS	Non-Event	685	263	**26**	1.65
	Event	724	221	**28**	2.84
	Difference	39	-42	**2**	1.19
	p-value	0	0	**0.114**	0

For this March tornado region, the most notable feature from the 300K pressure anomaly map (Fig 4.10) is that the greatest increase in pressure is located just to the northeast of the region with the axis of greatest increase stretching

through the center of the study region from southwest to northeast (as was also the case for the other regions discussed thus far). This would indicate a deepening of the trough into the region possibly adding moisture and uplift (discussed in detail below). Also of note is the tight gradient between isentropic troughing (positive values) and ridging (negative values) along the western edge of the study area, which indicates a steep slope on the isentropic surface as a transition between an isentropic ridge and trough. This feature enhances uplift through the study region as it moves through during the day. This pattern is also the likely reason why the Amarillo, TX station does not have a statistically significant change in pressure level of the isentropic surface since that station is located along this transition area.

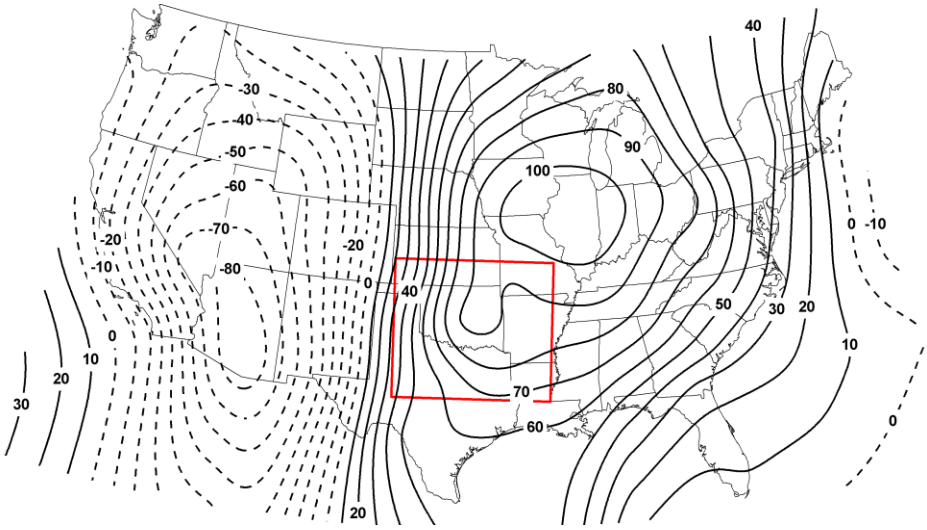

Fig. 4.10. 300K March Isentropic surface pressure difference calculated by taking the average pressure level of the 300K isentropic surface on tornado days minus the pressure level on non-tornado days. Solid lines indicate areas of increasing pressure (lowering heights) and dotted lines indicate areas of rising pressures (rising heights).

Uplift is a key aspect in not only the development of thunderstorms but also in maintaining their structure. On isentropic surfaces, enhanced areas of

uplift can be identified as resulting from wind flow between an area of high pressure (low heights) to areas of lower pressure (higher heights) on a given isentropic surface. Therefore, examination of the actual isentropic surface and the wind direction on the surface is important. The Kruskal-Wallis test of the median wind direction on non-tornado and tornado days resulted in every rawinsonde station within the study region having a statistically significant difference between the two cases on each isentropic surface. The most dramatic changes were noted on the 300K surface with an average backing wind from non-tornado to tornado days of 38.2 degrees, or a wind direction of 260.4 degrees (west) on non-tornado days and 222.2 degrees (southwest) on tornado days. This change in wind direction, as seen in Fig 4.11, shows that this backing wind leads to a greater amount of isentropic lift within the study region. During non-tornado days, a fairly zonal isentropic pattern exists with winds flowing nearly parallel to the contours. Conversely, on tornado days an amplified isentropic trough with an axis running almost directly south to north through the study region is present with winds flowing up the trough from areas of high pressure to low pressure. Such a pronounced isentropic trough indicates added uplift which could aid in thunderstorm development in the region. As noted in the other regions, wind speed did not show a significant statistical change between tornado and tornado days at all stations and of those that did show a significant change displayed minimal three to four knots change, so wind speed does not seem to be a factor in tornado development for this March region.

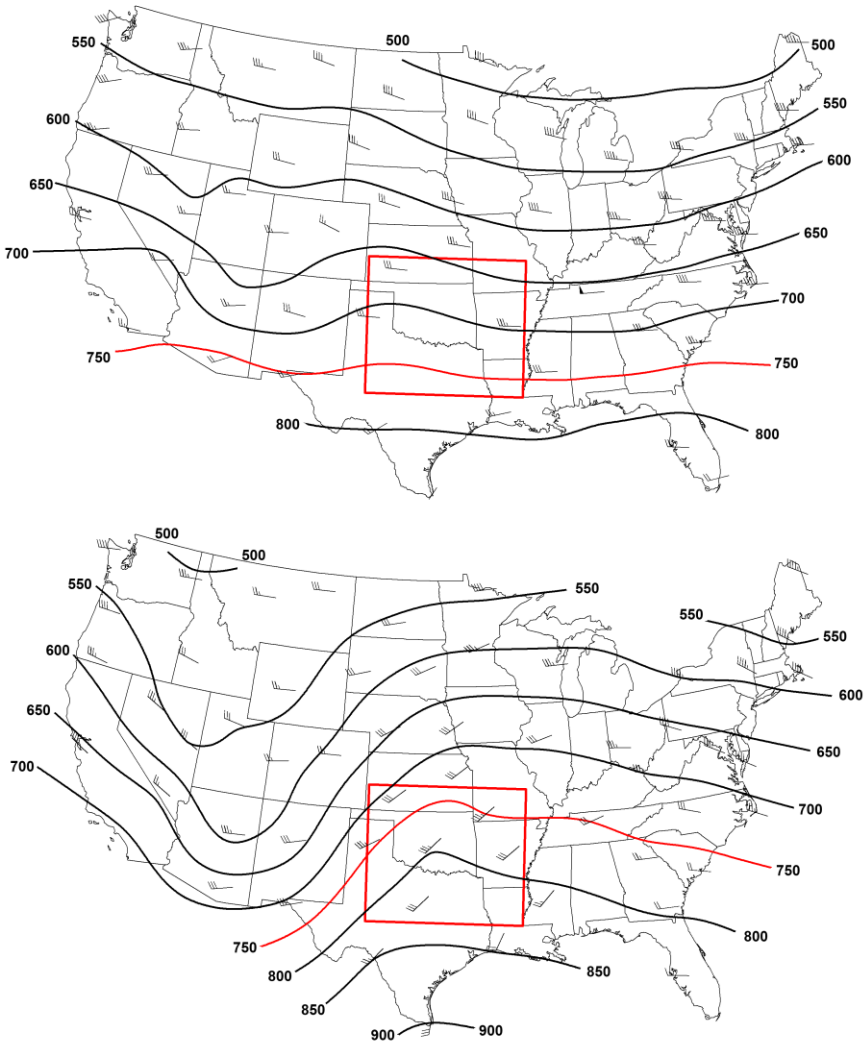

Fig. 4.11**.** (a) average 300K March isentropic surface and wind direction/speed for non-tornado days from 1974 through 2009 (b) same as the above but for tornado days. The 750 hPa isobar is highlighted in red to easily show the shift in pattern from non-tornado and tornado days.

A deepening isentropic trough across the study region should correspond with an increase in low-level moisture. To verify this hypothesis, I conducted a Kruskal-Wallis test on mixing ratio and found it to be significantly higher on tornado days compared to non-tornado days. The average increase over the study region on the 300 K isentropic surface between tornado and non-tornado days was 2.61g/kg. The greatest increase in mixing ratio was directly in the center of the

region with an axis of moisture increase running from the southern tip of Texas up through Wisconsin. This pattern (Fig 4.12) was created by calculating the difference between the average mixing ratio on tornado days from the average mixing ratio on non-tornado days. A tight moisture gradient can also be identified over the western side of the study region and could potentially mark a low-level dry line which could help aid thunderstorm development as well.

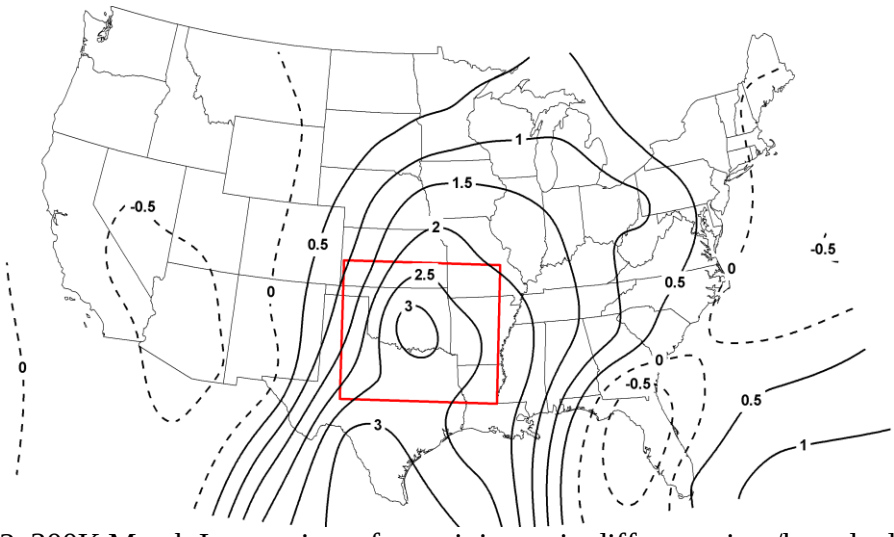

Fig. 4.12**.** 300K March Isentropic surface mixing ratio difference in g/kg calculated by taking the average mixing ratio of the 300K isentropic surface on tornado days minus the average mixing ratio on non-tornado days. Solid lines indicate areas of increased mixing ratio and dotted lines indicate areas of decreased mixing ratio.....

In summary, for this region in March, the pressure level at which an isentropic surface occurs, as well as wind direction and mixing ratio, has been found to be a valuable element to examine during tornado events. The pressure level of the 300K surface increased on average 56hPa, the wind direction was found to shift from 260 degrees to 222 degrees and the mixing ratio increased on average 2.61g/kg. While I focused primarily on the 300K isentropic surface, the above-mentioned variables were found to be statistically significant on the 305K,

310K and 315K surfaces as well. However, for this study region I would recommend using the 300K isentropic surface to obtain the best picture and changes within the atmosphere that could help forecast tornadoes.

e. March – Region 2 (southeastern United States region, excluding Florida)

With two areas indicating a high density of tornadoes, March was separated into two regions, with the first (central South Plains) being discussed in the section above. The second region for March was located in the southeastern United States and contained the states of Alabama, Georgia, South Carolina, northern Florida, southern Tennessee and central/eastern Mississippi. This region contained 717 (20 percent) of the 3,650 tornadoes reported between 1974 and 2009 for the month of March. Within that study region four upper air stations were used for analysis which included: Jackson, MS (72235), Peachtree City, GA (72215), Shelby, AL (72230) and Charleston, SC (72208).

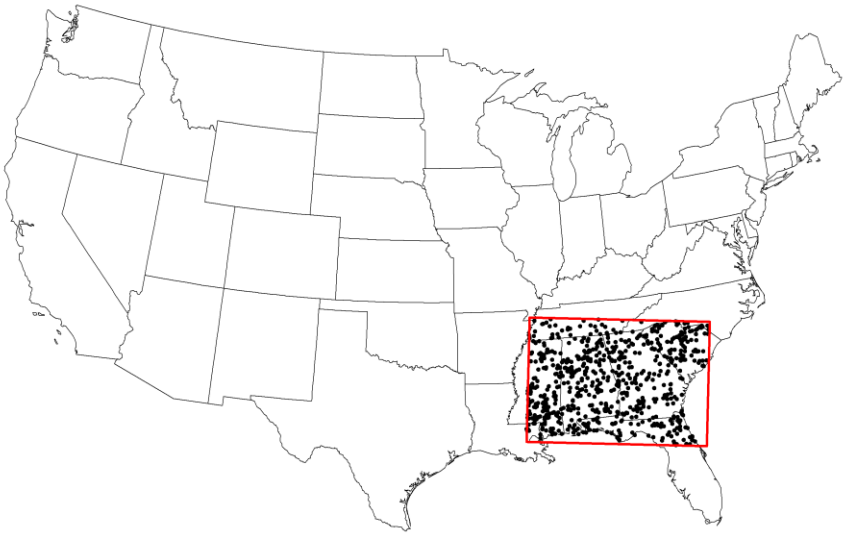

Fig. 4.13**.** Red box is the boundary for the study region for March. Black dots indicate tornado reports within the region for March from 1974 through 2009. This region contained 717 (20 percent) of the 3,650 tornado reports during this timeframe.

Using a Kruskal-Wallis test, I found that each of the stations within the region displayed a statistically significant change in the pressure level of the isentropic surface (315K, 310K, 305K and 300K) from non-tornado days to tornado days (Table 4.4). The greatest difference occurred on the 305K isentropic surface with an average increase in pressure over the study region of 50hPa, with the 300K isentropic surface having an average pressure increase of 48hPa. Even though the 305K isentropic surface indicated the highest change by 2hPa over the 300b K surface, for consistency and for the opportunity to better visualize the lower levels of the atmosphere, I will focus on the 300K isentropic surface.

Table 4.4**.** Kruskal-Wallis test results for the 300K isentropic level for the following variables: pressure level (hPa), wind direction (º from N), wind speed (kts) and mixing ratio (g/kg) for the five stations within study region 2 for March. Bolded values indicate those that were not significant at the 95 percentile confidence interval ($p < 0.05$). The entire table for the 315K, 310K, 305K and 300K can be found in the Appendix A.

		300K Pressure Level (hPa)	300K Wind Direction (°)	300K Wind Speed (knots)	300K Mixing Ratio (g/kg)
Jackson, MS	Non-Event	752	262	22	2.17
	Event	801	236	32	5.86
	Difference	49	-26	10	3.69
	p-value	0	0	0	0
Peachtree City, GA	Non-Event	743	268	**26**	1.77
	Event	793	229	**29**	5.69
	Difference	50	-39	3	3.92
	p-value	0	0	**0.423**	0
Shelby, AL	Non-Event	746	265	25	2.04
	Event	787	231	32	6.11
	Difference	41	-34	7	4.07
	p-value	0	0	0.031	0

Table 4.4 (continued)

Charleston, SC	Non-Event	738	268	24	1.82
	Event	791	234	22	5.39
	Difference	53	-34	-2	3.57
	p-value	0	0	0	0

The 300K isentropic pressure difference between tornado and non-tornado days shows markedly similar patterns to what was discussed in the February pattern. The largest pressure increase in the isentropic surface is noted to the northeast of the region with the largest decrease in pressure of the surface noted over eastern Colorado and western Kansas (Fig 4.14). The axis of highest increase in pressure runs from the panhandle of Florida up to the north-northwest into West Virginia, which is a line nearly directly through the center of the study region. This pattern results in a deepening isentropic trough centered over the study region and an amplified isentropic ridge setting up over the central plains. The transition zone from the isentropic trough to ridge is then located over Arkansas and Louisiana which is just to the west of the region and is marked by a tight gradient and switch from increasing to decreasing pressure. As noted in the above sections, this gradient could result in uplift across the region throughout the day as it moves through and is normally associated with a front as well (Moore and Smith, 1989; de Coning, 2000)

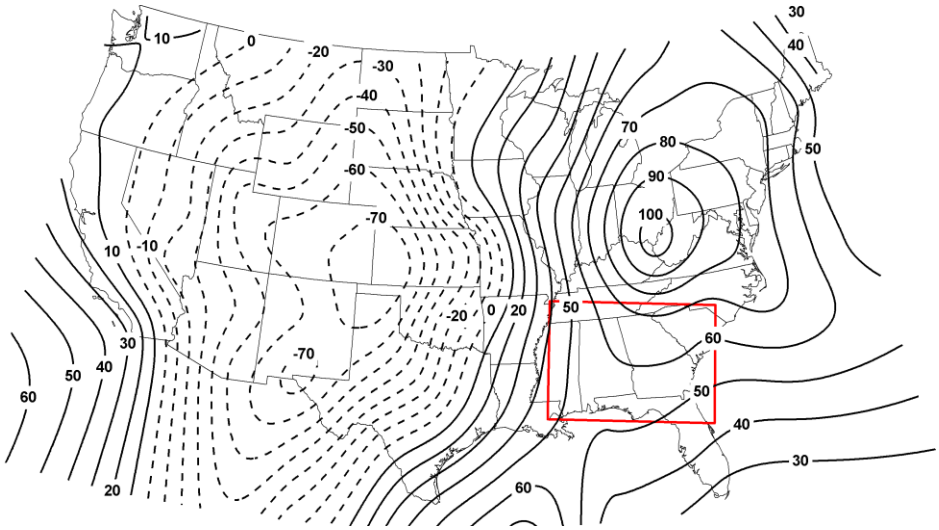

Fig. 4.14**.** 300K March Isentropic surface pressure difference calculated by taking the average pressure level of the 300K isentropic surface on tornado days minus the pressure level on non-tornado days. Solid lines indicate areas of increasing pressure (lowering heights) and dotted lines indicate areas of rising pressures (rising heights).

The amplification of the isentropic trough and ridge can clearly be seen by examining the actual 300K isentropic pattern on tornado versus non-tornado days. Fig 4.15 displays a very weak isentropic ridge over the study region with a weak isentropic trough over the Great Plains for non-tornado days, with a flow near parallel to the isentropic contours or even down-sloping flow over Georgia. For tornado days, a large isentropic trough can be seen directly over the region with up-sloping flow particularly in the eastern portion.

Conducting a Kruskal-Wallis test on wind direction for non-tornado versus tornado days, I found that each station at each isentropic level has a statistically significant change in wind direction on tornado days. A backing (counterclockwise change) wind of an average 33 degrees was noted on the 300K isentropic surface which once again results in air flowing from higher pressure to lower pressure on the isentropic surface which means uplift in the atmosphere,

potentially aiding in thunderstorm development/continuation. Similar to previously discussed regions, wind speed was found to be an insignificant factor to discriminate between tornado and non-tornado days, with Jackson, MS and Charleston, SC being the only stations to achieve any statistical significance and, at that, on average it was a change in wind speed of either minus two knots at Charleston or ten knots at Jackson on tornado days. This is a rather minimal change to detect on a day-to-day forecasting basis when average wind speeds for non-tornado and tornado days combined is in the twenty to thirty knot range.

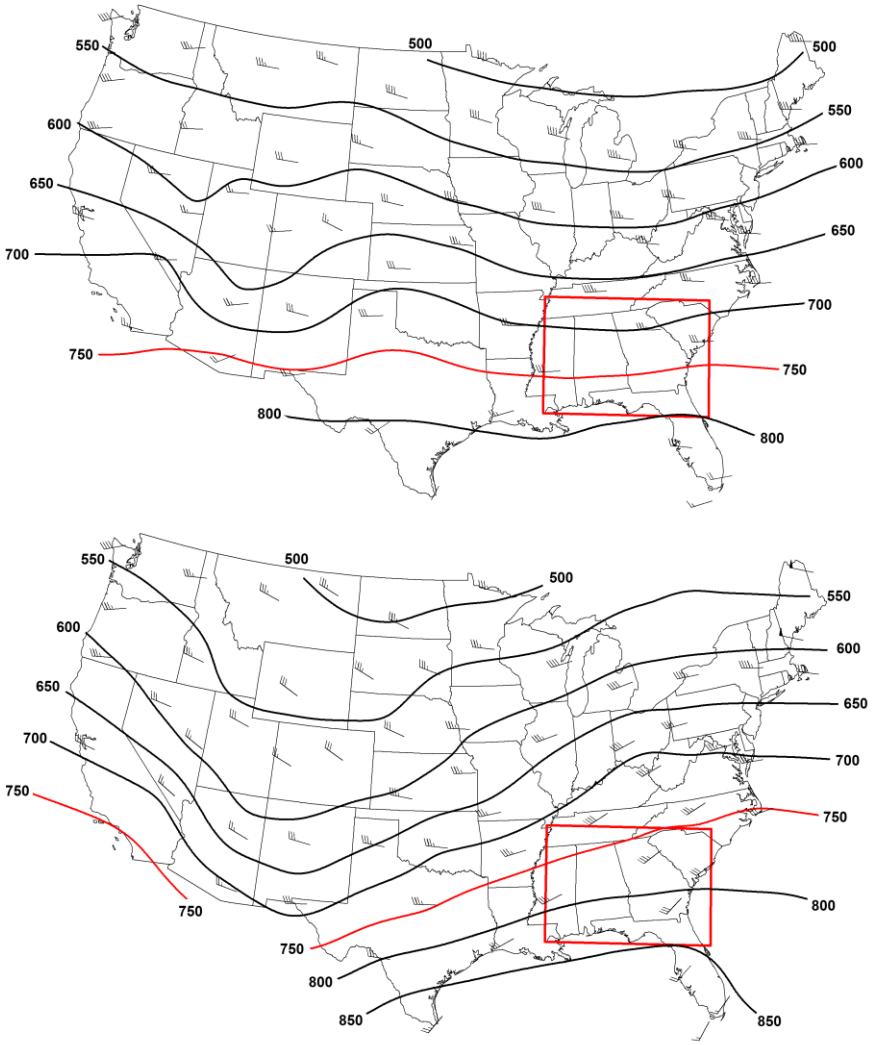

Fig. 4.15**.** (a) average 300K March isentropic surface and wind direction/speed for non-tornado days from 1974 through 2009 (b) same as the above but for tornado days. The 750 hPa isobar is highlighted in red to easily show the shift in pattern from non-tornado and tornado days.

Isentropic surface mixing ratio, however, displayed dramatic differences from tornado days as compared to non-tornado days. At each of the four stations within the region, and for all the tested isentropic surfaces, mixing ratio had a statistically significant increase during tornado days with the 300K surface displaying the highest increase. On tornado days the average median mixing ratio on the 300K surface was 5.76g/kg and on non-tornado days it was 1.95g/kg making for an average change in median across the study region of 3.81g/kg. The axis of greatest mixing ratio increase (Fig 4.16) is in a line from southwest to northeast directly across the study region. This coincides with the isentropic pressure difference pattern (Fig 4.14).

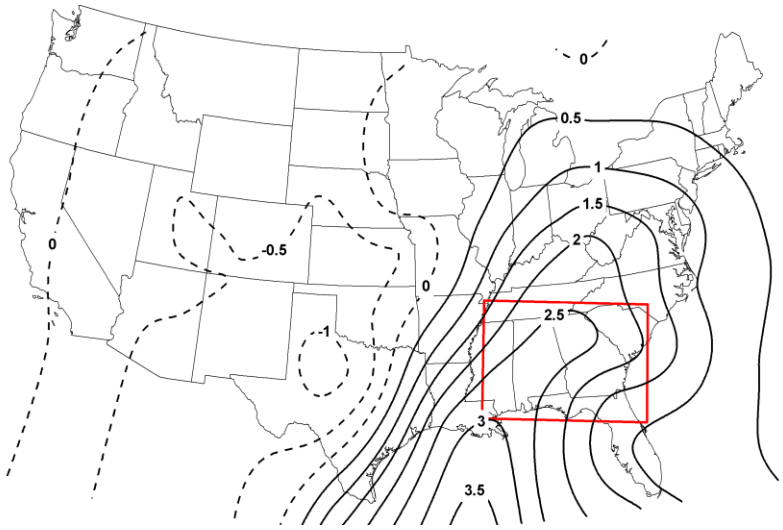

Fig. 4.16**.** 300K March Isentropic surface mixing ratio difference in g/kg calculated by taking the average mixing ratio of the 300K isentropic surface on tornado days minus the average mixing ratio on non-tornado days. Solid lines indicate areas of increased mixing ratio and dotted lines indicate areas of decreased mixing ratio.

In summary, similar to the other regions discussed thus far, three prominent variables on the 315K, 310K, 305K and 300K isentropic surfaces stand out as being useful forecasting aids during tornado events. Those variables are the pressure level, the wind direction and the mixing ratio of a given isentropic surface. The recommended isentropic surface to be used in this region in March is the 300K surface as all of the three above mentioned variables have the most notable changes on tornado days on that surface. On tornado days, the 300K isentropic surface increases in pressure by an average of 48hPa, the mixing ratio increased on average 3.81g/kg and the wind direction was found to be backing from westerly to a more southwesterly direction or, in other words, was found to be backing by 33 degrees. Overall, the isentropic pattern over this region on tornado days shows a deep isentropic trough over the region which aids in uplift and a dramatic increase in mixing ratio which helps to fuel thunderstorm development.

f. April – Region 1 (Southern Plains)

I selected the region for April to be located in the southern Plains, which include the states of Oklahoma, southern Kansas, southwest Missouri western/central Arkansas, northern Louisiana and northeast Texas (Fig 4.17). This region contained 1,437 (20 percent) of the 7,176 tornado reports in April from 1974 through 2009. Four upper air stations were located within the region and were used for the statistic analysis and included: Little Rock, AR (72340), Fort Worth, TX (72249), Norman, OK (72357) and Dodge City, KS (72451).

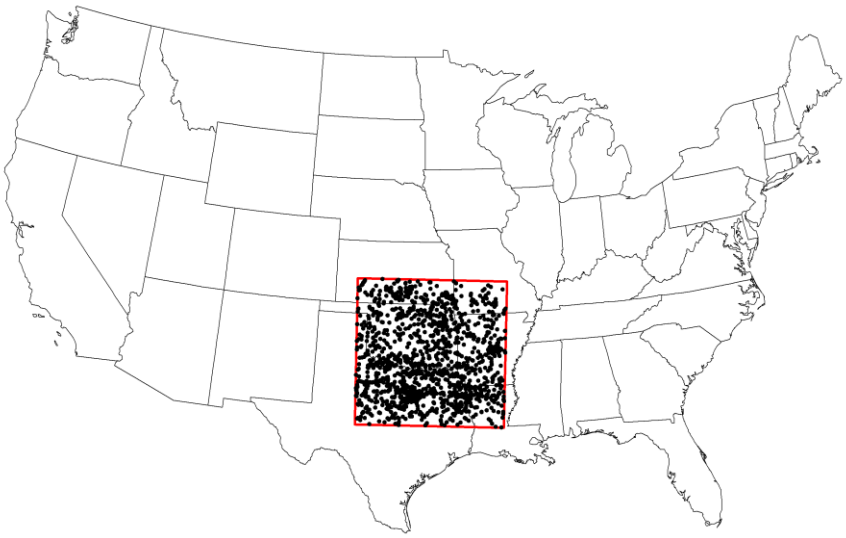

Fig. 4.17**.** Red box is the boundary for the study region for April. Black dots indicate tornado reports within the region for April from 1974 through 2009. This region contained 1,437 (20 percent) of the 7,176 tornado reports during this timeframe.

The first analysis was conducted on the pressure level at which a given isentropic surface was located. A Kruskal-Wallis test compared the median value of the isentropic pressure level on tornado days and non-tornado days between 1974 and 2009. Of the four upper air stations within the region, only one (Dodge City, KS) did not have a statistically significant change in the pressure level on each of the isentropic level (315K, 310K, 305K and 300K) on tornado days compared to that of non-tornado days (Table 4.5). The three other stations (Little Rock, AR, Fort Worth, TX and Norman, OK) recorded a significant increase in pressure on the isentropic surface, with the 300K surface having the greatest increase (lowering in height). Consequently, similar to previous sections, the 300K surface will be primary surface discussed in the below discussion.

Table 4.5**.** Kruskal-Wallis test results for the 300K isentropic level for the following variables: pressure level (hPa), wind direction (º from N), wind speed (kts) and mixing ratio (g/kg) for the five stations within study region 1 for April. Bolded values indicate those that were not significant at the 95 percentile

confidence interval ($p < 0.05$). The entire table for the 315K, 310K, 305K and 300K can be found in the Appendix A.

		300K Pressure Level (hPa)	300K Wind Direction (°)	300K Wind Speed (knots)	300K Mixing Ratio (g/kg)
Fort Worth, TX	Non-Event	817	233	23	3.76
	Event	875	205	28	9.31
	Difference	58	-28	5	5.55
	p-value	0	0	0.001	0
Little Rock, AR	Non-Event	759	269	**24**	2.44
	Event	828	225	**24**	6.12
	Difference	69	-44	0	3.68
	p-value	0	0	**0.39**	0
Norman, OK	Non-Event	785	250	26	3.02
	Event	843	213	30	7.3
	Difference	58	-37	4	4.28
	p-value	0	0	0.043	0
Dodge City, KS	Non-Event	747	264	**24**	2.79
	Event	766	233	**22**	4.12
	Difference	19	-31	-2	1.33
	p-value	0.043	0	**0.268**	0

The average increase in pressure of the 300K surface on tornado days was 51hPa with Little Rock, AR increasing 69hPa, Fort Worth, TX and Norman OK both increasing by 58hPa and Dodge City, KS increasing 19hPa. Lack of discrimination at Dodge City KS in tornado vs. non-tornado isentropic pressure is likely the result of the tight isentropic gradient (moving from ridge to trough flowing east) at the western border of the region. Fig 4.18 shows the anomaly change in the 300K isentropic surface in tornado versus non-tornado days with positive values indicating areas of isentropic troughing and negative values

indicating areas of isentropic ridging. Similar to previously discussed regions, the greatest increase in pressure is located just to the northeast of the region with an axis of greatest change running directly through the study region. In this case, the axis runs from the southwest corner up through the northeast corner of the region.

However, of particular note is the tight gradient from positive to negative change located along the western border of the region. This feature marks where the greatest potential for uplift exists and is likely to move through the region throughout the day. This feature is also the likely reason as to why Dodge City, KS did not show a significant change at each of the isentropic levels, as at higher isentropic levels Dodge City was directly along the border.

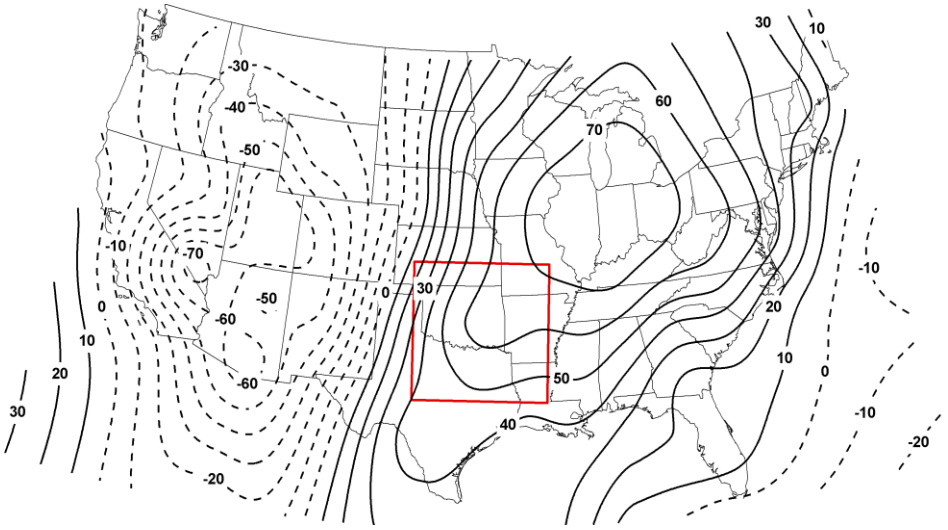

Fig. 4.18**.** 300K April Isentropic surface pressure difference calculated by taking the average pressure level of the 300K isentropic surface on tornado days minus the pressure level on non-tornado days. Solid lines indicate areas of increasing pressure (lowering heights) and dotted lines indicate areas of rising pressures (rising heights).

Second, I conducted a Kruskal-Wallis test on wind direction for the four stations within the study region. Each showed a statistically significant amount of backing wind (counterclockwise shift) on tornado days compared to the median

wind direction on non-tornado days. The average backing for the four stations was 35 degrees, or from a median wind direction of 254 degrees (west-southwest) on non-tornado days to 219 degrees (south-southwest) on tornado days. This change in wind direction and an amplified isentropic trough across the region produces an increase in uplift which could aid in thunderstorm development.

Fig 4.19 displays the average 300K isentropic pattern as well as wind speed and direction for non-tornado and tornado days. A weak isentropic trough is located across the study region on tornado days with flow oriented generally parallel to the isentropic isobars indicating little to no vertical motion within the atmosphere over the region. Conversely, the average 300K isentropic pattern for tornado days displays a well defined isentropic trough and flow nearly straight up the isentropic trough indicating a large amount of uplift. In this map as well, the boundary between the isentropic trough and ridge is visually evident along the western border of the region, as discussed above with the isentropic pressure change.

Wind speed was also statistically analyzed for differences between tornado and non-tornado days. However, as with previously discussed regions, no clear signal in wind speed emerged as most stations showed no significant change. Consequently, this study demonstrates that isentropic wind speed does not appear to be important when forecasting tornado occurrence.

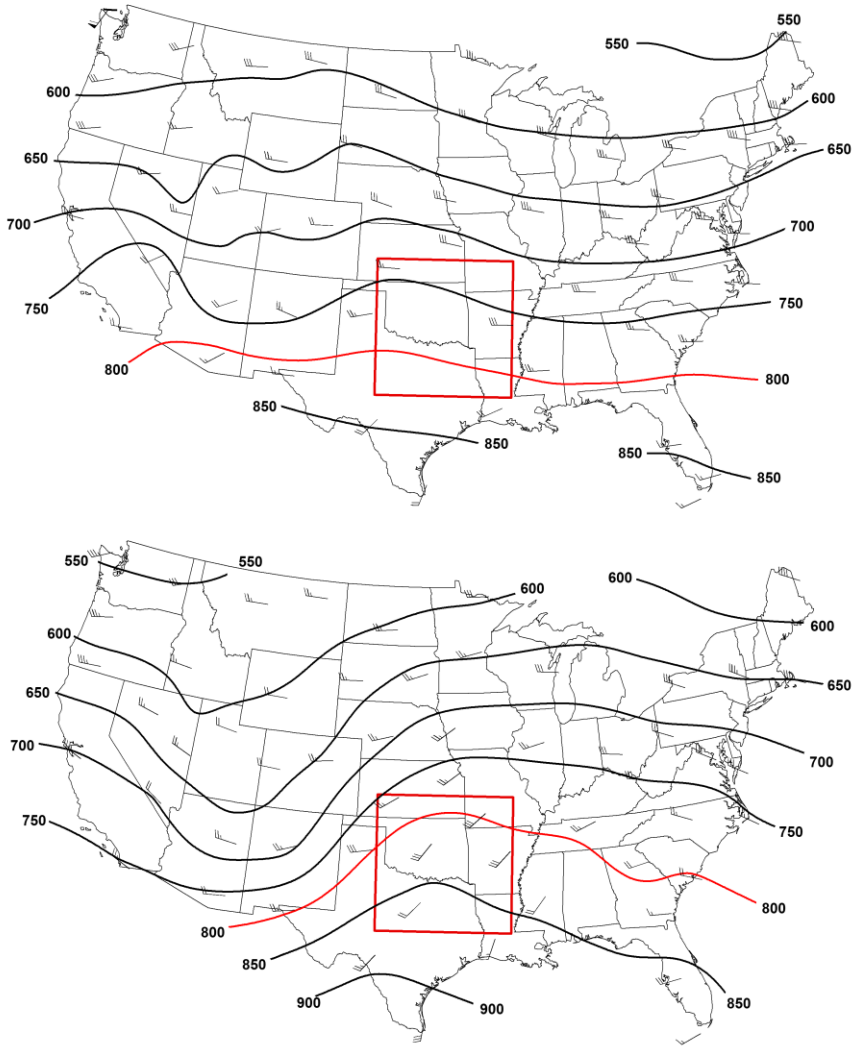

Fig. 4.19**.** (a) average 300K April isentropic surface and wind direction/speed for non-tornado days from 1974 through 2009 (b) same as the above but for tornado days. The 800 hPa isobar is highlighted in red to easily show the shift in pattern on non-tornado versus tornado days.

The deeper and more amplified isentropic trough across the region during tornado days not only leads to more uplift as a result of the wind direction shift, but it also results in the increase of moisture across the region which is a key ingredient for storm development. A Kruskal-Wallis test on mixing ratio for each of the isentropic pressure levels showed that each of the stations within the region had a statistically significant increase in mixing ratio on tornado days. The

median mixing ratio across the study region on average rose 3.71g/kg on tornado days (6.71g/kg on tornado days and 3.00g/kg on non-tornado days). This pattern (Fig 4.20) has the greatest increase located directly over the study region with an axis of maximum increase flowing from southern Texas up into Michigan. This pattern corresponds to the change in the pressure on the isentropic surface (Fig 4.18) closely.

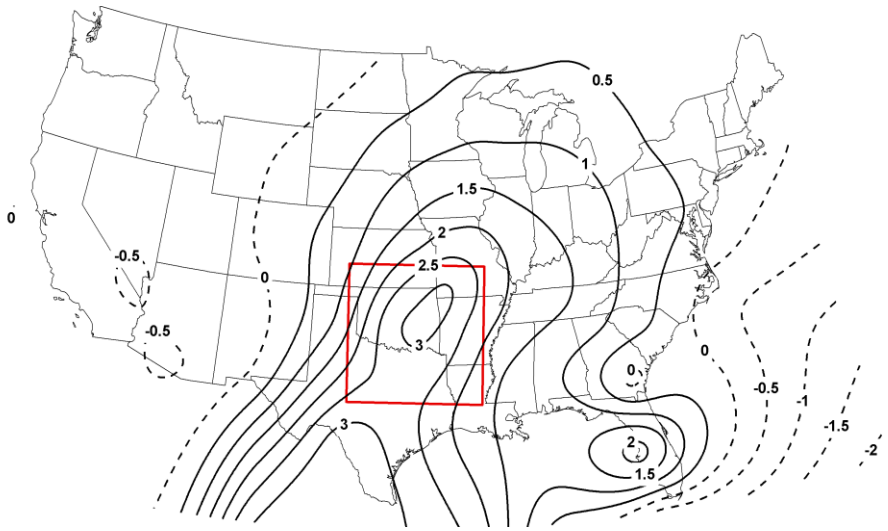

Fig. 4.20**.** 300K April Isentropic surface mixing ratio difference in g/kg calculated by taking the average mixing ratio of the 300K isentropic surface on tornado days minus the average mixing ratio on non-tornado days. Solid lines indicate areas of increased mixing ratio and dotted lines indicate areas of decreased mixing ratio.

In summary, this southern Plains region for April tornado occurrence has shown very similar results to region 1 (central southern Plains) for March in which the isentropic surface increases in pressure (decreases in height), the wind direction is backing and the mixing ratio increases on tornado days as compared to non-tornado days. For this region in April (as with previous regions), I recommend that forecasters focus on the 300K isentropic surface as it displayed the greatest change in all the above mentioned variables. On average for tornado

days, I found that the 300K isentropic surface increased in pressure 51hPa, wind direction was backing by 35 degrees and the mixing ratio increased 3.71g/kg. All of these changes on tornado days would result in additional uplift and added moisture into the region that could generate and continue to fuel tornadic storms.

g. May– Region 1 (central Great Plains)

The region I selected for May is located over the central and southern Plains and includes the states of northern Texas, Oklahoma, Kansas, and southern Nebraska. Within this region there were eight upper air stations that were used and include: Ft Worth, TX (72249), Amarillo, TX (72363), Norman, OK (72357), Dodge City, KS (72451), Topeka, KS (72456), Omaha, NE (72558), North Platte, NE (72562), and Midland, TX (72265). A total of 3,355 (28 percent) of the 11,921 tornado reports for the month of May between 1974 and 2009 were located within this region (Fig 4.21).

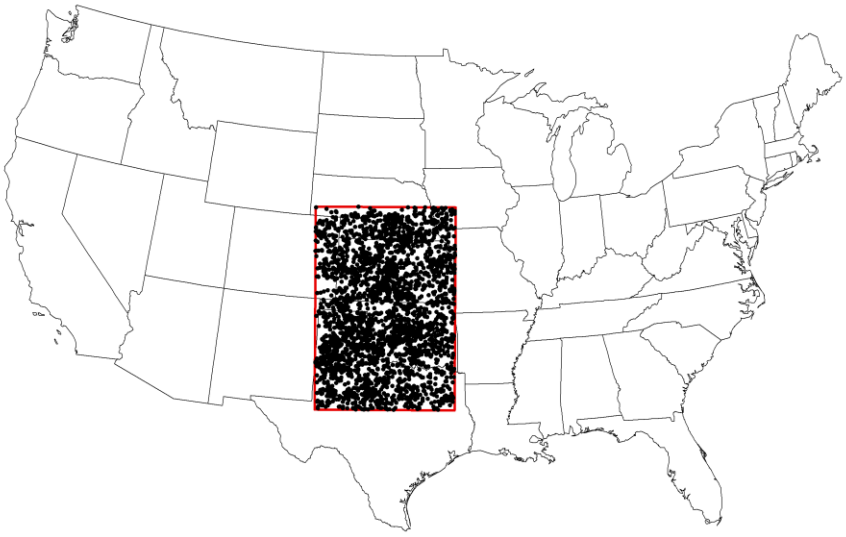

Fig. 4.21**.** Red box is the boundary for the study region for May. Black dots indicate tornado reports within the region for May from 1974 through 2009. This region contained 1,437 (20 percent) of the 7,176 tornado reports during this timeframe.

First, I conducted a Kruskal-Wallis tests on the pressure level of the four isentropic surfaces (315K, 310K, 305K and 300K), which compared the median pressure level of the isentropic surface for tornado and non-tornado days. While this month/region yielded similar results to those discussed earlier, there were several stations that were not found to be significant on each isentropic surface (Table 4.6). On the 315K isentropic surface Dodge City, KS, Omaha, NE and North Platte, KS were not statistically significant at the 95 percent confidence level, but still indicated an overall increase in pressure on tornado days. On the 310K and 305K surface North Platte, NE was the only station that was not significant but nevertheless showed a small (9hPa on 310K and 13hPa on 305K) increase in pressure on tornado days compared to non-tornado days. However, the best-performing isentropic surface as discussed for other regions above, the 300K isentropic surface, displayed a significant change in pressure on tornado days as compared to non-tornado days for all stations.

Table 4.6**.** Kruskal-Wallis test results for the 305K isentropic level for the following variables: pressure level (hPa), wind direction (º from N), wind speed (kts) and mixing ratio (g/kg) for the five stations within study region 1 for May. Bolded values indicate those that were not significant at the 95 percentile confidence interval ($p < 0.05$). The entire table for the 315K, 310K, 305K and 300K can be found in the Appendix A.

		305K Pressure Level (hPa)	305K Wind Direction (°)	305K Wind Speed (knots)	305K Mixing Ratio (g/kg)
Fort Worth, TX	Non-Event	785	233	18	6.19
	Event	827	210	23	8.21
	Difference	42	-23	5	2.02
	p-value	0	0	0.001	0

Table 4.6 (continued)

Amarillo, TX	Non-Event	760	232	21	4.75
	Event	791	224	24	5.93
	Difference	31	-8	3	1.18
	p-value	0	0.003	0	0
Norman, OK	Non-Event	757	241	**21**	5.23
	Event	801	220	**21**	7.28
	Difference	44	-21	0	2.05
	p-value	0	0	**0.733**	0
Dodge City, KS	Non-Event	732	250	**21**	4.01
	Event	764	223	**21**	5.37
	Difference	32	-27	0	1.36
	p-value	0	0	**0.402**	0
Topeka, KS	Non-Event	694	266	**22**	3.09
	Event	737	232	**21**	5.04
	Difference	43	-34	-1	1.95
	p-value	0	0	**0.206**	0
Omaha, NE	Non-Event	674	283	**25**	2.56
	Event	707	246	**22**	4.11
	Difference	33	-37	-3	1.55
	p-value	0.021	0	**0.098**	0
North Platte, NE	Non-Event	**698**	263	21	3.41
	Event	**711**	236	19	4.25
	Difference	13	-27	-2	0.84
	p-value	**0.06**	0	0.007	0
Midland, TX	Non-Event	814	197	18	6.54
	Event	854	189	25	7.09
	Difference	40	-8	7	0.55
	p-value	0	0.058	0	0

The rationale for several stations not indicating significant results at some of the isentropic surfaces is likely three-fold. First, the stations closest to the edge of the region, especially the north and west fringes of the region, would be

expected to show the weakest signal as the isentropic trough that has been identified in the other regions is normally directly centered within the region with a transition period on either side (especially the western side).

Second, during the month of May on non-tornado days a small but still apparent isentropic trough is located across the region at the higher isentropic surface (315K and 310K) which results in less of a change on those surfaces. This can be clearly seen in Fig 4.22 which shows the non-tornado and tornado pattern for each isentropic level using one pressure contour (315K: 550hPa, 310K: 650hPa, 305K: 750hPa and 300K: 850hPa) in order to obtain an idea of the pattern of each level with respect to the others.

Third, the 300K isentropic surface, which does have all stations displaying significant results, is the lowest isentropic surface to the ground. Consequently, it is most likely to discriminate critical surface contributions, especially moisture that the other surfaces might miss.

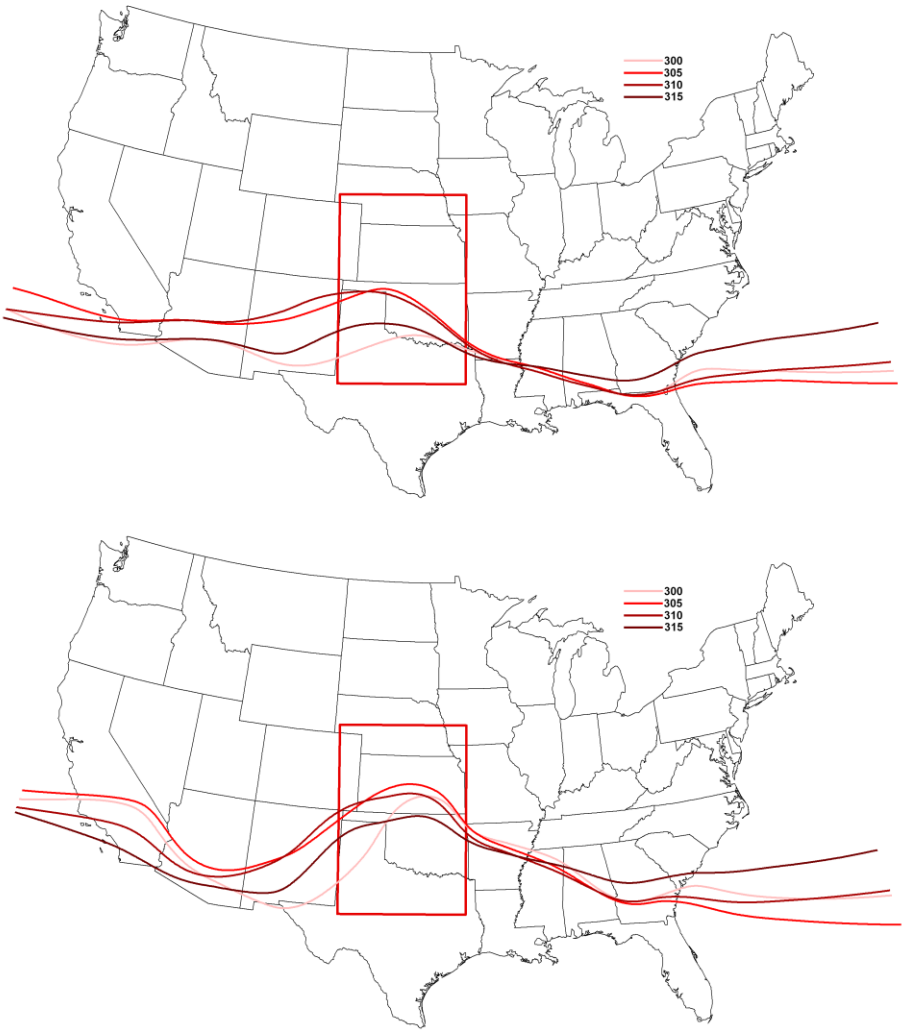

Fig. 4.22**.** Top image shows the average May isentropic pattern for a select contour for each isentropic level 315K: 550hPa, 310K: 650hPa, 305K: 750hPa and 300K: 850hPa for non-tornado days and the bottom Fig image is the same but for tornado days.

On average for tornado days the median pressure of the isentropic surface increased 35hPa with the greatest increase being 44hPa in Norman, Oklahoma on the 305K surface. This increase in pressure pattern can be seen by looking at the anomaly map for the region which I created by taking the average 305K isentropic pressure level on tornado days and subtracted out the average 305K isentropic pressure level on non-tornado days (Fig 4.23). The largest increase in

pressure, which means a more amplified trough, is located directly over the region. Also, as has been the case with all the other regions, the area of tightest gradient moving from increasing pressure (troughing) to decreasing pressure (ridging) is located just along the western border of the region. The change in pressure is not as great as has been seen in other regions primarily due to the fact that there is already the presence of a weak isentropic trough across the region for even non-tornado days.

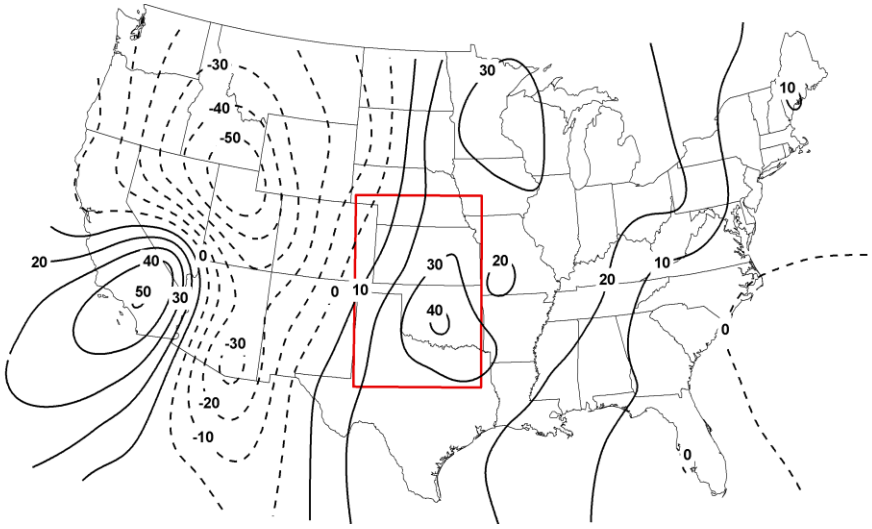

Fig. 4.23**.** 305K May Isentropic surface pressure difference calculated by taking the average pressure level of the 305K isentropic surface on tornado days minus the pressure level on non-tornado days. Solid lines indicate areas of increasing pressure (lowering heights) and dotted lines indicate areas of rising pressures (rising heights).

Secondly, wind direction may also be a key component to examine when forecasting tornadoes for this particular region. A Kruskal-Wallis test on wind direction comparing median wind direction on tornado versus non-tornado days each station on the 315K, 310K and 305K isentropic surface demonstrates a statistically significant difference. On the 300K surface, wind direction at Omaha, NE and Amarillo, TX were not significant and this is likely due to the fact they

are near the edge of the region as was discussed above. However, for all other stations, the average shift in wind direction across the region from non-tornado to tornado days was a backing wind of 23 degrees on the 305K surface. This change in wind direction and an increasing trough across the region creates added uplift. This change in both the isentropic pattern and wind direction can be seen in Fig 2.24, with a flow nearly horizontal to the contours on non-tornado days and nearly perpendicular to the contours on tornado days. When the wind direction results in a flow across isobars and up the isentropic trough, it produces uplift in the region since the flow is from higher pressure to lower pressure for the given isentropic surface. Thirdly, as was the case with the other regions, wind speed was tested but no significant difference was found with an average of around plus or minus five knots on tornado days versus non-tornado days.

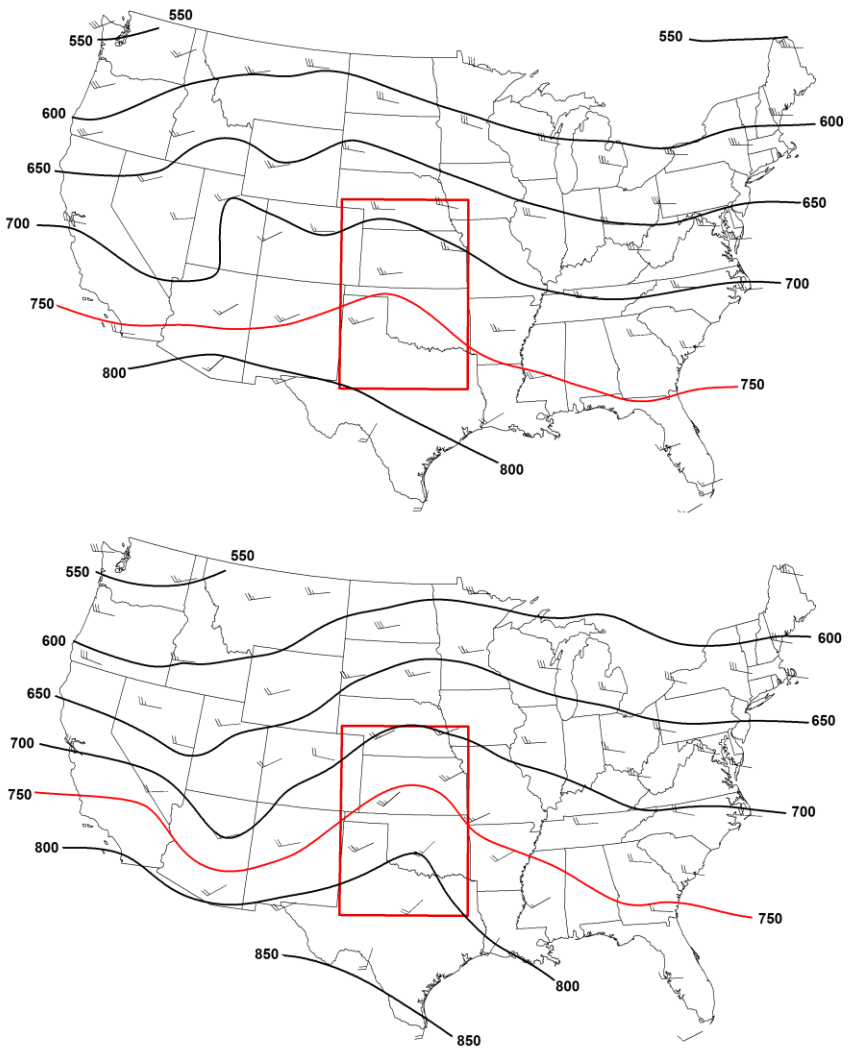

Fig. 4.24**.** (a) average 305K May isentropic surface and wind direction/speed for non-tornado days from 1974 through 2009 (b) same as the above but for tornado days. The 750 hPa isobar is highlighted in red to easily show the pattern shift from non-tornado and tornado days.

Moisture was the fourth variable examined. Given the isentropic trough that amplifies across the region on tornado days, it would be expected that moisture should increase as well. A Kurskal-Wallis test on mixing ratio does demonstrate with statistical significance that on tornado days on the 305K level that mixing ratio rises on average 1.44g/kg. All eight stations on all four isentropic surfaces displayed a statistically significant increase in mixing ratio on

tornado days as compared to non-tornado days. The greatest increase was located near the center of the region with no change, or a slight decrease, just to the west of the region (Fig. 4.25). With added moisture across the region and additional uplift as a result of the backing wind in the isentropic trough, thunderstorm development is more likely to occur and continue aiding in the possible formation of tornadic storms.

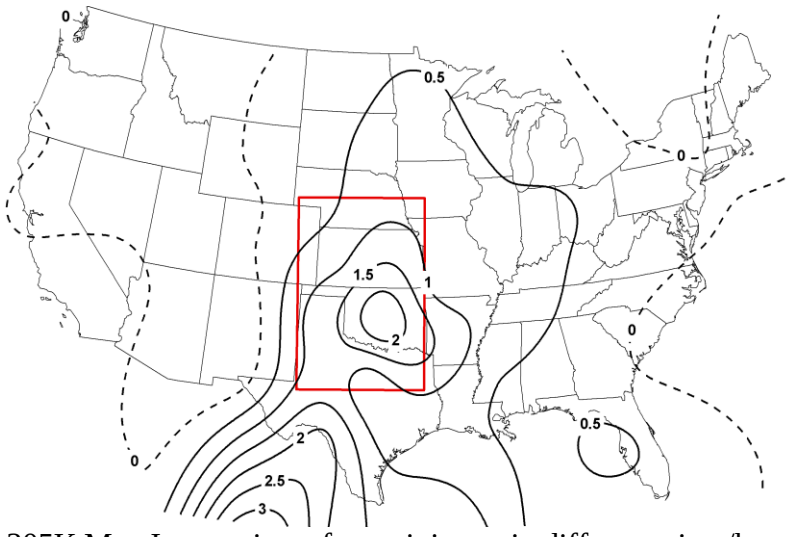

Fig. 4.25. 305K May Isentropic surface mixing ratio difference in g/kg calculated by taking the average mixing ratio of the 305K isentropic surface on tornado days minus the average mixing ratio on non-tornado days. Solid lines indicate areas of increased mixing ratio and dotted lines indicate areas of decreased mixing ratio.

In summary, several key points to examine when forecasting the possibility of tornadoes within this central Great Plains region for May is the pressure level at which an isentropic surface occurs, the wind direction and mixing ratio. For this region it is recommended to primarily use the 305K isentropic surface. With warmer temperatures across the region the 300K level in May is in rather close proximity to the surface which could actually result in the 300K surface going beneath the ground in certain locations. Even though

statistically the 300K surface shows strong results in an operational sense the 300K surface is still too close to the ground and may, during many severe weather days, go below ground level. Examining the 305K surface it was found that the surface increases in pressure on average 35hPa, the wind direction backs by 23 degrees and the mixing ratio increases on average 1.44g/kg on tornado days. All of these components come together to create added uplift and moisture in the region which can aid in thunderstorm development.

h. June – Region 1 (Upper Great Plains)

Two regions were selected to examine for the June time frame using the criterion of the distribution of tornado density across the United States. The first region was located across the Upper Plains and included the states of North Dakota, South Dakota, Nebraska, Kansas, Minnesota, western/central Iowa and the northwest portion of Missouri (Fig 4.26). Between January 1974 and December 2009, there were 2,981 tornado reports within the region which makes up twenty-two percent of the 10,363 tornado reports across the country. This was one of the largest regions examined and included eight upper air stations which included: Dodge City, KS (72451), Topeka, KS (72456), Omaha, NE (72558), North Platte, NE (72562), Rapid City, SD (72662), Aberdeen, SD (72659), Bismark, ND (72764) and Chanhassen, MN (72649).

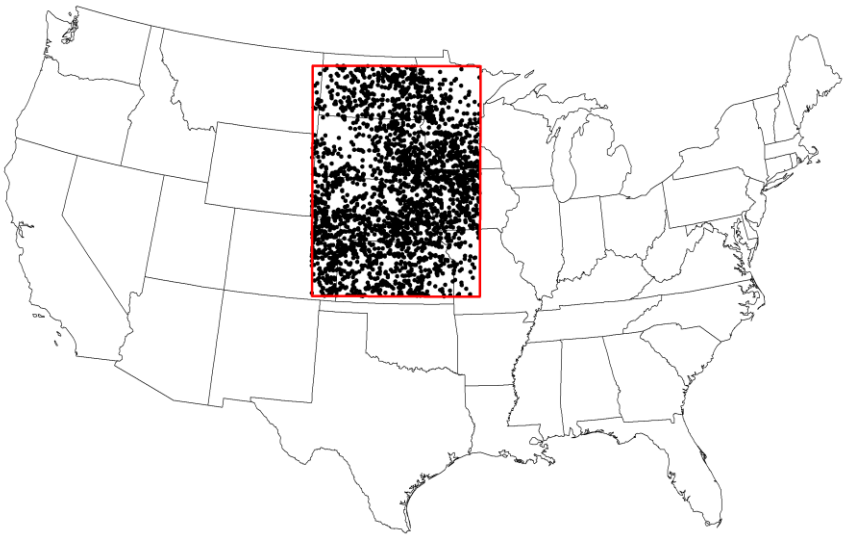

Fig. 4.26**.** Red box is the boundary for the study region for June. Black dots indicate tornado reports within the region for June from 1974 through 2009. This region contained 2,981 (22 percent) of the 10,363 tornado reports during this timeframe.

The first aspect was the pressure level at which the four isentropic levels occurred and I conducted a statistical test to determine if there was a difference in pressure on tornado days compared to non-tornado days. The Kruskal-Wallis test identified an increase in pressure on all four isentropic surfaces at all stations with each station also having a statistically significant change in pressure at the 95 percent confidence level, with the exception of the following stations: Aberdeen, SD on the 315K and 305K surfaces, Omaha, NE on the 315K surface and Bismark, ND on the 315K and 310K. The largest change in pressure was found to be on the 305K isentropic surface which coincides with the previous region and gives support for the selection during summer months of a higher potential temperature surface. This is particularly important given that a number of stations for tornado days had a pressure level of above 900hPa on the 300K surface which

could easily intersect the ground rendering the analysis useless. As a result, for the remainder of this section I will mainly focus on the 305K isentropic surface.

Table 4.7**.** Kruskal-Wallis test results for the 305K isentropic level for the following variables: pressure level (hPa), wind direction (º from N), wind speed (kts) and mixing ratio (g/kg) for the five stations within study region 1 for June. Bolded values indicate those that were not significant at the 95 percentile confidence interval ($p < 0.05$). The entire table for the 315K, 310K, 305K and 300K can be found in the Appendix A.

		305K Pressure Level (hPa)	305K Wind Direction (°)	305K Wind Speed (knots)	305K Mixing Ratio (g/kg)
Dodge City, KS	Non-Event	823	215	**16**	7.65
	Event	866	206	**17**	9.93
	Difference	43	-9	**1**	2.28
	p-value	0	0	**0.099**	0
Topeka, KS	Non-Event	781	257	**15**	7.03
	Event	838	240	**14**	8.9
	Difference	57	-17	**-1**	1.87
	p-value	0	0.027	**0.702**	0
Omaha, NE	Non-Event	753	275	**19**	5.43
	Event	795	233	**18**	6.96
	Difference				
	p-value	0.001	0	**0.427**	0
North Platte, NE	Non-Event	785	241	**15**	6.42
	Event	826	220	**15**	7.71
	Difference	41	-21	**0**	1.29
	p-value	0	0	**0.612**	0
Rapid City, SD	Non-Event	756	263	**17**	5.14
	Event	770	238	**17**	5.85
	Difference	14	-25	**0**	0.71
	p-value	0.042	0.003	**0.336**	0
Aberdeen, SD	Non-Event	**720**	282	20	**3.69**
	Event	**731**	253	20	**4.63**
	Difference	**11**	-29	0	**0.94**
	p-value	**0.136**	0	0.3	**0.068**

Table 4.7 (continued)

Bismarck, ND	Non-Event	702	283	**19**	3.35
	Event	717	265	**18**	4.29
	Difference	15	-18	**-1**	0.94
	p-value	0.036	0	**0.193**	0.001
Chanhassen, MN	Non-Event	705	**263**	**23**	3.32
	Event	735	**254**	**21**	4.49
	Difference	30	**-9**	**-2**	1.17
	p-value	0.007	**0.258**	**0.324**	0.019

First, the Kruskal-Wallis test yielded valuable results on the variation in pressure of an isentropic surface between tornado and non-tornado days. On the 305K surface, on average the median isentropic pressure level increased 30hPa on tornado days as compared to non-tornado days. The greatest increase was at Topeka, KS where the pressure increased 57hPa, which went from a pressure level on the 305K isentropic surface of 781hPa on non-tornado days to 838hPa on tornado days. The anomaly pattern for the 305K isentropic surface (Fig. 4.27) was created by taking the average 305K isentropic pattern on tornado days and subtracting it from the 305K isentropic pattern on non-tornado days. The largest increase in pressure was located directly over the study region with an axis of pressure increase dropping south from southeast South Dakota into north central Oklahoma. This is a slightly different pattern compared to the other regions/month combinations discussed thus far, as in those other cases the area of highest pressure increases was generally located to the northeast of the study region. This pattern of the greatest pressure increase directly over the region could mean that the isentropic trough ends near the top of the study region and that the

trough itself is more narrow (west to east) as compared to the other regions discussed so far.

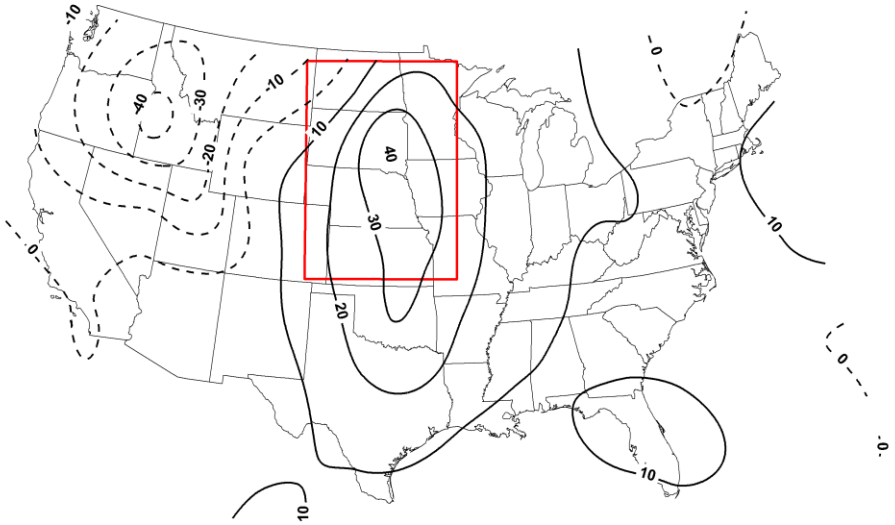

Fig. 4.27. 305K June Isentropic surface pressure difference calculated by taking the average pressure level of the 305K isentropic surface on tornado days minus the pressure level on non-tornado days. Solid lines indicate areas of increasing pressure (lowering heights) and dotted lines indicate areas of rising pressures (rising heights).

To further examine this isentropic pressure increase over the study region (suggesting a small isentropic trough as compared to other regions) , I created two maps with the first showing the average 305K isentropic surface on non-tornado days and the second displaying the average 305K isentropic surface for tornado days (Fig. 4.28).

During non-tornado days an isentropic trough is located across the southernmost portion of the study region in Kansas with a more zonal isentropic pattern across the central and northern portion of the region. Conversely, on tornado days, the isentropic trough which is normally located to the south builds northward and becomes well-established across the central portion of the study region. This leads to a slight flattening of the trough toward the north of the

region and is also the pattern that was expected to be seen based off the anomaly pattern (Fig. 4.27). This trough which is also fairly narrow in west to east extent could result in added uplift aiding thunderstorm development.

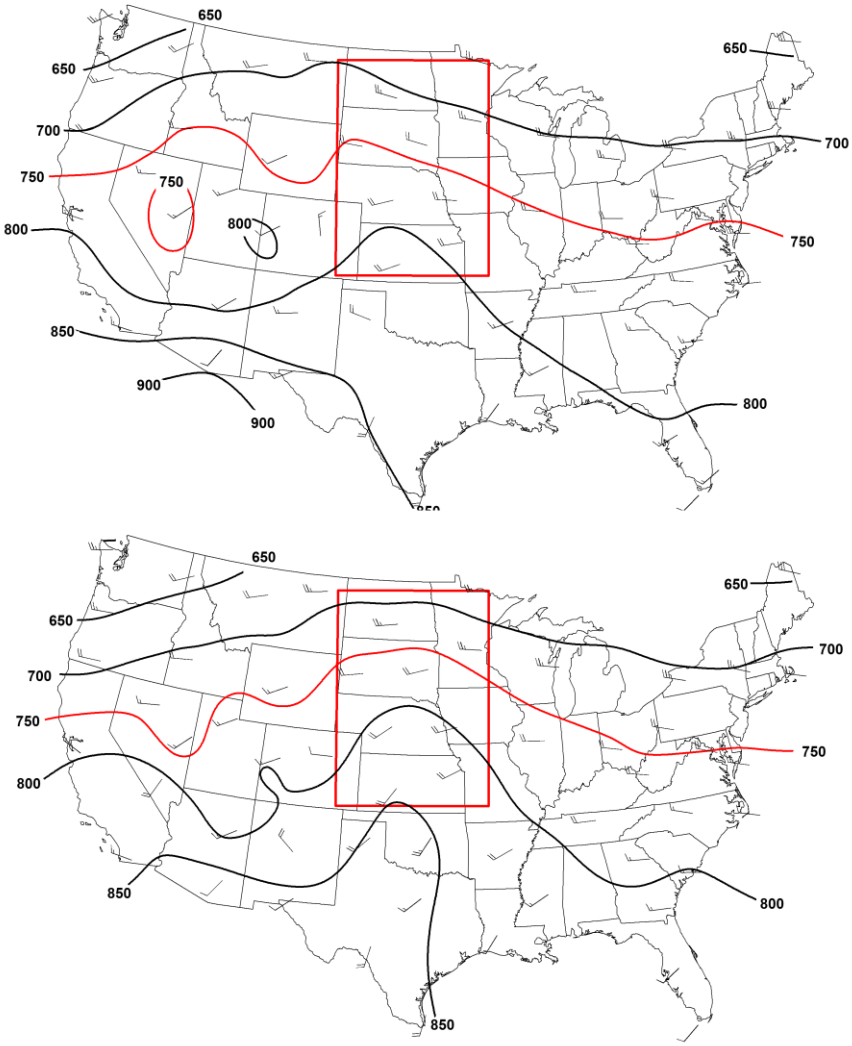

Fig. 4.28**.** (a) average 305K June isentropic surface and wind direction/speed for non-tornado days from 1974 through 2009 (b) same as the above but for tornado days. The 750 hPa isobar is highlighted in red to easily show the shift in pattern from non-tornado to tornado days.

While a deepening trough across a region can create uplift due to the elevation difference on the isentropic surface, wind direction and speed are crucial

to examine in order to determine flow (and hence uplift) on the given isentropic surface. I performed Kruskal-Wallis tests on both wind direction and wind speed comparing the medians of the two variables on tornado versus non-tornado days. First, wind direction has a significant difference at all stations with the exception of Topeka, KS on the 315K surface and Chanhassen, MN on the 315K, 310K and 305K surfaces. As has been the case in all the region/month combinations so far, the wind direction on tornado days was found to be backing (counterclockwise change) with the 305K surface backing on average 21 degrees from 260 degrees (west) on non-tornado days to 239 degrees (southwest) on tornado days. On non-tornado days, the wind direction is generally parallel to the isentropic surface in the northern and central portion of the region with slight up sloping flow found in the southern portion of the region associated with the isentropic trough. On tornado days a fairly dramatic shift can be seen, with wind direction crossing the isentropic isobars in the southern and central portion of the study region. This indicates up-sloping flow which could help induce the growth and continuation of tornadic thunderstorms in the region (Fig. 4.28).

Secondly, I analyzed wind speed but identified Dodge City, KS as the only station having a statistically significant change on tornado days and that change was only two to three knots, so for forecasting purposes wind speed (similar to previous region/month combinations) is not a key factor to examine when forecasting tornadoes using isentropic analysis.

With a deepening isentropic trough and backing winds across the region resulting in added uplift, moisture becomes the next key aspect to examine. The

general rule of thumb as first defined by Namias (1939) with isentropic analysis is that isentropic troughs are associated with an increase in moisture and I find that this rule holds true in this case. I conducted a Kruskal-Wallis test on mixing ratio comparing non-tornado and tornado days and each station for each isentropic level. With the exception of Aberdeen, SD on the 305K surface, all stations indicated a statistically significant, at the 95 percent confidence level, increase in mixing ratio on tornado days. The greatest increase was noted on the 305K isentropic surface with an average increase across the study region of 1.34g/kg. The largest increase was located in the southern portion of the study region with an axis of greatest increases running northward from the Kansas/Oklahoma state line up through Minnesota (Fig. 4.19). With this added moisture and uplift already shown to be increased thunderstorm initiation and continuation are highly probable within this region when this type of isentropic pattern is present.

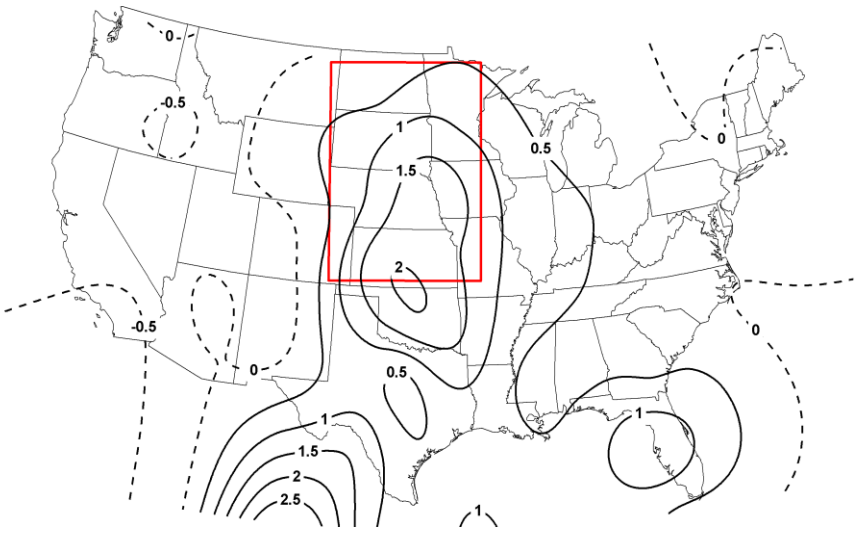

Fig. 4.29**.** 305K June Isentropic surface mixing ratio difference in g/kg calculated by taking the average mixing ratio of the 305K isentropic surface on tornado days minus the average mixing ratio on non-tornado days. Solid lines indicate areas of increased mixing ratio and dotted lines indicate areas of decreased mixing ratio.

In summary, I have shown three key factors on isentropic surfaces that could aid in the forecasting of severe thunderstorms within this region. Statistical analyses on the pressure level as well as the wind direction, wind speed and mixing ratio of each isentropic surface yielded a number of potential discriminators to tornadic activity in the upper Great Plains in June. First, it was found that on tornado days the 305K isentropic pressure surface on average increased 30hPa, which indicated an isentropic trough developing into the region. For this region it should be noted that it was a fairly narrow isentropic trough which could be seen in Figs. 4.27 and 4.28 with the greatest increase in troughing located in the central and southern portions of the region.

Second, with the isentropic trough present and an average backing wind across the region of 21 degrees, nearly every location with the exception of the very northern portion of the region, had an increase in uplift on the isentropic surface due to this change in wind direction on tornado days. Third and finally, the mixing ratio was also found to increase on average 1.34g/kg during tornado days. With the added uplift due to the isentropic trough and wind direction, as well as the increase in moisture content, all of which are important ingredients for thunderstorm development, I can conclude that isentropic analysis does a respectable job discriminating these condition on tornado days and could help forecasters more easily determine areas of greatest threat based on the location of the isentropic trough and subsequent wind direction shifts. It should be noted that the 305K surface was used as it demonstrated the greatest change in all the variables examined, with similar but less dramatic changes noted on the 310K and

315K surface. The 300K surface, used in previous month/region combinations, was disregarded in this region due to it's intersection with the ground across portion of the study region, so I recommend as to forecasters they should mainly focus on the 305K surface.

i. June – Region 2 (Great Lakes)

The second prominent region of high density tornado reports for June is located in the Great Lakes region which included the states of Illinois, Indiana and western Ohio (Fig. 4.30). Only sixty-three percent of the tornado reports from 1974 through 2009 were within this region as there was a high density of tornado reports which warranted an investigation into this area. Three upper air stations were located in this area and used for analysis which included: Davenport , IA (74455), Lincoln, IL (74560) and Wilmington, OH (72426).

Fig. 4.30**.** Red box is the boundary for the second study region for June. Black dots indicate tornado reports within the region for June from 1974 through 2009. This region contained 652 (3 percent) of the 10,363 tornado reports during this timeframe.

As with previous region/month combinations, I analyzed pressure level, wind direction, wind speed and mixing ratio of the isentropic surface for discrimination of tornado versus non-tornado conditions for the region. First, I compared the change in pressure level of the four isentropic surfaces (315K, 310K, 305K and 300K) on tornado versus non-tornado days using a Kruskal-Wallis test. Using this test, I found that each station within the region for each isentropic level displayed a statistically significant increase in pressure on tornado days at the 95 percent confidence level (Table 4.8).

Table 4.8**.** Kruskal-Wallis test results for the 305K isentropic level for the following variables: pressure level (hPa), wind direction (º from N), wind speed (kts) and mixing ratio (g/kg) for the five stations within study region 2 for June. Bolded values indicate those that were not significant at the 95 percentile confidence interval ($p < 0.05$). The entire table for the 315K, 310K, 305K and 300K can be found in the Appendix A.

		305K Pressure Level (hPa)	305K Wind Direction (°)	305K Wind Speed (knots)	305K Mixing Ratio (g/kg)
Davenport, IA	Non-Event	744	262	**19**	4.86
	Event	779	237	**20**	7.28
	Difference	35	-25	**1**	2.42
	p-value	0.013	0.005	**0.102**	0
Lincoln, IL	Non-Event	761	265	19	5.64
	Event	794	244	24	8.01
	Difference	33	-21	5	2.37
	p-value	0.001	0.001	0.039	0
Wilmington, OH	Non-Event	749	**262**	**19**	5.45
	Event	797	**247**	**20**	7.88
	Difference	48	**-15**	**1**	2.43
	p-value	0	**0.059**	**0.908**	0

The average increase in pressure on the 305K isentropic surface was 39hPa, with the highest increase being at Willmington, OH in the northeastern portion of the study region. As with the other region (Upper Great Plains) for June, I disregarded the 300K surface as some stations had a median pressure on the 300K surface around 925hPa which could go beneath the surface, resulting in erroneous values at the 300K isentropic level. As a result the 305K isentropic surface will primarily be discussed in this section and is recommended for use by anyone forecasting in this region.

I created the 305K anomaly pattern by subtracting the average isentropic pattern on tornado days from the isentropic pattern on non-tornado days and found that the greatest increase in pressure is along an axis from northeast of the region running down to southwest of the region (Fig. 4.1). Also of note is the anomalous isentropic ridge over the upper Midwest with the boundary between isentropic ridging and troughing being located just to the northwest of the study region which could induce additional uplift as it moves through the region.

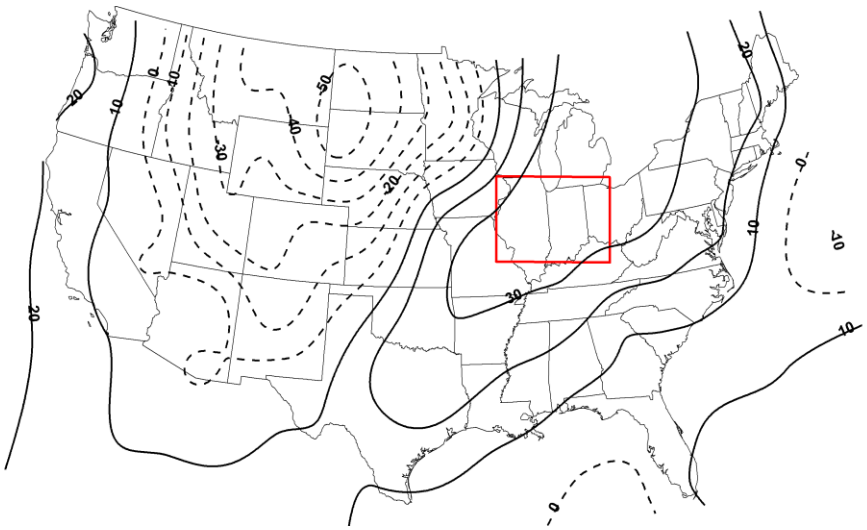

Fig. 4.31**.** 305K June Isentropic surface pressure difference calculated by taking the average pressure level of the 305K isentropic surface on tornado days minus the pressure level on non-tornado days. Solid lines indicate areas of increasing pressure (lowering heights) and dotted lines indicate areas of rising pressures (rising heights).

On the 305K surface (Fig. 4.32), and the same is observed on the 310K and 315K surface, a broad isentropic ridge is located across the study region during non-tornado days. The reverse is true for tornado days with a rather broad isentropic trough across the study region. The axis of the trough extrends from northern Michigan down through northern Missouri, indicating that it would move through the region throughout the day, resulting in possible uplift as the backside of the trough moved in (moving from higher pressure to lower pressures). While this trough is not as well-defined as the first region/month combination I examined, in June the impacts of the trough could be the same, when examining wind direction/speed and mixing ratio.

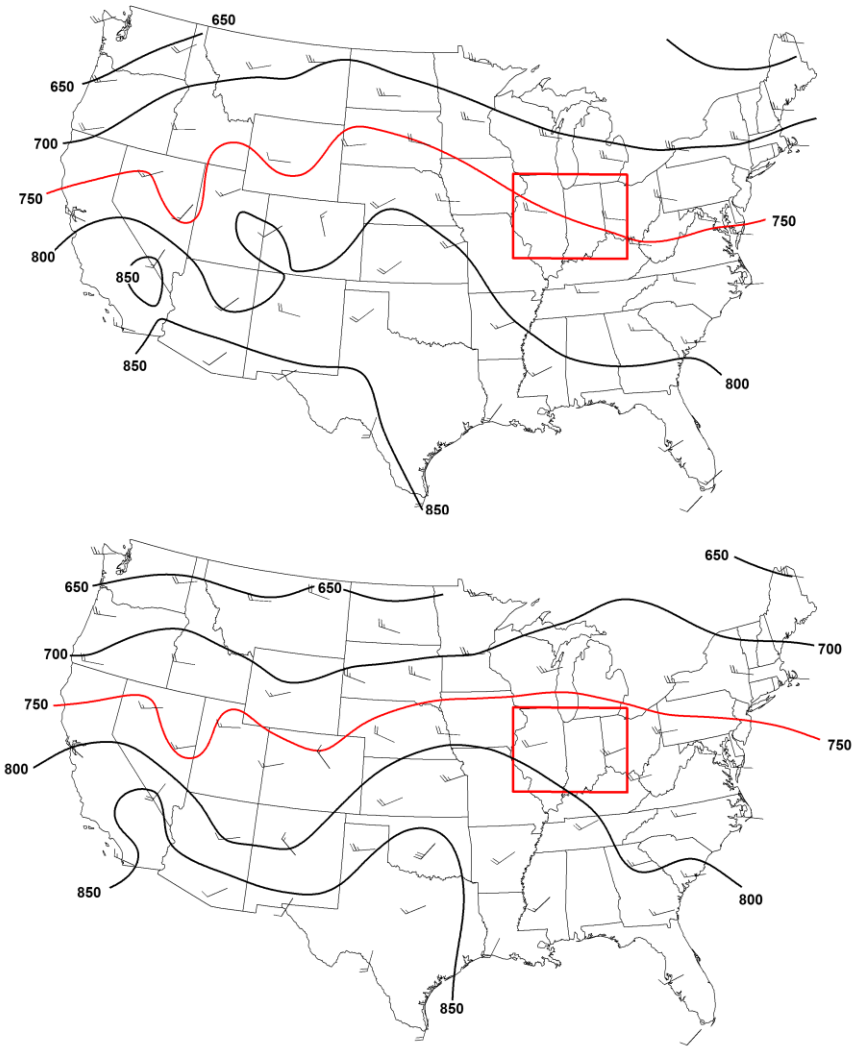

Fig. 4.32**.** (a) average 305K June isentropic surface and wind direction/speed for non-tornado days from 1974 through 2009 (b) same as the above but for tornado days. The 750 hPa isobar is highlighted in red to easily show the shift in pattern on non-tornado days compared to tornado days.

With a broad isentropic trough across the region on tornado days it is important to examine wind speed and direction to see if the trough is also associated with increased ascent due to the flow on the given isentropic surface. To conduct this analysis I used a Kruskal-Wallis test and found that each of the stations, with the exception of Wilmington, OH, had a statistically significant

change in wind direction on tornado days when compared to non-tornado days on each of the isentropic levels. Wilmington, OH likely did not have a statistically significant change due to its location on the very eastern edge of the study region. Given that only the 12Z soundings used in this dissertation , it is likely that the change was not as great that far across the region.

Even though Wilmington OH did not have a statistically significant change, it still indicated a backing (counterclockwise shift) wind on tornado days as did the other two stations within the region. On average the wind was found to back by 20 degrees, which takes the wind direction from an average of 263 degrees (west) on non-tornado days to 234 degrees (southwest) on tornado days. This shift in wind direction and the development of the isentropic trough on tornado days leads to increasing up slope flow on the isentropic surface (Fig. 2.24) with the wind no longer flowing parallel to the isobars like on non-tornado days, but to be more perpendicular indicating up-sloping flow across the region.

Once again, like the other regions/month combinations, wind direction was statistically significant and helped induce additional uplift across the study region. Also, as seen in the other region/month combinations, wind speed showed no consistent statistical significance with the largest changes being on the order of two to five knots. As a result of that test, wind speed is not considered to be important to examine for at least this scale of a study.

With increased uplift being found across the region, , thunderstorm development is likely if moisture is present. A Kruskal-Wallis test can establish if a difference in median mixing ratio was present for non-tornado and tornado days.

I found that each station on each isentropic level had a statistically significant increase in mixing ratio on tornado days compared to that of non-tornado days. On the 305K isentropic level, for example, the average median mixing ratio across the study region for non-tornado days was 5.31g/kg while on tornado days it was 7.72g/kg which results in an increase of 2.41g/kg on tornado days. Examining this spatially, the greatest increase in mixing ratio is over the western portion of the region with an axis running from northern Michigan into central Missouri, which closely matches the axis of the isentropic trough discussed above. With this added moisture and uplift from the isentropic trough and shift in wind direction, thunderstorm development is most certainly probable across this region.

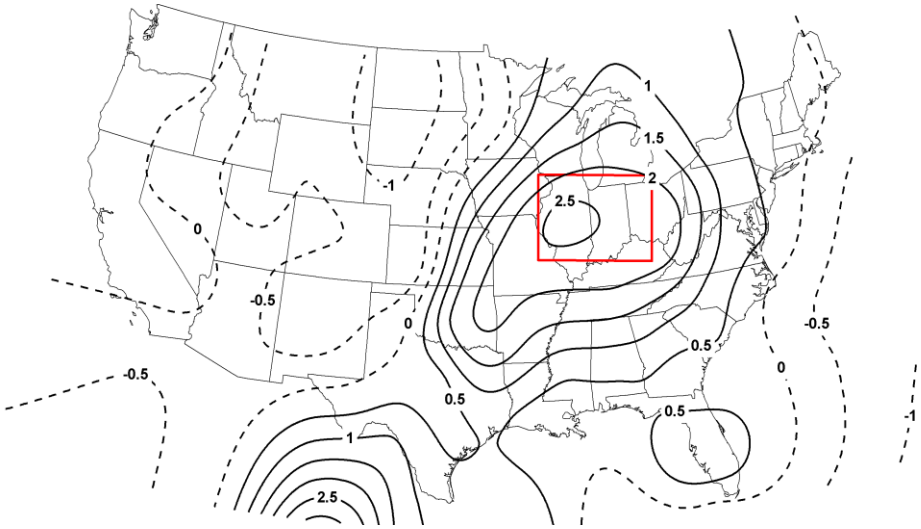

Fig. 4.35. 305K June Isentropic surface mixing ratio difference in g/kg calculated by taking the average mixing ratio of the 305K isentropic surface on tornado days minus the average mixing ratio on non-tornado days. Solid lines indicate areas of increased mixing ratio and dotted lines indicate areas of decreased mixing ratio

In summary, comparison of tornado versus non-tornado days for the Great Lakes region in June shows that isentropic analysis can be a useful tool in

forecasting tornadic conditions. Within this particular region both the pressure level of a given isentropic surface and the mixing ratio have statistically significant differences in median from non-tornado and tornado days for each station and isentropic surface. On tornado days the pressure level of each isentropic level increases by as much as 39hPa (305K surface). Mixing ratio also increases on each level during tornado days with an increase of 2.41g/kg on the 305K surface. Wind direction was found to be a significant variable with the exception of Wilmington, OH located on the very eastern edge of the region; however, on average, the median wind direction for Wilmington—as with the other stations—was found to be backing by 20 degrees on tornado days which resulted in a more up sloping flow on the 305K surface across the study region

j. July – Region 1 (Upper Plains)

For the month of July, two areas with a high density of tornado reports were found. The first was located over the upper Plains (Fig. 4.36) with a second major tornadic region located over the mid-Atlantic and eastern Great Lakes states. The first region contained 1,665 of the 5,866, or twenty-eight percent of tornado reports from 1974 through 2009. As was the case for the first region of June, this region was one of the largest and included nine upper air stations that were used in the analysis. These stations included: Denver, CO (72469), Dodge City, KS (72451), Topeka, KS (72456), Omaha, NE (72558), North Platte, NE (72562), Rapid City, SD (72662), Aberdeen, SD (72659), Bismark, ND (72764) and Chanhassen, MN (72649).

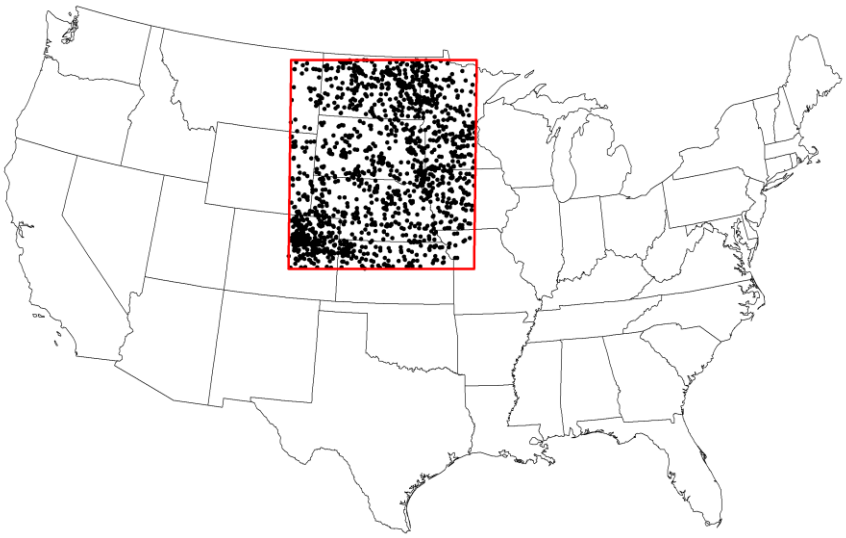

Fig. 4.36**.** Red box is the boundary for the study region for July. Black dots indicate tornado reports within the region for July from 1974 through 2009. This region contained 1,665 (28 percent) of the 5,866 tornado reports during this timeframe.

I started by examining the pressure level of the four isentropic levels (315K, 310K, 305K and 300K) using a Kruskal-Wallis test in order to assess whether there was a difference in median pressure on the isentropic surface for non-tornado days compared to tornado days. However, most importantly, I discovered that the lowest possible level that can be used is 310K, as the lower isentropic surfaces (300K and 305K) went below ground level rendering the isentropic analysis useless. As a result, for this region the primary focus will be on the 310K isentropic surface. With regards to pressure change between tornado and non-tornado days for the 310K surface, I found that unlike the other regions discussed so far, a number of upper air stations indicated a decrease in pressure (raising of height) for the isentropic surface on tornado days. Stations primarily in the northern portion of the region, specifically, Rapid City, SD, Aberdeen, SD and Bismarck, ND, had a decrease in pressure of the isentropic surface on tornado

days with Chanhassen indicating no change in median pressure on tornado days as compared to non-tornado days (Table 4.9).

Table 4.9**.** Kruskal-Wallis test results for the 310K isentropic level for the following variables: pressure level (hPa), wind direction (º from N), wind speed (kts) and mixing ratio (g/kg) for the five stations within study region 1 for July. Bolded values indicate those that were not significant at the 95 percentile confidence interval ($p < 0.05$). The entire table for the 315K, 310K, 305K and 300K can be found in the Appendix A.

		310K Pressure Level (hPa)	310K Wind Direction (°)	310K Wind Speed (knots)	310K Mixing Ratio (g/kg)
Dodge City, KS	Non-Event	795	226	15	8.39
	Event	830	219	16	9.5
	Difference	35	-7	1	1.11
	p-value	0	0.063	0.044	0
Topeka, KS	Non-Event	741	255	**17**	7.02
	Event	760	242	**18**	8.11
	Difference	19	-13	**1**	1.09
	p-value	0	0.018	**0.173**	0
Omaha, NE	Non-Event	**741**	**271**	**16**	7.14
	Event	**762**	**252**	**18**	7.88
	Difference	**21**	**-19**	**2**	0.74
	p-value	**0.077**	**0.06**	**0.059**	0.007
North Platte, NE	Non-Event	774	228	**14**	7.88
	Event	791	220	**13**	8.17
	Difference	17	-8	**-1**	0.29
	p-value	0.005	0.017	**0.058**	0
Rapid City, SD	Non-Event	**767**	266	**14**	6.15
	Event	**755**	252	**14**	6.68
	Difference	**-12**	-14	**0**	0.53
	p-value	**0.267**	0.037	**0.426**	0.004
Aberdeen, SD	Non-Event	**719**	**291**	**19**	**4.75**
	Event	**716**	**279**	**21**	**5.09**
	Difference	**-3**	**-12**	**2**	**0.34**
	p-value	**0.867**	**0.094**	**0.162**	**0.203**

Table 4.9 (continued)

Bismarck, ND	Non-Event	698	285	**19**	**4.25**
	Event	673	277	**21**	**4.19**
	Difference	-25	-8	**2**	**-0.06**
	p-value	0.005	0.027	**0.092**	**0.88**
Chanhassen, MN	Non-Event	**685**	**284**	**22**	**3.44**
	Event	**685**	**291**	**22**	**3.72**
	Difference	**0**	**7**	**0**	**0.28**
	p-value	**0.748**	**0.373**	**0.844**	**0.183**
Denver, CO	Non-Event	771	**267**	9	**6.62**
	Event	774	**255**	9	**6.57**
	Difference	3	**-12**	0	**-0.05**
	p-value	0.023	**0.301**	0.001	**0.904**

Of these stations, Bismarck, ND was the only station whose pressure change between tornado and non-tornado days was statistically significant at the 95 percent confidence level, but, an apparent spatial signal does exist in that the other northern stations indicated a decrease in pressure.

Conversely, the stations in the southern portion of the region, specifically, Dodge City, KS, Topeka, KS, Omaha, NE, North Platte, NE and Denver, CO all displayed an increase in the 310K isentropic pressure on tornado days, with the majority of those stations being statistically significant (the exception being Omaha, NE). The greatest change in pressure was evident at Dodge City, KS where the pressure on tornado days increased 35hPa and the greatest decrease in pressure was 25hPa in Bismarck, ND.

This contrasting spatial pattern is evident when examining the anomaly pattern. That pattern was created by taking the average 310K isentropic pattern

on tornado days and subtracting it from the average 310K isentropic pattern on non-tornado days (Fig. 4.37). The greatest increase in pressure was located across the southeast portion of the region stretching eastward into Illinois and Indiana, with the northern portion of the region, especially the northwest corner showing a decrease in pressure on the 310K surface. This type of pattern is likely the result of the monsoonal isentropic trough that develops across the entire western United States during the monsoon season as was found by Namias (1949).

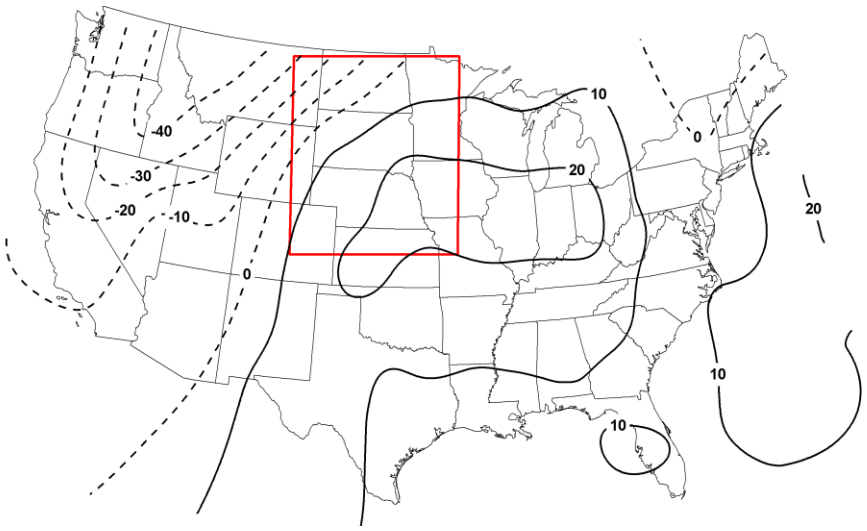

Fig. 4.37**.** 310K Isentropic surface pressure difference calculated by taking the average pressure level of the 310K July isentropic surface on tornado days minus the pressure level on non-tornado days. Solid lines indicate areas of increasing pressure (lowering heights) and dotted lines indicate areas of rising pressures (rising heights).

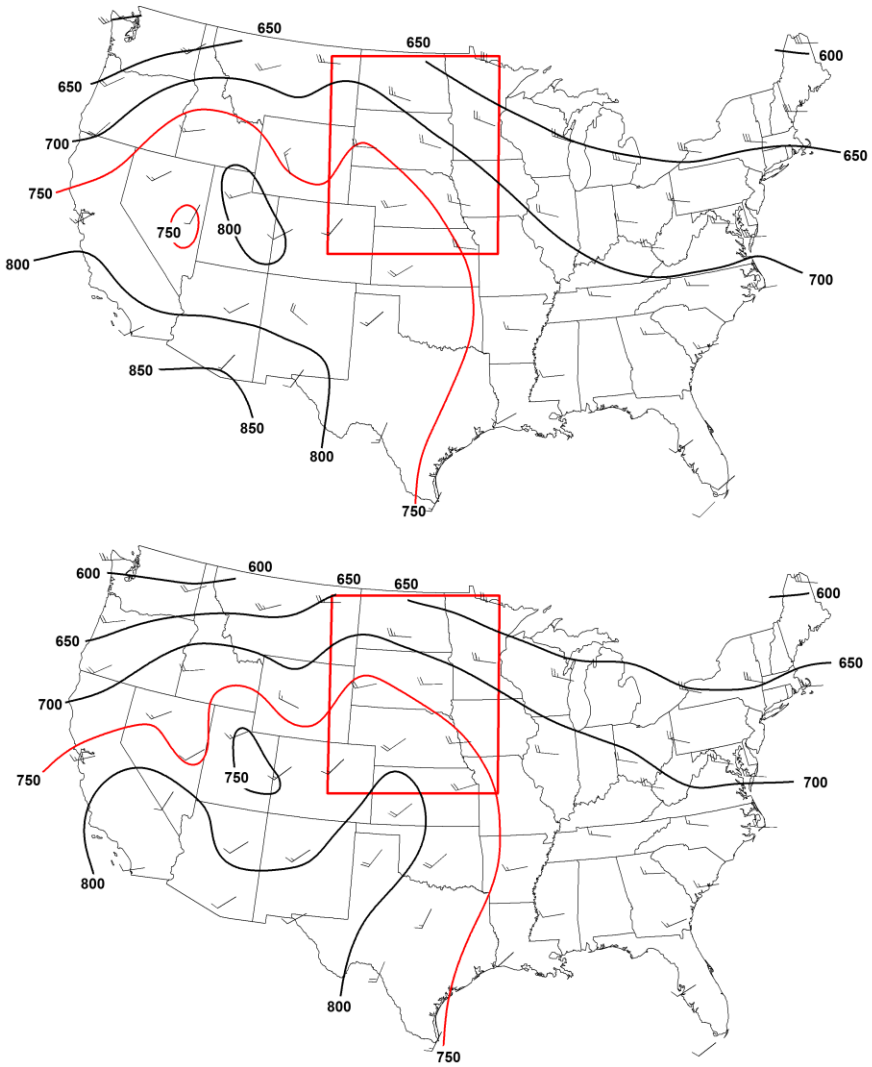

Fig. 4.38**.** (a) average 310K July isentropic surface and wind direction/speed for non-tornado days from 1974 through 2009 (b) same as the above but for tornado days. The 750 hPa isobar is highlighted in red to easily show the shift in pattern on non-tornado days compared to tornado days

This spatial difference is evident when the actual 310K surfaces for tornadoes and non-tornadoes area are plotted (Fig. 4.38) The prominent feature shown on both maps is the isentropic trough over the entire western United States which is associated with the North American Monsoon season. During non-tornado days this large scale isentropic trough seems to be well established across

the west with a north to south isentropic trough axis. On tornado days this prominent isentropic trough is seen to shift eastward with the isentropic trough axis running from the center of the study region down to the southwest into New Mexico. This shift in the large scale isentropic trough is likely the main reason why the northwest corner of the study region displays a decrease in pressure, whereas the southern portion shows an increase in pressure on the 310K surface as the monsoonal isentropic trough builds into that region. The shift of this trough could result in additional uplift as will be discussed in the next paragraphs.

Wind velocity is the next variable under examination for this region/month combination. I conducted a Kruskal-Wallis test and, similar to all previous region/month combinations, found a backing wind on tornado days compared to non-tornado days on the 310K surface for all stations, with the exception of Chanhassen, MN. On average across the study region the wind was found to be 264 degrees (west) on non-tornado days and 254 (west-southwest)_degrees on tornado days with the greatest change being in the southern portion of the region, where Omaha, NE had a backing wind of 19 degrees on tornado days. This shift in wind direction and isentropic pattern leads to additional uplift across primarily the southern and central portion of the region; however, it should be noted that even during non-tornado days isentropic lift across the region is high due to the overall synoptic pattern during this time of the year. Wind speed was also examined, but similar to other region/month combinations discussed thus far, had no statistical significance with change in wind speed on tornado versus non-tornado days. Changes were on the order of one to two knots. As a result, wind

direction is a much more useful element on the 310K surface to examine compared to wind speed.

I conducted a Kruskal-Wallis test on mixing ratio to determine if there was a difference in median mixing ratio values on tornado days versus non-tornado days. Each upper air station within the region indicated an increase in mixing ratio with the exception of Bismarck, ND and Denver, CO. These exceptions can be attributed to eastward movement of a large scale isentropic trough associated with the monsoon season during tornado days. The stations that indicated a statistically significant(95 percent confidence level) increase in mixing ratio were Dodge City, KS with an increase of 1.11g/kg, Topeka, KS +1.09g/kg, Omaha, NE, + 0.74g/kg, North Platte, NE +0.29g/kg and Rapid City, SD, + 0.53g/kg. This pattern can also be seen on a mixing ratio anomaly map (Fig. 4.39), with the highest increase in mixing ratio on the 310K surface located in the southeastern portion of the region and a slight decrease in mixing ratio in the northwest corner. This matches very closely with the amplified isentropic troughing and ridging seen in those areas of the region as well as supporting the eastward shift in the large scale isentropic trough as a key aspect to examine when forecasting tornadoes in this region.

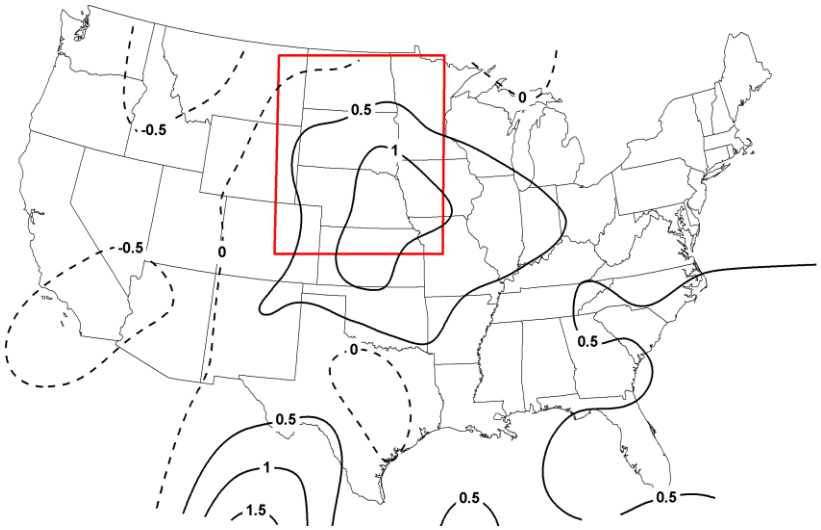

Fig. 4.39. 310K Isentropic surface mixing ratio difference in g/kg calculated by taking the average mixing ratio of the 310K isentropic surface on tornado days minus the average mixing ratio on non-tornado days. Solid lines indicate areas of increased mixing ratio and dotted lines indicate areas of decreased mixing ratio.

In summary, for the Upper Great Plains region in July an analysis on the pressure level, the wind speed, wind direction and mixing ratio for the 305 and 310K isentropic surfaces found that the patterns were not quite as clear as the other regions primarily due to the large scale monsoon-derived isentropic trough that develops during this time of year over the western United States. I found that during tornado days, the isentropic ridge that establishes itself across the western United States shifts eastward resulting in an increase in moisture and uplift across the study region. This can be seen in the northwest to southeast gradient in isentropic pressure and mixing ratio shift that was found statistically and visually. For this region I recommended using the 310K surface as lower isentropic surfaces will go below ground level rendering the map flawed with the key aspect to analyze being the positioning of the monsoon isentropic trough.

k. July – Region 2 (Mid-Atlantic)

The second area of high-density tornado occurrence in July is located across the mid-Atlantic region of the United States. This region contained 602 of the 5,866 tornado reports during the time frame of the study and had seven upper air stations which could be used (Fig 3.40). The upper air stations included: Wilmington, OH (72426), White Lake, MI (72632), Pittsburgh, PA (72520), Buffalo, NY (72528), Albany, NY (72518), Upton, NY (72501) and Sterling, VA (72403).

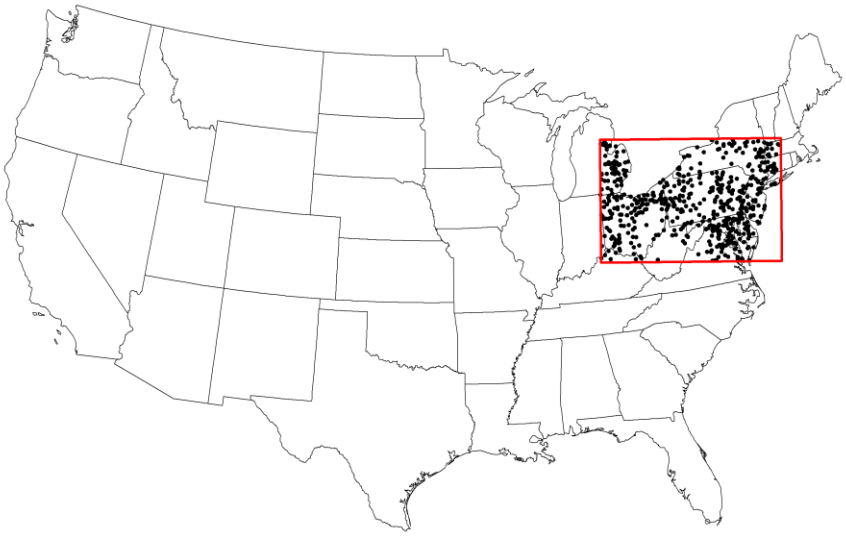

Fig. 4.40**.** Red box is the boundary for the second study region for July. Black dots indicate tornado reports within the region for July from 1974 through 2009. This region contained 602 (10 percent) of the 5,866 tornado reports during this timeframe.

I first conducted a Kruskal-Wallis test on the pressure level of the four isentropic surfaces (315K, 310K, 305K and 300K) for tornado occurrence versus non-tornado occurrence in July. I found that on each level all stations had a statistically significant (95 percent confidence level) increase in pressure on the four isentropic surfaces, with the exception of Wilmington, OH and White Lake, MI where they still displayed an increase but it was not statistically significant

(Table 4.10). In contrast to Region I (Upper Great Plains) for July, I have determined that for this region/month combination, the best isentropic level is 305K, as it shows the greatest change in pressure but also is the closest surface to the ground. While the 300K surface may be lower during certain conditions, on average it will intersect the ground through the region, so to ensure an accurate depiction of the isentropic surface, 305K should be used.

Table 4.10**.** Kruskal-Wallis test results for the 305K isentropic level for the following variables: pressure level (hPa), wind direction (º from N), wind speed (kts) and mixing ratio (g/kg) for the five stations within study region 2 for July. Bolded values indicate those that were not significant at the 95 percentile confidence interval ($p < 0.05$). The entire table for the 315K, 310K, 305K and 300K can be found in the Appendix A.

		305K Pressure Level (hPa)	305K Wind Direction (°)	305K Wind Speed (knots)	305K Mixing Ratio (g/kg)
Wilmington, OH	Non-Event	789	**272**	17	6.74
	Event	806	**270**	19	9.25
	Difference	17	**-2**	2	2.51
	p-value	0.034	**0.844**	0	0
White Lake, MI	Non-Event	**756**	**279**	16	4.02
	Event	**761**	**276**	19	7.17
	Difference	**5**	**-3**	3	3.15
	p-value	**0.464**	**0.419**	0.009	0
Pittsburgh, PA	Non-Event	767	275	14	5.67
	Event	798	263	17	9.17
	Difference	31	-12	3	3.5
	p-value	0	0	0	0
Buffalo, NY	Non-Event	740	279	18	3.94
	Event	761	260	20	6.63
	Difference	21	-19	2	2.69
	p-value	0	0	0.12	0
Albany, NY	Non-Event	737	280	**19**	4.51

Table 4.10 (continued)

	Event	758	269	**20**	6.29
	Difference	21	-11	**1**	1.78
	p-value	0	0.001	**0.744**	0
Upton, NY	Non-Event	756	275	**19**	5.36
	Event	780	265	**19**	7.7
	Difference	24	-10	**0**	2.34
	p-value	0.001	0.007	**0.759**	0
Sterling, VA	Non-Event	779	280	**14**	7.21
	Event	817	270	**16**	9.5
	Difference	38	-10	**2**	2.29
	p-value	0	0.01	**0.058**	0

While each station had an increase in pressure on each of the isentropic levels, the greatest change occurred on the 305K surface so that surface will be primarily discussed for this region/month combination. The greatest increase in pressure of the isentropic surface between tornado and non-tornado days occurred in Sterling, VA with an increase of 38hPa during tornado days while the average increases over the entire region were on the order of 19hPa. Examining the actual anomaly pattern reveals that on tornado days on the 305K surface the greatest increase is located centrally over the study region (Fig 4.41).

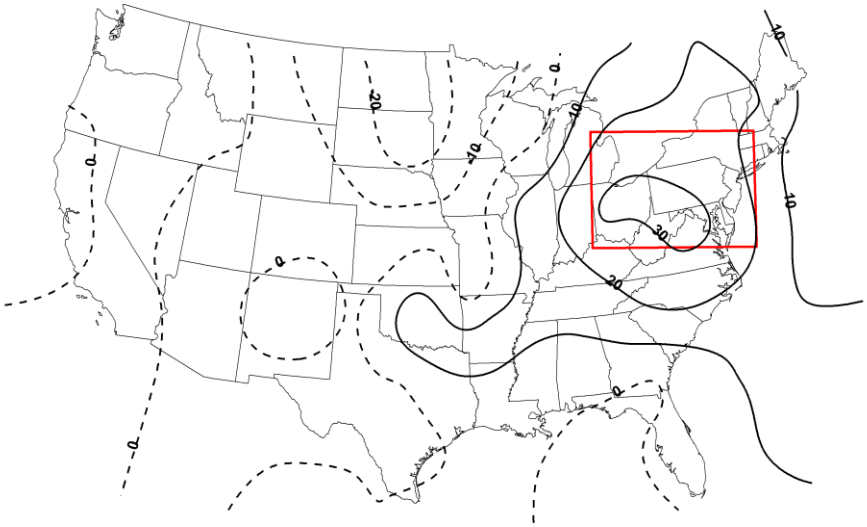

Fig. 4.41**.** 305K July Isentropic surface pressure difference for Region II calculated by taking the average pressure level of the 305K isentropic surface on tornado days minus the pressure level on non-tornado days. Solid lines indicate areas of increasing pressure (lowering heights) and dotted lines indicate areas of rising pressures (rising heights).

This pattern indicates amplified isentropic troughing over the study region and ridging over the central and western portion of the United States; but more detail can be discerned from the actual isentropic patterns. Fig. 4.42 displays the average 305K isentropic surface for non-tornado days (top) and tornado days (bottom). On non-tornado days a pronounced isentropic ridge is located across the entire eastern United States resulting in dry conditions. On tornado days the isentropic ridge breaks down and a slight isentropic trough develops, in particular two small-scale isentropic troughs are present within the region. One is located near the western border and the other is located on the eastern side of the region, possibly enhancing uplift. At this point in time no datasets of sufficient isentropic data density exist that allow for a finer examination into that small-scale feature.

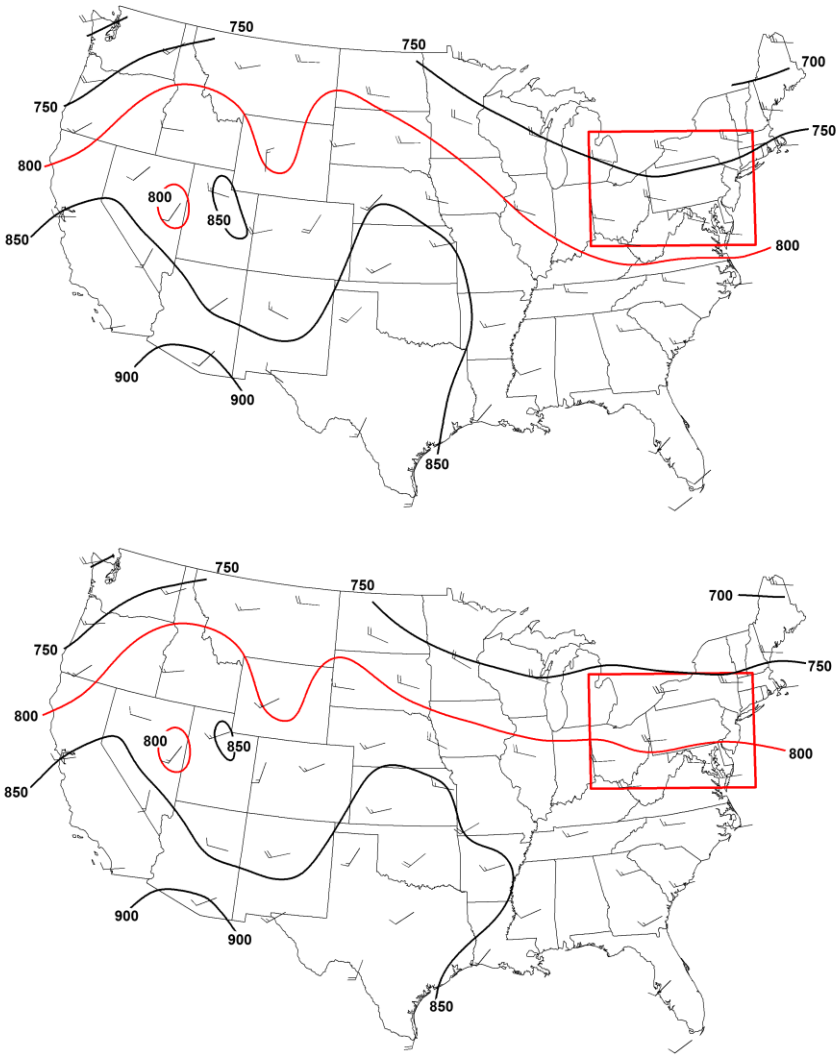

Fig. 4.42**.** (a) average 305K July isentropic surface and wind direction/speed for non-tornado days from 1974 through 2009 for Region II, (b) same as the above but for tornado days. The 850 hPa isobar is highlighted in red to easily show the shift in pattern from non-tornado days to tornado days.

Conducting a Kruskal-Wallis test on both wind speed and wind direction, I first found that wind speed had a statistically significant change on tornado days for this region in July but it was only on the order of two to three knots on the 305K surface, which would be extremely hard to discern in operational tornado forecasting. Wind direction has a statistically significant change in all stations between tornado and non-tornado day for this region with the exception of

Wilmington, OH and White Lake, MI. Even though these two stations did not produce statistically significant differences, all stations indicated a backing (counterclockwise) wind on tornado days with the greatest shift being in Buffalo, NY of 19 degrees. On average across the entire region the median wind was determined to be backing by 10 degrees, which is one of the smallest found in a region/month combination thus far but with troughing in the region such a shift would still enhance uplift. As seen in Fig 4.42, this backing wind results in a flow within the two small scale isentropic troughs to be up-sloping enhancing thunderstorm activity across those two regions.

This trough may also be apparent in the tornado reports shown in Fig. 4.40. Note the highest density is located in the eastern and western portion of the region which corresponds very closely to the two small isentropic troughs. Once again, for this study the isentropic data resolution is not high enough to further analyze this small-scale feature.

Mixing ratio is the fourth component to analyze for this region/month combination. I conducted a Kurskal-Wallis test on mixing ratio to compare tornado versus non-tornado days and found that each station on each isentropic level had a statistically significant (95 percent) increase in mixing ratio on tornado days. The highest increase of mixing ratio on the 305K surface was located at Buffalo, NY where the mixing ratio increased from 3.94g/kg on non-tornado days to 6.63g/kg on tornado days. On average across the entire region the median mixing ratio rose 2.61g/kg on tornado days. Spatially examining the pattern, the highest increase in mixing ratio was observed over the western portion of the

region (Fig. 4.43). This increase in moisture, an isentropic trough developing across the region, and an increased up sloping flow are all ingredients for added instability to initiate and continue the growth of thunderstorms across the region.

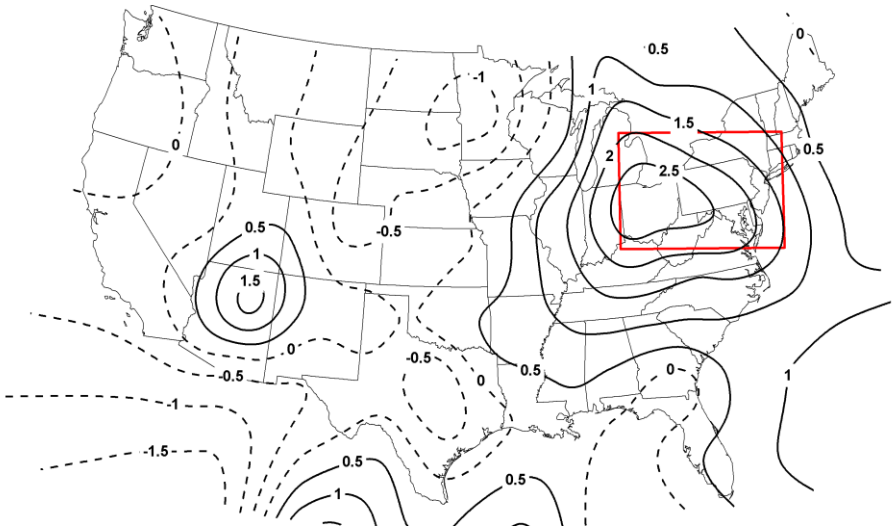

Fig. 4.43. 305K July Isentropic surface mixing ratio difference in g/kg calculated by taking the average mixing ratio of the 305K isentropic surface on tornado days minus the average mixing ratio on non-tornado days. Solid lines indicate areas of increased mixing ratio and dotted lines indicate areas of decreased mixing ratio.

In summary, within this Mid-Atlantic region for July, I found the isentropic surface, wind direction, wind speed and mixing ratio were altered on tornado days compared to non-tornado days for that region. The 305K isentropic surface across the region increased in pressure on average 19hPa, the wind direction was backing at 10 degrees and the mixing ratio increased 2.61g/kg across the region for tornado days versus non-tornado days. Wind speed was also found to change; however, it was only on the order of one to two knots which is insignificant for operational forecasting. One of the key aspects of this region/month combination is the presence of two smaller scale isentropic troughs which formed at the top of the larger scale trough. These two features may result

in added uplift, especially with the shift in wind direction. It is recommended that forecasters use the 305K surface when forecasting in this study region as all the variables discussed above had the greatest change on this level.

l. August – Region 1 (Great Lakes/Midwest)

For the month of August, I selected a region spanning portions of the Midwest and Great Lakes (Fig. 4.44). This region contained 15 percent, or 567 of the 3,837 tornado reports from 1974 through 2009. This region also contained eight upper air stations which were utilized in the analysis and included: Topeka, KS (72456), Omaha, NE (72558), Chanhassen, MN (72649), Davenport, IA (74455) Lincoln, IL (74560), Wilmington, OH (72426), White Lake, MI (72632) and Green Bay, WI (72645).

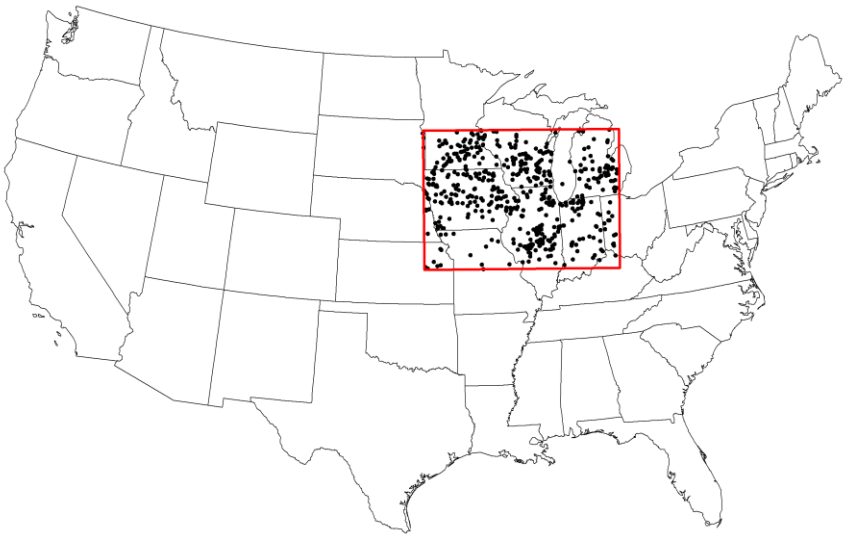

Fig. 4.44**.** Red box is the boundary for the study region for August. Black dots indicate tornado reports within the region for August from 1974 through 2009. This region contained 567 (15 percent) of the 3,837 tornado reports during this timeframe.

The first variable I examined was the pressure level of the four isentropic surfaces. While I conducted a Kruskal-Wallis test comparing the medians

pressure of the four of the isentropic surfaces (315K, 310K, 305K and 30K) for non-tornado and tornado days, the 300K surface will not be discussed in detail as, similar to discussions above, the isentropic surface at times throughout the region went below ground level, which results in an inaccurate isentropic surface. The level of most interest is the 305K surface as it is the isentropic surface closest to the ground, yet does not intersect it.

Upon conducting the Kruskal-Wallis nonparametric test on pressure differences between tornado and non-tornado days, I found that all stations on each isentropic level, with the exception of Omaha, NE, indicated an increase in pressure on tornado days (Table 4.11). In particular, on the 305K isentropic surface, all stations with the exception of Omaha, NE and Chanhassen, MN displayed a statistically significant increase in pressure of the isentropic surface at the 95 percent confidence level. The average increase over the entire study region was 18hPa, with the greatest increase (49hPa) occurring at Lincoln, IL indicating the greatest increase in pressure of the surface was located near the center of the region. The pressure change at Omaha, NE, though not statistically significant, was a decrease on tornado days of 3hPa. This is likely the result of that station being on the very western edge of the study region which has been shown in other regions to be the least responsive to changes in pressure between tornado and non-tornado days. This concept will be developed in more detail below.

Table 4.11**.** Kruskal-Wallis test results for the 305K isentropic level for the following variables: pressure level (hPa), wind direction (º from N), wind speed (kts) and mixing ratio (g/kg) for the five stations within study region 1 for August.

Bolded values indicate those that were not significant at the 95 percentile confidence interval ($p < 0.05$). The entire table for the 315K, 310K, 305K and 300K can be found in the Appendix A.

		305K Pressure Level (hPa)	305K Wind Direction (°)	305K Wind Speed (knots)	305K Mixing Ratio (g/kg)
Topeka, KS	Non-Event	852	**225**	10	9.75
	Event	884	**222**	11	11.85
	Difference	32	**-3**	1	2.1
	p-value	0	**0.145**	0.009	0
Omaha, NE	Non-Event	**855**	**225**	**13**	**8.86**
	Event	**852**	**235**	**15**	**9.26**
	Difference	**-3**	**10**	**2**	**0.4**
	p-value	**0.667**	**0.888**	**0.308**	**0.353**
Chanhassen, MN	Non-Event	**770**	**268**	**17**	5.07
	Event	**776**	**258**	**18**	6.35
	Difference	**6**	**-10**	**1**	1.28
	p-value	**0.752**	**0.175**	**0.319**	0.002
Davenport, IA	Non-Event	795	267	**14**	5.86
	Event	829	246	**16**	9.76
	Difference	34	-21	**2**	3.9
	p-value	0.008	0.006	**0.052**	0
Lincoln, IL	Non-Event	802	266	13	6.89
	Event	851	243	18	10.22
	Difference	49	-23	5	3.33
	p-value	0.002	0.09	0.006	0
Wilmington, OH	Non-Event	790	**271**	**14**	6.77
	Event	811	**257**	**15**	8.06
	Difference	21	**-14**	**1**	1.29
	p-value	0.002	**0.132**	**0.391**	0.021
White Lake, MI	Non-Event	755	**274**	16	4.32
	Event	780	**265**	17	6.48

Table 4.11 (continued)

	Difference	25	**-9**	1	2.16
	p-value	0.001	**0.128**	0.254	0.003

Green Bay, WI	Non-Event	745	281	**16**	3.53
	Event	760	262	**16**	5.95
	Difference	15	-19	**0**	2.42
	p-value	0	0	**0.551**	0

Statistically most stations, again with the exception of Omaha, NE, have an increase in the pressure level of a given isentropic surface for tornado days with the greatest increases occurring on the 305K surface. The anomaly pattern permits evaluation of where the greatest changes are occurring. I created the anomaly map shown in Fig. 4.45 by taking the average 305K isentropic pattern on tornado days and subtracting out the average 305K isentropic pattern for non-tornado days. The greatest increase in pressure on the 305K surface was located on a transect from southern Michigan to the southwest into central Oklahoma, indicating a deepening or developing isentropic trough across the region. Decreasing pressures are located across the western United States and working their way into the western and northwestern edge of the study region indicating a strengthening isentropic ridge.

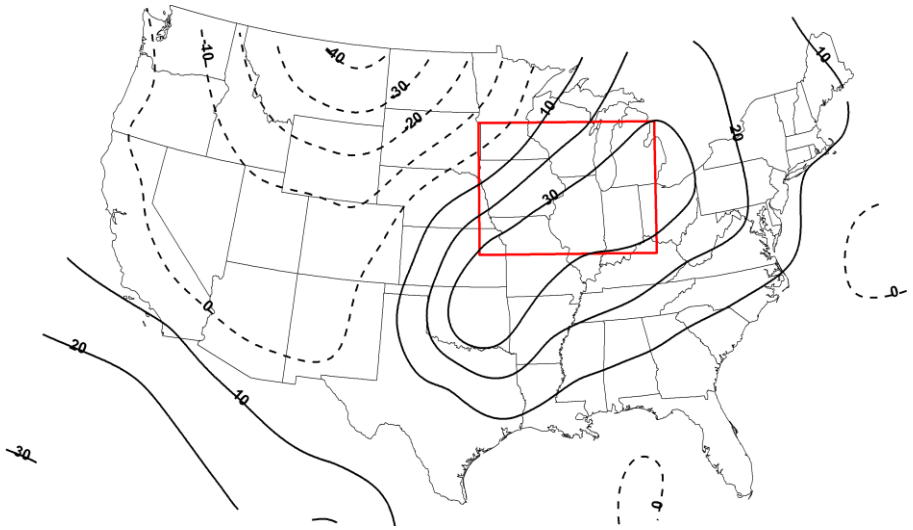

Fig. 4.45**.** 305K August Isentropic surface pressure difference calculated by taking the average pressure level of the 305K isentropic surface on tornado days minus the pressure level on non-tornado days. Solid lines indicate areas of increasing pressure (lowering heights) and dotted lines indicate areas of rising pressures (rising heights).

The actual 305K isentropic pattern provides supporting information on the overall synoptic pattern on non-tornado and tornado days for this region (Fig. 4.46). The most prevalent feature is the large-scale isentropic trough associated with the North American Monsoon Season across the western United States (Namias 1940), with the study region located at the front/top side of the trough. On tornado days, the large-scale isentropic trough weakens over the far western portion of the United States and amplifies across the plains with a trough axis running from the top of Texas up into the southern portion of Iowa. This pattern shift and trough axis matches closely with the anomaly pattern described above.

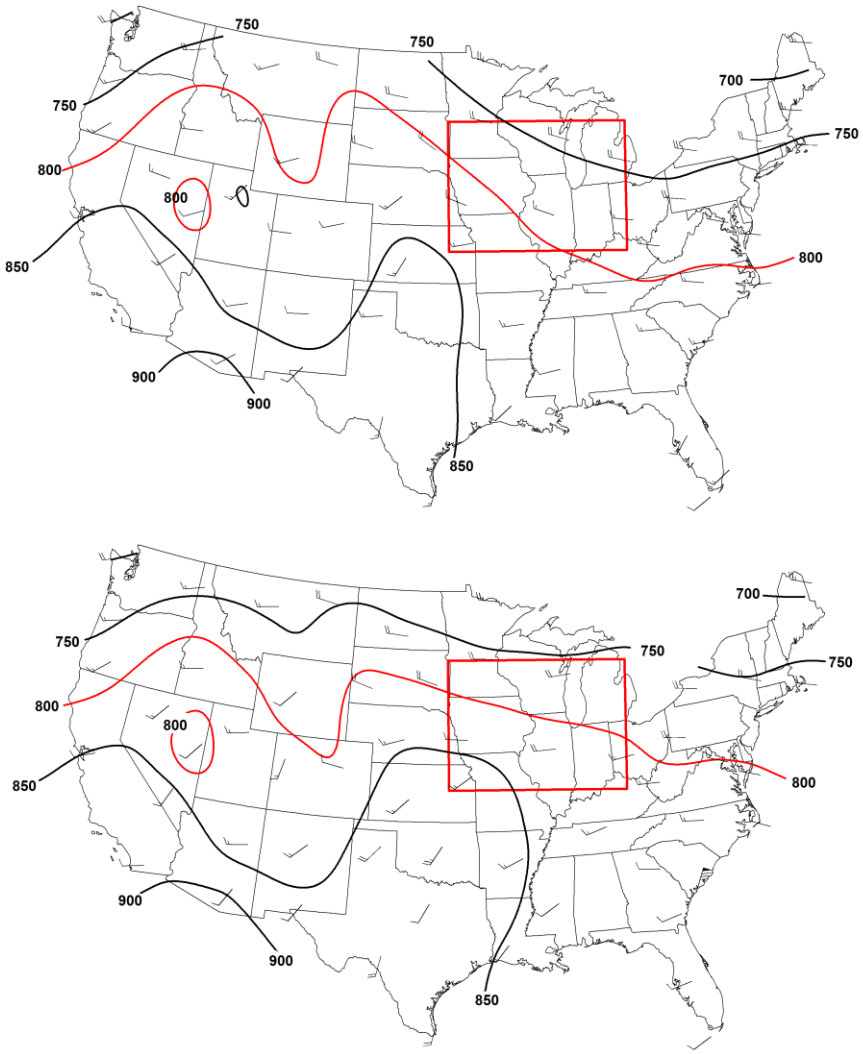

Fig. 4.46**.** (a) average 305K August isentropic surface and wind direction/speed for non-tornado days from 1974 through 2009 (b) same as the above but for tornado days. The 800 hPa isobar is highlighted in red to easily show the shift in pattern on non-tornado days compared to tornado days.

A shift in the pattern could result in a shift in wind direction and speed and therefore additional uplift across the region. I conducted a Kruskal-Wallis test on wind direction and speed comparing tornado and non-tornado days. All stations on the 305K surface, with the exception of Omaha, NE, had a backing (counterclockwise shift) wind on tornado days compared to non-tornado days. However, only Davenport, IA, Lincoln, IL and Green Bay, WI displayed

statistically significant changes in wind direction but the other stations did indicate a backing wind on tornado days. The greatest change in wind direction was at Lincoln, IL with a backing of 23 degrees from non-tornado wind directions and Davenport, IA with a backing of 21 degrees on tornado days compared to non-tornado days. On average across the region the wind shift was 11 degrees which is one of the smaller shifts in wind direction I have found thus far across a region/month combination, but, however slight, this shift does still result in additional uplift.

As seen in Fig 4.46, on non-tornado days the flow is parallel to the isobars of the isentropic surface indicating no vertical uplift on the adiabatic surface. Conversely, on tornado days in the southern and central portion of the region the winds are seen to be flowing slightly more perpendicular to the isobars indicating uplift since the flow is from higher pressure values to lower pressure values. This shift in pattern and wind direction could result in additional help in generating thunderstorms across the region. I also compared wind speed between tornado and non-tornado days for stations in this region but a change of only one to two knots is evident, making the significance of such a change both statistically and in an operational forecasting sense extremely limited.

Moisture is the last variable I examined for this region to see if there were increases in moisture to accompany the additional uplift mentioned above to generate severe thunderstorms in the region. Again, I performed a Kruskal-Wallis test on mixing ratio and found on tornado days each station at each isentropic level (again with the exception of Omaha, NE) had a statistically significant

increase in mixing ratio on tornado days, with the greatest increase observed on the 305K isentropic surface. Omaha, NE also had an increase in mixing ratio but it did not meet my significance criterion. On average across the entire region on the 305K surface the median mixing ratio increased 2.11g/kg on tornado days. The largest increase on the 305K surface occurred at Lincoln, IL with a rise of 3.9g/kg. The mixing ratio anomaly map (Fig. 4.47) has the greatest increase across the southern and central portion of the region. This closely matches the greatest increase in pressure of the isentropic surface for tornado days as well as the axis of the trough shown on the actual isentropic chart. With this amount of added moisture and the increased uplift, it is highly probable that these two ingredients would come together to create increased severe thunderstorm development across the region.

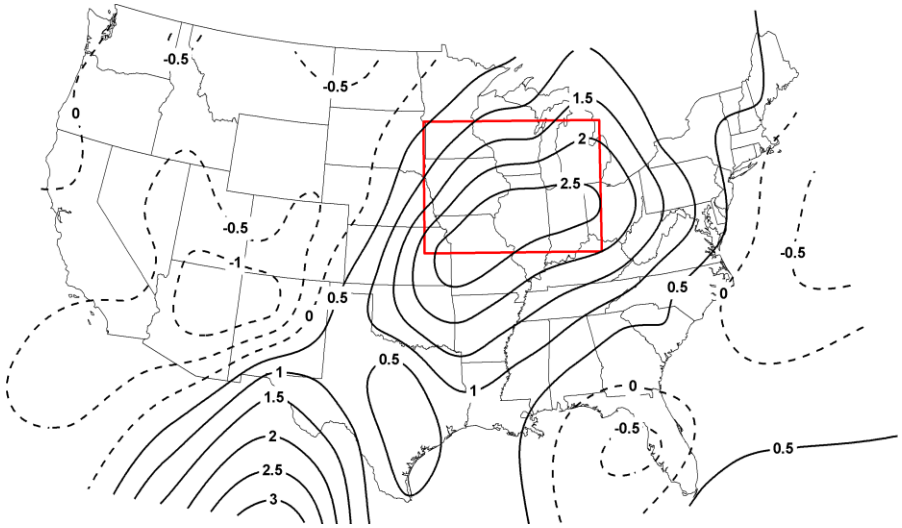

Fig. 4.47. 305K August Isentropic surface mixing ratio difference in g/kg calculated by taking the average mixing ratio of the 305K isentropic surface on tornado days minus the average mixing ratio on non-tornado days. Solid lines indicate areas of increased mixing ratio and dotted lines indicate areas of decreased mixing ratio.

In summary, for this Great Lakes/Midwest region for August, I have found several isentropic differences that may help forecast the likelihood of severe

thunderstorms developing across the region. First and foremost, the large-scale isentropic trough located across the entire western United States on non-tornado days is slightly weaker along the west coast of the United States and deeper across the Plain and into the study region. This deepening trough can be statistically seen across the region with an average increase in pressure of 18hPa for the isentropic surface. With this isentropic trough across the region, moisture also increases with an average increase of 2.11g/kg on tornado days. Finally, with the added moisture the wind direction was found to be backing by 11 degrees resulting in additional uplift. With the added moisture and uplift thunderstorm development is enhanced within the study region. Finally, I recommend that forecasters use the 305K isentropic surface as the lower 300K isentropic surface runs into the ground on several occasions rendering the analysis flawed.

m. September – Region 1(Gulf States)

The region I selected for September is located in the southeastern United States and included the states of Mississippi, Alabama, western Georgia, eastern/central Louisiana and southeastern Arkansas (Fig. 4.48). This region contains 402 (14 percent) of the 2,939 tornado reports from 1974 through 2009. Five upper air stations are also located within this region which included: Lake Charles, LA (72240), Little Rock, AR (72340), Jackson, MS (72235), Shelby, AL (72230) and Peachtree City, GA (72215).

Fig. 4.48**.** Red box is the boundary for the study region 1 for September. Black dots indicate tornado reports within the region for September from 1974 through 2009. This region contained 402 (14 percent) of the 2.939 tornado reports during this timeframe.

The first aspect I analyzed was the pressure level of the four isentropic surfaces. I conducted a Kruskal-Wallis test to identify if there was a difference in medians between non-tornado and tornado days. Each station at the 315K, 310K, 300K and 305K level had a statistically significant increase in pressure of the isentropic surface on tornado days at the 95 percent confidence level (Table 4.12). This increase was the most prominent on the 305K isentropic surface where the average increase across the region was 20hPa, with the largest increase in pressure noted at the Shelby, AL upper air station at 24hPa.

Table 4.12**.** Kruskal-Wallis test results for the 305K isentropic level for the following variables: pressure level (hPa), wind direction (º from N), wind speed (kts) and mixing ratio (g/kg) for the five stations within study region 1 for September. Bolded values indicate those that were not significant at the 95 percentile confidence interval ($p < 0.05$). The entire table for the 315K, 310K, 305K and 300K can be found in the Appendix A.

		305K Pressure Level (hPa)	305K Wind Direction (°)	305K Wind Speed (knots)	305K Mixing Ratio (g/kg)
Lake Charles, LA	Non-Event	819	**210**	10	8.97
	Event	834	**208**	16	10.27
	Difference	15	**-2**	6	1.3
	p-value	0	**0.166**	0	0
Little Rock, AR	Non-Event	789	**242**	12	7.06
	Event	813	**225**	13	9.57
	Difference	24	**-17**	1	2.51
	p-value	0	**0.052**	0.041	0
Jackson, MS	Non-Event	803	**226**	10	8
	Event	825	**219**	16	10.59
	Difference	22	**-7**	6	2.59
	p-value	0	**0.46**	0	0
Shelby, AL	Non-Event	796	**228**	11	7.55
	Event	821	**232**	20	10.62
	Difference	25	**4**	9	3.07
	p-value	0	**0.824**	0	0
Peachtree, GA	Non-Event	794	**235**	11	7.37
	Event	808	**214**	17	10.5
	Difference	14	**-21**	6	3.13
	p-value	0.023	**0.119**	0.003	0

A 305K pressure anomaly pattern was created for this region/month combination by taking the average 305K isentropic surface on tornado days and subtracting from that the average 305K isentropic surface on non-tornado days.

Over the majority of the eastern United States on tornado days, an increase in pressure occurs with the axis of increase stretching from Alabama/Mississippi up through Pennsylvania. A particular feature that is missing in this region that was present in most of the other southern region/month combinations is the tight positive to negative gradient on the western edge of the region. This feature is likely absent in this month as a result of the overall decaying isentropic trough that develops across the entire western United States during the North American Monsoon Season in September.

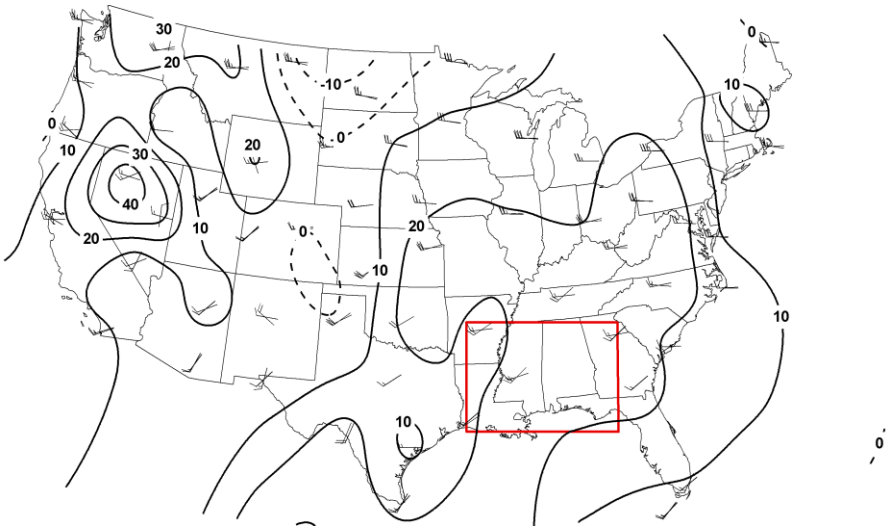

Fig. 4.49. 305K September isentropic surface pressure difference calculated by taking the average pressure level of the 305K isentropic surface on tornado days minus the pressure level on non-tornado days. Solid lines indicate areas of increasing pressure (lowering heights) and dotted lines indicate areas of rising pressures (rising heights).

While the pressure anomaly isentropic map (Fig. 4.49) does not show a very dramatic shift as noted in prior regions, the actual 305K pattern shows the shift that occurs on tornado versus non-tornado days slightly better (Fig. 4.50). On non-tornado days a well-established isentropic ridge is located across the region

with an isentropic trough over the Plains. Such a trough is likely the remnants of the large-scale isentropic trough associated with the North American Monsoon Season. On tornado days the trough in the Plains is seen to deepen and widen and a separate isentropic trough can also be seen across the study region. This shift in pattern from isentropic ridging to troughing over the region could result in an increase in moisture and uplift across the region, which will be discussed below.

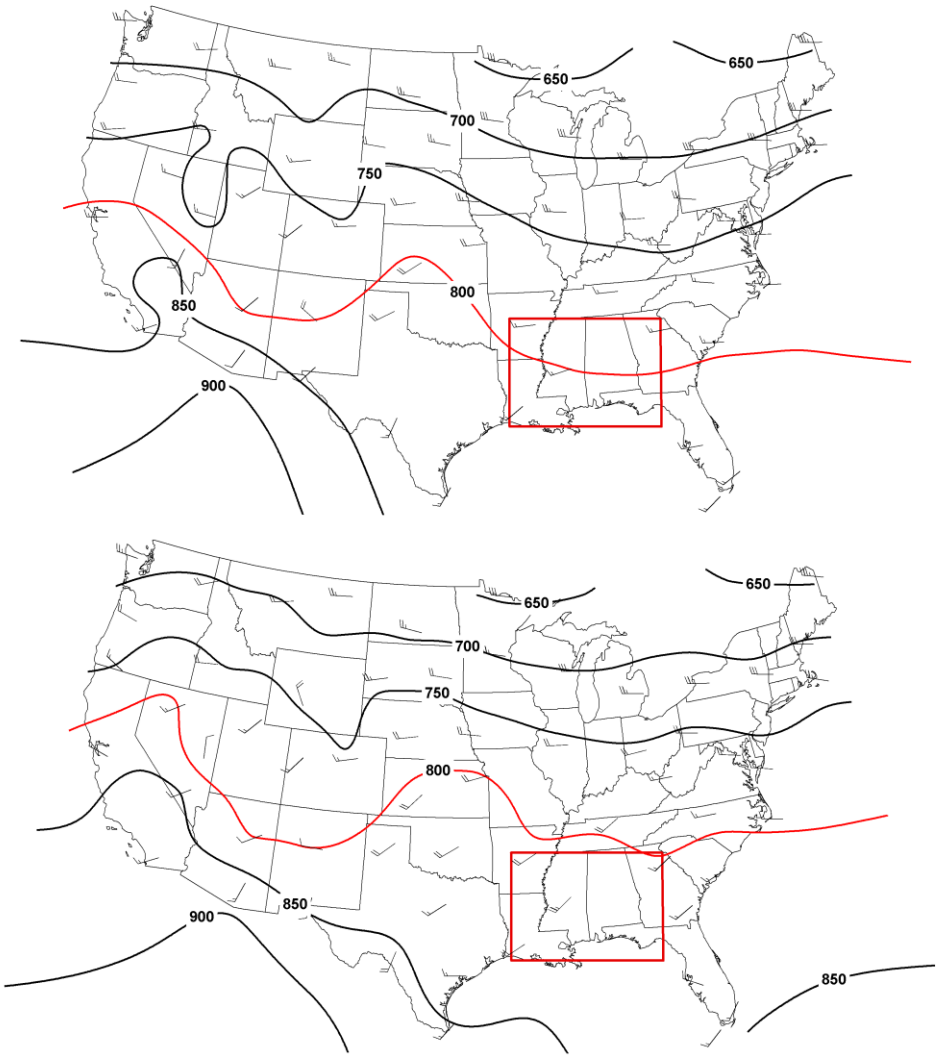

Fig. 4.50**. (a)** average 305K September isentropic surface and wind direction/speed for non-tornado days from 1974 through 2009 (b) same as the above but for tornado

days. The 800 hPa isobar is highlighted in red to easily show the shift in pattern from non-tornado days and tornado days.

Second, I examined the change in wind direction and speed as well to see if up-sloping or down-sloping flow increased on tornado days. I conducted a Kruskal-Wallis test on wind direction and speed and found that on the 305K surface none of the stations had met the significance criterion for changes in wind direction. However, they all indicated a non-significant backing wind that only on average 9 degrees with the highest backing wind (21 degrees) at Peachtree City, GA. Even though this shift in wind direction is not statistically significant, the actual isentropic pattern (Fig. 4.50) for non-tornado days has a fairly zonal wind while on tornado days the shift in the isentropic pattern and in wind direction results in flow oriented up the isentropic surface, indicating uplift across the region.

Additionally, I analyzed wind speed and found that each station actually had a statistically significant increase in wind speed on tornado days. However, as with the other region/month combinations, this change was only on the order of one to nine knots which, from a forecasting standpoint, is not a sufficient magnitude to easily identify on an operational basis so wind direction as opposed to wind speed is still recommended to be the isentropic variable of choice for operational forecasting.

With an isentropic trough across the region the likelihood of moisture advection is increased. To further ascertain such moisture increase, I conducted a Kruskal-Wallis test on mixing ratio for tornado and non-tornado days for this

region in September and found each station at each of the isentropic levels had a statistically significant increase in mixing ratio on tornado days at the 95 percent confidence level. The average increase in mixing ratio across the entire region was 2.52g/kg. Examining the mixing ratio anomaly map (Fig. 4.51), which was calculated in the same manner as the isentropic pressure anomaly map, shows the greatest increases in mixing ratio are located across the region. With this added moisture and lift as noted in the prior discussion, enhanced severe thunderstorm activity is probable across the region given this type of isentropic pattern.

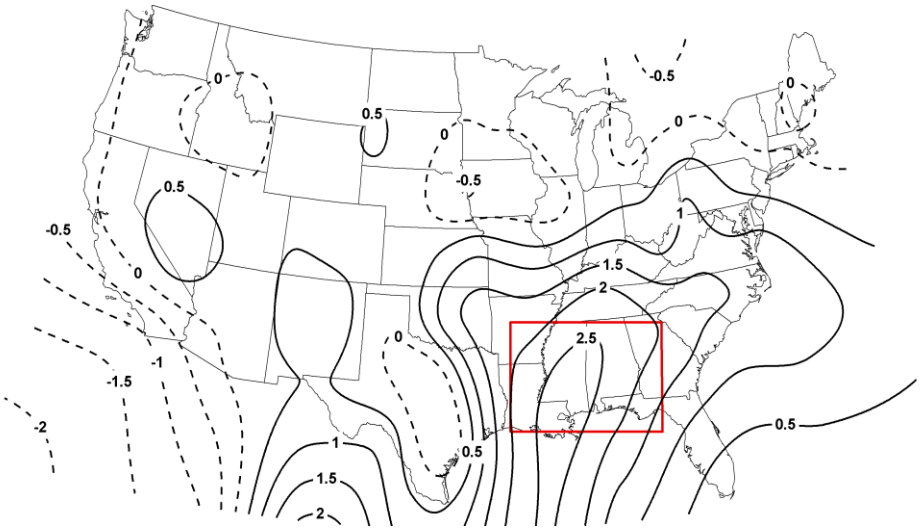

Fig. 4.51. 305K September isentropic surface mixing ratio difference in g/kg calculated by taking the average mixing ratio of the 305K isentropic surface on tornado days minus the average mixing ratio on non-tornado days. Solid lines indicate areas of increased mixing ratio and dotted lines indicate areas of decreased mixing ratio.

In summary for the Gulf States region in September for non-tornado and tornado days, I identified three aspects that could be discriminate the isentropic surfaces between tornado and non-tornado occurrences across the region. First is the increase in pressure of the isentropic surface on tornado days indicating troughing over the region with an average increase of 20hPa on the 305K surface.

This troughing over the region coupled with the slight nine-degree backing winds within the region results in the flow being up the isentropic trough resulting in uplift across the area. Additionally, moisture significantly increases across the region with the 305K isentropic surface having an increase in mixing ratio of 2.32g/kg on tornado days. With this added uplift and the increase in moisture, severe tornadic thunderstorms are highly probable given the isentropic pattern. For this region in September, I recommend forecasters use the 305K isentropic surface as it is the closest surface to ground level without going below.

n. October – Region 1 (Southern Great Plains)

The region I selected for October was located across the southern Plains and included the states of Louisiana, Arkansas, central and eastern Oklahoma and eastern Texas (Fig 4.52). This region contained five upper air stations which include: Lake Charles, LA (72240), Little Rock, AR (72340), Jackson, MS (72235), Fort Worth, TX (72249), and Norman, OK (72357). This region also contains 511 (25 percent) of the 2,027 tornado reports across the contiguous United States from the time period of 1974 through 2009.

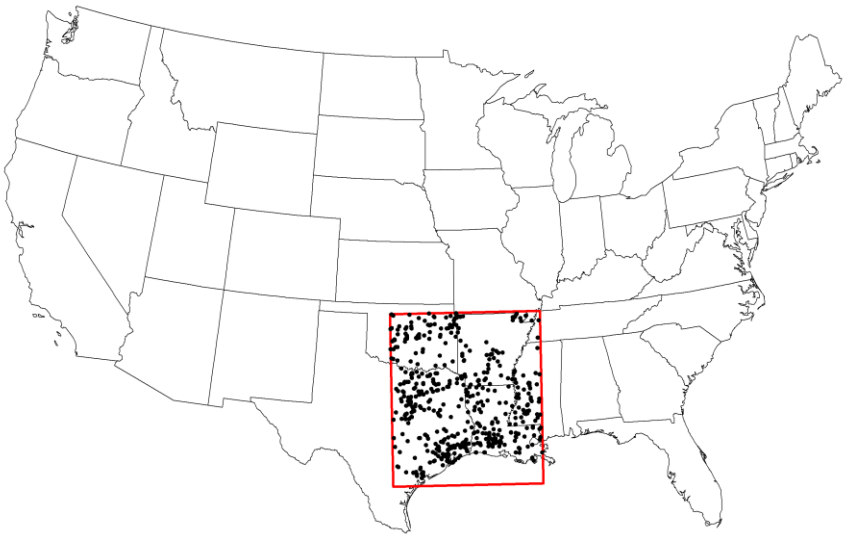

Fig. 4.52**.** Red box is the boundary for the study region 1 for October. Black dots indicate tornado reports within the region for October from 1974 through 2009. This region contained 511 (25 percent) of the 2,027 tornado reports during this timeframe.

I first examined the pressure level differences between tornado and non-tornado days for the four isentropic surfaces (315K, 310K, 305K and 300K). A Kruskal-Wallis test on the pressure level for tornado and non-tornado days determined that each station on each isentropic surface displayed a statistically significant increase in pressure of the isentropic surface on tornado days with the exception of Fort Worth, TX and Norman, OK, both of which are near the western edge of the study region. Specifically, on the 315K, 310K and 305K Norman, OK, though not statistically significant, indicate that the pressure level on the isentropic surfaces actually decreased on tornado days compared to non-tornado days (Table 4.13).

Table 4.13**.** Kruskal-Wallis test results for the 305K isentropic level for the following variables: pressure level (hPa), wind direction (º from N), wind speed (kts) and mixing ratio (g/kg) for the five stations within study region 1 for October. Bolded values indicate those that were not significant at the 95 percentile confidence interval ($p < 0.05$). The entire table for the 315K, 310K, 305K and 300K can be found in the Appendix A.

		305K Pressure Level (hPa)	305K Wind Direction (°)	305K Wind Speed (knots)	305K Mixing Ratio (g/kg)
Lake Charles, LA	Non-Event	772	241	12	3.5
	Event	805	201	19	8.6
	Difference	33	-40	7	5.1
	p-value	0	0	0	0
Little Rock, AR	Non-Event	726	260	17	2.55
	Event	747	225	24	5.8
	Difference	21	-35	7	3.25
	p-value	0.0001	0	0	0
Jackson, MS	Non-Event	747	252	13	2.77
	Event	780	219	17	6.78
	Difference	33	-33	4	4.01
	p-value	0	0	0.001	0
Fort Worth, TX	Non-Event	**770**	**236**	16	4.63
	Event	**771**	**224**	26	7.77
	Difference	**1**	**-12**	10	3.14
	p-value	**0.325**	**0.239**	0	0
Norman, OK	Non-Event	**747**	**240**	19	3.87
	Event	**737**	**236**	27	5.25
	Difference	**-10**	**-4**	8	1.38
	p-value	**0.57**	**0.248**	0	0.001

For this region and month, the 300K surface is occasionally at a higher pressure level than 900hPa, which means during certain events, the surface is

likely below ground level, particularly for the western portion of the region. As a result, for this region it is recommended to use the 305K isentropic surface and that surface will be the primary focus for this region/month combination. Additionally, the 305K surface also shows the greatest increase in pressure of the isentropic surface with an average increase on tornado days of 16hPa, indicating troughing over the region.

The pressure anomaly pattern (Fig. 4.53) was created by taking the average 305K isentropic surface on tornado days and subtracting out the average 305K surface on non-tornado days. That anomaly map demonstrates that the greatest increase is found over Ohio with an axis of greatest increase running from Ohio southwest into Louisiana (Fig. 4.53). The greatest increase over the region was over the southern and eastern portions with an actual decrease in pressure of the isentropic surface in the northwest corner which matches the statistical data presented above. Additionally, a tight positive to negative gradient is evident to the west of the study region and begins to encroach on the northwest portion of the region. This indicates an area of steep slope on the 305K isentropic surface which could enhance thunderstorm activity in the region as it moved through.

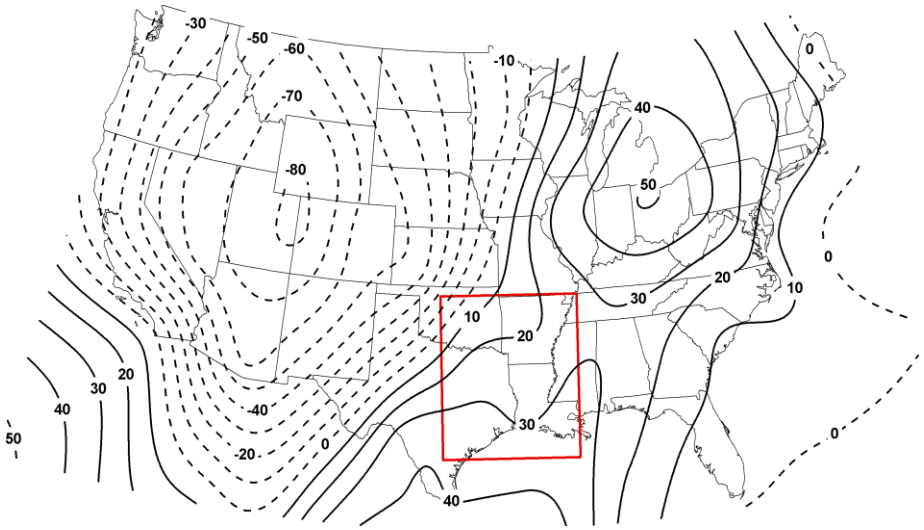

Fig. 4.53**.** 305K October Isentropic surface pressure difference calculated by taking the average pressure level of the 305K isentropic surface on tornado days minus the pressure level on non-tornado days. Solid lines indicate areas of increasing pressure (lowering heights) and dotted lines indicate areas of rising pressures (rising heights).

The actual isentropic pattern provides additional understanding of how the isentropic pattern is modified for tornado versus non-tornado days. On the 305K surface during non-tornado day, a well-developed isentropic trough is located across the central Plains just to the west of the study region and over the study region is an isentropic trough with fairly zonal flow (Fig. 4.54). On tornado days, the isentropic trough seen in the central Plains is replaced by a prominent isentropic trough across the entire western United States with an isentropic trough located across the study region, in particular over the western side of the region.

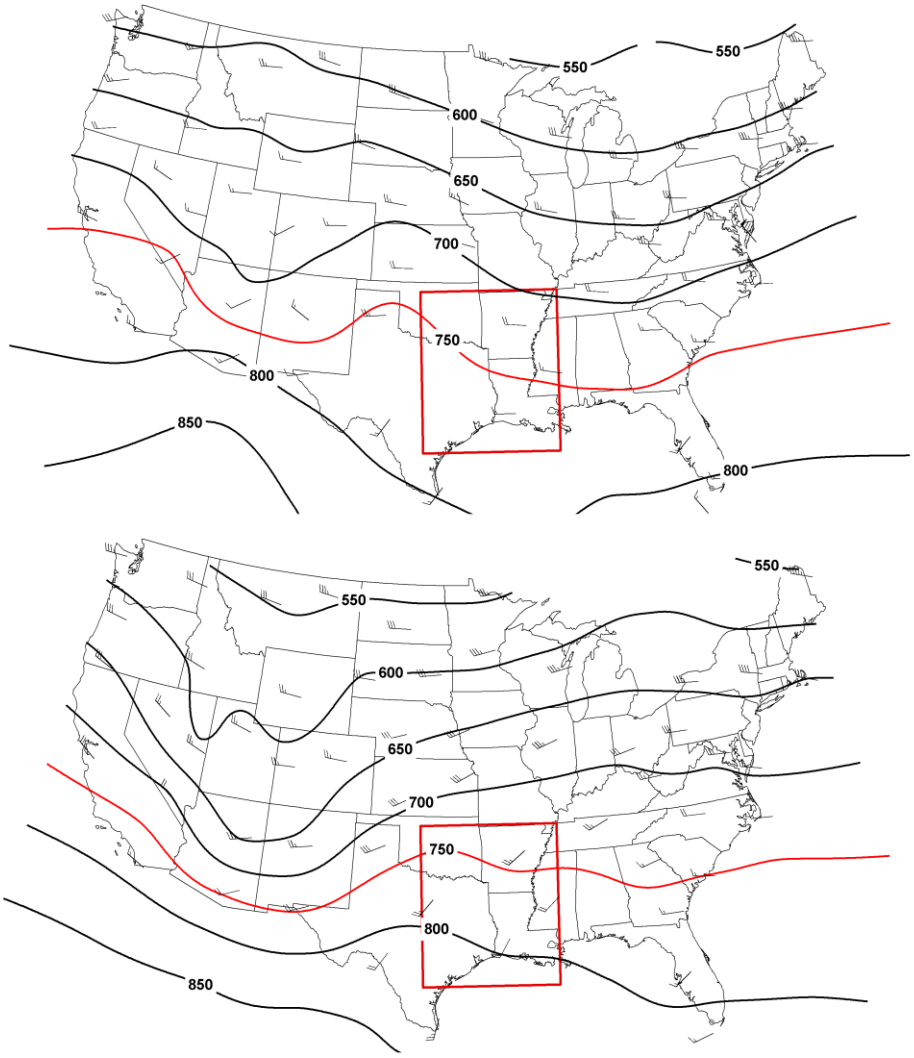

Fig. 4.54**.** (a) average October 305K isentropic surface and wind direction/speed for non-tornado days from 1974 through 2009 (b) same as the above but for tornado days. The 750 hPa isobar is highlighted in red to easily show the shift in pattern from non-tornado and tornado days.

Secondly, I examined both wind speed and direction differences in tornado and non-tornado days for this region/month combination using a Kruskal-Wallis test. On the 305K surface I found that three stations in the region had a statistically significant change in wind direction on tornado versus non-tornado days while Fort Worth, TX and Norman, OK did not. Each of three stations had a

backing (counterclockwise) wind between tornado and non-tornado days, with an average wind shift of 36 degrees. This shift in wind direction can be seen on Fig. 4.54, with non-tornado days having the wind flow parallel to the isentropic isobars and on non-tornado days the wind flow was nearly perpendicular to the isobars, especially over the central and eastern portions of the region. This perpendicular flow implies a large amount of uplift as wind flows up the isentropic surface from areas of high to low pressure values (low to high heights). The uplift from the backside of the isentropic trough itself moving through the region coupled with the up-sloping flow due to the wind direction shift, leads to uplift across the entire study region which could substantially increase thunderstorm activity across the region. I tested wind speed and found it to be statistically significant at all the stations within the region. However, the greatest increase in wind speed on tornado days was only ten knots at Fort Worth, TX with most stations only reporting a two to four knot change. This is too small a change to use in an operational forecasting algorithm, so wind direction is suggested to be the primary variable with respect to isentropic winds.

I have shown that the isentropic pattern dramatically shifts for the Southern Plains in October as well as the isentropic wind direction which all relate to increased uplift. I next examine the mixing ratio by conducting a Kruskal-Wallis test comparing tornado and non-tornado days. I found that each station within the region on the 315K, 310K and 305K isentropic surface has a statistically significant increase in mixing ratio on tornado days. The 305K surface shows the greatest increase with an average of 3.38g/kg across the study

region. An axis of moisture increase is located from the Louisiana/Texas border up through Illinois for tornado days (Fig. 4.55). This increase in moisture closely matches that of the isentropic trough axis that develops across the region on tornado days. This large of an increase in moisture at 305K aids in the generation of severe thunderstorms, especially given the increased uplift.

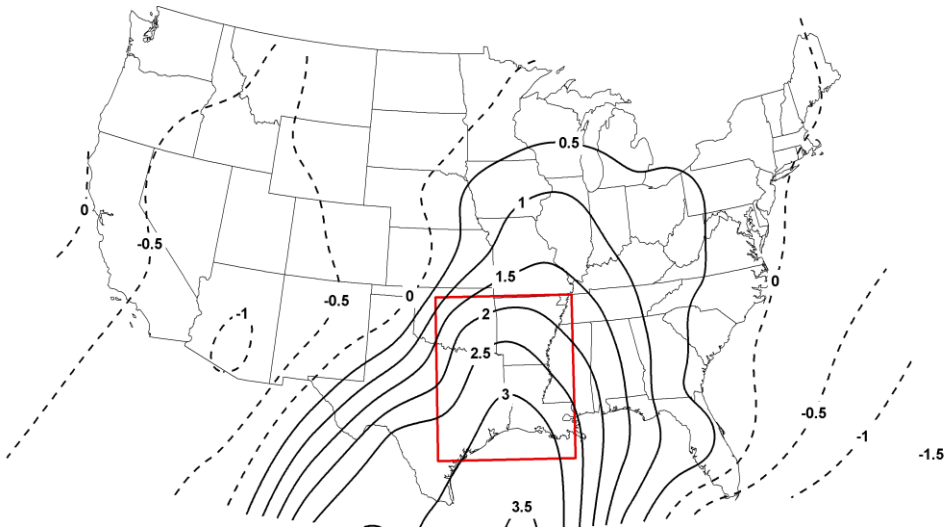

Fig. 4.55. 305K October isentropic surface mixing ratio difference in g/kg calculated by taking the average mixing ratio of the 305K isentropic surface on tornado days minus the average mixing ratio on non-tornado days. Solid lines indicate areas of increased mixing ratio and dotted lines indicate areas of decreased mixing ratio.

For this Southern Plains region in October, I have identified several key aspects on the isentropic surface that dramatically change on tornado days when compared to non-tornado days. First, an isentropic ridge which is over the region on non-tornado days is replaced on tornado days by an isentropic trough on average 16hPa higher in pressure (decrease in height). With the isentropic trough moving into the region from the west already increasing uplift within the atmosphere, wind direction backs (turns counterclockwise) by approximately 36 degrees resulting in flow perpendicular to the contour lines flowing up the

isentropic trough yielding even more uplift. With this amplified isentropic trough across the region, the mixing ratio value is also found to increase significantly by 3.38g/kg on tornado days. An increase in moisture coupled with an increase in uplift can most certainly result in more intense thunderstorm development and continuation which could result in an increase in tornado activity across the entire region. All of these changes are the most notable on the 305K surface with the 300K surface being too low during this time period as at times it could run into the ground. As a result, I would encourage forecasters to rely on the 305K isentropic surface when forecasting as it should give the most representative picture of the atmosphere.

o. November – Region 1(Gulf States)

For November, I selected a region located in the southeastern United States which included the states of Arkansas, Louisiana, Mississippi, Alabama, the panhandle of Florida, western Georgia and Tennessee (Fig 4.56). This region contained 39 percent (845 of 2,152) of the tornado reports from November between 1974 through 2009. This region also contained six upper air stations that were used in the statistical analysis and included: Little Rock, AR (72340), Jackson, MS (72235), Shelby, AL (72230), Nashville, TN (72327), Peachtree City, GA (72215), and Lake Charles, LA (72240).

Fig. 4.56**.** Red box is the boundary for the study region 1 for November. Black dots indicate tornado reports within the region for November from 1974 through 2009. This region contained 379 (31 percent) of the 1,220 tornado reports during this timeframe.

The isentropic pattern is crucial in determining the three dimensional representation of the atmosphere when conducting an isentropic analysis. I conducted a Kruskal-Wallis test on the pressure of a given isentropic surface on tornado and non-tornado days and determined that for each station within the region, and on each of the four isentropic levels (315K, 310K, 305K and 300K); there was a statistically significant increase in pressure on tornado days as compared to non-tornado days (Table 4.14). Of the four isentropic surfaces, the 300K surface had the largest increase in pressure, which is not unexpected since it is the lowest level to the surface and would indicate the level which should be used to gain the best representation of the atmosphere during this time of the year. As a result, the 300K surface is primarily discussed in this section and is the level I would recommend forecasters use in this region in November.

Table 4.14**.** Kruskal-Wallis test results for the 300K isentropic level for the following variables: pressure level (hPa), wind direction (º from N), wind speed (kts) and mixing ratio (g/kg) for the five stations within study region 1 for November. Bolded values indicate those that were not significant at the 95 percentile confidence interval ($p < 0.05$). The entire table for the 315K, 310K, 305K and 300K can be found in the Appendix A.

		300K Pressure Level (hPa)	300K Wind Direction (°)	300K Wind Speed (knots)	300K Mixing Ratio (g/kg)
Little Rock, AR	Non-Event	751	263	24	2.08
	Event	787	236	32	5.43
	Difference	36	-27	8	3.35
	p-value	0	0	0	0
Jackson, MS	Non-Event	782	255	18	2.44
	Event	836	218	25	7.79
	Difference	54	-37	7	5.35
	p-value	0	0	0	0
Shelby, AL	Non-Event	776	262	20	2.27
	Event	825	213	25	8.04
	Difference	49	-49	5	5.77
	p-value	0	0	0.018	0
Nashville, TN	Non-Event	730	259	28	1.85
	Event	784	223	32	6.04
	Difference	54	-36	4	4.19
	p-value	0	0	0.018	0
Peachtree, GA	Non-Event	773	268	21	2.08
	Event	812	227	23	7.12
	Difference	39	-41	2	5.04
	p-value	0	0	0.426	0
Lake Charles, LA	Non-Event	813	247	16	3.39
	Event	853	228	27	9.01
	Difference	40	-19	11	5.62
	p-value	0	0	0	0

Of the six stations in this region, the greatest increase in pressure on the 300K surface was 54hPa which occurred at both Jackson, MS and Nashville, TN. The average change in median pressure on tornado days across the entire region was 45hPa. The 300K anomaly isentropic pattern, computed by taking the 300K isentropic pattern on tornado days minus the 300K isentropic pattern on non-tornado days, shows that the greatest increase in pressure was over eastern Ohio with an axis of greatest increase running through eastern Louisiana (Fig 4.57). Additionally, a tight positive to negative gradient extends just to the east of the region. This feature indicates the area of transition between a deepening trough and an increasing ridge, which could enhance uplift as it moves through a region.

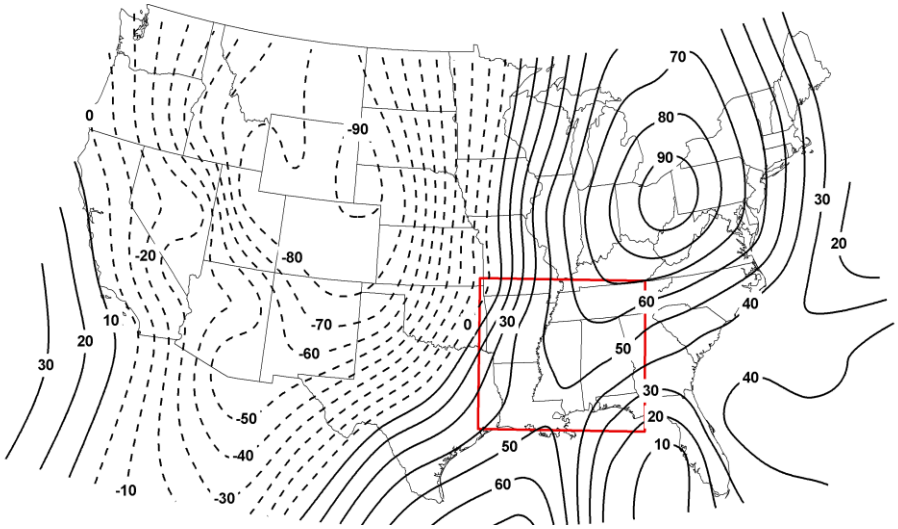

Fig. 4.57. 300K November isentropic surface pressure difference calculated by taking the average pressure level of the 300K isentropic surface on tornado days minus the pressure level on non-tornado days. Solid lines indicate areas of increasing pressure (lowering heights) and dotted lines indicate areas of rising pressures (rising heights).

During non-tornado days, a well established isentropic trough is located across the region with an isentropic ridge just to the west of the region (Fig. 4.58). Conversely, on tornado days an isentropic trough develops across the entire

eastern United States with a trough axis running from western New York down through Georgia. This trough, based on previous research and by examining the other region/month combinations, should result in an increase in moisture across the region and, if wind direction shifts, uplift should increase as well. These two aspects will be examined in more detail below.

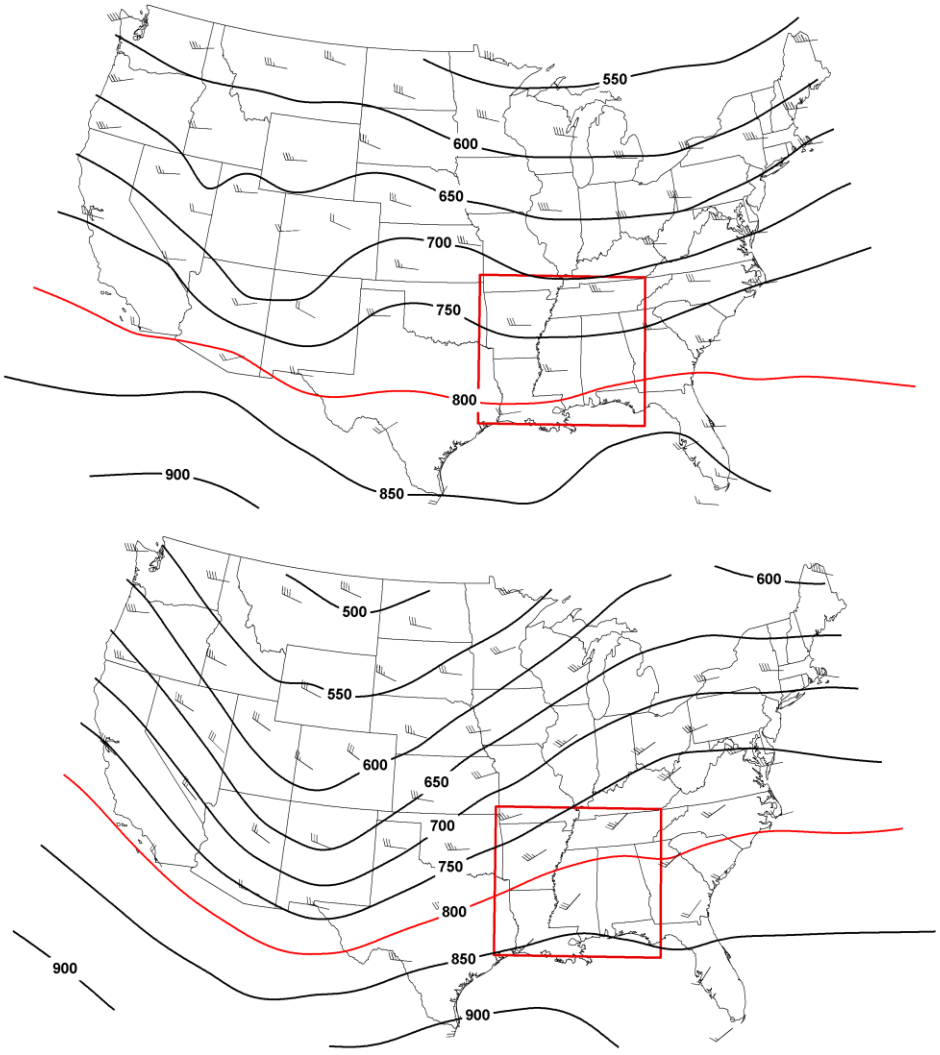

Fig. 4.58**.** (a) average 305K November isentropic surface and wind direction/speed for non-tornado days from 1974 through 2009 (b) same as the above but for tornado days. The 800hPa isobar is highlighted to easily show the shift in pattern from non-tornado to tornado days.

With an isentropic trough found to develop across the region during tornado days a shift in wind direction should result in added uplift as well. To examine wind direction I conducted a Kruskal-Wallis test on wind direction and wind speed comparing the median value on tornado and non-tornado days. First examining wind speed, I found that only on the 300K surface did all six stations have a statistically significant increase in wind speed, but was only on the order of two to eleven knots. While this change is statistically significant, in an operational sense this small of a change would be hard to easily recognize and base a forecast on so other variables such as wind direction would be of more importance/value.

Wind direction was statistically significant at all isentropic levels for each of the stations across the region, with the 300K surface having the largest change. In each case the wind was found to be backing (counterclockwise shift) with winds on the 300K surface changing from 259 degrees (west) on non-tornado days to 224 degrees (southwest) on tornado days, which is a backing wind of 35 degrees. Examining this change on the isentropic surface (Fig. 4.58), shows that during non-tornado days flow is primarily parallel to the isentropic isobars indicating no adiabatic uplift, while on tornado days the flow is found to be more perpendicular to the contours, especially in the central portion of the region. Since this flow is up the isentropic trough (from high pressure to low pressure values) it indicates uplift within the atmosphere which could initiate severe thunderstorms or help already developed thunderstorms to continue.

With an isentropic trough within the region and uplift shown on tornado days based on the flow on the 300K isentropic surface, moisture is the next aspect

to examine. I conducted a Kruskal-Wallis test on mixing ratio comparing non-tornado days and tornado days and found that all six stations within the region on each isentropic surface had a statistically significant increase on tornado days. The greatest increase was once again found on the 300K isentropic surface and on average across the region moisture increased by 4.89g/kg, with the highest increase at Shelby, AL. The highest increase in mixing ratio on the 300K surface occurred over the southern portion of the region with an axis of increase running from southern Louisiana up through Ohio (Fig. 4.59). This axis matches nearly identically to the change in pressure map (Fig. 4.57) which is not surprising given isentropic troughs are generally associated with an increase in moisture, which can aid in thunderstorm development.

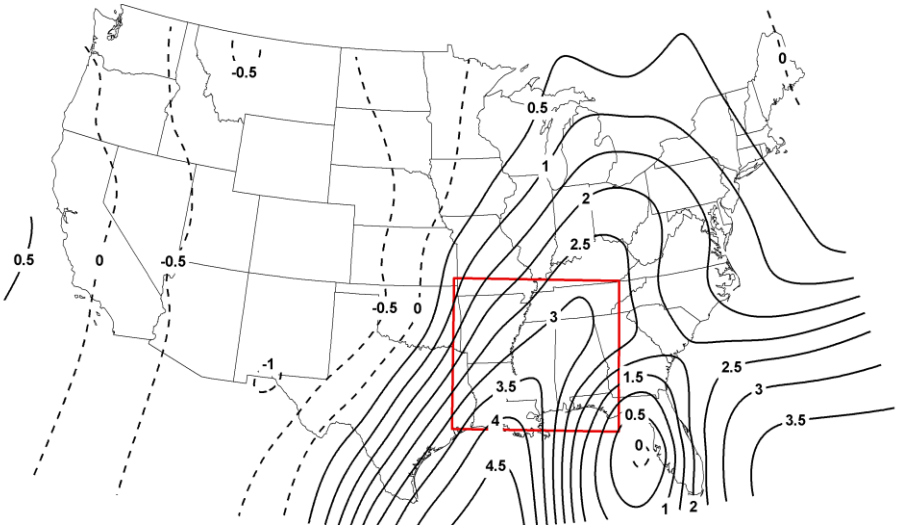

Fig. 4.59**.** 300K November Isentropic surface mixing ratio difference in g/kg calculated by taking the average mixing ratio of the 300K isentropic surface on tornado days minus the average mixing ratio on non-tornado days. Solid lines indicate areas of increased mixing ratio and dotted lines indicate areas of decreased mixing ratio.

In summary, there is a significant shift in the isentropic surfaces when comparing tornado and non-tornado days for the Gulf States in November. First,

an anomalously strong isentropic trough develops across the region, with an average increase in pressure over the region of 45hPa on tornado days. With a strengthening isentropic trough across the region, mixing ratio is also found to increase on average 4.89g/kg with an axis of increase running from Louisiana up through Ohio which matches nearly identically with the axis of greatest pressure increase on the 300K surface. I also determined the wind direction to be backing across the region between tornado and non-tornado days on average 35 degrees which with the trough over the region results in substantial uplift since the wind is flowing up the isentropic trough. With the added moisture and added uplift in the region it is not surprising that tornadoes tend to occur when the isentropic pattern, as I have described, is over the region. Finally, I suggest forecasters use the 300K isentropic surface when forecasting in this region in order to obtain an accurate representation of the lower levels of the atmosphere.

p. December – Region 1 (Lower Mississippi River)

For December the region I choose was located across the lower Mississippi river valley which from 1974 through 2009 included 379 (31 percent) of the 1,220 tornado reports during that time frame (Fig 4.60). This region included three upper air stations that were used in the analysis, which included: Little Rock, AR (72340), Jackson, MS (72235), and Lake Charles, LA (72240).

Fig. 4.60**.** Red box is the boundary for the study region 1 for December. Black dots indicate tornado reports within the region for December from 1974 through 2009. This region contained 379 (31 percent) of the 1,220 tornado reports during this timeframe.

The primary variable to examine when conducting an isentropic analysis is the pressure at which a given isentropic surface occurs. For the Lower Mississippi River region in December I examined the 315K, 310K, 305K and 300K isentropic surfaces using a Kruskal-Wallis test to determine if there was a difference in median for tornado and non-tornado day. Upon conducting this test, I found that each of the three stations at each isentropic level had a statistically significant at the 95 percent confidence level, increase in pressure (Table 4.15).

Table 4.15**.** Kruskal-Wallis test results for the 300K isentropic level for the following variables: pressure level (hPa), wind direction (º from N), wind speed (kts) and mixing ratio (g/kg) for the five stations within study region 1 for December. Bolded values indicate those that were not significant at the 95 percentile confidence interval ($p < 0.05$). The entire table for the 315K, 310K, 305K and 300K can be found in the Appendix A.

		300K Pressure Level (hPa)	300K Wind Direction (°)	300K Wind Speed (knots)	300K Mixing Ratio (g/kg)
Little Rock, AR	Non-Event	711	264	31	1.32
	Event	760	232	35	4.99
	Difference	49	-32	4	3.67
	p-value	0	0	0.023	0
Jackson, MS	Non-Event	745	260	26	1.83
	Event	800	209	30	6.38
	Difference	55	-51	4	4.55
	p-value	0	0	0.07	0
Lake Charles, LA	Non-Event	778	258	21	2.3
	Event	834	206	30	8.02
	Difference	56	-52	9	5.72
	p-value	0	0	0	0

While each isentropic surface had a significant increase in pressure, the 300K isentropic surface has the greatest increase with an average median increase of 53hPa. Since the 300K isentropic level displays the largest change and since it is the level that is closest to the surface I recommend this surface to be used in forecasting in this region and will be the primary level of focus within this section. The largest increase was at Lake Charles, LA, where on tornado days the median pressure of the 300K surface increased 56hPa. By examining the statistical results, the greatest increase in pressure occurs at the stations in the

eastern portion of the region with a smaller increase on the western side of the region. Similarly, the 300K anomaly pattern (the average 300K isentropic pattern for tornado days was subtracted from the average pattern on non-tornado days, Fig. 4.61) has the largest increase across the contiguous United States over Ohio, to the northeast of the study region with an axis of increase running down through the panhandle of Florida. As was found in other region/month combinations in the south, one of the keys features to examine is the location of the troughing to ridging gradient which is located to the west of the study region. As this moves through the region it would result in enhanced uplift as it generally indicates a front and moving from higher pressure (lower heights) to lower pressures (higher heights).

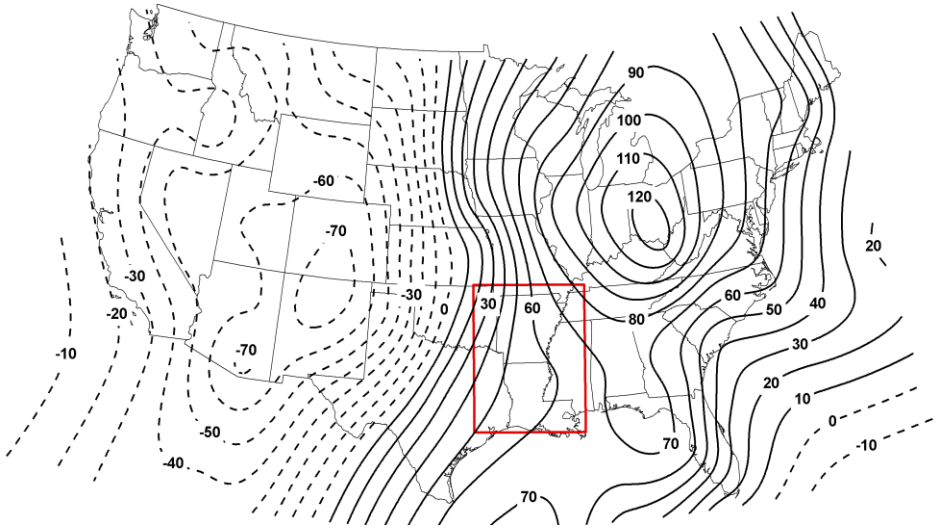

Fig. 4.61. 300K December Isentropic surface pressure difference calculated by taking the average pressure level of the 300K isentropic surface on tornado days minus the pressure level on non-tornado days. Solid lines indicate areas of increasing pressure (lowering heights) and dotted lines indicate areas of rising pressures (rising heights).

Examining the actual 300K isentropic pattern, on non-tornado days a fairly flat and zonal isentropic pattern is noted across the study region (Fig. 4.62).

On the other hand, on tornado days a rather pronounced isentropic trough can be seen across the region with the trough axis running from eastern Tennessee down through Georgia. A large isentropic ridge is located over the western United States, which verifies the location of the ridge to trough gradient to the west of the study region which could enhance uplift as it moved through the region. With this shift in the isentropic pattern, an examination into the wind speed and direction is also important to determine if uplift changes with the change in the overall isentropic pattern.

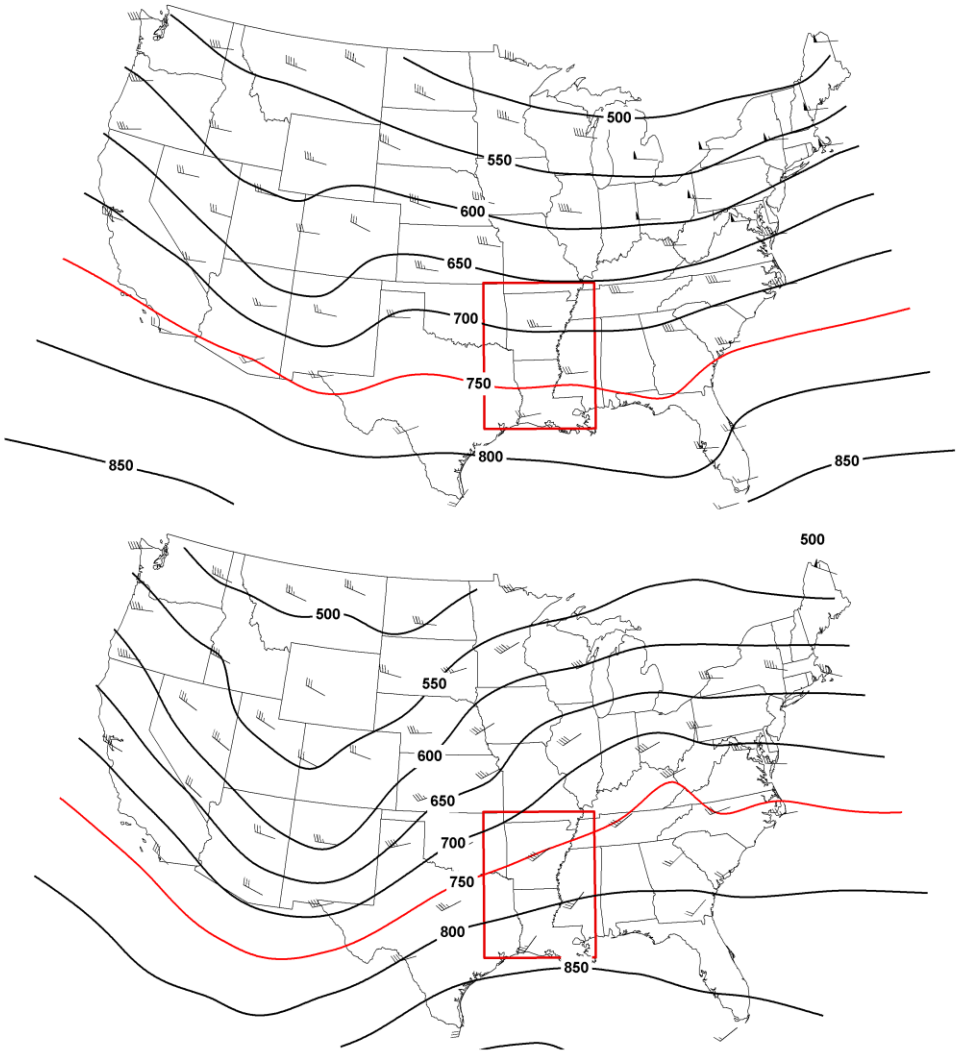

Fig. 4.62**.** (a) average 300K December isentropic surface and wind direction/speed for non-tornado days from 1974 through 2009 (b) same as the above but for tornado days. The 750hPa isobar is highlighted in red to easily show the shift in pattern from non-tornado to tornado days.

To examine how wind speed and direction change on tornado versus non-tornado days, I used the Kruskal-Wallis test. For each station within the region on each of the four isentropic levels, the median wind direction showed a statistically significant change on tornado days as compared to non-tornado days. Each of the stations indicated a backing (counterclockwise shift) wind which, once again, showed the greatest shift in wind direction was found on the 300K isentropic surface. On average, the median wind direction shifted from 260 degrees (west) on non-tornado days to 216 degrees (south-southwest) on tornado days. The isentropic pattern (Fig. 4.62) shows that on non-tornado days the flow is primarily parallel to the isentropic isobars indicating no up-sloping or down-sloping flow within the atmosphere. On tornado days the shift results in wind flowing across the isobars and, in this case, from high pressures (low heights) to low pressures (high heights) indicating a large amount of uplift in the atmosphere across the region. I compared wind speed with a Kruskal-Wallis test for tornado and non-tornado days and each station at the 300K isentropic level showed a statistically significant change at the 95 percent confidence level, but the change was only on the order of four to nine knots which, by an operational forecasting standpoint, would not be of sufficient magnitude to use as a forecasting parameter, as a result wind direction should be used for analysis.

I analyzed mixing ratio on tornado and non-tornado days using a Kruskal-Wallis test and determined that, like wind direction and pressure on the isentropic surface, mixing ratio for each station and isentropic surface had a statistically significant change on tornado days. In fact, the median mixing ratio average across the study region on the 300K surface increased 3.64g/kg. The greatest increase was located across the southern and eastern portion of the study region (Fig. 4.63) which is closely linked with the greatest increase in pressure on the isentropic surface seen in Fig. 4.61. With this added moisture, the isentropic trough and the shift in wind direction resulting in enhanced uplift thunderstorm development across this region is plausible.

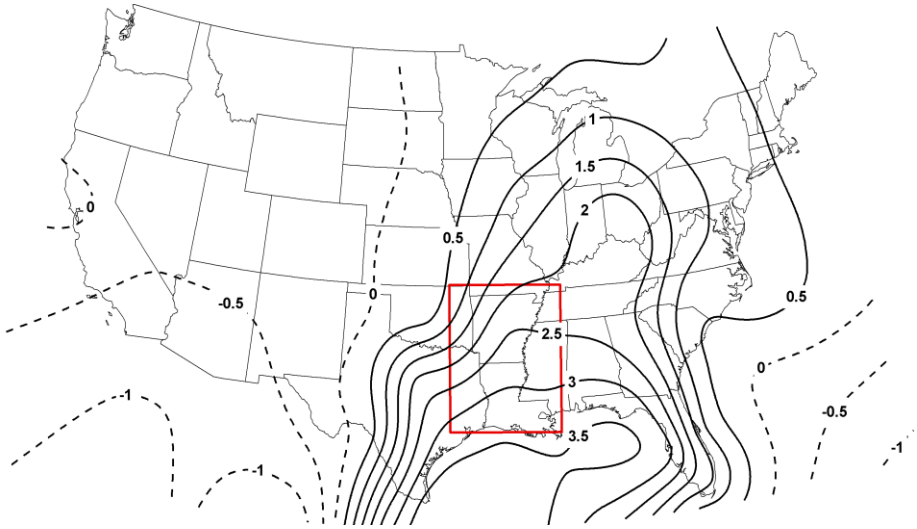

Fig. 4.63**.** 300K December isentropic surface mixing ratio difference in g/kg calculated by taking the average mixing ratio of the 300K isentropic surface on tornado days minus the average mixing ratio on non-tornado days. Solid lines indicate areas of increased mixing ratio and dotted lines indicate areas of decreased mixing ratio.

In summary, for the Lower Mississippi River region in December, I found the pressure on a given isentropic surface, the wind direction; wind speed and

mixing ratio had statistically significant changes in median value when comparing tornado and non-tornado days. The main isentropic surface used in this section was the 300K surface since it is the closest to the ground and displayed the greatest changes. On tornado days, an amplified isentropic trough developed across the region, with an average pressure increase on the 300K surface of 56hPa. With this trough across the region, it advected in moisture with an average increase of 3.64g/kg across the study region. The wind direction also was found to be backing on average 44 degrees, which results in a flow up the isentropic trough (from high pressure to low pressure) indicating a large amount of uplift across the region. With an increase in moisture and additional uplift across the region as a result of the wind direction shift and isentropic trough, this could aid in the development and continuation of thunderstorm activity across the region. For forecasters, I recommend using the 300K isentropic level in this region in December due to the fact that the largest changes were noted on this level.

q. Summary

I first divided the contiguous United States into different regions throughout each month using tornado densities. Once the regions were defined I used rawinsonde data from 1974 through 2009 in order to determine the conditions on the 315K, 310K, 305K and 300K isentropic surfaces for non-tornado and tornado days. This was carried out in both the statistical and visual sense. I used the non-parametric Kruskal-Wallis test to determine if there was a significant difference in median value on tornado and non-tornado days for the

following variables: pressure level of the isentropic surface, wind direction, wind speed and mixing ratio.

Upon conducting the statistical tests and visually examining the isentropic maps presented throughout this chapter, the following are the major findings that were common across each of the regions I selected:

a) On tornado days an isentropic trough developed over the regions of interest. This was indicated by an increase in pressure on each of the isentropic surfaces tested which included the 315K, 310K, 305K and 300K surfaces. This isentropic trough is the most basic but essential aspect of producing thunderstorms across a region as isentropic troughs have been linked to an increase in moisture and isentropic troughs can result in added uplift. Uplift can be increased within an isentropic trough two ways: (1) by having wind flow up the isentropic trough, meaning flow from higher pressure (lower heights) to low pressure (higher heights), and (2) by having the back side of a trough move through a given region resulting in air being forced up the isentropic surface from higher pressure to lower pressure purely due to the change in height of the isentropic surface, which is generally marked by the passage of a front.

b) Wind direction shifted counterclockwise or backing at nearly every station in each region between tornado days and non-tornado days. On non-tornado days the flow was parallel to the isentropic isobars indicating little, if any, adiabatic uplift within the atmosphere, whereas the more backing winds on tornado days led to a flow that was perpendicular to the

isentropic pressure contours which resulted in adiabatic uplift. This uplift on tornado days was nearly always up the isentropic trough as described above.

c) Changes in wind speed in each region/month combinations were found to be of a magnitude too small to use in an operational forecasting scheme. Maximum changes in wind speed were less than 10 knots for tornado versus non-tornado days. This small change in wind speed on a day-to-day forecasting scale would be extremely hard to determine. As a result, wind speed is not a parameter to examine on isentropic surfaces in operational forecasting.

d) Mixing ratio in each region/month combination is significantly higher on tornado days as compared to non-tornado days. This is likely the result of the formation of the isentropic trough across the region which allowed moisture to flow into the area from the south.

In this chapter, I have examined the results from the statistical tests and mapped data which were accompanied by a discussion of those results which demonstrated the usefulness of forecasting tornadoes using isentropic analysis. The next chapter presents the results of an independent evaluation of these findings using tornado data from 2010 and 2011. Such an independent test will provide useful verification of the results presented in this chapter.

Chapter 5

INDEPENDENT DATASET VERIFICATION

a. Introduction

In Chapter 4, I examined and discussed how the isentropic surface changed on tornado versus non-tornado days using visual and statistical tests, which included the following variables: pressure level of the given isentropic surface, wind speed, wind direction and mixing ratio. For that portion of the study I used rawinsonde data from 1974 through 2009 which were obtained from the CD-ROM "Radiosonde Data of North America 1946-1996" produced by Forecast System Laboratory, supplemented with data between the years of 1997 through 2009 using data supplied online via National Climatic Data Center (Forecast Systems Laboratory 1997).

In this chapter I used observations independent of those used in Chapter 4 in order to ascertain if the operational aspects of my finding hold true for a separate dataset and for individual tornado cases. To complete this I used the 2010 to 2011 rawinsonde data found online via National Climatic Data Center (Forecast Systems Laboratory 1997). For the 2010 through 2011 time frame, I selected individual tornado events that occurred within each of the fifteen regions and compare them with the findings in Chapter 4. To select the days to use in each region I examined tornado reports from 2010 through 2011 for each month and selected the event that had the most tornado reports within the given region. The tornado reports for this time frame were obtained from the Storm Prediction Center (Storm Prediction Center, 2011) and, since these reports are recent, no

final report of the tornado intensities was available. As a result, the intensity of the tornadoes were not a factor in selecting the event day but was primarily based on the location of the tornado reports.

This chapter is divided into the fifteen separate regions which correlate to the same region/month couplets discussed in Chapter 4 and will conclude with the overall accuracy of the operational aspect of using isentropic analysis in forecasting tornado events.

b. January – Region 1 (Lower Mississippi River Valley)

For this region I selected January 20, 2010 which had twenty-one tornado reports all located within the study region (Fig 5.1a). The first tornado was reported at 2055Z and the last was reported at 650Z.

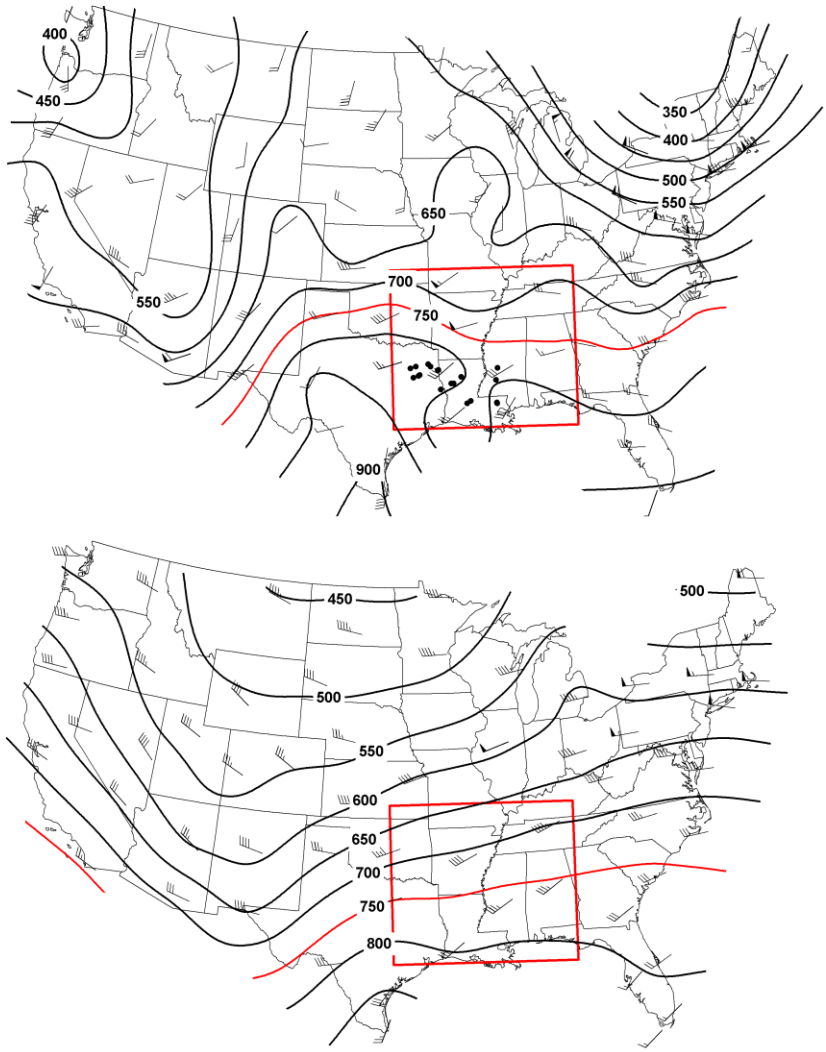

Fig. 5.1**.** (a) 300K isentropic surface with isobars every 50hPa for January 20, 2010 at 12Z. Black dots indicate individual tornado event occurrences. (b) average 12Z January 300K isentropic surface for tornado days across the Lower Mississippi River region from 1974 through 2009. The 750hPa isobar has been highlighted in red on both Figs to more easily compare the pattern.

For this 300K isentropic pattern (Lower Mississippi River region/January) a well-defined isentropic trough stretches from Texas into the northern portion of Louisiana (Fig 5.1a). A smaller scale ridge is located over Louisiana, which by the evening hours would likely shift to the east and out of the study region. Wind direction across the region is also seen to be from the southwest which is up the

isentropic surface, indicating uplift within the atmosphere. For this event, the winds on the 300K surface are most perpendicular to the isobars above and near the location that tornadoes were reported.

Comparing this case study 300K pattern (Fig 5.1a) with the average 300K pattern for tornado days across the Lower Mississippi River region (Fig 5.1b), a number of similarities can be identified. The first and foremost similarity is the location of the isentropic trough across the entire southern United States in both cases, albeit the trough is deeper in the case study, which would be expected given it is being compared to the average tornado pattern. Also, the wind flow was to the southwest, which is forcing air up the isentropic trough in each case, yielding increased uplift. The main difference is the small scale isentropic ridge noted across Louisiana which is likely the result of a small scale feature associated with this particular storm system.

c. February – Region 1 (southeastern Mississippi River)

I selected February 24, 2011 as the independent case example for this region. On this day twenty-seven tornado reports were received (Fig 5.2a), with the first occurring at 2155Z and the last at 510Z (Feb 24, 2011).

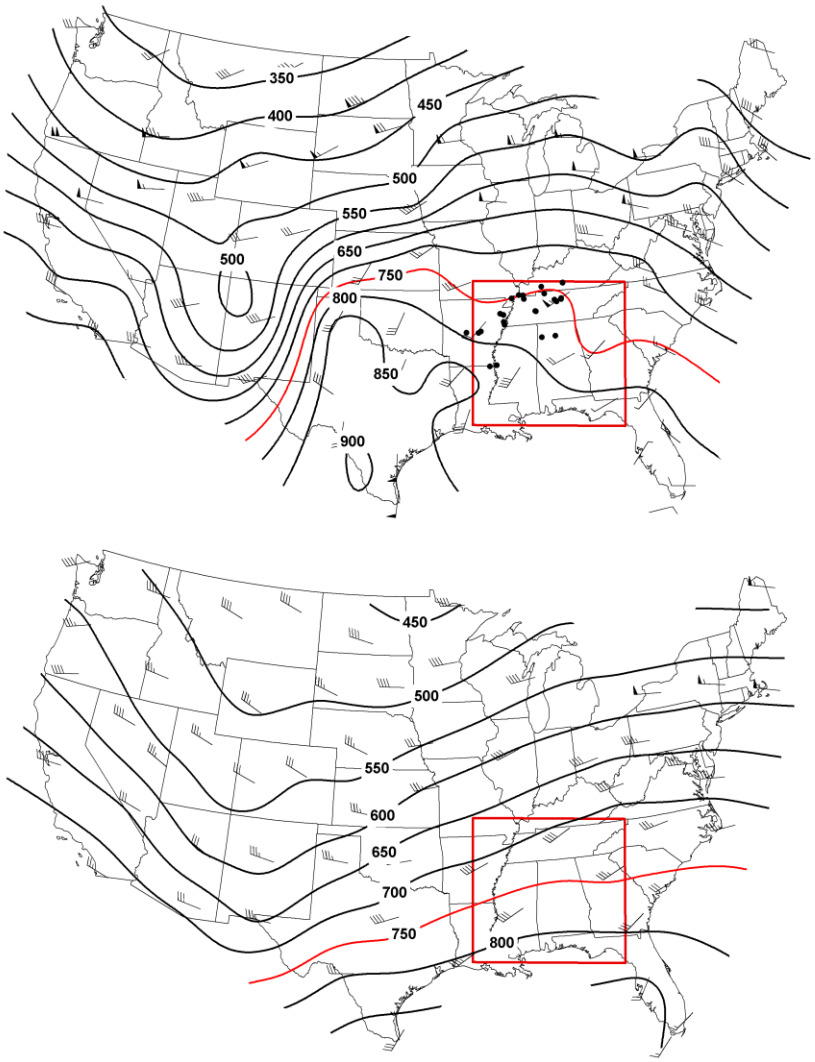

Fig. 5.2**.** (a) 300K isentropic surface with isobars every 50hPa for February 24, 2011 at 12Z. Black dots indicate individual tornado event occurrences. (b) average 12Z February 300K isentropic surface for tornado days across the southeastern Mississippi River region from 1974 through 2009. The 750hPa isobar has been highlighted in red on both Figs to more easily compare the pattern.

The 300K isentropic pattern (Fig 5.2a) indicates an isentropic trough is located over the entire southern United States with two trough axes. The first located over Texas and the second over Tennessee. The wind flow to the west of the region is from the southwest which is directly up the isentropic trough

indicating a large amount of uplift across the region in which tornadoes were reported.

The average 12Z 300K isentropic surface for tornado days in the southern Mississippi River region between 1974 and 2009 (Fig 5.2b) showed a similar pattern to that of the case study shown in Fig 5.2a. In both cases a trough is located across the southern United States, which is actually best shown in the case study with a much deeper and amplified trough across the region with tornadoes. This can be noted by examining the 750hPa isobar in which in the case study is located across the Tennessee/Kentucky border and in the average pattern it is located across northern Mississippi and Alabama. The general wind flow between the case study and average pattern are similar; however, the case study shows a slightly more southerly component to the wind resulting in even more uplift present on the isentropic surface compared to that which was found in the average pattern. The main difference is the presence of a well defined smaller scale isentropic trough directly located across the region that had tornadoes on February 24, 2011, which may have induced additional thunderstorm development to that specific area.

d. March – Region 1 (central Southern Plains)

On March 10, 2010 seven tornadoes were reported in the southern United States with five of those occurring within the study region (Fig 5.3a). The first report occurred at 2217Z and the last was at 905Z (March 11, 2010).

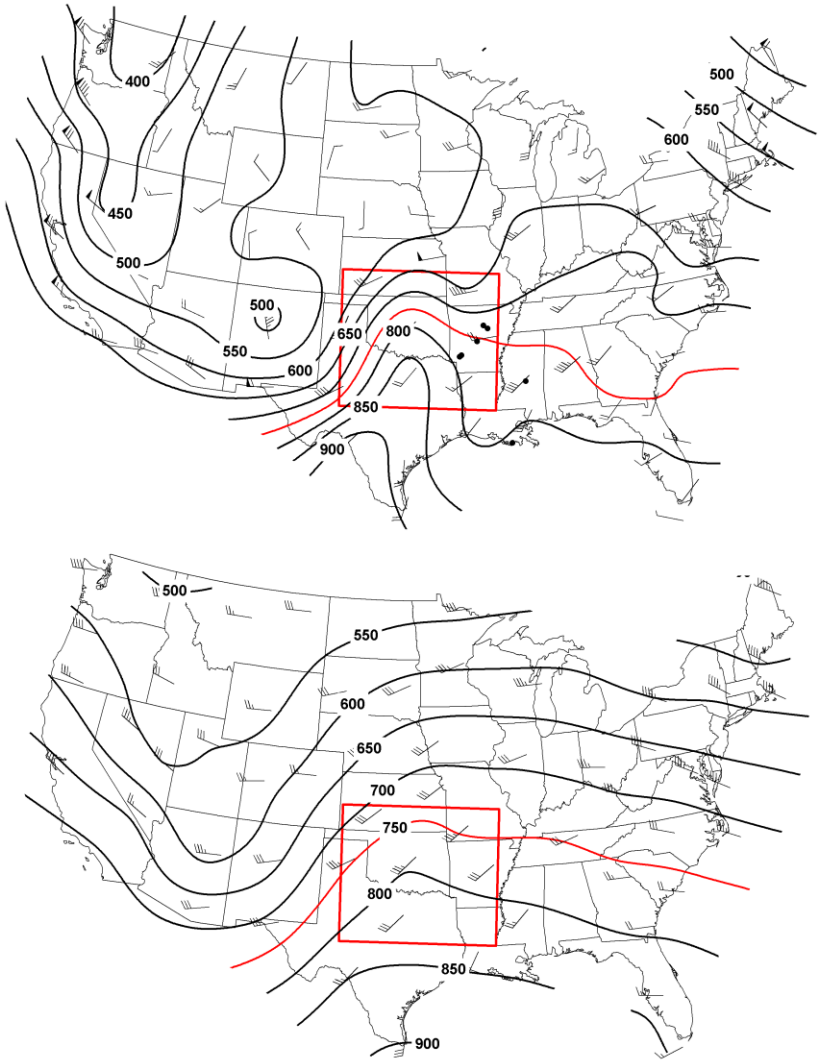

Fig. 5.3**.** (a) 300K isentropic surface with isobars every 50hPa for March 10, 2010 at 12Z. Black dots indicate individual tornado event occurrences. (b) Average 12Z March 300K isentropic surface for tornado days across the central Southern Plains region from 1974 through 2009. The 750hPa isobar has been highlighted in red on both Figs to more easily compare the pattern.

For this event I found an amplified isentropic trough located over central/eastern Texas stretching up into Oklahoma and Nebraska, with a broader trough located across the entire southern United States (Fig 5.3a). On the whole examining where the tornado reports were found, ample moisture was present and with flow up the isentropic trough in those regions increasing uplift, it is not too

surprising that tornadic events occurred within this region with this type of pattern.

Several similarities and differences are seen when comparing this case study (Fig 5.3a) with the average 12Z 300K isentropic pattern for tornado days across the southern Plains region (Fig. 5.3b). The location of the isentropic trough is similar for both analyses. The main difference is the isentropic trough across Texas and Oklahoma is better defined in the case study with a broader trough noted in the average pattern. However, even though the trough is more defined in the case study, it has a slightly shallower trough which is seen by analysis of the 750hPa isobar. This isobar is located across northern Oklahoma for the case study but is further north in southern Kansas for the average pattern. This shift is likely due to the storm system in the case study having a slightly more southerly position compared to the average position of storms in the average pattern from 1974 through 2009. Another similarity is the wind direction, with both the case study and average pattern showing near identical wind direction within the region.

e. March – Region 2 (southeastern United States region, excluding Florida)

The event I selected to verify this region occurred on March 9, 2011, and included twenty-five tornado reports (Fig 5.4a). The first tornado report was recorded at 1208Z and the last was at 1920Z.

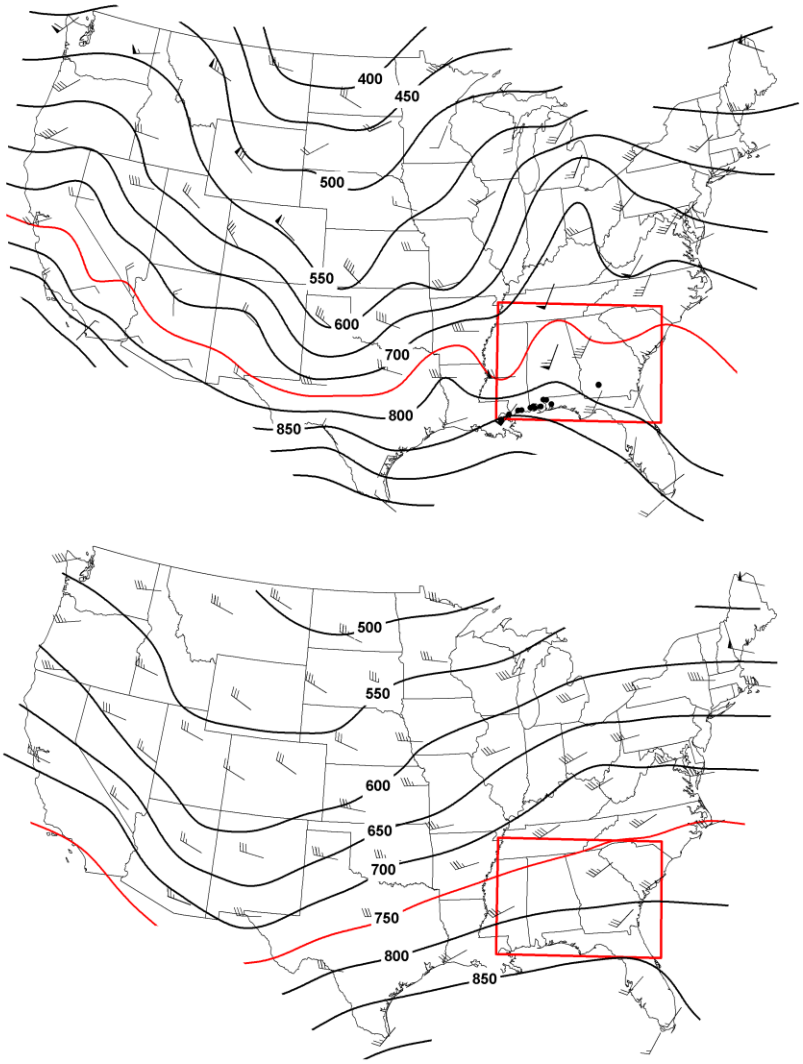

Fig. 5.4**.** (a) 300K isentropic surface with isobars every 50hPa for March 9, 2011 at 12Z. Black dots indicate individual tornado event occurrences. (b) Average 12Z March 300K isentropic surface for tornado days across the southeastern United States region (excluding Florida) from 1974 through 2009. The 750hPa isobar has been highlighted in red on both Figs to more easily compare the pattern.

The 12Z 300K isentropic surface on March 9, 2011 displays an isentropic trough over the eastern United States, with a trough axis located from the panhandle of Florida up through eastern Michigan (Fig 5.4a). A southwesterly wind direction is present across the region, in particular in the location around the tornado reports. This southwesterly wind results in flow up the isentropic trough

indicating uplift across the region. With the added uplift due to the positioning of the isentropic trough and an increase in moisture across the region likely with the positioning of the trough, the increase in tornadic events is plausible.

When comparing the March 9, 2011 case study (Fig 5.4a) with the average 12Z 300K isentropic pattern for tornado days over the southeastern United States region between 1975 through 2009 (Fig. 5.4b), the case study shows a more detailed pattern compared to that of the average pattern. The first difference is the smaller scale isentropic troughs and ridges within the broad large scale isentropic trough across the eastern United States. Also, a rather significant difference is the wind direction, with the case study having primarily a southerly wind flowing directly up the isentropic trough indicating an abundant amount of isentropic lift, while the average pattern shows a southwesterly flow indicating less uplift compared to that of the case study. However, even with these differences and the case study showing a much more dramatic isentropic picture, the primary features of an isentropic trough and flow up the isentropic trough do hold true for both cases.

f. April – Region 1 (Southern Plains)

For this region I selected the April 25, 2011 event which included a total of fifty-nine tornado reports (Fig 5.5a). This first tornado report was at 1405Z with the last report of the day occurring at 740Z (April 26, 2011).

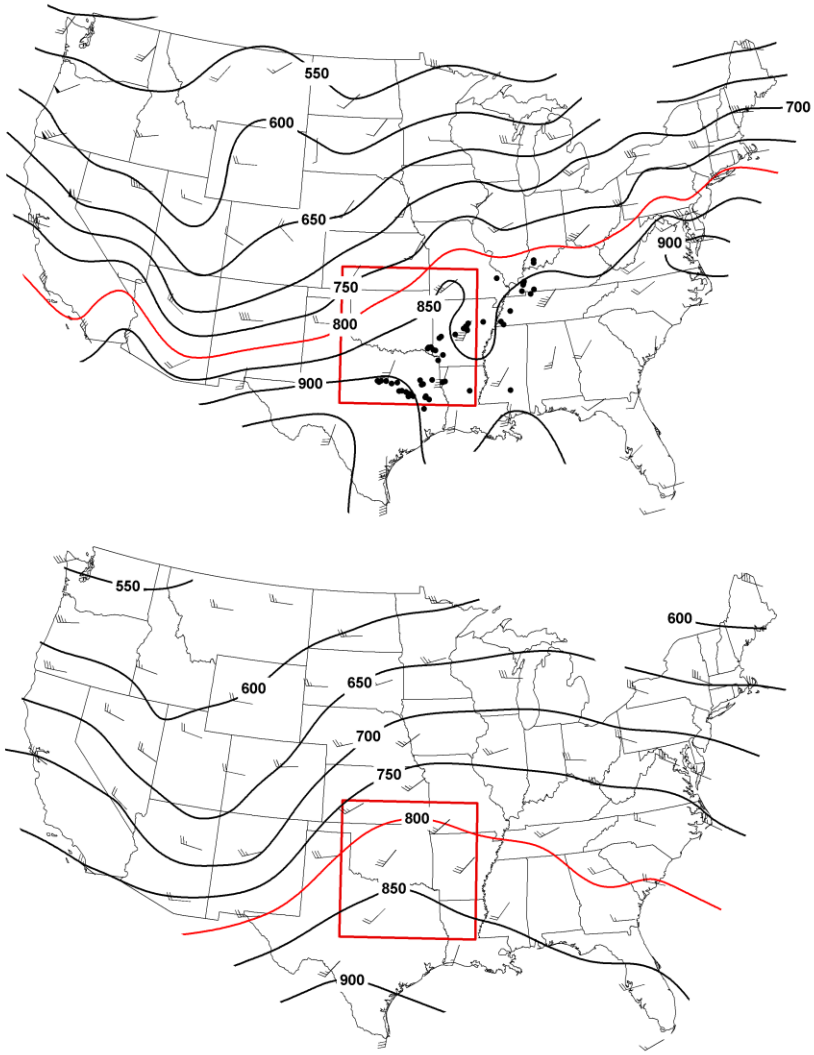

Fig. 5.5**.** (a) 300K isentropic surface with isobars every 50hPa for April 25, 2011 at 12Z. Black dots indicate individual tornado event occurrences. (b) Average 12Z April 300K isentropic surface for tornado days across the southern Plains region from 1974 through 2009. The 800hPa isobar has been highlighted in red on both Figs to more easily compare the pattern.

On April 25, 2011 at 12Z, an isentropic trough is present on the 300K isentropic surface, with a trough axis running from south-central Texas up to the northeast into central Missouri (Fig 5.5a). Within this trough the wind direction is from the south-southwest resulting in flow nearly completely perpendicular the isobars over and to the west of the area in which tornadoes occurred. This flow

indicates vertical motion in the atmosphere as it rises up the isentropic surface from areas of high pressure to low pressure.

Again, this case study on April 25, 2011 and the average 300K isentropic pattern for tornado days across the southern Plains from 1974 through 2009 (Fig 5.5b) yield some similarities and differences. On average, the case study (Fig 5.5a) displays a more amplified trough across the region with tornado reports, whereas the average pattern (Fig 5.5b) still shows an isentropic trough across the region; however, it is shallower and is not as well defined. With regard to the isentropic pattern, there are also smaller scale features within the case study such as the small scale isentropic trough and ridge over southern Missouri and Arkansas, directly over the region with tornadoes, which is a similar pattern that was seen in the case study conducted for January. The wind direction in both the average pattern and case study are nearly identical with both having a south-southwesterly wind direction which is up the isentropic trough indicating uplift across the region possibly enhancing thunderstorm activity.

g. May– Region 1 (central Great Plains)

For independent verification in this region I selected the tornado outbreak that occurred on May 10, 2010. Throughout the day forty-two tornadoes were reported with the first occurring at 1830Z and the last at 150Z (May 11, 2010).

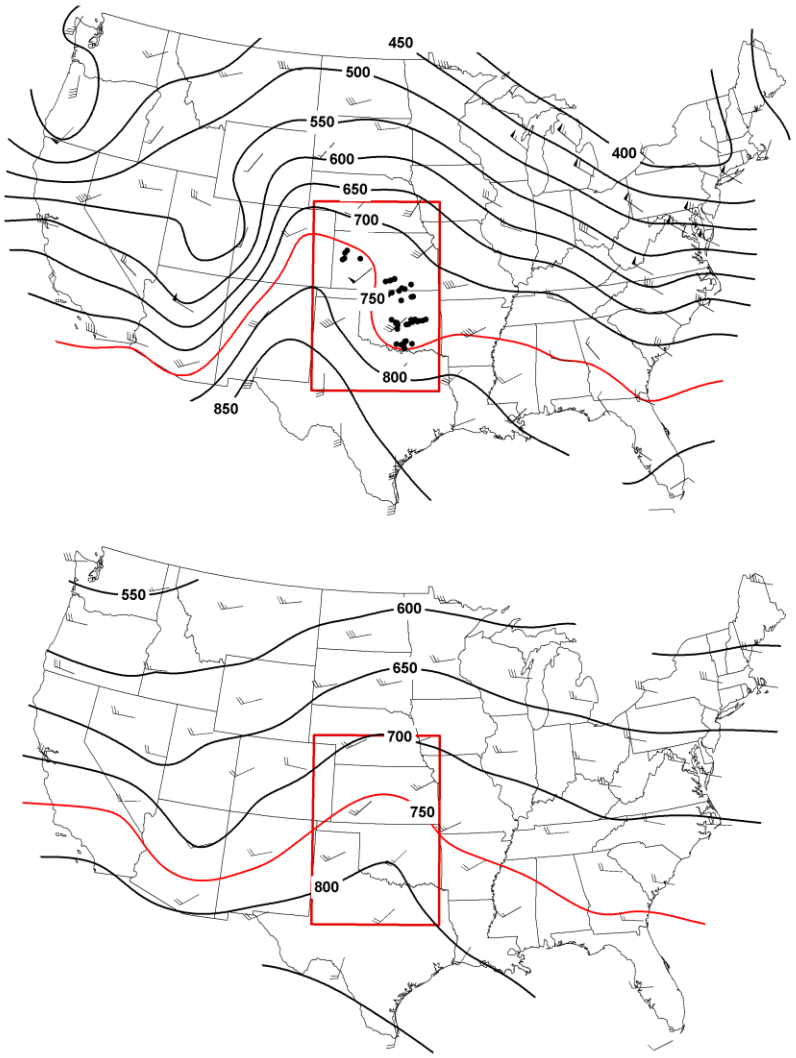

Fig. 5.6**.** (a) 305K isentropic surface with isobars every 50hPa for May 10, 2010 at 12Z. Black dots indicate individual tornado event occurrences. (b) average 12Z May 305K isentropic surface for tornado days across the central Great Plains region from 1974 through 2009. The 750hPa isobar has been highlighted in red on both Figs to more easily compare the pattern.

At 12Z on May 10, 2010 the 305K isentropic pattern shows an isentropic trough across the New Mexico/Texas state line running northward into Nebraska (Fig 5.6a). Examining the wind direction on this surface shows over the region where tornadoes developed, the wind direction was nearly perpendicular to the isobars, resulting in the most isentropic lift possible on the 305K surface. This lift

and moisture associated with the isentropic trough could result in enhanced thunderstorms across the region.

Comparing the 12Z 305K isentropic surface for May 10, 2010 (Fig 5.6a) and the average 12Z 305K isentropic surface for tornado days in the Great Plains region (Fig 5.6b) yielded similar results. In both cases, an isentropic trough of similar depth was located across the region, with the main difference being the location of the trough axis. In the case study, the axis was located along the Colorado/Kansas state line, whereas in the average pattern it was located nearly directly over the center of the study region. The other major difference is the small scale isentropic ridge located over Oklahoma in the case study. This same small scale ridge is also evident in the January and May case studies and is something for more detailed investigation in future studies especially when a less coarse dataset becomes available. Wind direction was also found to be similar in the average pattern and in the case study with a southwesterly wind resulting in flow up the isentropic trough.

h. June – Region 1 (Upper Great Plains)

June 17, 2010 is the event I chose to use in order to verify the findings in section 4.h. This event had a total of one hundred fifteen tornado reports mainly across northeastern portion of the study region (Fig 5.7a). The first tornado report was at 1931Z and the last for the day was reported at 308Z (June 18, 2010).

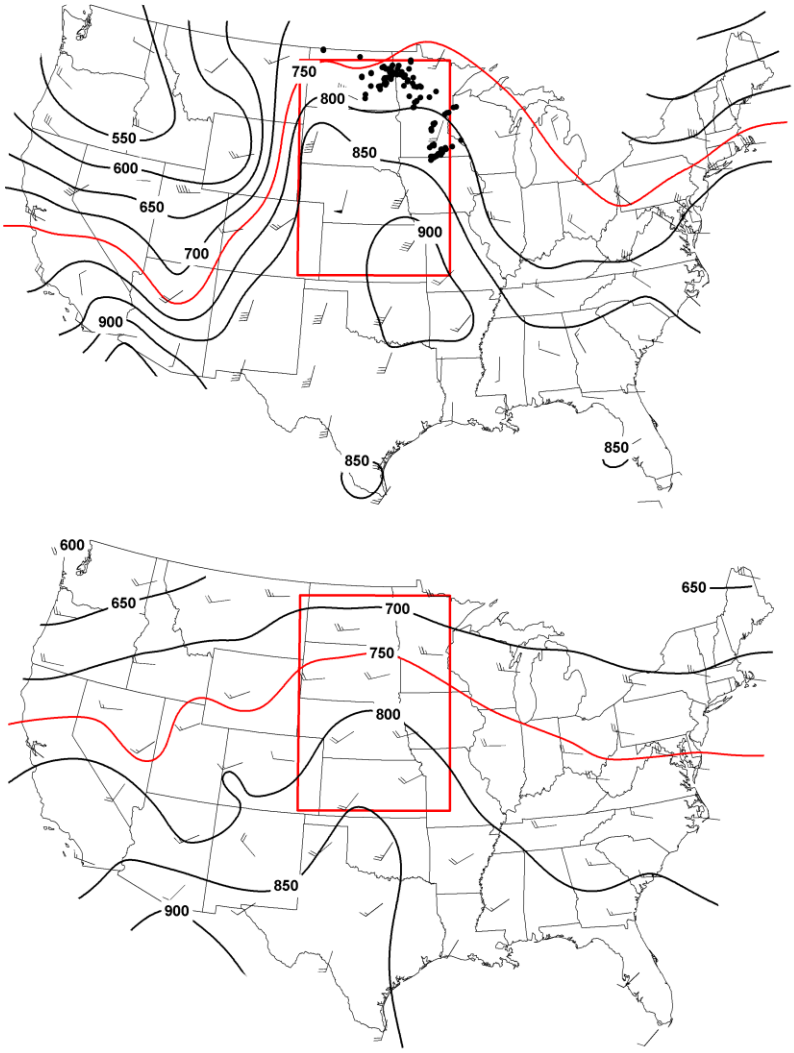

Fig. 5.7**.** (a) 305K isentropic surface with isobars every 50hPa for June 17, 2010 at 12Z. Black dots indicate individual tornado event occurrences. (b) Average 12Z June 305K isentropic surface for tornado days across the Upper Great Plains region from 1974 through 2009. The 750hPa isobar has been highlighted in red on both Figs to more easily compare the pattern.

A highly amplified isentropic trough is seen to be located across the entire plains with an axis running from the southern tip of Florida straight up through North Dakota (Fig 5.7a). The tornadoes that occurred on this day were located just to the east of the trough axis. Also the southerly and southwesterly wind direction in and around the area with tornadoes, given the isentropic pattern,

results in flow up the isentropic surface which likely helped to enhance thunderstorms across the region leading to tornadic storms.

On the 305K isentropic surface an isentropic trough can be seen in the region for both the 12Z June 17, 2010 case study (Fig 5.7a) and the average 305K isentropic surface for tornado days within the Great Lakes region from 1974 through 2009 (Fig 5.7b). The isentropic trough is indeed deeper and shifted slightly northward compared to the average pattern; however, this is likely the result of the tornado in the case study being in the northern portion of the study region which would result in the northern portion of the isentropic trough being further north compared to that of the average pattern where it is located in nearly the center of the region. Wind direction is different in the case study compared to the average pattern. In the case study the winds were primarily from the south-southwest directly up the isentropic trough resulting in a great deal of isentropic lift. On the average pattern the flow was more southwesterly to westerly, which still results in uplift as a result of the overall isentropic pattern but is not as dramatic as found in this case study. However, with one hundred and fifteen tornadoes being reported on June 17, 2010, it would be expected to have well above average uplift across the region with such a large outbreak.

i. June – Region 2 (Great Lakes region)

June 5, 2010 sixty-seven tornadoes were reported and was the event I selected for the case study for the Great Lake region (Fig 5.8a). The first tornado report came in at 1751Z and the last was at 934Z.

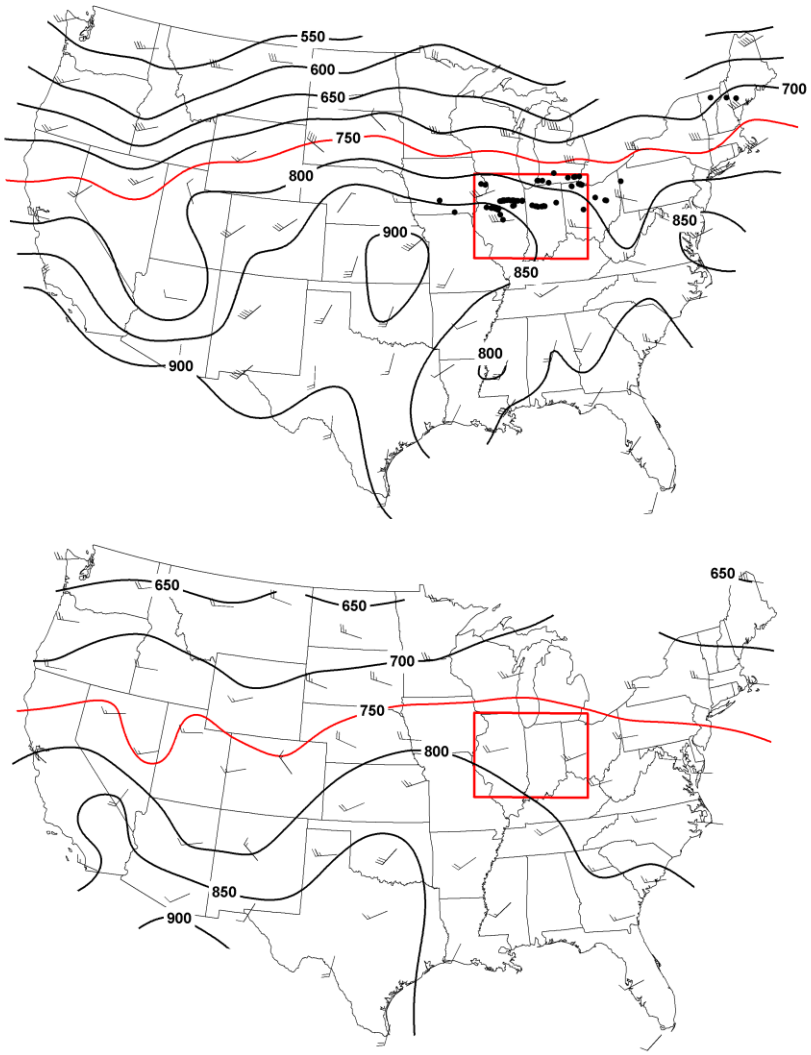

Fig. 5.8**.** (a) 305K isentropic surface with isobars every 50hPa for June 5, 2010 at 12Z. Black dots indicate individual tornado event occurrences. (b) Average 12Z June 305K isentropic surface for tornado days across the Great Lakes region from 1974 through 2009. The 750hPa isobar has been highlighted in red on both Figs to more easily compare the pattern.

The 305K isentropic trough axis was located along a line from south-central Texas up through Illinois, which is just to the west of the locations of tornado reports (Fig 5.8a). The wind direction within the region where tornadoes occurred is nearly parallel the isobars to the west and east of the tornado reports.

Around the specific region of the tornado reports, a flow more perpendicular to the isobars was present, indicating added uplift in the atmosphere.

Comparing the 305K isentropic surface at 12Z June 5, 2010 case study (Fig 5.8a) with the average 305K isentropic surface for tornado days in the Great Lakes region from 1974 through 2009 (Fig 5.8b), several similarities emerge. In both cases an isentropic trough is located across the region. The only difference is the trough has an axis shifted eastward stretching into Illinois and Indiana for the case study which would be expected given the location of the tornado reports. The trough is also deeper for the case study compared to the average pattern. Wind direction is near identical across the region in both cases with primarily westerly flow.

j. July – Region 1 (Upper Plains)

For July, I choose an event that had fifteen tornado reports and occurred on July 10, 2011 (Fig 5.9a). The first tornado was reported at 1940Z with the last occurring at 148Z (July 12, 2011).

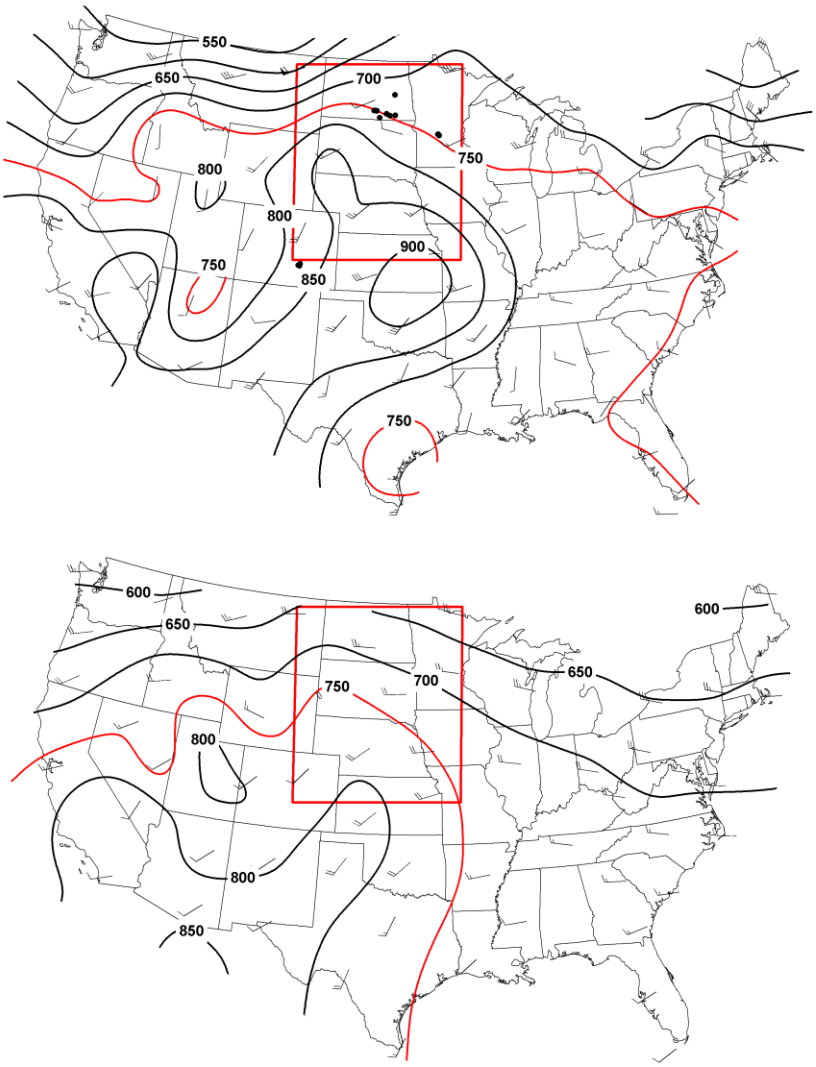

Fig. 5.9**.** (a) 310K isentropic surface with isobars every 50hPa for July 10, 2011 at 12Z. Black dots indicate individual tornado event occurrences. (b) Average 12Z July 310K isentropic surface for tornado days across the Upper Plains region from 1974 through 2009. The 750hPa isobar has been highlighted in red on both Figs to more easily compare the pattern.

A large isentropic trough is noted across nearly the entire United States, with a slightly deeper trough located along a line from southern New Mexico up through South Dakota (Fig 5.9a). With this trough, the wind flow in the western regions of North Dakota and South Dakota were up the isentropic trough indicating uplift. Since this region of uplift is located just to the west of the

tornado reports, it seems plausible that this isentropic lift would move over the region throughout the day enhancing thunderstorms.

Both the case study (Fig 5.9a) and the average 310K isentropic surface for tornado days across the Upper Plains between 1974 and 2009 (Fig 5.9b) show similarities. The first is the location of the large scale isentropic trough with an axis running from Texas up through North Dakota and South Dakota. In this case study the northern extent of the trough is shifted further north compared to the average pattern which can be seen by examining the 750hPa isobar, with the average pattern 750hPa isobar located across South Dakota, and in the case study that isobar is across North Dakota. This is likely due to the positioning of the tornadoes in the case study. With the tornado reports in the northern portion of the region for the case study, it would seem reasonable that the isentropic trough would also be shifted up to the northern portion of the study region. Wind direction, with the exception of the station in northeast South Dakota, displays similar results from the average pattern and the case study.

k. July – Region 2 (Mid-Atlantic)

For the second region in July, located across the Mid-Atlantic, I selected July 24, 2010, which had seven tornado reports within the area (Fig 5.10a). The first tornado was reported at 2040Z with the last being reported at 2345Z.

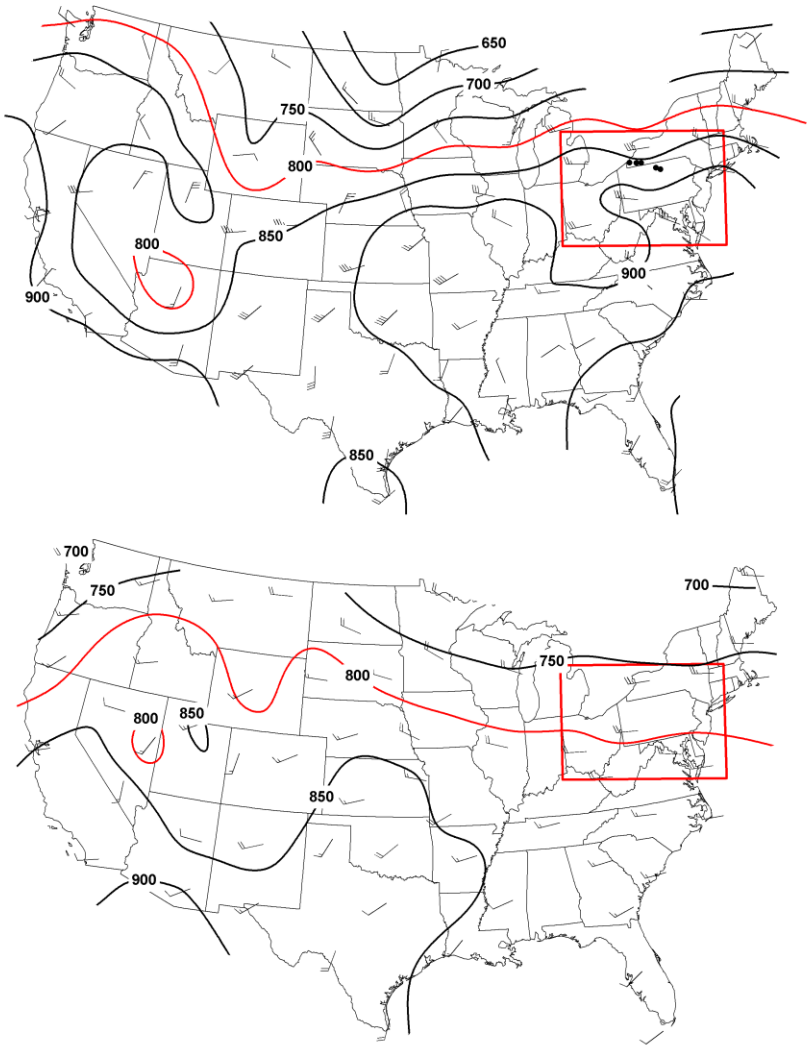

Fig. 5.10**.** (a) 305K isentropic surface with isobars every 50hPa for July 24, 2010 at 12Z. Black dots indicate individual tornado event occurrences. (b) average 12Z July 305K isentropic surface for tornado days across the Mid-Atlantic region from 1974 through 2009. The 800hPa isobar has been highlighted in red on both Figs to more easily compare the pattern.

Fig 5.10a shows the 12Z 305K isentropic pattern on July 24, 2010. Of most interest, is the presence of two small scale isentropic troughs within the study region. The first was located over eastern Michigan and the second over eastern New York. With the two small scale isentropic troughs likely resulting in

uplift as they move through the region, mixing ratio is also found to be elevated which could enhance thunderstorm development.

Some remarkable similarities are present when comparing the 305K isentropic surface for the 12Z July 24, 2010 case study (Fig 5.10a) with that of the average pattern on tornado days in the Mid-Atlantic region from 1974 through 2009 (Fig. 5.10b). The most notable feature is the presence of two small scale isentropic troughs located on the east and west sides of the study region. Unfortunately, a higher resolution isentropic dataset would need to be created to analyze these in more detail. But, given that these features were found in both the long term average and in the case study, these troughs are certainly features that need to be explored in greater detail when such data sources become available. Wind direction also shows great similarity with primarily a westerly flow across the region.

l. August – Region 1 (Great Lakes/Midwest)

On August 23, 2011, five tornado reports occurred within the study region and was the event I selected to verify the Great Lakes/Midwest Region (Fig 5.11a). The first tornado was reported at 2205Z with the last being at 205Z (August 24, 2011).

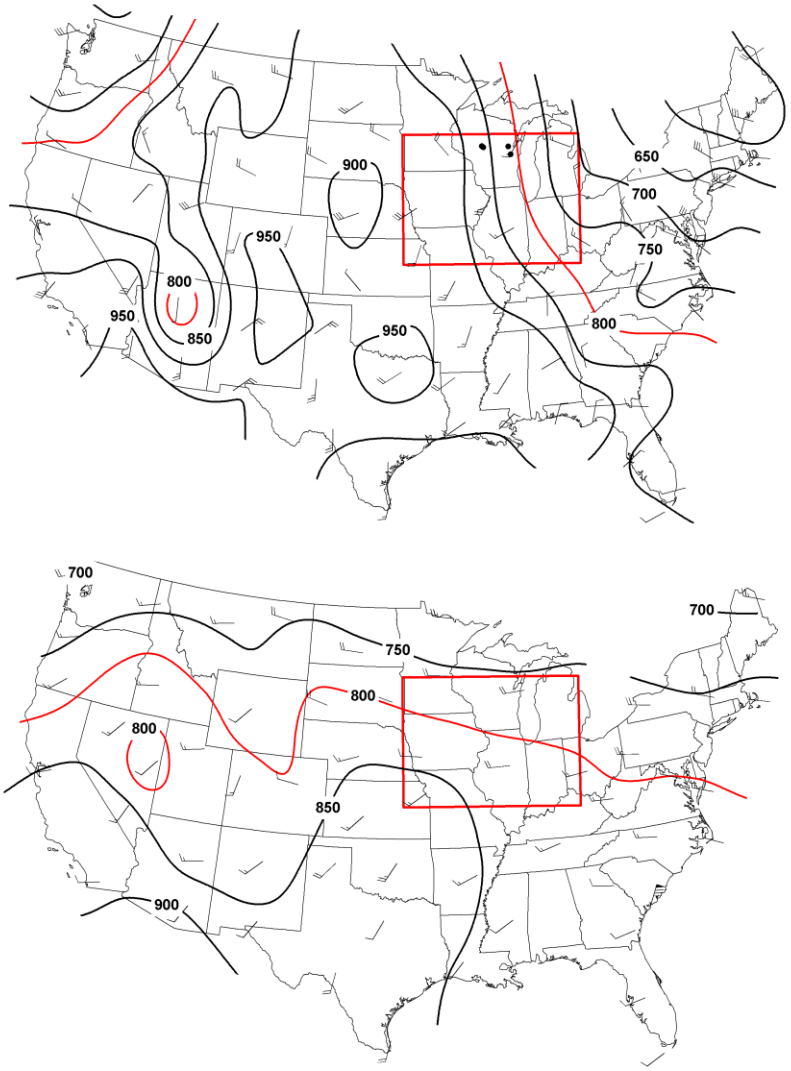

Fig. 5.11**.** (a) 305K isentropic surface with isobars every 50hPa for August 23, 2011 at 12Z. Black dots indicate individual tornado event occurrences. (b) Average 12Z August 305K isentropic surface for tornado days across the Great Lakes/Midwest region from 1974 through 2009. The 800hPa isobar has been highlighted in red on both Figs to more easily compare the pattern.

A large scale isentropic trough was located across the western and central portion of the United States, which is likely the nearly stationary isentropic trough associated with the North American Monsoon (Namias 1940, Cerveny et. Al. 2010) (Fig 5.11a). All of the tornado reports of this event are located on the

eastern perimeter of the isentropic trough where the flow is also found to be from the southwest which is moving up the isentropic trough.

Comparing the 12Z August 23, 2011 case study showing the 305K isentropic pattern (Fig 5.11a) with the average 305K isentropic pattern from tornado days within the Great Lakes/Midwestern region from 1974 through 2009 (Fig 5.11b) several similarities are noted. The first is the broad isentropic trough associated with the North American Monsoon. In the case study the trough is more amplified which should be expected given that this high amplification would be averaged out in the long term pattern. Wind direction, when comparing the two patterns, is slightly different with the average pattern having a westerly flow across the region and the case study having a more southwesterly flow across the region. Even though the direction is slightly varying in both cases, the flow presented results in flow up the isentropic trough, which is important for increased uplift.

m. September – Region 1(Gulf States)

I selected September 4, 2011 to verify the results from section 4.m. On this day, nineteen tornadoes were reported, with the majority occurring in Mississippi (Fig 5.12a). The first tornado was reported at 1243Z and the last at 821Z (September 5, 2011). This is also a slightly different event than those previously discussed as this was the day that Tropical Storm Lee made landfall along the Louisiana coast.

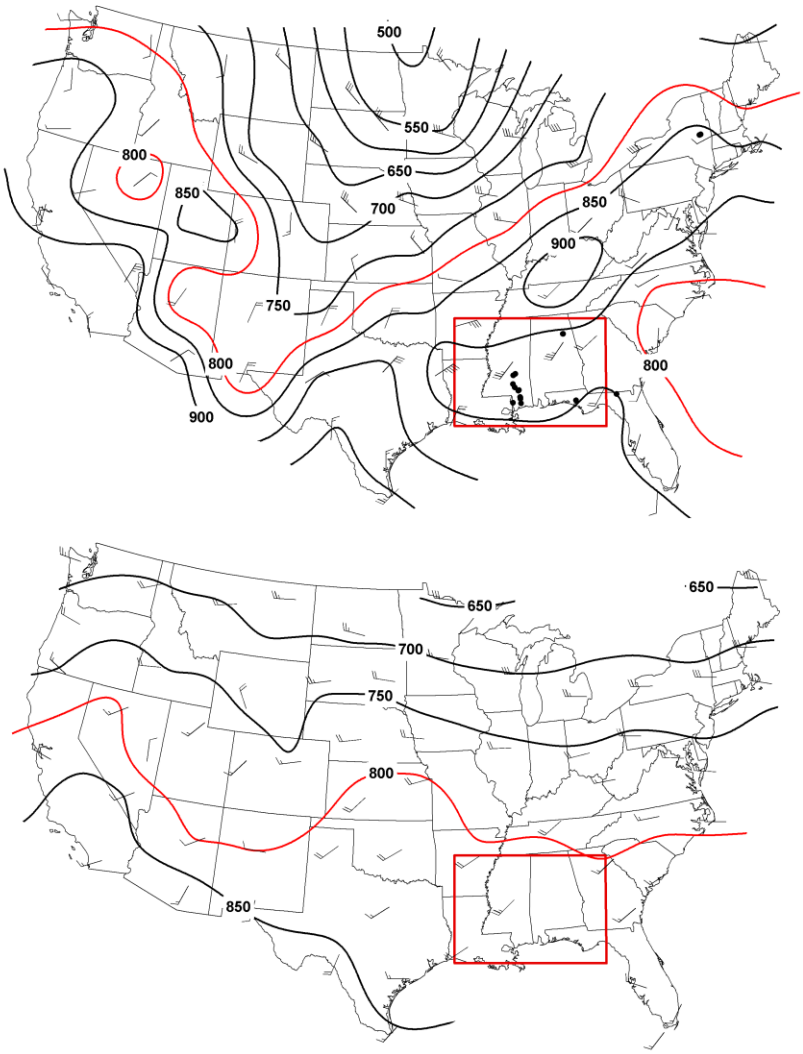

Fig. 5.12**.** (a) 305K isentropic surface with isobars every 50hPa for September 4, 2011 at 12Z. Black dots indicate individual tornado event occurrences. (b) Average 12Z September 305K isentropic surface for tornado days across the Gulf States region from 1974 through 2009. The 800hPa isobar has been highlighted in red on both Figs to more easily compare the pattern.

The 305K isentropic surface for this day shows an isentropic trough over the southern and eastern portion of the Unites States, with an isentropic ridge over the central and western portion of the United States (Fig 5.12a). For the specific area of tornado reports, the wind is from the southwest, producing flow up the isentropic trough which indicates uplift on the isentropic surface. Of much interest

is the down sloping northeasterly flow just to the west of the tornado reports. While this abrupt switch in wind direction over Mississippi and Louisiana is likely the result of Tropical Storm Lee, isentropic analysis does indicate areas of enhanced uplift within a smaller scale system resulting in the possibility of better forecasting areas of severe thunderstorms.

Several aspects on the 305K isentropic surface are found to be different while many others are found to be similar, when comparing the 12Z September 4, 2011 case study (Fig 5.12a) with the average isentropic pattern for tornado days in the Gulf States region between 1974 and 2009 (Fig 5.12b). The most notable is the rather amplified isentropic trough across the entire eastern United States in the case study, whereas the average pattern shows a fairly zonal surface with smaller scale isentropic troughs located with the large scale pattern. Wind direction, within the tornado region, are similar to the case study and average pattern with flow on average up the isentropic trough.

n. October – Region 1 (Southern Great Plains)

I chose October 24, 2010 to verify the October region discussed in section 4.n. On this date twenty tornado reports were made, with the first occurring at 2030Z and the last being reported at 1020Z (October 25, 2010).

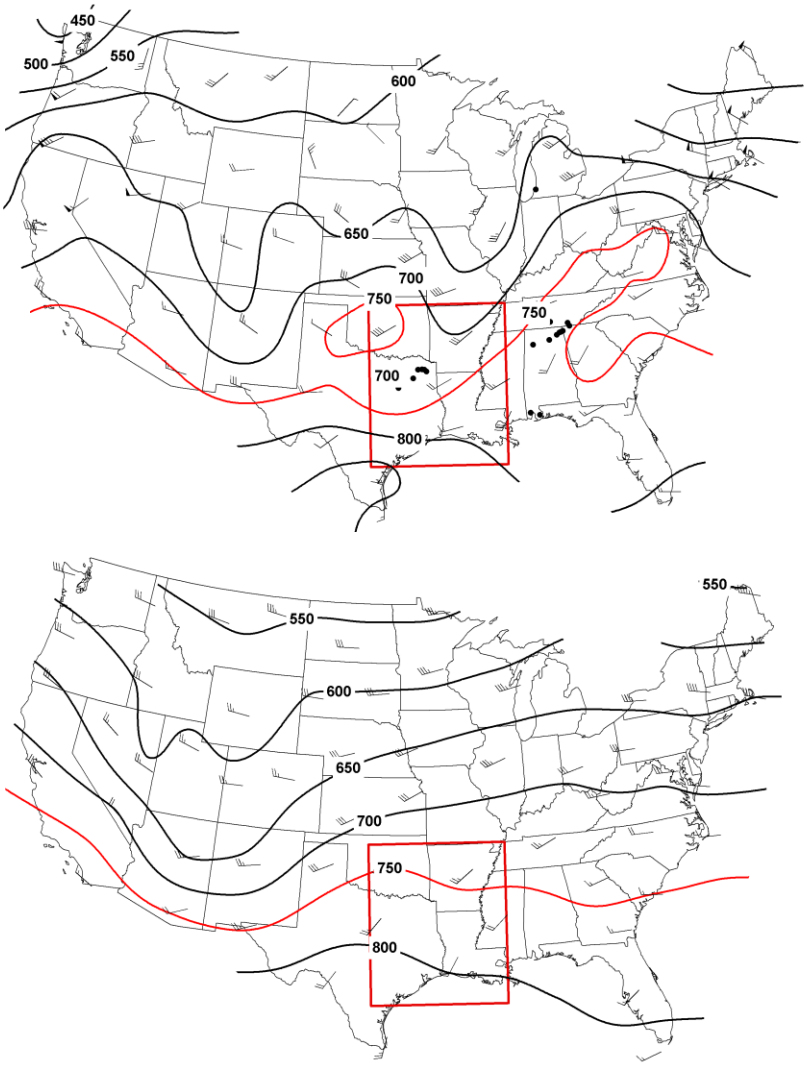

Fig. 5.13**.** (a) 305K isentropic surface with isobars every 50hPa for October 24, 2010 at 12Z. Black dots indicate individual tornado event occurrences. (b) Average 12Z October 305K isentropic surface for tornado days across the Southern Great Plains region from 1974 through 2009. The 750hPa isobar has been highlighted in red on both Figs to more easily compare the pattern.

On October 24, 2010 at 12Z the 305K isentropic surface reveals a broad isentropic trough across the southern Plains (Fig 5.13a). The overall flow across the region is from the southwest which results in air moving from higher pressure values to low pressure values and indicates uplift across the region. Also of note is the closed isentropic trough identified by the 750hPa isobar. This is a feature

that would need to be examined closer once a higher resolution isentropic dataset becomes available. While not associated with this region being discussed, something of note is the highly amplified isentropic trough and wind flow directly up the trough in the region associated with the tornadoes over northern Alabama and southern Tennessee, which I point out as the same isentropic pattern that has been seen in previous sections that was associated with tornado events.

When comparing the 12Z October 24, 2010 case study on the 305K surface (Fig 5.13a) with the average 305K isentropic pattern on tornado days across the Southern Great Plains between 1974 and 2009 (Fig 5.13b), similar isentropic troughs are evident in both analyses. In the average pattern a more pronounced trough is located across Oklahoma and in the case study the trough actually forms a closed feature, particularly for the 750 hPa isobar, over Oklahoma. Even though this closed feature is not shown on the average pattern, a lower 305K isentropic surface is located across this region as noted by the deeper trough in the average pattern. Wind direction on both maps across the region is from the southwest with flow up the isentropic trough resulting in added uplift.

o. November – Region 1(Gulf States)

I selected November 29, 2010 as the date to use for verifying results in section 4.o. On this day, twenty-five tornadoes reports were contained within the region with the first report occurring at 2113Z and the last being at 1150Z (November 30, 2010).

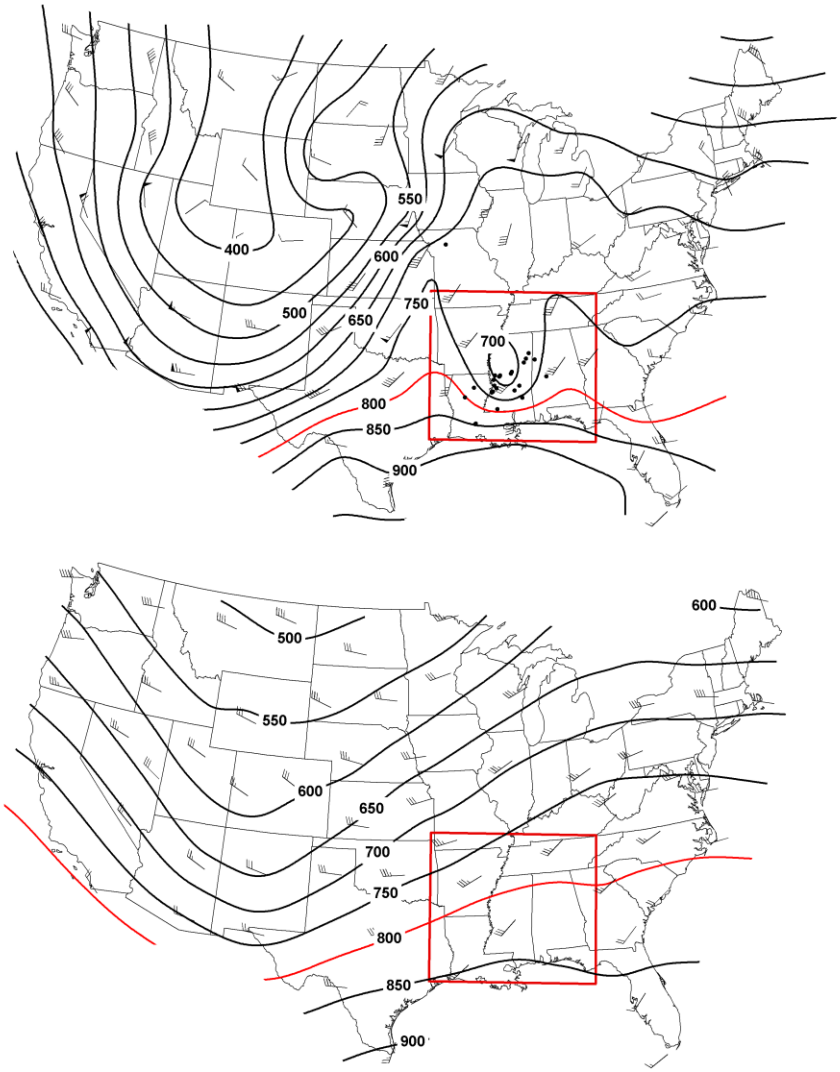

Fig. 5.14**.** (a) 300K isentropic surface with isobars every 50hPa for November 29, 2010 at 12Z. Black dots indicate individual tornado event occurrences. (b) Average 12Z November 300K isentropic surface for tornado days across the Gulf States region from 1974 through 2009. The 800hPa isobar has been highlighted in red on both Figs to more easily compare the pattern.

The 300K isentropic pattern for 12Z on November 29, 2010 yields an intriguing pattern. An isentropic ridge is noted over the western United States and an isentropic trough over the eastern United States (Fig 5.14a). The most notable feature is the closed 700hPa isobar over Northern Mississippi which results in the two well defined isentropic troughs on either side of the feature. All the tornado

reports for this event occurred to the south and east sides of the closed feature. While initially this appears to be an isentropic ridge possibly inhibiting uplift, the wind flow around this feature is from the southwest which actually results in up sloping flow on the southern side of the feature which could enhance thunderstorm activity across the region, especially with the tight gradient with pressure decreasing on the surface roughly 150hpa from southern Louisiana to central Mississippi over northern Mississippi.

Several notable differences can be seen when comparing the November 29, 2010 300K isentropic pattern (Fig 5.14a) with the average 300K isentropic pattern for tornado days in the Gulf States region from 1974 through 2009 (Fig 5.14b). The most striking difference, as was discussed above, is the presence of a closed isentropic trough over northern Mississippi. This feature is not seen on the average pattern and is likely the result of special dynamics associated primarily with this storm situation. With the location of this smaller scale feature, two sharp isentropic troughs are present on either side of the location of tornado reports. Even though these features are not shown in the average pattern, it still indicates isentropic troughing over the study region, resulting in added uplift based on the wind direction and an increase in moisture since isentropic troughs have been closely linked to moisture increase.

p. December – Region 1 (Lower Mississippi River)

Sixty-six tornadoes were reported on December 31, 2010 which was the largest outbreak to occur around the Lower Mississippi Valley from 2010 through

2011, which was why I selected it for the verification case study (Fig 5.15a). The first report was at 1205Z and the last was at 905Z (January 1, 2011).

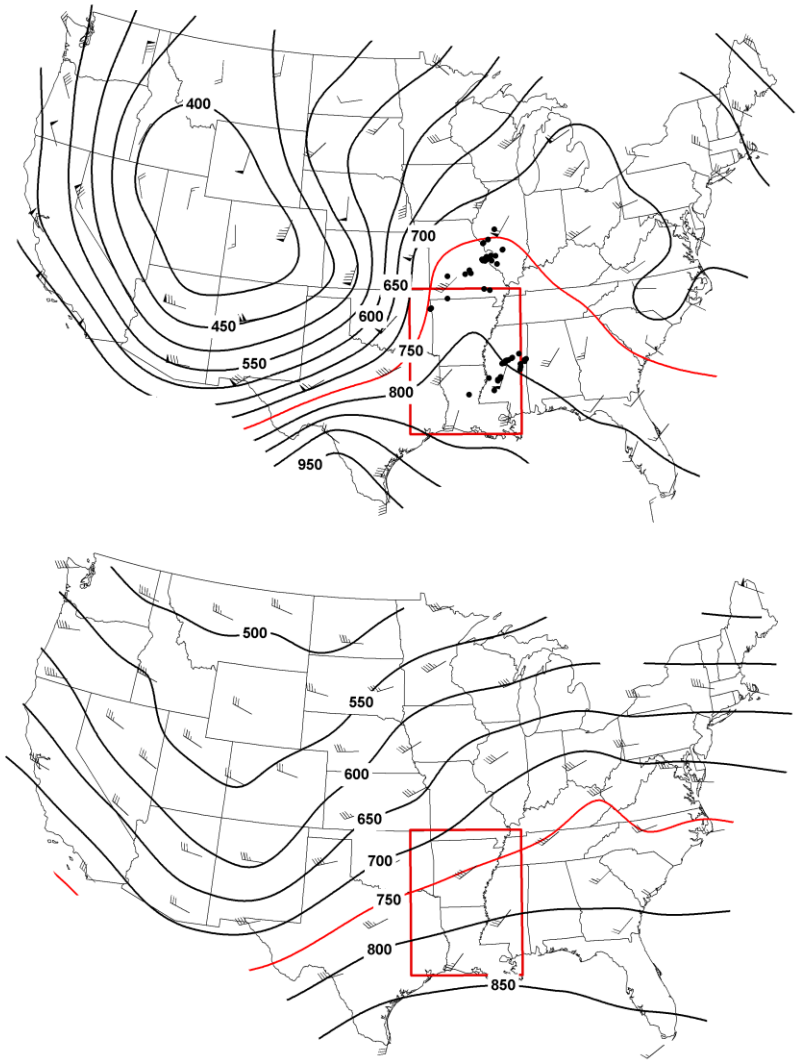

Fig. 5.15**.** (a) 300K isentropic surface with isobars every 50hPa for December 31, 2010 at 12Z. Black dots indicate individual tornado event occurrences. (b) Average 12Z December 300K isentropic surface for tornado days across the Lower Mississippi River region from 1974 through 2009. The 750hPa isobar has been highlighted in red on both Figs to more easily compare the pattern.

The 12Z 300K isentropic pattern for December 31, 2010, indicates a large isentropic ridge across the western United States. A prominent isentropic trough axis extends from Louisiana through Missouri, which is west of the majority of

the tornado reports for the day (Fig 5.15a). Also, within the trough the wind direction was from the southwest which results in flow up the isentropic surface indicating uplift across the region.

Comparing the December 31, 2010 case study (Fig 5.15a) with the average pattern for tornado days in December from 1974 to 2009 for the Lower Mississippi River region (Fig 5.15b), similar isentropic troughs are visible in each analysis. In the case study the isentropic trough is deeper and more pronounced compared to that in the average pattern, especially when examining the 750hPa isobar. Wind direction is nearly identical across the region in both cases, with a southwesterly wind direction, resulting in flow up the isentropic trough. However, with the deeper trough in the case study, a steeper slope across the region would result in increased uplift. Overall, both maps indicated a trough and additional uplift across the region likely resulting in enhanced thunderstorm development.

q. Summary

In this chapter I used independent data in order to verify results from Chapter 4. In Chapter 4 I used rawinsonde data from 1974 through 2009 (Forecast Systems Laboratory 1997) and for this chapter I found individual tornado cases for each region examined from 2010 through 2011. Following identification of case study dates, I created an isentropic map to analyze and compare the features to that found in Chapter 4.

For each of the independent case studies, I found that they matched fairly closely with the results for that of Chapter 4. While the individual case studies presented in the chapter had a more coarse pattern compared to the average

pattern in Chapter 4, the overall patterns where nearly the same. In each case, three primary results emerged:

(1) In many cases, the isentropic features were more accented for the case studies. This is not surprising as amplification would tend to be averaged out in the long term pattern.

(2) In general, the case study analysis produced an isentropic trough axis over, or just to the west of, the tornado report locations;

(3) The wind direction resulted in a flow up the isentropic trough over and near the tornadic events, indicating uplift within the atmosphere that could enhance thunderstorm activity.

Since the results were found in both the main dataset and the independent dataset, it can be concluded that isentropic analysis is looking to be a promising tool in forecasting tornadic events. The main caveat is that the only dataset currently available to conduct an isentropic analysis is using the rawinsonde database, which is fairly coarse, making the ability to find the smaller scale features on each surface extremely difficult. As stated in prior sections, one of the reasons for this dissertation is to show the need for a finer resolution database in isentropic coordinates so further research can be conducted based on the finding presented.

The next chapter presents the specific conclusions of this research presented in this dissertation. This includes a discussion of the justification for this dissertation, development of the hypothesis, critical literature addressed, the

methods and findings discussed, and an overall determination of the acceptance or rejection of the hypotheses developed in this research.

Chapter 6

SUMMARY AND CONCLUSIONS

a. Introduction

While techniques of analyzing constant pressure charts over the past few decades have allowed for more accurate short-term and long-term forecasting, additional analyses other than constant pressure surfaces could be of great significance. In particular, one synoptic technique that could improve forecasting of severe weather is isentropic analysis.

This type of analysis is based on using the concept of potential temperatures, which is the temperature of an air parcel that is brought down to 1000hPa of pressure adiabatically, or without any loss or gain of energy (Holton, 1992). It is a tool that can be used in determining where dry and moist areas reside (Byers, 1938; Pierce, 1938; Namias, 1938; Namias, 1939; Wexler and Namias, 1939; Namias 1940), along with the ability to determine where rising or sinking air is occurring (Green, 1966),.

From a broad-based perspective, this research is designed to close the large gap in literature since only an isolated set of studies have been published within the last decade on the topic of isentropic analysis (de Coning, 2000, Balling et al., 2011; Cerveny et al., 2011). The second broad-based goal for this dissertation is to demonstrate the usefulness of isentropic analysis in day-to-day forecasting in an effort to not only bring this type of analysis back into the mainstream forecasting toolset but also to potentially set in motion the development of a finer resolution dataset in the isentropic coordinates system

such as is currently available for isobaric coordinates. A finer resolution dataset would allow for the more subtle features within the flow to be examined, possibly enhancing even further the usefulness in forecasting tornadoes using isentropic analysis.

Both of these broad-based goals for this research will allow those who depend on severe weather forecasts, to be able to make better informed decisions when faced with events that can be severely impacted by weather and allow researchers the opportunity to better understand the atmosphere.

b. Hypothesis

In this dissertation, I have examined the question "*to what degree does climatological (monthly) isentropic analysis, based on modern weather observations, show identifiable distinct patterns associated with the occurrence of tornadoes within the contiguous United States?"* My hypothesis for this question, based on prior research discussed in Chapter 2, include the following patterns that may be present on the average isentropic surface for tornado days:

(1) A well-defined isentropic trough would be located across the given region experiencing tornadoes;

(2) With isentropic troughs linked to an increase in moisture, I also hypothesis that moisture will significantly increase in a region experiencing tornadoes;

(3) The wind direction on the given isentropic surface for a given region experiencing tornadoes will shift in a direction resulting in up sloping flow on the isentropic surface, meaning the flow would be from an area of high

pressures (low heights) to low pressures (high heights) which would result in added lift in the atmosphere; and

(4) Wind speed will increase across a given region experiencing tornadoes which would result in added uplift as such an increase would be coupled with the switch in wind direction flowing up the isentropic trough.

All these changes in variables on the isentropic surfaces would result in increased instability within the atmosphere lending itself to the development of thunderstorms which could potentially result in the development of tornadoes.

c. Data

Two datasets were utilized in this research, which included tornado data and rawinsonde data. I collected tornado data from the years of 1974 through 2009 from Storm the Prediction Center (Storm Prediction Center, 2010). Years prior to 1974 were missing many data fields including exact start latitude and longitude, such that an initial start year of 1974 was selected for this study. Tornado data from 2009 through 2010 was used in the verification case studies. For the case studies, tornado reports were collected from the Storm Prediction Center but reports were collected only for the given days, as discussed in Chapter 3e.

For the second dataset, I acquired raw rawinsonde data from the CD-ROM "Radiosonde Data of North America 1946-1996" produced by Forecast System Laboratory, supplemented with data between the years of 1997 through 2010 using data supplied online via National Climatic Data Center (Forecast Systems Laboratory 1997). These data were run through a quality control program (as

outlined in Chapter 3), and were used to map the isentropic pattern for tornado and non-tornado days and to create the daily files used for the statistical analysis carried out within each region. Also, I only collected the 12Z sounding data as those data in general are acquired prior to the occurrence of tornadic activity so forecasters would be identifying these isentropic synoptic patterns prior to the occurrence of the tornado.

d. Results

The first and main portion dealt with a more climatological examination of isentropic analysis and tornadoes. This was completed by creating and analyzing average isentropic maps for varying regions across the country for tornado days and non-tornado days between the years of 1974 and 2009. I then conducted both synoptic and statistical analyses of the isentropic data from the stations within the different regions throughout the year. The statistical analysis was conducted through a Kruskal-Wallis test which examined the difference in median value on tornado compared to non-tornado days for the flowing variables: pressure level of the given isentropic surface, mixing ration, wind speed and wind direction.

By undertaking the two above mentioned analyses, several fundamental observations emerged within each region experiencing tornadoes:

(1) Each region and month couplet had a statistically significant increase in pressure of the given isentropic surface on tornado days for the region in question. This increase in pressure (decrease in height) of the isentropic surface indicates an isentropic trough was located over the region;

(2) Mixing ratio was also found to be statistically significant, with an increase in mixing ratio on tornado days;

(3) A statistically significant difference in wind direction between tornado and non-tornado days occurred for each region/ month couplet. On tornado days I found that the wind direction primarily shifted to a more southerly to southwesterly direction resulting in flow up the isentropic surface, indicating greater uplift on tornado days; and

(4) Wind speed did not significantly increase or decrease between tornado versus non-tornado days.

With the results from the climatological study noted above, I then analyzed case studies (not part of the original climatological analysis) for each month/region couplet in order to examine if the climatological pattern found to be significant held true in a single day analysis. The case studies were selected from an independent dataset of tornado events for the years of 2010 through 2011. Using these case studies, I evaluated the synoptic differences and similarities to the pattern found in the first portion of this dissertation. The fundamental results that emerged from this independent test included:

(1) The isentropic pattern is more amplified in the single day case studies when compared to the average pattern. This is expected given that more amplified patterns will be averaged/smoothed anytime a long time scale such as the 1974 through 2009 is used;

(2) Though more amplified, as mentioned above, an isentropic trough is present in the location where tornadoes were reported as is seen in the average maps, or is shifted slightly westward of the tornado reports; and (3) Wind direction is shifted to a more southerly direction in the tornadic case studies corresponding favorably to the average pattern. This would suggest more uplift across the region where tornadoes were reported.

From examination of the climatological results and the case study verification, I can validate my hypothesis that climatological (monthly) isentropic analysis does have distinct patterns associated with tornado days for regions across the contiguous United States. These associated patterns include: an isentropic trough location over the tornado region, higher mixing ratio present within the trough and a wind direction resulting in flow up the isentropic surface, yielding additional uplift across the region. Forecasters can use these results discussed here to identify patterns that were found to be associated with tornado days when using isentropic analysis for given tornado regions across the contiguous United States.

e. Future Work

Based upon the results presented within this dissertation, I would recommend the following future work:

- Begin the development of a gridded dataset in isentropic coordinates, like is currently available from NCEP with constant pressure levels. This will allow for a clearer and more detailed depiction of the isentropic surface possibly yielding more clues

regarding how isentropic analysis can be beneficial in long-term and short-term forecasting.

- With the gridded dataset, examine the smaller scale features, such as the closed trough features found on tornado days over Oklahoma on tornado days or the two small scale isentropic troughs located across the Mid-Atlantic States on tornado days. This will aid in the understanding of how the smaller scale feature on isentropic analysis can impact the weather, similar to principles of shortwaves in isobaric coordinates.

f. Significance

This is the first research that examines the ability to identify distinct climatological isentropic patterns associated with monthly tornado regions. By conducting this research, I have (1) shown that climatological isentropic analysis yields significant pattern shifts when comparing tornado versus non-tornado days for monthly tornado regions across the contiguous United States, and (2) shown the need to create a finer resolution dataset in isentropic coordinates in order to analyze the more subtle features associated with the pattern over the tornado regions.

This research also continues to bridge the large literature gap from when the use of isentropic analysis was as its peak in the late 1930s and early 1940s to the current time with only a few recent studies being done (de Coning, 2000, Cerveny et al. 2011, Balling et al. 2011). By continuing to bridge the large gap in

literature, this research promotes the daily use of isentropic analysis. This would result in concerned parties, both public and private, that are impacted by severe weather to receive the best possible forecast available.

REFERENCES

Balling Jr., Robert C, K. DeBiasse, M. B. Pace, R. S. Cerveny. 2011. Long-term precipitation trend as a function of isentropic variability. *Atmospheric Environment*. 45(32): 5822-5827.

Benjamin, Stanley, G. Grell, J. Brown, T. Smirnova. 2004. Mesoscale Weather Prediction with the RUC Hybrid Isentropic‑Terrain-Following Coordinate Model. *Monthly Weather Review*. 132: 473-494.

Bleck, Rainer. 1973. Numerical Forecasting Experiments Based on the Conservation of Potential Vorticity on Isentropic Surfaces. *Journal of Applied Meteorology* 12 (5): 737-752.

Byers, Horace. 1938. On the Thermodynamic Interpretation of Isentropic Charts. *Monthly Weather Review* 66 (3): 63-68.

Cerveny, Randall S., K. DeBiasse, M. B. Pace, A. W. Ellis, and R. C. Balling, Jr.. 2011. Revitalization of Namias's Climatological Isentropic Analysis: Detection and Evaluation of Monsoonal, Severe Storm, Drought, and Flood Events. *Annals of the Association of American Geographers*. 101 (6): 1204-1220.

Crum, Francis and D. Stevens. 1987. A Case Study of Atmospheric Blocking Using Isentropic Analysis. *Monthly Weather Review* 116: 223-241.

Danielsen, EF. 1959. The Laminar structure of the atmosphere and its relation to the concept of the tropopause. *Arch Meteorology Geophysics Bioklim Service 11: 232-293.*

Danielsen, EF. 1961. Trajectories: Isobaric, Isentropic and Actual. *Journal of Meteorology. 18: 479-486.*

De Coning, E. 2000. PCGRIDDS-based Isentropic Analysis as a Forecasting Tool in the South African Weather Bureau. Water SW 26 (3): 377-387.

De Coning, E., G.S. Forbes, E. Poolman, 1998: Heavy rain and flooding on 12-14 February 1996 over the summer rainfall regions of South Africa: Synoptic and isentropic analyses. NWA Digest 22(3), 25-368.

Doswell, Charles A., H. E. Brooks and N. Dotzek. 2009. On the implementation of the enhanced Fujita scale in the USA. *Atmospheric Research*. 93(1-3): 554-563.

Forecast Systems Laboratory, 1997 Forecast Systems Laboratory Radiosonde Data of North America, 1946–1996 [CD-Rom] National Climatic Data Center, Asheville (1997).

Gilman, Donald. 1985. Long-Range Forecasting: The Present and the future. *Bulletin of the American Meteorological Society* 66 (2): 159-164.

Green, J.S.A., F. Ludlam, J. McIlveen. 1965. Isentropic relative-flow analysis and the parcel theory. *Quarterly Journal of the Royal Meteorological Society*. 92 (392): 210-219.

Hollander, Myels and D. A. Wolfe. 1999. Nonparametric: Statistical Methods (2 ed), John Wiley & Sons, pp 191.

Holton, J.R., 1992 An introduction to dynamic meteorology (3 ed), *Academic Press London*, pp 511.

Hoskins, B.J., M. McIntyre, A. Robertson. 1985. On the use and significance of isentropic potential vorticity maps. *Quarterly Journal of Meteorological Society*. 111(470): 877-946.

John, Robert and C. Doswell III. 1992. Severe Local Storm Forecasting. *Weather and Forecasting* 7 (4): 588-612.

Johnson, D.R., T. Zapotocny, F. Reames, B. Wolf, P. Bradely. 1993. A comparison of simulated precipitation by hybrid isentropic−sigma and sigma models. *Monthly Weather Review*. 121(3): 2088-2114.

Kalnay, E., M. Kanamitsu, R. Kistler, W. Collins, D. Deaven, L. Gandin, M. Iredell, S. Saha, G. White, J. Woollen, Y. Zhu, A. Leetmaa, B. Reynolds, M. Chelliah, W. Ebisuzaki, W. Higgins, J. Janowiak, K.C. Mo, C. Ropelewski, J. Wang, R. Jenne, and D. Joseph, 1996: The NCEP/NCAR 40-Year Reanalysis Project. *Bulletin of the American Meteorological Society*, 77, 437 – 471.

Mitchell, Val L. 1976. The Regionalization of Climate in the Western United States. *Journal of Applied Meteorology* 15 (9): 920-927.

Moore, J.T., 1992: Isentropic analysis and interpretation: Operational applications to synoptic and mesoscale forecasting problems. Dept. of Earth and Atmospheric Sciences. St. Louis University.

Moore, James and K. Smith. 1989. Diagnosis of Anafronts and Katafronts. *Weather and Forecasting* 4 (1): 61-72.

Namias, Jerome. 1938. The Forecasting Significance of Anticylclonic Eddies on the Isentropic Chart. *Transaction, American Geophysical Union.*

Namias, Jerome. 1938. Thunderstorm Forecasting with the Aid of Isentropic Charts. Bulletin of the American Meteorological Society 19 (1): 1-14.

Namias, Jerome. 1939. The Use of Isentropic Analysis in Short Term Forecasting. *Journal of the Aeronautical Sciences* 6 (7): 295-298.

Namias, Jerome. 1940. Isentropic Analysis. *Air Mass and Isentropic Analysis*. The American Meteorological Society: Milton, Mass. Oct 1940.

Pierce, Charles. 1938. On the Use of Vertical Cross Sections in Studying Isentropic Flow. *Monthly Weather Review* 66 (9): 263-267.

Read, R. J., and E. F. Danielsen, 1960: Fronts in the vicinity of the tropopause. *Arch. Meteor. Geophys. Bioklimatol*., 11A, 1-17.

Reiter, Elmar. 1963. A Case Study of Radioactive Fallout . Department of Atmospheric Science Colorado State University. 42.

Rossby, C.G., D.P. Keily, J.W.W. Osmin and J. Namias, 1937: Isentropic analysis. Bulletin of the American Metrological. Society. 18:201-209.

Storm Prediction Center. 2011. National Oceanic and Atmospheric Administration. [http://www.spc.noaa.gov/wcm/].

Tubbs, Anthony. 1972. Summer Thunderstorms Over Southern California. *Monthly Weather Review* 100 (11): 799-807.

Wagner, James. 1989. Medium- and Long-Range Forecasting. *Weather and Forecasting* 4 (3): 413-426.

Wexler H. and J. Namias. 1939. Mean Monthly Isentropic Charts and Their Relation to Departure of Summer Rainfall. Papers, Joint Meeting, Meteorology and Oceanography.

Yang, H and T. Pierrehumbert. 1994. Production of Dry Air by Isentropic Mixing. *Journal of the Atmospheric Sciences* 23 (51): 3437-3454.

APPENDIX A

KRUSKAL-WALLIS TESTS

RESULTS FOR JANUARY REGION 1

		315K Pressure Level (hPa)	315K Wind Direction (°)	315K Wind Speed (knots)	315K Mixing Ratio (g/kg)
Lake Charles, LA	Non-Event	502	262	41	0.57
	Event	520	239	46	0.72
	Difference	18	-23	5	0.15
	p-value	0	0	0.008	0.028
Little Rock, AR	Non-Event	409	267	58	0.25
	Event	447	236	62	0.38
	Difference	38	-31	4	0.13
	p-value	0	0	0.191	0
Jackson, MS	Non-Event	465	264	49	0.46
	Event	501	239	47	0.62
	Difference	36	-25	-2	0.16
	p-value	0	0	0.76	0.001
Shelby, AL	Non-Event	447	265	57	0.29
	Event	495	246	45	0.55
	Difference	48	-19	-12	0.26
	p-value	0	0	0.002	0.001
Nashville, TN	Non-Event	389	265	59	0.24
	Event	444	246	59	0.57
	Difference	55	-19	0	0.33
	p-value	0	0	0.084	0

		310K Pressure Level	310K Wind Direction	310K Wind Speed	310K Mixing Ratio
Lake Charles, LA	Non-Event	573	261	34	0.89
	Event	599	236	40	1.34
	Difference	26	-25	6	0.45
	p-value	0	0	0	0
Little Rock, AR	Non-Event	504	268	48	0.48
	Event	531	239	53	0.75
	Difference	27	-29	5	0.27

(continued)

	p-value	0	0	0.1	0
Jackson, MS	Non-Event	544	265	41	0.75
	Event	571	238	42	1.05
	Difference	27	-27	1	0.3
	p-value	0	0	0.481	0
Shelby, AL	Non-Event	535	267	47	0.54
	Event	572	240	41	1.25
	Difference	37	-27	-6	0.71
	p-value	0	0	0.026	0
Nashville, TN	Non-Event	478	266	56	0.43
	Event	531	243	53	0.94
	Difference	53	-23	-3	0.51
	p-value	0	0	0.256	0

		305K Pressure Level	305K Wind Direction	305K Wind Speed	305K Mixing Ratio
Lake Charles, LA	Non-Event	529	262	27	1.43
	Event	670	231	35	2.77
	Difference	141	-31	8	1.34
	p-value	0	0	0	0
Little Rock, AR	Non-Event	577	269	40	0.795
	Event	612	238	45	1.28
	Difference	35	-31	5	0.485
	p-value	0	0	0.015	0
Jackson, MS	Non-Event	627	365	34	1.15
	Event	680	235	38	2.25
	Difference	53	-130	4	1.1
	p-value	0	0	0.088	0
Shelby, AL	Non-Event	613	268	41	0.91
	Event	659	239	35	2.73
	Difference	46	-29	-6	1.82
	p-value	0	0	0.072	0
Nashville, TN	Non-Event	552	267	49	0.7
	Event	611	242	45	1.81

(continued)

	Difference	59	-25	-4	1.11
	p-value	0	0	0.155	0
		300K Pressure Level	300K Wind Direction	300K Wind Speed	300K Mixing Ratio
Lake Charles, LA	Non-Event	755	261	22	2.1
	Event	811	224	32	6.29
	Difference	56	-37	10	4.19
	p-value	0	0	0	0
Little Rock, AR	Non-Event	675	270	34	1.2
	Event	717	240	37	3.1
	Difference	42	-30	3	1.9
	p-value	0	0	0.003	0
Jackson, MS	Non-Event	725	266	28	1.62
	Event	776	233	24	5.05
	Difference	51	-33	-4	3.43
	p-value	0	0	0.001	0
Shelby, AL	Non-Event	714	269	33	1.45
	Event	765	227	32	4.84
	Difference	51	-42	-1	3.39
	p-value	0	0	0.696	0
Nashville, TN	Non-Event	636	268	41	0.99
	Event	715	241	40	2.93
	Difference	79	-27	-1	1.94
	p-value	0	0	0.294	0

RESULTS FOR FEBRUARY REGION 1

		315K Pressure Level (hPa)	315K Wind Direction (°)	315K Wind Speed (knots)	315K Mixing Ratio (g/kg)
Peachtree City, GA	Non-Event	455	265	56	0.315
	Event	504	245	47	0.71
	Difference	49	-20	-9	0.395
	p-value	0.002	0	0.018	0.004
Shelby, AL	Non-Event	448	265	57	0.31
	Event	501	245	50	1.02
	Difference	53	-20	-7	0.71
	p-value	0	0	0.057	0
Jackson, MS	Non-Event	449	264	49	0.43
	Event	501	240	49	0.7
	Difference	52	-24	0	0.27
	p-value	0	0	0.781	0
Nashville, TN	Non-Event	378	267	62	0.21
	Event	450	241	61	0.56
	Difference	72	-26	-1	0.35
	p-value	0	0	0.458	0
Little Rock, AR	Non-Event	406	267	56	0.24
	Event	439	240	61	0.44
	Difference	33	-27	5	0.2
	p-value	0	0	0.056	0
		310K Pressure Level	310K Wind Direction	310K Wind Speed	310K Mixing Ratio
Peachtree City, GA	Non-Event	537	265	49	0.59
	Event	570	246	41	1.37
	Difference	33	-19	-8	0.78
	p-value	0	0	0.034	0
Shelby, AL	Non-Event	536	265	49	0.58
	Event	578	246	48	2.15
	Difference	42	-19	-1	1.57
	p-value	0	0	0.565	0

(continued)

Jackson, MS	Non-Event	536	265	42	0.69
	Event	571	239	43	1.7
	Difference	35	-26	1	1.01
	p-value	0	0	0.051	0
Nashville, TN	Non-Event	468	267	55	0.38
	Event	534	240	51	1.53
	Difference	66	-27	-4	1.15
	p-value	0	0	0.358	0
Little Rock, AR	Non-Event	502	269	47	0.44
	Event	528	241	50	0.74
	Difference	26	-28	3	0.3
	p-value	0	0	0.066	0
		305K Pressure Level	305K Wind Direction	305K Wind Speed	305K Mixing Ratio
Peachtree City, GA	Non-Event	621	265	41	0.97
	Event	675	241	36	2.22
	Difference	54	-24	-5	1.25
	p-value	0	0	0.313	0
Shelby, AL	Non-Event	617	265	39	0.84
	Event	688	240	39	3.22
	Difference	71	-25	0	2.38
	p-value	0	0	0.772	0
Jackson, MS	Non-Event	626	265	34	1.1
	Event	679	242	38	2.5
	Difference	53	-23	4	1.4
	p-value	0	0	0.001	0
Nashville, TN	Non-Event	548	267	47	0.61
	Event	619	240	44	2.05
	Difference	71	-27	-3	1.44
	p-value	0	0	0.368	0
Little Rock, AR	Non-Event	574	269	38	0.77
	Event	613	242	43	1.54
	Difference	39	-27	5	0.77
	p-value	0	0	0.016	0

(continued)

		300K Pressure Level	300K Wind Direction	300K Wind Speed	300K Mixing Ratio
Peachtree City, GA	Non-Event	719	267	32	1.36
	Event	760	235	33	4.5
	Difference	41	-32	1	3.14
	p-value	0	0	0.892	0
Shelby, AL	Non-Event	721	267	31	1.22
	Event	775	230	33	4.86
	Difference	54	-37	2	3.64
	p-value	0	0	0.674	0
Jackson, MS	Non-Event	727	266	27	1.53
	Event	784	234	35	5.37
	Difference	57	-32	8	3.84
	p-value	0	0	0	0
Nashville, TN	Non-Event	634	268	39	0.98
	Event	723	237	35	4.24
	Difference	89	-31	-4	3.26
	p-value	0	0	0.39	0
Little Rock, AR	Non-Event	678	270	31	1.18
	Event	725	240	36	3.8
	Difference	47	-30	5	2.62
	p-value	0	0	0.002	0

RESULTS FOR MARCH REGION 1

		315K Pressure Level (hPa)	315K Wind Direction (º)	315K Wind Speed (knots)	315K Mixing Ratio (g/kg)
Little Rock, AR	Non-Event	415	268	49	0.28
	Event	474	244	41	0.67
	Difference	59	-24	-8	0.39
	p-value	0	0	0	0
Fort Worth, TX	Non-Event	456	264	40	0.35
	Event	506	234	40	0.45
	Difference	50	-30	0	0.1
	p-value	0	0	0.851	0.021
Amarillo, TX	Non-Event	408	265	44	0.25
	Event	408	230	56	0.28
	Difference	0	-35	12	0.03
	p-value	0.562	0	0	0.319
Norman, OK	Non-Event	419	267	46	0.26
	Event	464	234	42	0.4
	Difference	45	-33	-4	0.14
	p-value	0	0	0.719	0.009
Dodge City, KS	Non-Event	353	267	45	0.17
	Event	395	228	51	0.22
	Difference	42	-39	6	0.05
	p-value	0.002	0	0.009	0.01
		310K Pressure Level	310K Wind Direction	310K Wind Speed	310K Mixing Ratio
Little Rock, AR	Non-Event	514	268	49	0.28
	Event	570	240	35	1.15
	Difference	56	-28	-14	0.87
	p-value	0	0	0	0
Fort Worth, TX	Non-Event	550	265	31	0.87
	Event	596	232	34	1.56
	Difference	46	-33	3	0.69

(continued)

	p-value	0	0	0.336	0
Amarillo, TX	Non-Event	513	264	34	0.54
	Event	519	231	46	0.72
	Difference	6	-33	12	0.18
	p-value	0.983	0	0	0.031
Norman, OK	Non-Event	517	269	36	0.54
	Event	557	235	38	1.2
	Difference	40	-34	2	0.66
	p-value	0	0	0.682	0
Dodge City, KS	Non-Event	464	268	37	0.4
	Event	502	228	41	0.65
	Difference	38	-40	4	0.25
	p-value	0.006	0	0.013	0

		305K Pressure Level	305K Wind Direction	305K Wind Speed	305K Mixing Ratio
Little Rock, AR	Non-Event	601	269	34	0.99
	Event	683	235	31	2.06
	Difference	82	-34	-3	1.07
	p-value	0	0	0.002	0
Fort Worth, TX	Non-Event	665	262	25	181
	Event	731	224	30	3.73
	Difference	66	-38	5	-177.27
	p-value	0	0	0.055	0
Amarillo, TX	Non-Event	609	264	27	1.15
	Event	636	229	37	1.78
	Difference	27	-35	10	0.63
	p-value	0.32	0	0	0
Norman, OK	Non-Event	610	265	30	1.11
	Event	698	230	30	2.61
	Difference	88	-35	0	1.5
	p-value	0	0	0.98	0
Dodge City, KS	Non-Event	560	269	30	0.88
	Event	600	229	33	1.67

(continued)

	Difference	40	-40	3	0.79
	p-value	0.001	0	0.025	0
		300K Pressure Level	300K Wind Direction	300K Wind Speed	300K Mixing Ratio
Little Rock, AR	Non-Event	712	271	28	1.69
	Event	786	229	27	4.96
	Difference	74	-42	-1	3.27
	p-value	0	0	0	0
Fort Worth, TX	Non-Event	761	252	24	2.95
	Event	827	209	36	7.21
	Difference	66	-43	12	4.26
	p-value	0	0	0	0
Amarillo, TX	Non-Event	726	256	24	2.15
	Event	749	232	31	2.83
	Difference	23	-24	7	0.68
	p-value	0.01	0	0	0
Norman, OK	Non-Event	726	260	26	2.08
	Event	806	220	32	5.75
	Difference	80	-40	6	3.67
	p-value	0	0	0.004	0
Dodge City, KS	Non-Event	685	263	26	1.65
	Event	724	221	28	2.84
	Difference	39	-42	2	1.19
	p-value	0	0	0.114	0

RESULTS FOR MARCH REGION 2

		315K Pressure Level (hPa)	315K Wind Direction (º)	315K Wind Speed (knots)	315K Mixing Ratio (g/kg)
Jackson, MS	Non-Event	464	266	40	0.47
	Event	502	244	50	0.65
	Difference	38	-22	10	0.18
	p-value	0	0	0	0
Peachtree City, GA	Non-Event	452	270	47	0.5
	Event	515	243	46	1.32
	Difference	63	-27	-1	0.82
	p-value	0	0	0.739	0
Shelby, AL	Non-Event	456	267	45	0.34
	Event	504	243	48	1
	Difference	48	-24	3	0.66
	p-value	0	0	0.283	0
Charleston, SC	Non-Event	457	270	48	0.45
	Event	515	259	42	1.24
	Difference	58	-11	-6	0.79
	p-value	0	0	0	0
		310K Pressure Level	310K Wind Direction	310K Wind Speed	310K Mixing Ratio
Jackson, MS	Non-Event	553	267	33	0.78
	Event	580	239	44	1.36
	Difference	27	-28	11	0.58
	p-value	0	0	0	0
Peachtree City, GA	Non-Event	543	270	40	0.73
	Event	582	239	40	1.76
	Difference	39	-31	0	1.03
	p-value	0	0	0.633	0
Shelby, AL	Non-Event	544	267	39	0.76
	Event	578	248	41	1.87
	Difference	34	-19	2	1.11
	p-value	0	0	0.103	0
Charleston, SC	Non-Event	543	270	39	0.75
	Event	593	252	36	1.55

(continued)

	Difference	50	-18	-3	0.8
	p-value	0	0	0.001	0
		305K Pressure Level	305K Wind Direction	305K Wind Speed	305K Mixing Ratio
Jackson, MS	Non-Event	654	265	27	1.43
	Event	699	240	37	2.67
	Difference	45	-25	10	1.24
	p-value	0	0	0	0
Peachtree City, GA	Non-Event	638	269	32	1.13
	Event	699	234	32	3.5
	Difference	61	-35	0	2.37
	p-value	0	0	0.744	0
Shelby, AL	Non-Event	645	266	32	1.3
	Event	670	239	37	3.87
	Difference	25	-27	5	2.57
	p-value	0	0	0.039	0
Charleston, SC	Non-Event	634	268	32	1.25
	Event	704	243	27	2.2
	Difference	70	-25	-5	0.95
	p-value	0	0	0.003	0
		300K Pressure Level	300K Wind Direction	300K Wind Speed	300K Mixing Ratio
Jackson, MS	Non-Event	752	262	22	2.17
	Event	801	236	32	5.86
	Difference	49	-26	10	3.69
	p-value	0	0	0	0
Peachtree City, GA	Non-Event	743	268	26	1.77
	Event	793	229	29	5.69
	Difference	50	-39	3	3.92
	p-value	0	0	0.423	0
Shelby, AL	Non-Event	746	265	25	2.04
	Event	787	231	32	6.11
	Difference	41	-34	7	4.07
	p-value	0	0	0.031	0

(continued)

Charleston, SC	Non-Event	738	268	24	1.82
	Event	791	234	22	5.39
	Difference	53	-34	-2	3.57
	p-value	0	0	0	0

RESULTS FOR APRIL REGION 1

		315K Pressure Level (hPa)	315K Wind Direction (°)	315K Wind Speed (knots)	315K Mixing Ratio (g/kg)
Fort Worth, TX	Non-Event	503	269	32	0.52
	Event	523	424	36	1.24
	Difference	20	155	4	0.72
	p-value	0	0	0.253	0
Little Rock, AR	Non-Event	466	243	40	0.44
	Event	504	251	35	0.72
	Difference	38	8	-5	0.28
	p-value	0	0	0	0
Norman, OK	Non-Event	463	268	37	0.38
	Event	497	238	40	0.63
	Difference	34	-30	3	0.25
	p-value	0	0	0.041	0
Dodge City, KS	Non-Event	429	267	37	0.31
	Event	435	235	45	0.41
	Difference	6	-32	8	0.1
	p-value	0.203	0	0	0.019
		310K Pressure Level	310K Wind Direction	310K Wind Speed	310K Mixing Ratio
Fort Worth, TX	Non-Event	595	267	26	1.26
	Event	671	234	30	2.77
	Difference	76	-33	4	1.51
	p-value	0	0	0.326	0
Little Rock, AR	Non-Event	555	273	34	0.83
	Event	598	247	30	1.81
	Difference	43	-26	-4	0.98
	p-value	0	0	0	0
Norman, OK	Non-Event	562	269	30	0.99
	Event	608	236	34	1.95
	Difference	46	-33	4	0.96

(continued)

	p-value	0	0	0.085	0
Dodge City, KS	Non-Event	531	267	32	0.77
	Event	541	235	37	1.17
	Difference	10	-32	5	0.4
	p-value	0.17	0	0	0
		305K Pressure Level	305K Wind Direction	305K Wind Speed	305K Mixing Ratio
Fort Worth, TX	Non-Event	719	254	25	2.37
	Event	774	219	29	6.01
	Difference	55	-35	4	3.64
	p-value	0	0	0.016	0
Little Rock, AR	Non-Event	661	273	29	1.44
	Event	722	236	26	3.56
	Difference	61	-37	-3	2.12
	p-value	0	0	0.019	0
Norman, OK	Non-Event	694	264	27	1.99
	Event	742	230	29	4.01
	Difference	48	-34	2	2.02
	p-value	0	0	0.205	0
Dodge City, KS	Non-Event	640	255	28	1.76
	Event	667	232	30	2.17
	Difference	27	-23	2	0.41
	p-value	0.098	0	0.059	0
		300K Pressure Level	300K Wind Direction	300K Wind Speed	300K Mixing Ratio
Fort Worth, TX	Non-Event	817	233	23	3.76
	Event	875	205	28	9.31
	Difference	58	-28	5	5.55
	p-value	0	0	0.001	0
Little Rock, AR	Non-Event	759	269	24	2.44
	Event	828	225	24	6.12
	Difference	69	-44	0	3.68

(continued)

	p-value	0	0	0.39	0
Norman, OK	Non-Event	785	250	26	3.02
	Event	843	213	30	7.3
	Difference	58	-37	4	4.28
	p-value	0	0	0.043	0
Dodge City, KS	Non-Event	747	264	24	2.79
	Event	766	233	22	4.12
	Difference	19	-31	-2	1.33
	p-value	0.043	0	0.268	0

RESULTS FOR MAY REGION 1

		315K Pressure Level (hPa)	315K Wind Direction (º)	315K Wind Speed (knots)	315K Mixing Ratio (g/kg)
Fort Worth, TX	Non-Event	567	269	20	1.78
	Event	589	242	21	2.49
	Difference	22	-27	1	0.71
	p-value	0	0	0.85	0
Amarillo, TX	Non-Event	538	267	22	1.46
	Event	551	244	27	1.64
	Difference	13	-23	5	0.18
	p-value	0.024	0	0	0.044
Norman, OK	Non-Event	549	269	25	1.27
	Event	560	251	25	1.91
	Difference	11	-18	0	0.83
	p-value	0.005	0	0.888	0
Dodge City, KS	Non-Event	522	270	26	1
	Event	532	243	27	1.34
	Difference	10	-27	1	0.34
	p-value	0.075	0	0.078	0
Topeka, KS	Non-Event	512	276	31	0.78
	Event	526	248	27	1.21
	Difference	14	-28	-4	0.43
	p-value	0	0	0.06	0
Omaha, NE	Non-Event	489	584	35	0.6
	Event	506	252	36	1.12
	Difference	17	-332	1	0.52
	p-value	0.085	0	0.318	0
North Platte, NE	Non-Event	493	274	29	0.79
	Event	498	238	29	0.96
	Difference	5	-36	0	0.17
	p-value	0.736	0	0.864	0.003
Midland, TX	Non-Event	568	260	19	1.93
	Event	588	245	23	2.25
	Difference	20	-15	4	0.32

(continued)

	p-value	0	0	0	0
		310K Pressure Level	310K Wind Direction	310K Wind Speed	310K Mixing Ratio
Fort Worth, TX	Non-Event	683	255	19	3.49
	Event	735	227	20	4.94
	Difference	52	-28	1	1.45
	p-value	0	0	0.336	0
Amarillo, TX	Non-Event	662	255	20	2.94
	Event	708	245	25	3.26
	Difference	46	-10	5	0.32
	p-value	0	0	0	0.004
Norman, OK	Non-Event	650	265	24	267
	Event	1	238	23	3.95
	Difference	-649	-27	-1	-263.05
	p-value	0	0	0.48	0
Dodge City, KS	Non-Event	613	264	23	2.35
	Event	642	238	24	3
	Difference	29	-26	1	0.65
	p-value	0	0	0.518	0
Topeka, KS	Non-Event	589	276	26	1.47
	Event	619	244	24	2.47
	Difference	30	-32	-2	1
	p-value	0	0	0.102	0
Omaha, NE	Non-Event	575	288	29	1.39
	Event	590	251	28	2.15
	Difference	15	-37	-1	0.76
	p-value	0.032	0	0.293	0
North Platte, NE	Non-Event	579	271	25	1.6
	Event	588	240	23	2.23
	Difference	9	-31	-2	0.63
	p-value	0.311	0	0.129	0
Midland, TX	Non-Event	713	232	17	3.98
	Event	747	221	21	5.07

(continued)

	Difference	34	-11	4	1.09
	p-value	0	0	0	0
		305K Pressure Level	305K Wind Direction	305K Wind Speed	305K Mixing Ratio
Fort Worth, TX	Non-Event	785	233	18	6.19
	Event	827	210	23	8.21
	Difference	42	-23	5	2.02
	p-value	0	0	0.001	0
Amarillo, TX	Non-Event	760	232	21	4.75
	Event	791	224	24	5.93
	Difference	31	-8	3	1.18
	p-value	0	0.003	0	0
Norman, OK	Non-Event	757	241	21	5.23
	Event	801	220	21	7.28
	Difference	44	-21	0	2.05
	p-value	0	0	0.733	0
Dodge City, KS	Non-Event	732	250	21	4.01
	Event	764	223	21	5.37
	Difference	32	-27	0	1.36
	p-value	0	0	0.402	0
Topeka, KS	Non-Event	694	266	22	3.09
	Event	737	232	21	5.04
	Difference	43	-34	-1	1.95
	p-value	0	0	0.206	0
Omaha, NE	Non-Event	674	283	25	2.56
	Event	707	246	22	4.11
	Difference	33	-37	-3	1.55
	p-value	0.021	0	0.098	0
North Platte, NE	Non-Event	698	263	21	3.41
	Event	711	236	19	4.25
	Difference	13	-27	-2	0.84
	p-value	0.06	0	0.007	0
Midland, TX	Non-Event	814	197	18	6.54

(continued)

	Event	854	189	25	7.09
	Difference	40	-8	7	0.55
	p-value	0	0.058	0	0
		300K Pressure Level	300K Wind Direction	300K Wind Speed	300K Mixing Ratio
Fort Worth, TX	Non-Event	890	199	6	0.74
	Event	910	196	22	10.69
	Difference	20	-3	16	9.95
	p-value	0	0.08	0	0
Amarillo, TX	Non-Event	851	216	22	5.94
	Event	863	216	24	7.61
	Difference	12	0	2	1.67
	p-value	0	0.97	0.05	0
Norman, OK	Non-Event	863	215	18	6.99
	Event	890	201	20	10.67
	Difference	27	-14	2	3.68
	p-value	0	0	0.241	0
Dodge City, KS	Non-Event	835	214	18	5.57
	Event	861	204	7	7.7
	Difference	26	-10	-11	2.13
	p-value	0	0	0.049	0
Topeka, KS	Non-Event	792	525	20	4.75
	Event	855	208	21	7.43
	Difference	63	-317	1	2.68
	p-value	0	0	0.687	0
Omaha, NE	Non-Event	781	258	22	4
	Event	770	237	20	6.3
	Difference	11	-21	-2	2.3
	p-value	0.02	0.086	0.344	0
Midland, TX	Non-Event	878	189	24	7.29
	Event	891	196	25	7.67
	Difference	13	7	1	0.38
	p-value	0	0.029	0.037	0

RESULTS FOR JUNE REGION 1

		315K Pressure Level (hPa)	315K Wind Direction (°)	315K Wind Speed (knots)	315K Mixing Ratio (g/kg)
Dodge City, KS	Non-Event	598	259	18	3.17
	Event	647	236	20	3.93
	Difference	49	-23	2	0.76
	p-value	0	0	0.003	0
Topeka, KS	Non-Event	578	261	21	2.34
	Event	599	252	20	2.68
	Difference	21	-9	-1	0.34
	p-value	0	0.112	0.998	0.001
Omaha, NE	Non-Event	559	278	26	1.59
	Event	573	261	27	2.49
	Difference				
	p-value	0.053	0.012	0.744	0.002
North Platte, NE	Non-Event	574	277	22	2.51
	Event	596	250	23	3.17
	Difference	22	-27	1	0.66
	p-value	0	0	0.543	0
Rapid City, SD	Non-Event	545	275	23	1.53
	Event	550	258	26	2.14
	Difference	5	-17	3	0.61
	p-value	0.71	0	0.025	0
Aberdeen, SD	Non-Event	531	281	30	1.09
	Event	525	264	31	1.55
	Difference	-6	-17	1	0.46
	p-value	0.774	0	0.691	0.061
Bismarck, ND	Non-Event	525	278	27	1.04
	Event	525	263	30	1.3
	Difference	0	-15	3	0.26
	p-value	0.767	0	0.112	0.01
Chanhassen, MN	Non-Event	527	270	29	0.86
	Event	547	265	28	1.32
	Difference	20	-5	-1	0.46
	p-value	0.038	0.199	0.433	0.004

(continued)

		310K Pressure Level	310K Wind Direction	310K Wind Speed	310K Mixing Ratio
Dodge City, KS	Non-Event	720	238	17	5.48
	Event	774	221	18	6.96
	Difference	54	-17	1	1.48
	p-value	0	0	0.044	0
Topeka, KS	Non-Event	682	258	18	4.6
	Event	718	243	18	5.45
	Difference	36	-15	0	0.85
	p-value	0	0.004	0.792	0
Omaha, NE	Non-Event	652	281	21	3.3
	Event	696	252	23	4.51
	Difference	44	-29	2	1.21
	p-value	0.01	0	0.733	0.002
North Platte, NE	Non-Event	686	266	18	4.55
	Event	731	235	18	5.66
	Difference	45	-31	0	1.11
	p-value	0	0	0.978	0
Rapid City, SD	Non-Event	647	273	21	3.31
	Event	668	255	20	4.21
	Difference	668	-18	20	4.21
	p-value	0.07	0	0.728	0
Aberdeen, SD	Non-Event	607	285	24	1.99
	Event	619	260	24	2.96
	Difference	12	-25	0	0.97
	p-value	0	0	0.736	0.035
Bismarck, ND	Non-Event	600	278	23	1.88
	Event	605	265	24	2.46
	Difference	5	-13	1	0.58
	p-value	0.169	0	0.448	0.006
Chanhassen, MN	Non-Event	601	268	25	1.85
	Event	634	261	24	2.4
	Difference	33	-7	-1	0.55
	p-value	0.014	0.564	0.313	0.017

(continued)

		305K Pressure Level	305K Wind Direction	305K Wind Speed	305K Mixing Ratio
Dodge City, KS	Non-Event	823	215	16	7.65
	Event	866	206	17	9.93
	Difference	43	-9	1	2.28
	p-value	0	0	0.099	0
Topeka, KS	Non-Event	781	257	15	7.03
	Event	838	240	14	8.9
	Difference	57	-17	-1	1.87
	p-value	0	0.027	0.702	0
Omaha, NE	Non-Event	753	275	19	5.43
	Event	795	233	18	6.96
	Difference				
	p-value	0.001	0	0.427	0
North Platte, NE	Non-Event	785	241	15	6.42
	Event	826	220	15	7.71
	Difference	41	-21	0	1.29
	p-value	0	0	0.612	0
Rapid City, SD	Non-Event	756	263	17	5.14
	Event	770	238	17	5.85
	Difference	14	-25	0	0.71
	p-value	0.042	0.003	0.336	0
Aberdeen, SD	Non-Event	720	282	20	3.69
	Event	731	253	20	4.63
	Difference	11	-29	0	0.94
	p-value	0.136	0	0.3	0.068
Bismarck, ND	Non-Event	702	283	19	3.35
	Event	717	265	18	4.29
	Difference	15	-18	-1	0.94
	p-value	0.036	0	0.193	0.001
Chanhassen, MN	Non-Event	705	263	23	3.32
	Event	735	254	21	4.49
	Difference	30	-9	-2	1.17
	p-value	0.007	0.258	0.324	0.019

(continued)

		300K Pressure Level	300K Wind Direction	300K Wind Speed	300K Mixing Ratio
Dodge City, KS	Non-Event	887	198	15	9
	Event	905	199	14	10.78
	Difference	18	1	-1	1.78
	p-value	0	0.362	0.432	0
Topeka, KS	Non-Event	887	274	12	9.38
	Event	915	225	12	11.2
	Difference	28	-49	0	1.82
	p-value	0	0.002	0.577	0
Omaha, NE	Non-Event	881	232	15	7.32
	Event	906	193	13	9.43
	Difference	25	-39	-2	2.11
	p-value	0.001	0	0.016	0
North Platte, NE	Non-Event	866	224	12	7.57
	Event	878	218	10	9.07
	Difference	12	-6	-2	1.5
	p-value	0	0.002	0.008	0
Rapid City, SD	Non-Event	859	215	13	6.09
	Event	859	202	12	6.91
	Difference	0	-13	-1	0.82
	p-value	0.061	0.074	0.367	0
Aberdeen, SD	Non-Event	822	248	16	5.62
	Event	858	236	17	6.3
	Difference	36	-12	1	0.68
	p-value	0.034	0.022	0.643	0.013
Bismarck, ND	Non-Event	806	283	18	5.12
	Event	840	272	17	6.15
	Difference	34	-11	-1	1.03
	p-value	0.003	0.017	0.119	0
Chanhassen, MN	Non-Event	805	241	19	5.31
	Event	845	239	17	6.71
	Difference	40	-2	-2	1.4
	p-value	0.013	0.649	0.045	0.003

RESULTS FOR JUNE REGION 2

		315K Pressure Level (hPa)	315K Wind Direction (°)	315K Wind Speed (knots)	315K Mixing Ratio (g/kg)
Davenport, IA	Non-Event	560	274	25	1.29
	Event	576	242	24	2.56
	Difference	16	-32	-1	1.27
	p-value	0.022	0	0.859	0
Lincoln, IL	Non-Event	566	270	26	1.58
	Event	586	242	23	2.98
	Difference	20	-28	-3	1.4
	p-value	0.024	0.001	0.301	0
Wilmington, OH	Non-Event	566	263	25	1.63
	Event	580	253	25	2.86
	Difference	14	-10	0	1.23
	p-value	0.003	0.058	0.473	0
		310K Pressure Level	310K Wind Direction	310K Wind Speed	310K Mixing Ratio
Davenport, IA	Non-Event	643	271	21	2.83
	Event	671	240	20	5.25
	Difference	28	-31	-1	2.42
	p-value	0.028	0	0.777	0
Lincoln, IL	Non-Event	657	267	22	2.79
	Event	680	237	24	5.22
	Difference	23	-30	2	2.43
	p-value	0.012	0.001	0.863	0
Wilmington, OH	Non-Event	652	263	21	2.63
	Event	684	250	23	4.93
	Difference	32	-13	2	2.3
	p-value	0.001	0.22	0.771	0
		305K Pressure Level	305K Wind Direction	305K Wind Speed	305K Mixing Ratio
Davenport, IA	Non-Event	744	262	19	4.86
	Event	779	237	20	7.28
	Difference	35	-25	1	2.42

(continued)

	p-value	0.013	0.005	0.102	0
Lincoln, IL	Non-Event	761	265	19	5.64
	Event	794	244	24	8.01
	Difference	33	-21	5	2.37
	p-value	0.001	0.001	0.039	0
Wilmington, OH	Non-Event	749	262	19	5.45
	Event	797	247	20	7.88
	Difference	48	-15	1	2.43
	p-value	0	0.059	0.908	0
		300K Pressure Level	300K Wind Direction	300K Wind Speed	300K Mixing Ratio
Davenport, IA	Non-Event	858	245	15	7.3
	Event	894	240	16	10.29
	Difference	36	-5	1	2.99
	p-value	0.013	0.342	0.313	0
Lincoln, IL	Non-Event	874	248	13	8
	Event	928	230	18	11
	Difference	54	-18	5	3
	p-value	0	0.336	0.254	0
Wilmington, OH	Non-Event	861	256	14	8.5
	Event	927	230	12	11.3
	Difference	66	-26	-2	2.8
	p-value	0	0.036	0.649	0

RESULTS FOR JULY REGION 1

		315K Pressure Level (hPa)	315K Wind Direction (°)	315K Wind Speed (knots)	315K Mixing Ratio (g/kg)
Dodge City, KS	Non-Event	667	234	13	5.35
	Event	705	228	16	6.23
	Difference	38	-6	3	0.88
	p-value	0	0.123	0.001	0
Topeka, KS	Non-Event	633	266	16	3.75
	Event	645	254	17	4.45
	Difference	12	-12	1	0.7
	p-value	0	0.345	0.684	0
Omaha, NE	Non-Event	634	285	17	3.77
	Event	643	273	19	4.48
	Difference	9	-12	2	0.71
	p-value	0.226	0.113	0.445	0.045
North Platte, NE	Non-Event	662	263	16	4.96
	Event	694	247	16	5.5
	Difference	32	-16	0	0.54
	p-value	0.001	0.016	0.915	0
Rapid City, SD	Non-Event	645	276	17	4.17
	Event	625	263	19	4.2
	Difference	-20	-13	2	0.03
	p-value	0.177	0.001	0.001	0.335
Aberdeen, SD	Non-Event	607	294	23	2.48
	Event	589	282	26	2.94
	Difference	-18	-12	3	0.46
	p-value	0.361	0.002	0.09	0.211
Bismarck, ND	Non-Event	584	287	23	1.96
	Event	566	275	26	2.17
	Difference	-18	-12	3	0.21
	p-value	0	0	0.003	0.501
Chanhassen, MN	Non-Event	588	295	27	1.96
	Event	580	292	26	2
	Difference	-8	-3	-1	0.04
	p-value	0.396	0.861	0.613	0.745

(continued)

Denver, CO	Non-Event	716	279	11	5.1
	Event	721	277	12	4.95
	Difference	5	-2	1	-0.15
	p-value	0.026	0.168	0.048	0.752
		310K Pressure Level	310K Wind Direction	310K Wind Speed	310K Mixing Ratio
Dodge City, KS	Non-Event	795	226	15	8.39
	Event	830	219	16	9.5
	Difference	35	-7	1	1.11
	p-value	0	0.063	0.044	0
Topeka, KS	Non-Event	741	255	17	7.02
	Event	760	242	18	8.11
	Difference	19	-13	1	1.09
	p-value	0	0.018	0.173	0
Omaha, NE	Non-Event	741	271	16	7.14
	Event	762	252	18	7.88
	Difference	21	-19	2	0.74
	p-value	0.077	0.06	0.059	0.007
North Platte, NE	Non-Event	774	228	14	7.88
	Event	791	220	13	8.17
	Difference	17	-8	-1	0.29
	p-value	0.005	0.017	0.058	0
Rapid City, SD	Non-Event	767	266	14	6.15
	Event	755	252	14	6.68
	Difference	-12	-14	0	0.53
	p-value	0.267	0.037	0.426	0.004
Aberdeen, SD	Non-Event	719	291	19	4.75
	Event	716	279	21	5.09
	Difference	-3	-12	2	0.34
	p-value	0.867	0.094	0.162	0.203
Bismarck, ND	Non-Event	698	285	19	4.25
	Event	673	277	21	4.19
	Difference	-25	-8	2	-0.06
	p-value	0.005	0.027	0.092	0.88

(continued)

Chanhassen, MN	Non-Event	685	284	22	3.44
	Event	685	291	22	3.72
	Difference	0	7	0	0.28
	p-value	0.748	0.373	0.844	0.183
Denver, CO	Non-Event	771	267	9	6.62
	Event	774	255	9	6.57
	Difference	3	-12	0	-0.05
	p-value	0.023	0.301	0.001	0.904
		305K Pressure Level	305K Wind Direction	305K Wind Speed	305K Mixing Ratio
Dodge City, KS	Non-Event	877	215	14	10.86
	Event	885	211	14	12.12
	Difference	8	-4	0	1.26
	p-value	0	0.417	9.49	0
Topeka, KS	Non-Event	857	242	16	10.17
	Event	874	235	18	11.77
	Difference	17	-7	2	1.6
	p-value	0	0.258	0.026	0
Omaha, NE	Non-Event	857	236	13	10.07
	Event	876	237	15	11.92
	Difference	19	1	2	1.85
	p-value	0.039	0.785	0.385	0
North Platte, NE	Non-Event	863	206	12	9.93
	Event	868	195	11	10.89
	Difference	5	-11	-1	0.96
	p-value	0.019	0.11	0.003	0
Rapid City, SD	Non-Event	860	212	13	7.74
	Event	854	214	13	8.43
	Difference	-6	2	0	0.69
	p-value	0.098	0.216	0.368	0.001
Aberdeen, SD	Non-Event	817	257	17	7.12
	Event	833	243	17	8.15
	Difference	16	-14	0	1.03
	p-value	0.385	0.23	0.665	0.078

(continued)

Bismarck, ND	Non-Event	807	260	16	6.05
	Event	793	266	15	6.6
	Difference	-14	6	-1	0.55
	p-value	0.039	0.789	0.453	0.085
Chanhassen, MN	Non-Event	779	275	17	5.37
	Event	783	285	17	5.84
	Difference	4	10	0	0.47
	p-value	0.949	0.401	0.829	0.154
Denver, CO	Non-Event	*	*	*	*
	Event	*	*	*	*
	Difference	*	*	*	*
	p-value	*	*	*	*

		300K Pressure Level	300K Wind Direction	300K Wind Speed	300K Mixing Ratio
Dodge City, KS	Non-Event	916	200	9	11.66
	Event	919	200	8	11.99
	Difference	3	0	-1	0.33
	p-value	0.017	0.755	0.139	0
Topeka, KS	Non-Event	932	219	13	11.55
	Event	943	204	12	13.2
	Difference	11	-15	-1	1.65
	p-value	0	0.057	0.53	0
Omaha, NE	Non-Event	933	185	8	11.38
	Event	939	180	7	11.97
	Difference	6	-5	-1	0.59
	p-value	0.016	0.086	0.188	0.001
North Platte, NE	Non-Event	898	209	8	10.4
	Event	901	194	6	11.32
	Difference	3	-15	-2	0.92
	p-value	0.041	0.001	0.001	0
Rapid City, SD	Non-Event	888	0	0	8.57
	Event	888	1	1.5	8.88
	Difference	0	1	1.5	0.31
	p-value	0.147	0.998	0.73	0

(continued)

Aberdeen, SD	Non-Event	925	213	18	9.16
	Event	922	200	19	10.5
	Difference	-3	-13	1	1.34
	p-value	0.898	0.119	0.943	0.001
Bismarck, ND	Non-Event	891	218	15	8.06
	Event	884	229	14	8.58
	Difference	-7	11	-1	0.52
	p-value	0.025	0.452	0.218	0.066
Chanhassen, MN	Non-Event	901	240	13	8.46
	Event	887	245	15	9.13
	Difference	-14	5	2	0.67
	p-value	0.807	0.514	0.448	0.477
Denver, CO	Non-Event	*	*	*	*
	Event	*	*	*	*
	Difference	*	*	*	*
	p-value	*	*	*	*

RESULTS FOR JULY REGION 2

		315K Pressure Level (hPa)	315K Wind Direction (°)	315K Wind Speed (knots)	315K Mixing Ratio (g/kg)
Wilmington, OH	Non-Event	602	281	19	2.14
	Event	601	275	26	3.39
	Difference	-1	-6	7	1.25
	p-value	0.933	0.505	0	0.014
White Lake, MI	Non-Event	577	289	23	1.39
	Event	572	273	31	2.6
	Difference	-5	-16	8	1.21
	p-value	0.996	0.001	0.001	0.003
Pittsburgh, PA	Non-Event	592	279	20	1.7
	Event	604	266	25	3.06
	Difference	12	-13	5	1.36
	p-value	0	0	0	0
Buffalo, NY	Non-Event	564	278	25	1.3
	Event	581	262	27	2.46
	Difference	17	-16	2	1.16
	p-value	0	0	0.005	0
Albany, NY	Non-Event	567	273	27	1.46
	Event	583	266	28	2.63
	Difference	16	-7	1	1.17
	p-value	0	0.074	0.199	0
Upton, NY	Non-Event	582	268	26	1.23
	Event	590	260	27	2.97
	Difference	8	-8	1	1.74
	p-value	0.02	0.189	0.963	0
Sterling, VA	Non-Event	600	272	21	2.14
	Event	610	262	22	3.93
	Difference	10	-10	1	1.79
	p-value	0	0.017	0.068	0
		310K Pressure Level	310K Wind Direction	310K Wind Speed	310K Mixing Ratio
Wilmington, OH	Non-Event	704	277	17	3.95

(continued)

	Event	695	271	24	6.32
	Difference	-9	-6	7	2.37
	p-value	0.715	0.325	0	0
White Lake, MI	Non-Event	667	285	20	2.29
	Event	659	273	27	4.3
	Difference	-8	-12	7	2.01
	p-value	0.768	0.044	0	0
Pittsburgh, PA	Non-Event	682	278	18	2.87
	Event	702	266	23	5.71
	Difference	20	-12	5	2.84
	p-value	0	0	0	0
Buffalo, NY	Non-Event	647	280	21	1.99
	Event	666	262	25	4.28
	Difference	19	-18	4	2.29
	p-value	0	0	0.005	0
Albany, NY	Non-Event	649	276	23	2.36
	Event	669	269	24	3.83
	Difference	20	-7	1	1.47
	p-value	0	0.008	0.425	0
Upton, NY	Non-Event	665	271	22	2.65
	Event	681	265	25	5.31
	Difference	16	-6	3	2.66
	p-value	0.012	0.149	0.694	0
Sterling, VA	Non-Event	693	275	18	3.91
	Event	705	261	19	6.08
	Difference	12	-14	1	2.17
	p-value	0	0.001	0.044	0

		305K Pressure Level	305K Wind Direction	305K Wind Speed	305K Mixing Ratio
Wilmington, OH	Non-Event	789	272	17	6.74
	Event	806	270	19	9.25
	Difference	17	-2	2	2.51
	p-value	0.034	0.844	0	0
White Lake, MI	Non-Event	756	279	16	4.02

(continued)

	Event	761	276	19	7.17
	Difference	5	-3	3	3.15
	p-value	0.464	0.419	0.009	0
Pittsburgh, PA	Non-Event	767	275	14	5.67
	Event	798	263	17	9.17
	Difference	31	-12	3	3.5
	p-value	0	0	0	0
Buffalo, NY	Non-Event	740	279	18	3.94
	Event	761	260	20	6.63
	Difference	21	-19	2	2.69
	p-value	0	0	0.12	0
Albany, NY	Non-Event	737	280	19	4.51
	Event	758	269	20	6.29
	Difference	21	-11	1	1.78
	p-value	0	0.001	0.744	0
Upton, NY	Non-Event	756	275	19	5.36
	Event	780	265	19	7.7
	Difference	24	-10	0	2.34
	p-value	0.001	0.007	0.759	0
Sterling, VA	Non-Event	779	280	14	7.21
	Event	817	270	16	9.5
	Difference	38	-10	2	2.29
	p-value	0	0.01	0.058	0

		300K Pressure Level	300K Wind Direction	300K Wind Speed	300K Mixing Ratio
Wilmington, OH	Non-Event	906	235	9	10.41
	Event	927	235	9	12.1
	Difference	21	0	0	1.69
	p-value	0.008	0.785	0.248	0.003
White Lake, MI	Non-Event	851	270	13	7.28
	Event	880	258	15	9.96
	Difference	29	-12	2	2.68
	p-value	0.054	0.04	0.264	0
Pittsburgh, PA	Non-Event	869	247	9	9.03

(continued)

	Event	897	225	9	12.05
	Difference	28	-22	0	3.02
	p-value	0	0.008	0.087	0
Buffalo, NY	Non-Event	834	277	15	6.95
	Event	872	255	15	9.45
	Difference	38	-22	0	2.5
	p-value	0	0	0.657	0
Albany, NY	Non-Event	830	282	14	7.44
	Event	859	260	13	9.38
	Difference	29	-22	-1	1.94
	p-value	0	0	0.607	0
Upton, NY	Non-Event	859	272	15	8.06
	Event	894	246	12	10.33
	Difference	35	-26	-3	2.27
	p-value	0	0	0.02	0
Sterling, VA	Non-Event	884	280	11	10.13
	Event	915	263	11	12.34
	Difference	31	-17	0	2.21
	p-value	0	0	0.781	0

RESULTS FOR AUGUST REGION 1

		315K Pressure Level (hPa)	315K Wind Direction (°)	315K Wind Speed (knots)	315K Mixing Ratio (g/kg)
Topeka, KS	Non-Event	630	264	14	3.77
	Event	643	250	19	5.26
	Difference	13	-14	5	1.49
	p-value	0.001	0.007	0	0
Omaha, NE	Non-Event	624	275	17	3.53
	Event	626	271	21	4.14
	Difference	2	-4	4	0.61
	p-value	0.787	0.887	0	0.1
Chanhassen, MN	Non-Event	584	287	24	1.59
	Event	579	270	26	2.79
	Difference	-5	-17	2	1.2
	p-value	0.714	0.005	0.094	0
Davenport, IA	Non-Event	603	288	20	1.99
	Event	612	267	22	3.58
	Difference	9	-21	2	1.59
	p-value	0.164	0.003	0.053	0.001
Lincoln, IL	Non-Event	615	280	19	2.1
	Event	627	254	23	3.87
	Difference	12	-26	4	1.77
	p-value	0.114	0.001	0.004	0
Wilmington, OH	Non-Event	605	277	19	1.89
	Event	623	259	19	3.33
	Difference	18	-18	0	1.44
	p-value	0.043	0.109	0.632	0.008
White Lake, MI	Non-Event	581	278	22	1.42
	Event	600	269	27	2.93
	Difference	19	-9	5	1.51
	p-value	0.009	0.326	0.002	0
Green Bay, WI	Non-Event	564	284	23	1.32
	Event	580	264	26	2.2
	Difference	16	-20	3	0.88

(continued)

	p-value	0	0	0.144	0
		310K Pressure Level	310K Wind Direction	310K Wind Speed	310K Mixing Ratio
Topeka, KS	Non-Event	736	248	13	6.68
	Event	765	240	19	8.91
	Difference	29	-8	6	2.23
	p-value	0	0.032	0	0
Omaha, NE	Non-Event	737	264	16	6.1
	Event	726	275	19	6.74
	Difference	-11	11	3	0.64
	p-value	0.698	0.666	0.046	0.106
Chanhassen, MN	Non-Event	685	280	21	3.01
	Event	685	274	20	5.06
	Difference	0	-6	-1	2.05
	p-value	0.88	0.045	0.488	0
Davenport, IA	Non-Event	709	278	17	3.74
	Event	716	265	18	584
	Difference	7	-13	1	580.26
	p-value	0.15	0.049	0.144	0
Lincoln, IL	Non-Event	716	277	16	4.18
	Event	738	256	20	7.46
	Difference	22	-21	4	3.28
	p-value	0.035	0.002	0	0
Wilmington, OH	Non-Event	703	274	16	3.89
	Event	718	263	16	5.33
	Difference	15	-11	0	1.44
	p-value	0.01	0.261	0.248	0.045
White Lake, MI	Non-Event	676	276	20	2.31
	Event	692	271	22	4.55
	Difference	16	-5	2	2.24
	p-value	0.022	0.295	0.072	0
Green Bay, WI	Non-Event	651	281	19	2.16
	Event	671	266	21	3.85

(continued)

	Difference	20	-15	2	1.69
	p-value	0	0	0.482	0
		305K Pressure Level	305K Wind Direction	305K Wind Speed	305K Mixing Ratio
Topeka, KS	Non-Event	852	225	10	9.75
	Event	884	222	11	11.85
	Difference	32	-3	1	2.1
	p-value	0	0.145	0.009	0
Omaha, NE	Non-Event	855	225	13	8.86
	Event	852	235	15	9.26
	Difference	-3	10	2	0.4
	p-value	0.667	0.888	0.308	0.353
Chanhassen, MN	Non-Event	770	268	17	5.07
	Event	776	258	18	6.35
	Difference	6	-10	1	1.28
	p-value	0.752	0.175	0.319	0.002
Davenport, IA	Non-Event	795	267	14	5.86
	Event	829	246	16	9.76
	Difference	34	-21	2	3.9
	p-value	0.008	0.006	0.052	0
Lincoln, IL	Non-Event	802	266	13	6.89
	Event	851	243	18	10.22
	Difference	49	-23	5	3.33
	p-value	0.002	0.09	0.006	0
Wilmington, OH	Non-Event	790	271	14	6.77
	Event	811	257	15	8.06
	Difference	21	-14	1	1.29
	p-value	0.002	0.132	0.391	0.021
White Lake, MI	Non-Event	755	274	16	4.32
	Event	780	265	17	6.48
	Difference	25	-9	1	2.16
	p-value	0.001	0.128	0.254	0.003
Green Bay, WI	Non-Event	745	281	16	3.53

(continued)

	Event	760	262	16	5.95
	Difference	15	-19	0	2.42
	p-value	0	0	0.551	0
		300K Pressure Level	300K Wind Direction	300K Wind Speed	300K Mixing Ratio
Topeka, KS	Non-Event	925	207	9	11.47
	Event	945	190	10	12.62
	Difference	20	-17	1	1.15
	p-value	0	0.001	0.493	0
Omaha, NE	Non-Event	931	195	9	10.83
	Event	936	74	9	11.22
	Difference	5	-121	0	0.39
	p-value	0.309	0.066	0.857	0.351
Chanhassen, MN	Non-Event	873	250	15	8.34
	Event	882	241	15	9.24
	Difference	9	-9	0	0.9
	p-value	0.575	0.547	0.771	0.022
Davenport, IA	Non-Event	896	229	12	9.4
	Event	927	237	13	12.08
	Difference	31	8	1	2.68
	p-value	0.003	0.257	0.054	0
Lincoln, IL	Non-Event	915	217	11	10.5
	Event	935	218	10	13
	Difference	20	1	-1	2.5
	p-value	0	0.95	0.704	0
Wilmington, OH	Non-Event	899	228	12	9.85
	Event	930	79	9	11.09
	Difference	31	-149	-3	1.24
	p-value	0.001	0.001	0.029	0.065
Green Bay, WI	Non-Event	832	282	12	6.41
	Event	860	264	11	9.05
	Difference	28	-18	-1	2.64
	p-value	0	0	0.052	0

RESULTS FOR SEPTEMBER REGION 1

		315K Pressure Level (hPa)	315K Wind Direction (°)	315K Wind Speed (knots)	315K Mixing Ratio (g/kg)
Lake Charles, LA	Non-Event	628	236	10	3.38
	Event	640	235	16	4.63
	Difference	12	-1	6	1.25
	p-value	0	0.475	0	0.001
Little Rock, AR	Non-Event	604	253	14	2.12
	Event	618	229	17	3.97
	Difference	14	-24	3	1.85
	p-value	0.003	0.003	0.032	0
Jackson, MS	Non-Event	618	248	11	2.37
	Event	632	221	18	4.75
	Difference	14	-27	7	2.38
	p-value	0	0	0	0
Shelby, AL	Non-Event	615	248	13	1.86
	Event	631	212	17	5.86
	Difference	16	-36	4	4
	p-value	0	0.019	0.017	0
Peachtree, GA	Non-Event	615	250	12	1.97
	Event	635	206	11	5.68
	Difference	20	-44	-1	3.71
	p-value	0.002	0.004	0.779	0

		310K Pressure Level	310K Wind Direction	310K Wind Speed	310K Mixing Ratio
Lake Charles, LA	Non-Event	723	220	10	5.74
	Event	732	228	14	6.75
	Difference	9	8	4	1.01
	p-value	0	0.726	0	0
Little Rock, AR	Non-Event	704	246	12	4.04
	Event	714	232	16	6.15
	Difference	10	-14	4	2.11
	p-value	0.024	0.196	0.008	0

(continued)

Jackson, MS	Non-Event	713	239	10	4.67
	Event	723	220	15	7.03
	Difference	10	-19	5	2.36
	p-value	0.001	0.015	0	0
Shelby, AL	Non-Event	709	236	12	3.77
	Event	722	220	17	7.71
	Difference	13	-16	5	3.94
	p-value	0.001	0.265	0	0
Peachtree, GA	Non-Event	711	240	10	4.25
	Event	727	213	14	7.53
	Difference	16	-27	4	3.28
	p-value	0.012	0.049	0.137	0
		305K Pressure Level	305K Wind Direction	305K Wind Speed	305K Mixing Ratio
Lake Charles, LA	Non-Event	819	210	10	8.97
	Event	834	208	16	10.27
	Difference	15	-2	6	1.3
	p-value	0	0.166	0	0
Little Rock, AR	Non-Event	789	242	12	7.06
	Event	813	225	13	9.57
	Difference	24	-17	1	2.51
	p-value	0	0.052	0.041	0
Jackson, MS	Non-Event	803	226	10	8
	Event	825	219	16	10.59
	Difference	22	-7	6	2.59
	p-value	0	0.46	0	0
Shelby, AL	Non-Event	796	228	11	7.55
	Event	821	232	20	10.62
	Difference	25	4	9	3.07
	p-value	0	0.824	0	0
Peachtree, GA	Non-Event	794	235	11	7.37
	Event	808	214	17	10.5

(continued)

	Difference	14	-21	6	3.13
	p-value	0.023	0.119	0.003	0
		300K Pressure Level	300K Wind Direction	300K Wind Speed	300K Mixing Ratio
Lake Charles, LA	Non-Event	933	202	9	13.59
	Event	946	199	12	15.08
	Difference	13	-3	3	1.49
	p-value	0.001	0.457	0	0
Little Rock, AR	Non-Event	887	221	11	9.78
	Event	906	214	10	12.09
	Difference	19	-7	-1	2.31
	p-value	0	0.101	0.814	0
Jackson, MS	Non-Event	905	219	8	11.43
	Event	918	204	11	13.81
	Difference	13	-15	3	2.38
	p-value	0	0.009	0	0
Shelby, AL	Non-Event	914	225	13	11.16
	Event	924	235	20	13.61
	Difference	10	10	7	2.45
	p-value	0.103	0.582	0	0
Peachtree, GA	Non-Event	902	213	14	10.71
	Event	912	218	18	13.15
	Difference	10	5	4	2.44
	p-value	0.424	0.58	0.003	0.001

RESULTS FOR OCTOBER REGION 1

		315K Pressure Level (hPa)	315K Wind Direction (°)	315K Wind Speed (knots)	315K Mixing Ratio (g/kg)
Lake Charles, LA	Non-Event	589	262	15	1.33
	Event	612	229	21	2.7
	Difference	23	-33	6	1.37
	p-value	0	0	0	0
Little Rock, AR	Non-Event	546	265	24	0.94
	Event	567	236	30	1.96
	Difference	21	-29	6	1.02
	p-value	0	0	0	0
Jackson, MS	Non-Event	570	265	18	1.12
	Event	594	244	21	2.51
	Difference	24	-21	3	1.39
	p-value	0	0	0.363	0
Fort Worth, TX	Non-Event	582	255	20	1.43
	Event	585	232	31	3.05
	Difference	3	-23	11	1.62
	p-value	0.673	0.011	0	0
Norman, OK	Non-Event	554	255	23	0.98
	Event	549	239	39	1.42
	Difference	-5	-16	16	0.44
	p-value	0.13	0	0	0.024
		310K Pressure Level	310K Wind Direction	310K Wind Speed	310K Mixing Ratio
Lake Charles, LA	Non-Event	690	252	13	2.15
	Event	712	216	17	5.04
	Difference	22	-36	4	2.89
	p-value	0	0	0	0
Little Rock, AR	Non-Event	626	264	20	1.64
	Event	646	228	27	3.46
	Difference	20	-36	7	1.82

(continued)

	p-value	0.001	0	0	0
Jackson, MS	Non-Event	659	262	15	1.74
	Event	693	236	18	4.01
	Difference	34	-26	3	2.27
	p-value	0	0	0.17	0
Fort Worth, TX	Non-Event	684	248	17	2.6
	Event	680	234	26	4.98
	Difference	-4	-14	9	2.38
	p-value	0.725	0.166	0	0
Norman, OK	Non-Event	644	252	20	1.98
	Event	634	241	32	2.9
	Difference	-10	-11	12	0.92
	p-value	0.099	0.002	0	0.017

		305K Pressure Level	305K Wind Direction	305K Wind Speed	305K Mixing Ratio
Lake Charles, LA	Non-Event	772	241	12	3.5
	Event	805	201	19	8.6
	Difference	33	-40	7	5.1
	p-value	0	0	0	0
Little Rock, AR	Non-Event	726	260	17	2.55
	Event	747	225	24	5.8
	Difference	21	-35	7	3.25
	p-value	0.0001	0	0	0
Jackson, MS	Non-Event	747	252	13	2.77
	Event	780	219	17	6.78
	Difference	33	-33	4	4.01
	p-value	0	0	0.001	0
Fort Worth, TX	Non-Event	770	236	16	4.63
	Event	771	224	26	7.77
	Difference	1	-12	10	3.14
	p-value	0.325	0.239	0	0

(continued)

Norman, OK	Non-Event	747	240	19	3.87
	Event	737	236	27	5.25
	Difference	-10	-4	8	1.38
	p-value	0.57	0.248	0	0.001
		300K Pressure Level	300K Wind Direction	300K Wind Speed	300K Mixing Ratio
Lake Charles, LA	Non-Event	862	218	12	6.29
	Event	907	196	19	12.62
	Difference	45	-22	7	6.33
	p-value	0	0	0	0
Little Rock, AR	Non-Event	816	253	16	4.05
	Event	852	214	20	9.2
	Difference	36	-39	4	5.15
	p-value	0	0	0	0
Jackson, MS	Non-Event	838	242	12	4.65
	Event	879	207	16	9.65
	Difference	41	-35	4	5
	p-value	0	0	0.001	0
Fort Worth, TX	Non-Event	865	215	5.92	4.5
	Event	892	212	9.64	9
	Difference	27	-3	3.72	4.5
	p-value	0.078	0.58	0	0.742
Norman, OK	Non-Event	853	226	19	5.95
	Event	857	226	22	7.94
	Difference	4	0	3	1.99
	p-value	0.971	0.95	0.182	0

RESULTS FOR NOVEMBER REGION 1

		315K Pressure Level (hPa)	315K Wind Direction (°)	315K Wind Speed (knots)	315K Mixing Ratio (g/kg)
Little Rock, AR	Non-Event	507	265	41	0.62
	Event	520	235	49	0.85
	Difference	13	-30	8	0.23
	p-value	0.001	0	0	0
Jackson, MS	Non-Event	531	261	32	0.81
	Event	557	234	35	1.11
	Difference	26	-27	3	0.3
	p-value	0	0	0.013	0
Shelby, AL	Non-Event	524	265	37	0.6
	Event	560	239	38	1.3
	Difference	36	-26	1	0.7
	p-value	0	0	0.962	0
Nashville, TN	Non-Event	486	262	45	0.26
	Event	522	238	46	1.13
	Difference	522	238	46	1.13
	p-value	0	0	0.866	0
Peachtree, GA	Non-Event	525	265	38	0.53
	Event	554	242	32	1.38
	Difference	29	-23	-6	0.85
	p-value	0	0	0.174	0
Lake Charles, LA	Non-Event	554	260	26	0.92
	Event	571	237	35	1.22
	Difference	17	-23	9	0.3
	p-value	0	0	0	0

		310K Pressure Level	310K Wind Direction	310K Wind Speed	310K Mixing Ratio
Little Rock, AR	Non-Event	574	264	34	0.92
	Event	595	235	44	1.46
	Difference	21	-29	10	0.54

(continued)

	p-value	0.001	0	0	0
Jackson, MS	Non-Event	606	261	26	1.23
	Event	641	232	31	1.98
	Difference	35	-29	5	0.75
	p-value	0	0	0.001	0
Shelby, AL	Non-Event	599	265	31	0.98
	Event	635	237	31	2.32
	Difference	36	-28	0	1.34
	p-value	0	0	0.85	0
Nashville, TN	Non-Event	556	261	39	0.91
	Event	594	235	40	1.94
	Difference	38	-26	1	1.03
	p-value	0	0	0.682	0
Peachtree, GA	Non-Event	602	266	31	0.89
	Event	638	239	29	1.66
	Difference	36	-27	-2	0.77
	p-value	0.001	0	0.557	0
Lake Charles, LA	Non-Event	638	260	21	1.42
	Event	671	235	32	2.44
	Difference	33	-25	11	1.02
	p-value	0	0	0	0

		305K Pressure Level	305K Wind Direction	305K Wind Speed	305K Mixing Ratio
Little Rock, AR	Non-Event	667	264	28	1.4
	Event	699	237	37	3.17
	Difference	32	-27	9	1.77
	p-value	0	0	0	0
Jackson, MS	Non-Event	706	258	21	1.8
	Event	739	230	29	4.5
	Difference	33	-28	8	2.7
	p-value	0	0	0	0
Shelby, AL	Non-Event	705	263	25	1.61

(continued)

	Event	737	228	27	4.97
	Difference	32	-35	2	3.36
	p-value	0	0	0.295	0
Nashville, TN	Non-Event	640	261	32	1.35
	Event	695	231	35	3.68
	Difference	55	-30	3	2.33
	p-value	0	0	0.225	0
Peachtree, GA	Non-Event	703	270	25	1.47
	Event	729	232	25	4.6
	Difference	26	-38	0	3.13
	p-value	0.003	0	0.853	0
Lake Charles, LA	Non-Event	733	255	17	2.16
	Event	760	232	28	4.73
	Difference	27	-23	11	2.57
	p-value	0	0	0	0

		300K Pressure Level	300K Wind Direction	300K Wind Speed	300K Mixing Ratio
Little Rock, AR	Non-Event	751	263	24	2.08
	Event	787	236	32	5.43
	Difference	36	-27	8	3.35
	p-value	0	0	0	0
Jackson, MS	Non-Event	782	255	18	2.44
	Event	836	218	25	7.79
	Difference	54	-37	7	5.35
	p-value	0	0	0	0
Shelby, AL	Non-Event	776	262	20	2.27
	Event	825	213	25	8.04
	Difference	49	-49	5	5.77
	p-value	0	0	0.018	0
Nashville, TN	Non-Event	730	259	28	1.85
	Event	784	223	32	6.04
	Difference	54	-36	4	4.19
	p-value	0	0	0.018	0

(continued)

Peachtree, GA	Non-Event	773	268	21	2.08
	Event	812	227	23	7.12
	Difference	39	-41	2	5.04
	p-value	0	0	0.426	0
Lake Charles, LA	Non-Event	813	247	16	3.39
	Event	853	228	27	9.01
	Difference	40	-19	11	5.62
	p-value	0	0	0	0

RESULTS FOR DECEMBER REGION 1

		315K Pressure Level (hPa)	315K Wind Direction (º)	315K Wind Speed (knots)	315K Mixing Ratio (g/kg)
Little Rock, AR	Non-Event	447	264	53	0.34
	Event	497	230	54	0.69
	Difference	50	-34	1	0.35
	p-value	0	0	0.861	0
Jackson, MS	Non-Event	502	261	44	0.61
	Event	529	233	42	0.88
	Difference	27	-28	-2	0.27
	p-value	0	0	0.106	0.002
Lake Charles, LA	Non-Event	525	257	38	0.73
	Event	547	230	40	0.99
	Difference	22	-27	2	0.26
	p-value	0	0	0.059	0.029
		310K Pressure Level	310K Wind Direction	310K Wind Speed	310K Mixing Ratio
Little Rock, AR	Non-Event	533	264	45	0.59
	Event	565	228	47	1.46
	Difference	32	-36	2	0.87
	p-value	0	0	0.598	0
Jackson, MS	Non-Event	569	261	38	0.93
	Event	610	228	36	1.67
	Difference	41	-33	-2	0.74
	p-value	0	0	0.325	0
Lake Charles, LA	Non-Event	602	258	31	1.1
	Event	643	227	35	1.9
	Difference	41	-31	4	0.8
	p-value	0	0	0.025	0
		305K Pressure Level	305K Wind Direction	305K Wind Speed	305K Mixing Ratio

(continued)

Little Rock, AR	Non-Event	610	263	38	0.92
	Event	667	237	43	2.68
	Difference	57	-26	5	1.76
	p-value	0	0	0.118	0
Jackson, MS	Non-Event	665	263	31	1.37
	Event	719	223	33	3.48
	Difference	54	-40	2	2.11
	p-value	0	0	0.678	0
Lake Charles, LA	Non-Event	707	257	25	1.6
	Event	737	216	33	4.61
	Difference	30	-41	8	3.01
	p-value	0	0	0	0

		300K Pressure Level	300K Wind Direction	300K Wind Speed	300K Mixing Ratio
Little Rock, AR	Non-Event	711	264	31	1.32
	Event	760	232	35	4.99
	Difference	49	-32	4	3.67
	p-value	0	0	0.023	0
Jackson, MS	Non-Event	745	260	26	1.83
	Event	800	209	30	6.38
	Difference	55	-51	4	4.55
	p-value	0	0	0.07	0
Lake Charles, LA	Non-Event	778	258	21	2.3
	Event	834	206	30	8.02
	Difference	56	-52	9	5.72
	p-value	0	0	0	0